Response Control of Structural Systems Using Semi-Actively Controlled Interactions

Thesis by

Jeffrey Clyde Hayen

In Partial Fulfillment of the Requirements

for the Degree of

Doctor of Philosophy

California Institute of Technology

Pasadena, California

1996

(Submitted August 9, 1995)

Dedication

To My Lord and Savior, Jesus Christ

To My Grandparents, Douglas E. Decker and Eleanor J. White

To My Parents, Clyde J. Hayen and Sandra J. Decker

To My Wife, Celeste L. VanHollebeke

Acknowledgments

I would like to express my sincere appreciation to my principal advisor, Professor Wilfred D. Iwan, for the support, encouragement, and guidance that he has provided to me during my efforts on this research project. He is certainly a man to be esteemed and emulated in many respects, and I look forward to an ongoing association with him in the future. He is also responsible for giving me the opportunity to participate as a graduate teaching assistant for several courses in the Department of Applied Mechanics, as well as to pursue a minor field of study in Physics, both for which I am especially grateful.

Special thanks should also be extended to my former advisor, Professor Fredric Raichlen, who helped ease me over several academic hurdles — most notably, the oral Ph.D. candidacy examinations. He is also responsible for giving me the opportunity to participate as a graduate research assistant on a project with which I was briefly involved: a study to investigate the effects upon coastal regions produced by the initial wave trains associated with a tsunami. Furthermore, the efforts made on my behalf by Professors Allan J. Acosta, Christopher E. Brennen, and Edward E. Zukoski of the Department of Mechanical Engineering were particularly instrumental in helping me to secure admission to the California Institute of Technology (Caltech).

Professor John F. Hall was extremely helpful in answering my questions regarding structural and computational mechanics issues. Some key conversations with Dr. José A. Inaudi, University of California (Berkeley), and Professor Bill F. Spencer, University of Notre Dame, greatly influenced certain areas of focus in this thesis.

Many individuals associated with Caltech have assisted my research and writing efforts: Jonathan Melvin and Thomas Welmers, Computer Aided Design, Research, and Education (CADRE) Facilities; Thomas Boyce and Wayne Waller, Campus Computing Organization (CCO) Facilities; Donna Covarrubias, Jim O'Donnell, and Philip Roché, Earthquake Engineering Research Library (EERL); and Sharon Beckenbach and Denise

Okamoto, Structures and Soils Group in the Department of Civil Engineering.

I have received an excellent education during my stay at Caltech, and I am grateful for the financial support that has been faithfully provided to me. The willingness of the members of my thesis defense committee — Professors Wilfred D. Iwan, John F. Hall, James L. Beck, and Melany L. Hunt — to spend their time reviewing the thesis is very much appreciated.

The support, encouragement, and love of my family in San Diego, California have been invaluable to me during my studies at Caltech. My parents, grandparents, and sister and her family were instrumental in motivating and counseling me during my academic endeavors and providing physical, spiritual, and emotional "care packages" at critically-needed times. In addition, the Choe, Harris, Hill, Pentecost, and Wiens families of the Seekers Class at Lake Avenue Congregational Church offered a meaningful alternative to the often wearisome life of a graduate student in the form of the Tuesday Night Home Fellowship and Bible Study, which will be fondly remembered by both my wife and myself.

Finally, I want to express my deep gratitude to and abiding love for my wife and faithful companion, Celeste, who has endured with much sacrifice and patience the rigorous demands and irregular lifestyle associated with graduate study. Her Godly character and example have been an unending source of stability and perspective for me during some very difficult and demanding, yet challenging and rewarding experiences.

Abstract

The objective of the research described herein is to demonstrate conditions under which controlled interactions between two structures or structural components can be made effective in reducing the response of structures that are subjected to seismic excitation. It is shown that the effectiveness depends upon such factors as the control strategy implementation, the interaction element mechanical properties, and the parameters which characterize the dynamic behavior of the structural systems.

A study is conducted to examine the performance of a structural response control approach referred to as Active Interface Damping (AID). This control approach utilizes controlled interactions between two distinct structural systems — or different components of a single structural system — to reduce the resonance buildup that develops during an external excitation. Control devices or elements may be employed to physically produce the interactions between the systems. The proposed control approach differs from some other control approaches in that the sensors, processors, and switching components all operate actively, whereas the interaction elements function passively. The major advantage of this semi-active control technology is that relatively large control forces can be generated with minimal power requirements, which is of prime importance for the control of relatively massive systems, such as structures.

In the most simple form, the strategy of the control approach is to remove energy associated with vibration from only one system (the primary system). This process is accomplished through the transfer of energy to another system (the auxiliary system) by means of interaction elements, the dissipation of energy directly in the interaction elements, or a combination of both these methods. In a more complex form, the control strategy may be to minimize some composite response measure of the combined primary-auxiliary system. Only the most simple form of the control strategy is considered in the present study.

Several physical interpretations of the control approach are possible: one is that the systems represent two adjacent multi-story buildings; another is that the primary system represents a single multi-story building, while the auxiliary system could represent either an externally-situated resilient frame or a relatively small, unrestrained mass — or even be completely absent (in this latter scenario, the interaction elements are internally-mounted control devices). The interactions consist of reaction forces that are developed within and transmitted through the elements which are located between the two systems (or different points of a single system). The mechanical properties of these elements can be altered in real time by control signals, so the reaction forces applied to the systems may be changed, and the response control objective is achieved by actively changing the interactions at the interface of the two systems (or different points of a single system).

Initially, a preliminary study of the proposed control approach is conducted within the specialized setting of linear single-degree-of-freedom (SDOF) primary and auxiliary systems. Numerical simulations are performed for a series of control cases using horizontal ground accelerations from an ensemble of earthquake time histories as excitation input. Subsequently, a follow-on study of the proposed control approach is conducted for linear multiple-degree-of-freedom (MDOF) primary and auxiliary systems intended to represent actual structural systems. Based upon the investigation and insight obtained from the preliminary study, a limited number of control cases are considered which include those deemed most effective and implementable. Numerical simulations are again performed using the same excitation input as for the SDOF systems. The control approach is targeted at reducing the response contribution from the fundamental or dominant mode of vibration associated with the primary system. Uniformly-discretized models of a 6-story primary structural system capable of only lateral deformations are considered in most cases. A few cases involving models of a 3-story primary structural system are also examined.

Table of Contents

List of Figures

List of Tables

Chapter 1

Introduction and Background

1.1 Introduction

During the last two decades, a growing interest in the intelligent control of civil engineering structures has developed, and many analytical, numerical, and experimental studies have been conducted by various investigators with this objective in mind. This interest is confirmed by the appearance of numerous journal papers and technical reports on structural control in the literature (see [1–5] for an extensive review), as well as the convocation of several conferences and workshops on this topic. Such an interest has arisen in part because of the ambitious efforts by architects and engineers to create large-scale structures such as high-rise buildings and towers, long-span bridges and cables, and deep-water offshore platforms.

Yang and Soong [3] have remarked that improvements in structural analysis and design methods coupled with the development of high-strength materials have permitted the construction of taller and larger structural systems. In fact, it has been predicted that the next generation of buildings may be one order of magnitude taller than those currently considered feasible. But the inherent flexibility and low intrinsic-damping properties of the materials used to fabricate these structures produces an increased vulnerability to external excitations in the form of vibratory response. As a result, a control system might become an integral member of a structural system in order to maintain both its stability and integrity during response to routine and excessive loading conditions.

There is a natural desire for the protection and preservation of structures, their occupants, and their contents during critical periods of usage or catastrophic excitation episodes. Situations in which a structure is subjected to unpredictable environmental excitations associated with atmospheric, oceanic, or seismic events (*e.g.*, wind gusts,

water waves, or earthquakes) are of particular concern. The incorporation of control devices into a structure to guard against these events should be viewed as a means of alleviating such concerns, and this preventative measure has become viable because of the technological successes achieved in such areas of applied scientific endeavor as control theory and actuation, signal detection and processing, and fluid power utilization.

Several well-developed approaches (and their associated systems) to the problem of controlling a structure subjected to an external excitation have emerged and are discussed in the next section.

1.2 Background

As indicated by Leipholz and Abdel-Rohman [6], structural control involves the regulation of pertinent structural characteristics in order to ensure a desirable structural response while under the effect of loading. This regulation is achieved by modifying the dynamic behavior of the structure through the application of control forces. The control forces may be produced by either *passive* or *active* control systems. Passive control systems operate without the need for energy from an external source. As such, these systems must develop forces which are *reactive* in nature. Often, their main function is simply to dissipate mechanical energy (*i.e.*, all forms of kinetic and potential energy) that has accumulated within the structure. Alternatively, active control systems operate only when an external supply of energy is available. But their advantage over passive control systems lies in the fact that, within reasonable bounds, they are capable of producing arbitrarily prescribed control forces for application to the structure. This feature permits a strong connection between active control systems and modern control theory.

Some traditional approaches which have been used to suppress unwanted vibration in *mechanical* systems produced by an external excitation are:

- Alter the mechanical properties of the system to shift the natural frequencies of vibration (*i.e.*, the resonant frequencies) away from the dominant frequencies of excitation.

- Introduce energy dissipating or *damping* mechanisms into the system to prevent excessive vibration at or near the resonant frequencies.

- Employ vibration absorbers to counteract forces exerted on the system by the excitation.

- Employ vibration isolators to reduce transmission of forces to the system by the excitation.

- Actively generate applied forces to counteract forces exerted on the system by the excitation.

It is not surprising then that extended versions of these basic approaches constitute the primary methods used for most *structural* control applications. The principal areas of technological development that have met with some measure of success are structural base isolation, energy dissipation by internal devices, and active force application. Among the latter two areas, Soong [7] has reported the following examples of structural control systems: tuned mass dampers; tuned liquid dampers; sliding-friction dampers; supplemental viscous dampers; viscoelastic dampers; active mass drivers; active brace and tendon restraints; and pulsed gas-jet thrusters.

One of the earliest proponents for the application of modern control theory to civil engineering structures subjected to external excitations and other loading conditions was Yao [8], who in 1972 advocated

> "... an error-activated structural system ... defined as a structural system the behavior of which varies automatically in accordance with unpredictable variations in the loading as well as environmental conditions and thereby produces desirable responses under all possible loading conditions."

In their initial efforts, structural control investigators have drawn upon the results and techniques developed by the electrical and mechanical engineering communities for such diverse applications as servomechanism devices, chemical production processes, and guidance of aerospace vehicles. However, applications involving externally excited structures often possess characteristics and present challenges that depart from or even invalidate the assumptions and conditions upon which these results and techniques have been based.

In an address at a recent conference on structural control, Housner [9] has aptly pointed out the fact that much of the theoretical basis in the development of active structural control is rooted in modern control theory. For example, control algorithms used to govern the operation of control systems intended for civil engineering structures are often based upon standard solutions to the linear quadratic regulator (LQR) problem. However, some of the features associated with structural control applications which differ from the conventional LQR formulation are:

- a dynamical system typically characterized by only a few critical modes of response, permitting the option of reduced-order modelling
- a limited number of available sensors and actuators, suggesting the need for an optimal placement of these devices
- a relatively massive system, necessitating the influence of large and sustainable control forces
- a control objective focusing on the reduction of selected maximum response quantities but tolerating substantial imprecision in the state space trajectory for the system
- a requirement for robust, reliable, and possibly fault-tolerant control system performance under conditions for which the external excitation is generally unpredictable
- a control algorithm that is both computationally implementable and physically achievable

Because of their capability to provide arbitrarily prescribed control forces for application to the structure, active control systems are more effective than passive control systems. However, this superior effectiveness is accompanied by: increased complexity (*e.g.*, requirements for sensors, processors, and actuators); higher costs necessary to construct, operate, and maintain such systems; and questionable reliability. On the contrary, passive systems usually require minimal maintenance, do not need a power supply in order to function, and are simple and extremely reliable.

From these considerations emerges the concept of a *hybrid* control system, which consists of a combination of active and passive control systems. This system represents a

compromise between the two control approaches, and it is intended to be more efficient than either of these systems taken separately when all of the performance costs and benefits are taken into account. Typically, the active part of such a control system is operated for only brief intervals of time, as directed by a control algorithm, whereas the passive part is always ready to function. As may be verified in the literature, there has been an explosive growth in the number of hybrid control systems proposed for structural control applications during the last several years.

Historically, aseismic design procedures for structural systems have relied upon the ductility of structural members in the event of excessive loading conditions [10]. Materials which exhibit ductile behavior have the ability to dissipate energy during inelastic deformation. However, such deformation generally leaves the structure in a damaged condition with a compromised load-carrying capacity. Various researchers have demonstrated that energy dissipating devices are an effective and reliable means of reducing structural response during seismic excitation. Pall and Marsh [11] proposed and tested sliding-friction devices mounted at the intersection of diagonally-crossed braces connecting adjacent structural floors. The two ends of such a device are normally resistant to relative motion but will slip when a predetermined level of restraint force is exceeded. Because of the hysteretic behavior of the force-deformation curves for such a device undergoing cyclic loading, mechanical energy is dissipated. Filiatrault and Cherry [12] developed a simplified design procedure for determining the level of slip force to be used during operation of these braced sliding-friction devices. It is based upon the observation that a uniform distribution of slip force levels along the height of the structure is nearly as effective as an optimally-determined distribution of slip force levels, which vary with the height.

Another combination of active and passive control systems is manifested in the concept of a *semi-active* control system. The idea behind this approach appears to have first been elucidated by Karnopp *et al.* [13]. A semi-active control device consists of a

passive mechanical element (or combination of elements) across which the force is controllable. The variability in force will generally depend upon the instantaneous mechanical properties of the element and the states of the dynamical systems with which the element interacts. As described by Karnopp and Allen [14],

> "The concept involves a damping mechanism for force generation which can be modulated through a feedback control signal. The scheme requires only signal level power and small transducers to generate large, controllable forces in the damper."

In principle and practice, any forces which are actively generated during operation of a semi-active control device are not permitted to do work directly on the systems to be controlled. The resulting energy changes of these systems can only occur through the effect of reactive forces developed by the device. As an example, consider a control device that consists of friction plates which are attached between two structures. When there is relative motion of the two ends of the device, a normal force must be generated and applied to the plates in order to develop and sustain a resisting force between the structures. It is assumed that this normal force may be adjusted so that the resisting force is varied in a manner which has an optimal control effect upon the structures involved. However, the energy changes associated with this process are not a result of the normal force doing work on either of the systems to effect these energy changes. Rather, the normal force merely alters the mechanical properties of the device (*i.e.*, the slip force level) that is responsible for the interactions between the structures.

A number of investigators have performed analytical, numerical, and experimental studies involving the incorporation of semi-active devices into structural systems for control purposes. Hrovat *et al.* [15] investigated a semi-active tuned mass damper for the control of wind induced vibrations in tall buildings. The tuned mass damper utilized an auxiliary viscous damper whose properties could be controlled. They demonstrated that the performance of this control system is superior to passive systems and comparable to active systems. Akbay and Aktan [16] proposed an actively regulated friction-slip brace.

The operation of the brace was controlled by varying the clamping force on the friction interface of the slip device in order to regulate the reactive force transmitted to the structure. Dowdell and Cherry [17] performed a numerical study to demonstrate the effectiveness of varying in time the slip force levels associated with braced sliding-friction devices. Two control algorithms were investigated for the operation of these devices: one involved a simple clamp-and-release scheme; the other used a linear state feedback law motivated by optimal control theory.

Sack and Patten [18] introduced a semi-active hydraulic actuator as a means of achieving a variable viscous damper. The actuator utilized an adjustable flow orifice in the fluid return path connecting the high-pressure and low-pressure compartments of a piston-cylinder mechanism. Such a device is capable of providing large control forces, and it could be realized by installing a variable flow restriction on an otherwise generic shock absorber. In addition, Hirsch *et al.* [19] conceived, constructed, and tested a semi-active tuned mass damper which utilized a controllable viscous damper that can be activated or deactivated with electromagnetic forces.

Kobori *et al.* [20–23] advanced an active variable stiffness approach in which auxiliary braces are alternately engaged by or disengaged from the primary support frame for the structure. This engagement or disengagement is accomplished by piston-cylinder mechanisms which may be rapidly locked and unlocked. These braces and locking devices have actually been installed in the Kajima Technical Research Institute (KaTRI) No. 21 building in Tokyo [24]. Two methods are proposed for regulating the operation of the devices in order to achieve a desired control effect for the structure: one uses an open-loop approach based upon the excitation input characteristics in an effort to avoid resonance conditions; the other uses a closed-loop approach based upon an adaptive self-balancing principle.

In addition, it has been suggested that semi-active control systems be incorporated into other kinds of structural systems. For example, Kawashima and Unjoh [25] proposed

using active variable damping and variable stiffness for the seismic response control of bridges, while Yang and Lu [26] considered using semi-active friction damping for the seismic response control of bridges.

More recently, increased attention is being devoted to control methodologies which are based upon the theory of *variable structure systems* or *sliding mode control* [27–29]. Such methods of control bear a strong resemblance to those developed for the singular optimal control of linear systems [30]. Structural control research efforts following this approach are found in [31, 32]. The basic idea is that variable structure systems possess different dynamic properties in different regions of the state space. The change in the properties of the controlled system is idealized to occur instantaneously as the trajectory of system states crosses a *switching surface*, which separates one region from another. The switching surfaces are selected so as to produce a favorable control effect on the system as its trajectory migrates through the state space, eventually being driven to the origin. This method is also reminiscent of active variable damping and variable stiffness approaches.

Another novel method proposed for the mitigation of excessive structural response during seismic excitation involves the interaction of two distinct structural systems or components of a single structural system. Kobori *et al.* [33] advocated the use of tuned steel connectors between adjacent buildings for seismic response control. Each connector consists of a passive joint damper whose function is to dissipate energy upon elastoplastic deformation under loading conditions. The joint dampers are mounted to permit relative motion between the buildings in any direction, rendering them effective in suppressing both lateral and rotational motions. Such passive devices have actually been installed in the steel-reinforced concrete Kajima Intelligent (KI) building in Tokyo, which is comprised of a 5-story "A" building linked to a 9-story "B" building. Sera *et al.* [34] performed numerical and experimental analyses on a model of a four-winged, 12-story building with an internal atrium. The wings of the building were interconnected by link

members of fixed stiffness and damping properties. Simulations were performed, and different values were considered for these properties in separate simulation cases. Their results indicated that this configuration produced special "link modes" of vibration, which were effective in reducing deformations in each wing during seismic excitation.

1.3 Description and Organization of the Thesis

This thesis documents an exploratory study that has been initiated to examine the performance of a structural response control approach referred to as *Active Interface Damping*. This control approach utilizes controlled *interactions* between two distinct structural systems — or different components of a single structural system — to reduce the resonance buildup that develops during an external excitation. Control devices or *elements* may be employed to physically produce the interactions between the systems; these interaction elements are fully described in Chapters 3 and 4. The proposed control approach differs from some other control approaches in that the sensors, processors, and switching components involved all operate actively, whereas the interaction elements function passively. The major advantage of this semi-active control technology is that relatively large control forces can be generated with minimal power requirements, which is of prime importance for the control of relatively massive systems, such as structures.

In the most simple form, the strategy of the control approach is to remove energy associated with vibration from only one system (the *primary system*). This process is accomplished through the transfer of energy to another system (the *auxiliary system*) by means of the interaction elements, the dissipation of energy directly in the interaction elements, or a combination of both these methods. In a more complex form, the control strategy may be to minimize some composite response measure of the combined primary-auxiliary system. This study focuses on the simple form of the strategy and presents conditions under which the strategy will be effective in reducing only the response of the primary system. In this situation, the auxiliary system must be capable of absorbing any

additional energy received as a result of the control effort.

Several physical interpretations of the control approach are possible: one is that the systems represent two adjacent multi-story buildings; another is that the primary system represents a single multi-story building, while the auxiliary system could represent either an externally-situated resilient frame or a relatively small, unrestrained mass — or even be completely absent (in this latter scenario, the interaction elements are internally-mounted control devices). The interactions consist of reaction forces that are developed within and transmitted through the elements which are located between the two systems (or different points of a single system). The mechanical properties of these elements can be altered in real time by control signals, so the reaction forces applied to the systems may be changed, and the response control objective is achieved by actively changing the interactions at the *interface* of the two systems (or different points of a single system).

The objective of the research described herein is to establish under what conditions the proposed control approach is effective in reducing the response of the primary system when subjected to seismic excitation. As will be shown, this effectiveness depends upon such factors as the method of control strategy implementation, the interaction element mechanical properties, and the parameters characterizing the dynamic behavior of the primary and auxiliary systems.

Before proceeding to case studies of the proposed control approach, the concepts and theory of *classical*, *instantaneous*, and *incremental* optimal control methods are first considered. This body of material is introduced and developed in Chapter 2, and it is addressed in order to understand what constitutes an optimal control process and to offer some alternatives for coping with the difficulties which arise when the external excitation is unpredictable. As mentioned earlier, much of the theoretical basis that has been used to treat structural control problems is rooted in modern control theory, for which the notion of an optimal control process is essential. Some results are obtained that may be valuable for fully-active control systems and might prove effective in the response control

of structural systems subjected to seismic excitations. It is hoped that these results will also lay a foundation for further studies in the field of structural control.

In Chapter 3, a preliminary study of the proposed control approach is conducted within the specialized setting of linear single-degree-of-freedom (SDOF) primary and auxiliary systems. Numerical simulations are performed for a series of control cases using horizontal ground accelerations from an ensemble of earthquake time-histories as excitation input. In each of the control cases, the system parameters are specified and a particular type of interaction element is considered. The effectiveness of the control approach is judged by comparing the response of the controlled primary system to that of an uncontrolled primary system. The simplicity of this study is beneficial in formulating the structural control problem, guiding the selection of a specific set of parameters, and suggesting appropriate values for the chosen parameters. Most importantly, this study facilitates the development of a basic methodology for the implementation of the control strategy that is extendible to multiple-degree-of-freedom (MDOF) systems.

In Chapter 4, a follow-on study of the proposed control approach is conducted for linear MDOF primary and auxiliary systems intended to represent actual structural systems. Based upon the investigation and insight obtained from the results presented in Chapter 3, a limited number of control cases are considered which include those deemed most effective and implementable. Numerical simulations are again performed using the same excitation input as for the SDOF system study. The control approach is targeted at reducing the response contribution from the fundamental or dominant mode of vibration associated with the primary system. Uniformly-discretized models of a 6-story primary structural system capable of only lateral deformations are considered in most cases. A few cases involving models of a 3-story primary structural system are also examined.

A summary of the work and results presented in this thesis is provided in Chapter 5. There, overall conclusions are drawn, effects that have not been taken into account are mentioned, and recommendations for future work are indicated.

It should be emphasized that the control approach adopted herein is an outgrowth of both the active variable stiffness system invented by Kobori and the concept of semi-active control introduced by Karnopp. However, the control approach presented in the following chapters is much broader than has been previously considered, and it can be applied to situations involving the interaction of two structural systems — or between different components of a single structural system — and may include the effects of additional mass, stiffness, damping, or some combination of these mechanical properties.

Of particular significance are the control strategy employed and its relation to the reduction of certain structural displacements (the so-called *story drifts*) associated with the primary system, and the control algorithms used to operate the interaction elements upon which the control approach is based. As will be seen in Chapters 3 and 4, bounds can be established for the absolute structural displacements by considering a particular kind of vibrational energy. The control strategy is intimately related to this vibrational energy and the manner in which it evolves with time. It is believed that the adoption of such a framework for the description and analysis of structural control problems, including the concept of controlled interactions, sets apart the methodologies and studies presented herein from the previous investigations discussed in the preceding section.

References for Chapter 1

1. T. T. Soong, "Active Structural Control in Civil Engineering," *Engrg. Struct.*, Vol. 10, No. 2, Apr. 1988, pp. 74–84.
2. T. Kobori, "Active Seismic Response Control," *Proc. of Ninth World Conf. on Earthquake Engrg.*, Paper SE-R2, Vol. 8, Tokyo/Kyoto, Aug. 1988, pp. 435–446.
3. J. N. Yang and T. T. Soong, "Recent Advances in Active Control of Civil Engineering Structures," *Probabilistic Engrg. Mech.*, Vol. 3, No. 4, Dec. 1988, pp. 179–188.
4. T. Kobori, "State-of-the-Art of Seismic Response Control Research in Japan," *Proc. of U.S. Natnl. Workshop on Struct. Control Research*, ed. by G. W. Housner and S. F. Masri, USC Pub. No. CE-9013, Los Angeles, Oct. 1990, pp. 1–21.
5. T. T. Soong, "State-of-the-Art of Structural Control in U.S.A.," *Proc. of U.S. Natnl. Workshop on Struct. Control Research*, ed. by G. W. Housner and S. F. Masri, USC Pub. No. CE-9013, Los Angeles, Oct. 1990, pp. 48–65.
6. H. H. E. Leipholz and M. Abdel-Rohman, *Control of Structures*, Mechanics of Elastic Stability Series, Boston: Martinus Nijhoff Publishers, 1986, Chap. 1.
7. T. T. Soong, *Active Structural Control — Theory and Practice*, Essex, England: Longman Scientific and Technical (Publishers), 1990, Chap. 1–5.
8. J. T. P. Yao, "Concept of Structural Control," *Jour. of Struct. Div., Proc. of ASCE*, Vol. 98, No. ST7, July 1972, pp. 1567–1574.
9. G. W. Housner, T. T. Soong, and S. F. Masri, "Second Generation of Active Structural Control in Civil Engineering," *Proc. of First World Conf. on Struct. Control*, Vol. 1, Los Angeles, Aug. 1994, pp. 3–18 (Panel Sect.).
10. "Design and Identification of Steel for Structures," *Uniform Building Code*, Whittier, Calif.: International Conference of Building Officials, 1991, Chap. 27.
11. A. S. Pall and C. Marsh, "Response of Friction Damped Braced Frames," *Jour. of Struct. Div., Proc. of ASCE*, Vol. 108, No. ST6, June 1982, pp. 1313–1323.
12. A. Filiatrault and S. Cherry, "A Simplified Seismic Design Procedure for Friction Damped Structures," *Proc. of Fourth U.S. Natnl. Conf. on Earthquake Engrg.*, Vol. 3, Palm Springs, Calif., May 1990, pp. 479–488.

13. D. Karnopp, M. J. Crosby, and R. A. Harwood, "Vibration Control Using Semi-Active Force Generators," *Jour. of Engrg. for Indus., Trans. of ASME*, Vol. 96, Ser. B, No. 2, May 1974, pp. 619–626.

14. D. Karnopp and R. R. Allen, "Semiactive Control of Multimode Vibratory Systems Using the ILSM Concept," *Jour. of Engrg. for Indus., Trans. of ASME*, Vol. 98, Ser. B, No. 3, Aug. 1976, pp. 914–918.

15. D. Hrovat, P. Barak, and M. Rabins, "Semi-Active versus Passive or Active Tuned Mass Dampers for Structural Control," *Jour. of Engrg. Mech.*, Vol. 109, No. 3, June 1983, pp. 691–705.

16. Z. Akbay and H. M. Aktan, "Intelligent Energy Dissipation Devices," *Proc. of Fourth U.S. Natnl. Conf. on Earthquake Engrg.*, Vol. 3, Palm Springs, Calif., May 1990, pp. 427–435.

17. D. J. Dowdell and S. Cherry, "Semi-Active Friction Dampers for Seismic Response Control of Structures," *Proc. of Fifth U.S. Natnl. Conf. on Earthquake Engrg.*, Vol. 1, Chicago, July 1994, pp. 819–828.

18. R. L. Sack and W. N. Patten, "Semiactive Hydraulic Structural Control," *Proc. of Intnl. Workshop on Struct. Control*, ed. by G. W. Housner and S. F. Masri, USC Pub. No. CE-9311, Honolulu, Aug. 1993, pp. 417–431.

19. G. Hirsch, G. Hüffmann, and A. Kleine-Tebbe, "Semi-Active Control of Earthquake Induced Oscillations of Structures," Paper SE-14, *Proc. of Ninth World Conf. on Earthquake Engrg.*, Vol. 8, Tokyo/Kyoto, Aug. 1988, pp. 483–488.

20. T. Kobori, H. Kanayama, and S. Kamagata, "A Proposal of New Anti-Seismic Structure with Active Seismic Response Control System — Dynamic Intelligent System," Paper SE-11, *Proc. of Ninth World Conf. on Earthquake Engrg.*, Vol. 8, Tokyo/Kyoto, Aug. 1988, pp. 465–470.

21. T. Kobori, M. Sakamoto, M. Takahashi, N. Koshika, and K. Ishii, "Seismic Response Controlled Structure with Active Mass Driver System and Active Variable Stiffness System," *Proc. of U.S. Natnl. Workshop on Struct. Control Research*, ed. by G. W. Housner and S. F. Masri, USC Pub. No. CE-9013, Los Angeles, Oct. 1990, pp. 151–162.

22. T. Kobori and S. Kamagata, "Dynamic Intelligent Buildings — Active Seismic Response Control," *Intelligent Structures – 2: Monitoring and Control, Proc. of Intnl. Workshop on Intel. Systems*, ed. by Y. K. Wen, Perugia, Italy, 1991, London:

Elsevier Science Pub. Ltd., 1992, pp. 279–292.

23. T. Kobori and S. Kamagata, "Active Variable Stiffness System — Active Seismic Response Control," *Proc. of U.S.-Italy-Japan Workshop/Symposium on Struct. Control and Intel. Systems*, ed. by G. W. Housner, S. F. Masri, F. Casciati, and H. Kameda, USC Pub. No. CE-9210, Sorrento/Genoa, July 1992, pp. 140–153.

24. M. Sakamoto and T. Kobori, "Practical Applications of Active and Hybrid Response Control Systems," *Proc. of Intnl. Workshop on Struct. Control*, ed. by G. W. Housner and S. F. Masri, USC Pub. No. CE-9311, Honolulu, Aug. 1993, pp. 432–446.

25. K. Kawashima and S. Unjoh, "Variable Dampers and Variable Stiffness for Seismic Control of Bridges," *Proc. of Intnl. Workshop on Struct. Control*, ed. by G. W. Housner and S. F. Masri, USC Pub. No. CE-9311, Honolulu, Aug. 1993, pp. 283–297.

26. C. Yang and L.-W. Lu, "Seismic Response Control of Cable-Stayed Bridges by Semi-Active Friction Damping," *Proc. of Fifth U.S. Natnl. Conf. on Earthquake Engrg.*, Vol. 1, Chicago, July 1994, pp. 911–920.

27. V. I. Utkin, "Variable Structure Systems with Sliding Modes," *IEEE Trans. on Automatic Control*, Vol. AC-22, No. 2, Apr. 1977, pp. 212–222.

28. J.-J. E. Slotine and W. Li, *Applied Nonlinear Control*, Englewood Cliffs, N.J.: Prentice-Hall, Inc., 1991, Chap. 7.

29. R. R. Mohler, *Nonlinear Systems, Volume II — Applications to Bilinear Control*, Englewood Cliffs, N.J.: Prentice-Hall, Inc., 1991, Chap. 6.

30. B. D. O. Anderson and J. B. Moore, *Linear Optimal Control*, Network Series, Englewood Cliffs, N.J.: Prentice-Hall, Inc., 1971, Chap. 12.

31. J. A. Inaudi and J. M. Kelly, "Variable-Structure Homogeneous Control Systems," *Proc. of Intnl. Workshop on Struct. Control*, ed. by G. W. Housner and S. F. Masri, USC Pub. No. CE-9311, Honolulu, Aug. 1993, pp. 224–238.

32. J. N. Yang, Z. Li, and J. C. Wu, "Discontinuous Nonlinear Control of Base-Isolated Buildings," *Proc. of Intnl. Workshop on Struct. Control*, ed. by G. W. Housner and S. F. Masri, USC Pub. No. CE-9311, Honolulu, Aug. 1993, pp. 551–563.

33. T. Kobori, T. Yamada, Y. Takaneka, Y. Maeda, and I. Nishimura, "Effect of Dynamic Tuned Connector on Reduction of Seismic Response — Application to

Adjacent Office Buildings" Paper 7-10-3, *Proc. of Ninth World Conf. on Earthquake Engrg.*, Vol. 5, Tokyo/Kyoto, Aug. 1988, pp. 773–778.

34. K. Sera, T. Nagao, S. Sudo, Y. Kitakawa, and Y. Matsusima, "A Study on Inter-Building Coupling Behavior with Link-Members," *Proc. of Tenth World Conf. on Earthquake Engrg.*, Vol. 4, Madrid, July 1992, pp. 2161–2165.

Chapter 2

Classical, Instantaneous, and Incremental Optimal Control Methods

2.1 Introduction

In this chapter, the concepts and theory of what will be referred to as *classical*, *instantaneous*, and *incremental* optimal control methods are introduced and developed primarily within the context of structural control applications. The structural systems of interest are assumed to be linear, with time-invariant properties, and to be described by a discrete set of state variables (see [1–3] for further discussion on state space representation of dynamical systems). In addition, these systems are subject to external excitations — in particular, horizontal base acceleration as a result of the strong ground motion brought about by seismic disturbances.

2.2 Definition and Formulation of an Optimal Control Process

In this section, a special case of the basic problem encountered in the classical theory of optimal control processes is formulated. Such a case is sufficiently general, though, to include the class of structural systems considered. The development of the material presented here is partially adapted from the accounts given in [4, 5].

The objective of an optimal control process is to achieve a performance optimum for some actual system. This is accomplished by optimizing the dynamic behavior and control requirements of an ideal system associated with the actual system. The dynamic behavior and control requirements are quantitatively characterized by a performance index. The ideal system is a mathematical representation or *model* of the actual system, and it is typically based upon many simplifying assumptions. If the actual system is adequately approximated by the ideal system, then satisfactory physical performance

should result. In what follows, the term *system* will be used to denote the ideal system.

First, suppose that the dynamic condition or *state* of the system at any time t is fully described by a set of m real scalar quantities $z_1, \ldots, z_m$, known as *system state variables*, which are functions of t. These quantities form the components of a vector $\boldsymbol{z} = (z_1, \ldots, z_m)^{\mathsf{T}}$, $\boldsymbol{z} \in R^m$. It is assumed that the dynamic behavior of the system can be controlled to some extent by specifying values for the r real scalar quantities $u_1, \ldots, u_r$, known as *control input variables*. These quantities form the components of a vector $\boldsymbol{u} = (u_1, \ldots, u_r)^{\mathsf{T}}$, $\boldsymbol{u} \in R^r$. Furthermore, it is assumed that the system state variables are governed by ordinary differential equations of the form

$$\frac{dz_i}{dt} = g_i(z_1, \ldots, z_m, u_1, \ldots, u_r, t) \tag{2-1}$$

on a time interval $t_a \le t \le t_b$, where $i \in \{1, \ldots, m\}$. The functions $g_i(\boldsymbol{z}, \boldsymbol{u}, t)$, which also form a vector $\boldsymbol{g} = (g_1, \ldots, g_m)^{\mathsf{T}}$, $\boldsymbol{g} \in R^m$, are assumed to be defined and continuous, together with their partial derivatives

$$\frac{\partial g_i}{\partial z_j},\ j \in \{1, \ldots, m\};\quad \frac{\partial g_i}{\partial u_k},\ k \in \{1, \ldots, r\} \tag{2-2}$$

for all $\boldsymbol{z} \in R^m$ and $\boldsymbol{u} \in R^r$.

Next, suppose that a real vector function $\boldsymbol{u}(t) \in R^r$ is prescribed $\forall t \in [t_a, t_b]$. Upon substituting $\boldsymbol{u} = \boldsymbol{u}(t)$ into (2-1), a system of ordinary differential equations is obtained

$$\frac{dz_i}{dt} = g_i(z_1, \ldots, z_m, u_1(t), \ldots, u_r(t), t) \tag{2-3}$$

If the requirements of the *Cauchy-Lipshitz theorem* are satisfied, then this system of differential equations possesses a definite solution on the time interval $t_a \le t \le t_b$, known as a *state space trajectory*, for every initial condition $\boldsymbol{z}_a \equiv \boldsymbol{z}(t_a)$.

The aggregate of mathematical objects

$$U = \left\{\boldsymbol{z}_a,\ t_a,\ t_b;\ \boldsymbol{u}(t),\ t_a \le t \le t_b\right\} \tag{2-4}$$

will be called a *control process*. Thus, it is evident that to every control process U, there corresponds a unique trajectory, with definite initial and final states, which is a solution

to (2-3). It should be mentioned that although the aggregate is sufficient to yield a unique trajectory, the objects comprising U may not all be *a priori* known. Indeed, one of the tasks involved in the synthesis of an optimal control process is to determine each of these objects if some freedom exists in their selection.

Now, let

$$L = L(\dot{z}_1, \ \dots \ , \dot{z}_m, z_1, \ \dots \ , z_m, u_1, \ \dots \ , u_r, t) \tag{2-5}$$

be a real scalar function which is assumed to be defined and continuous, together with its partial derivatives

$$\frac{\partial L}{\partial \dot{z}_j}, \ \frac{\partial L}{\partial z_j}, \ j \in \{1, \ \dots \ , m\}; \ \frac{\partial L}{\partial u_k}, \ k \in \{1, \ \dots \ , r\} \tag{2-6}$$

for all $\dot{z}, z \in R^m$ and $\boldsymbol{u} \in R^r$, and let

$$\varphi = \varphi(z_1, \ \dots \ , z_m, t) \tag{2-7}$$

be a real scalar, nonnegative definite function which is also assumed to be defined and continuous, together with its partial derivatives

$$\frac{\partial \varphi}{\partial z_j}, \ j \in \{1, \ \dots \ , m\}; \ \frac{\partial \varphi}{\partial t} \tag{2-8}$$

For every control process U, a real scalar quantity $J[U]$, known as a *performance index*, may be assigned by a relation of the form

$$J[U] = \varphi(z_b, t_b) + \int_{t_a}^{t_b} L(\dot{z}, z, \boldsymbol{u}, t)\, dt \tag{2-9}$$

where $z_b \equiv z(t_b)$. Thus, $J[U]$ is a functional defined on some set of control processes. The control process $\hat{U}$ is said to be *optimal* if the inequality

$$J[\hat{U}] \leq J[U] \tag{2-10}$$

holds for any other control process U which transfers the initial state $z(t_a) = z_a$ to the final state $z(t_b) = z_b$, where $z(t)$ is the trajectory corresponding to U. Likewise, the trajectory $\hat{z}(t)$ corresponding to $\hat{U}$ is an optimal trajectory for the system.

In many practical applications, it is assumed that some class of *admissible* control

processes has been identified in advance. An admissible control process utilizes only those functions $u_1(t)$, ... , $u_r(t)$ which have values such that $\boldsymbol{u}(t) \in \Omega$, $\forall t \in [t_a, t_b]$, and $\Omega \subset R^r$ has been selected to incorporate the restrictions on u_1, ... , u_r corresponding to any physical constraints. The admissible control input functions considered herein are assumed to be at least piecewise continuous.

2.3 Necessary Conditions for an Optimal Control Process

With the formulation of the basic problem in the classical theory of optimal control processes complete, it is then useful to find necessary conditions which characterize the optimal control process and the optimal trajectory. A special case of the basic optimal control problem is now examined: the initial state z_a and initial time t_a are specified, whereas the final state z_b and final time t_b may each be either specified or unspecified. In cases for which z_b and t_b are free to be specified, it is necessary to simultaneously determine these quantities along with $\boldsymbol{u}(t)$.

The first class of optimal control problems considered are those for which $\Omega \equiv R^r$. In such a case, the *calculus of variations* may be used in conjunction with the *method of Lagrange multipliers* to find the desired necessary conditions. Using these mathematical tools, the necessary conditions for a solution to this class of optimal control problems may be derived [4] as

$$\dot{z} = \frac{\partial H}{\partial \lambda}, \quad \dot{\lambda} = \frac{d}{dt}\left[\frac{\partial H}{\partial \dot{z}}\right] - \frac{\partial H}{\partial z}, \quad \frac{\partial H}{\partial \boldsymbol{u}} = 0; \quad \forall t \in [t_a, t_b] \tag{2-11}$$

subject to the boundary conditions

$$\left[\frac{\partial \varphi}{\partial z} - \lambda + \frac{\partial H}{\partial \dot{z}}\right]^{\mathsf{T}}\Bigg|_{t_b} dz_b = 0, \quad \left[\frac{\partial \varphi}{\partial t} + H - \frac{\partial H}{\partial \dot{z}}^{\mathsf{T}} \boldsymbol{g}\right]\Bigg|_{t_b} dt_b = 0 \tag{2-12}$$

where H is a *Hamiltonian state function*, defined as

$$H(\lambda, \dot{z}, z, \boldsymbol{u}, t) \equiv \lambda^{\mathsf{T}} \boldsymbol{g}(z, \boldsymbol{u}, t) + L(\dot{z}, z, \boldsymbol{u}, t) \tag{2-13}$$

and λ is the *system costate vector*, whose components are Lagrange multipliers.

In cases for which the control input vector is constrained to belong to some specified set of admissible functions; $\boldsymbol{u} \in \Omega$, with $\Omega \subset R^r$; the *minimum principle of Pontryagin* [5] is used (see Appendix A). This principle states, in essence, that all of the necessary conditions in (2-11) and (2-12) remain in effect except for the last condition in (2-11), which is replaced by

$$H(\lambda, \dot{z}, z, \boldsymbol{u}, t) \leq H(\lambda, \dot{z}, z, \bar{\boldsymbol{u}}, t); \quad \forall \bar{\boldsymbol{u}} \in \Omega, \quad \forall t \in [t_a, t_b] \tag{2-14}$$

where the optimal values for λ, $\dot{z}$, z, and $\boldsymbol{u}$ are used in (2-14).

2.4 Classical Optimal Control Methods

A standard problem known as the *homogeneous* linear quadratic regulator (LQR) is now considered. A regulator is a feedback controller designed to maintain the state of a dynamical system within an acceptable deviation from a reference condition (if it were suddenly perturbed away from this condition) by using a minimum amount of control effort [6]. Solutions to this problem have formed the basis for much of the early work in structural control applications, as previously mentioned in Chapter 1.

The dynamical system is assumed to be governed by a linear (and, as will be seen from the relation between $\boldsymbol{u}$ and z, homogeneous) differential equation of the form

$$\dot{z} = Az + B\boldsymbol{u} \tag{2-15}$$

where the matrices A and B are time-invariant, and the associated performance index is selected to have the quadratic form

$$J = \tfrac{1}{2} z_b^{\mathsf{T}} P_b z_b + \int_{t_a}^{t_b} \tfrac{1}{2} \left[z^{\mathsf{T}} Q z + \boldsymbol{u}^{\mathsf{T}} R \boldsymbol{u} \right] dt \tag{2-16}$$

where P_b and Q are symmetric, nonnegative definite matrices while R is a symmetric, positive definite matrix. This choice for J has acceptable physical implications for the system behavior and yields desirable mathematical properties for obtaining a solution. In a sense, the functional form selected for J can be viewed as a constitutive relation for use

with the necessary conditions given in (2-11) through (2-14).

The particular case of interest is that for which z_b is free but t_b is fixed, and $\Omega \equiv R^r$. From the form given in (2-13), the Hamiltonian H for this problem is

$$H(\lambda, z, \boldsymbol{u}) = \lambda^{\mathsf{T}}(Az + B\boldsymbol{u}) + \tfrac{1}{2}\left[z^{\mathsf{T}}Qz + \boldsymbol{u}^{\mathsf{T}}R\boldsymbol{u}\right] \tag{2-17}$$

For an optimal control process to exist in this case, the necessary conditions are

$$\dot{z} = Az + B\boldsymbol{u}, \quad -\dot{\lambda} = Qz + A^{\mathsf{T}}\lambda, \quad R\boldsymbol{u} + B^{\mathsf{T}}\lambda = 0; \quad \forall t \in [t_a, t_b] \tag{2-18}$$

with the accompanying boundary conditions

$$\lambda(t_b) = P_b z_b; \quad z_a, t_a, t_b, P_b \text{ specified} \tag{2-19}$$

The solution to this problem which satisfies the conditions in (2-18) and (2-19) was first obtained by Kalman [7]. A technique known as the *sweep method* [6] is employed here to solve this *two-point* boundary value problem. Let

$$\lambda(t) = P(t)z(t) \tag{2-20}$$

where $P(t)$ is some matrix function of t, whose form is to be determined. In order to obtain a relation that may be used to find this form, (2-20) is differentiated to give

$$\dot{\lambda} = \dot{P}z + P\dot{z} = \dot{P}z + P(Az + B\boldsymbol{u}) \tag{2-21}$$

The second of the necessary conditions in (2-18) requires that

$$-\dot{\lambda} = Qz + A^{\mathsf{T}}\lambda = \left[Q + A^{\mathsf{T}}P\right]z \tag{2-22}$$

while the last of the necessary conditions in (2-18) demands that

$$\boldsymbol{u} = -R^{-1}B^{\mathsf{T}}\lambda = -R^{-1}B^{\mathsf{T}}Pz \tag{2-23}$$

in which case, by using (2-22) and (2-23), (2-21) becomes

$$-\dot{P}z = \left[A^{\mathsf{T}}P + PA - PBR^{-1}B^{\mathsf{T}}P + Q\right]z \tag{2-24}$$

Since the relation in (2-24) must hold at each z along the optimal trajectory for any given z_a, it is necessary that

$$-\dot{P} = A^{\mathsf{T}}P + PA - PBR^{-1}B^{\mathsf{T}}P + Q; \quad \forall t \in [t_a,\ t_b],\ \ P(t_b) = P_b \tag{2-25}$$

where the boundary condition is deduced from (2-20). Equation (2-25) is known as a matrix *differential Ricatti equation*, and if a solution $P = P(t)$ to (2-25) exists with final condition $P(t_b) = P_b$, then (2-24) is satisfied and (2-20) is valid. The solution to (2-25) is discussed in [6, 8], and under some general conditions which incorporate the assumptions stated for the parameter matrices, P will be a nonnegative definite matrix. Consider the limiting case for which $t_b - t_a \to \infty$. Upon examining (2-25), it is possible that a finite, steady-state solution $P = \overline{P}$ exists and possesses the property $\dot{P} = 0$, in which case

$$A^{\mathsf{T}}\overline{P} + \overline{P}A - \overline{P}BR^{-1}B^{\mathsf{T}}\overline{P} + Q = 0; \quad \forall t \in [t_a,\ t_b],\ \ t_b - t_a \to \infty \tag{2-26}$$

Equation (2-26) is known as a matrix *algebraic Ricatti equation*. In either case, the solution for P is then used with the result in (2-23) to obtain the optimal $\boldsymbol{u}$.

Another problem that is perhaps more closely related to control applications for structural systems which are subject to external excitations is the *inhomogeneous* LQR. The solution to this problem is credited in [6] to Garber, who has shown that for a dynamical system governed by a linear (and, by the presence of $\boldsymbol{v}$, which is unrelated to z, inhomogeneous) differential equation of the form

$$\dot{z} = Az + B^{u}\boldsymbol{u} + B^{v}\boldsymbol{v} \tag{2-27}$$

with the performance index given in (2-16), the optimal $\boldsymbol{u}$ is given by

$$\boldsymbol{u} = -R^{-1}B^{u\mathsf{T}}(Pz + \boldsymbol{w}) \tag{2-28}$$

where $P(t)$ satisfies (2-25), and $\boldsymbol{w}(t)$ is a solution to the vector differential equation

$$-\dot{\boldsymbol{w}} = \left[A^{\mathsf{T}} - PB^{u}R^{-1}B^{u\mathsf{T}}\right]\boldsymbol{w} + PB^{v}\boldsymbol{v}; \quad \forall t \in [t_a,\ t_b],\ \ \boldsymbol{w}(t_b) = 0 \tag{2-29}$$

where $\boldsymbol{v}(t)$ is an excitation input vector function which forces the system state to evolve in time. However, for applications involving seismic excitations, the functional form of $\boldsymbol{v}(t)$ is generally not available in advance. This prohibitive condition leads to the

realization that other approaches must be considered in the pursuit of "optimal" control methods for structural systems.

2.5 Instantaneous Optimal Control Methods

As demonstrated in the previous section, the classical theory of optimal control processes is well developed for linear dynamical systems which are subjected to *a priori* known external excitations (this includes the specialized case of unforced systems, for which the excitation input is zero but a dynamic response follows from nonzero initial conditions that may be caused by a perturbation). For a seismically-excited structure, a complete knowledge of the ground motion is generally not available when the control input must be determined and applied. This situation has motivated the development of *instantaneous* optimal control methods, which are founded upon the concept of attaining the best performance possible for the system while utilizing only information available at the current instant in time (and, possibly, that from previous instants in time).

The Instantaneous Optimal Control Method of Yang *et al.*

The first instantaneous optimal control method for structural systems appears to have been introduced by Yang *et al.* [9]. The key idea behind the proposed method is to use a *time-dependent* performance index in lieu of the standard integral performance index given in (2-16). This time-dependent performance index also has a quadratic functional dependence upon z and $\boldsymbol{u}$, like the integrand in (2-16). The implication inherent to the method is that the performance index is minimized at *every* instant in time. In practice though, the performance index is minimized only at discrete, regularly-spaced points in time. An abbreviated development of this method will be carried out here. The intention of duplicating the efforts of the investigators is to illustrate a generalization to their approach and draw attention to some puzzling aspects of their results. The presentation of the method here is somewhat different from that in [9], but the main features are essentially equivalent.

Consider again a dynamical system governed by the linear equation given in (2-27). In the case of a linear structural system, a typical equation of motion would be

$$M\ddot{x} + C\dot{x} + Kx = L^u u + L^v v \tag{2-30}$$

where $x \in R^n$ is the generalized coordinate vector, $u \in R^r$ is the control input vector, and $v \in R^s$ is the excitation input vector. The parameter matrices M, C, and K, assumed to be symmetric and positive definite, are directly related to the kinetic, dissipative, and elastic properties of the uncontrolled structural system, respectively. The matrices L^u and L^v represent mappings between the control and excitation forces acting on the system and the control and excitation inputs, respectively. The form in (2-27) is then obtained by introducing the mathematical objects

$$z \equiv \begin{Bmatrix} x \\ \dot{x} \end{Bmatrix}; \; A = \begin{bmatrix} 0 & I \\ -M^{-1}K & -M^{-1}C \end{bmatrix}, \; B^u = \begin{bmatrix} 0 \\ M^{-1}L^u \end{bmatrix}, \; B^v = \begin{bmatrix} 0 \\ M^{-1}L^v \end{bmatrix} \tag{2-31}$$

The time-dependent performance index is given by

$$J(t) = \tfrac{1}{2}\left[z^{\mathrm{T}}(t)Qz(t) + u^{\mathrm{T}}(t)Ru(t)\right] \tag{2-32}$$

The equations of motion in (2-27) can be uncoupled by using the transformation

$$z(t) \equiv Ty(t) \tag{2-33}$$

where T is an invertible matrix whose columns consist of the complex eigenvectors of A, and A is assumed to be a stable matrix (*i.e.*, the eigenvalues of A all have negative real parts). Substituting (2-33) into (2-27) and rearranging terms yields

$$\dot{y} = Dy + w; \; D = T^{-1}AT, \; w = T^{-1}\left(B^u u + B^v v\right) \tag{2-34}$$

where D is a diagonal matrix whose entries consist of the complex eigenvalues of A. If the system conditions are known at some initial time t_c, the solution to (2-34) is given by

$$y(t) = e^{(t-t_c)D}y(t_c) + \int_{t_c}^{t} e^{(t-\bar{t})D}w(\bar{t})\,d\bar{t} \tag{2-35}$$

in which $e^{(\bullet)}$ is the *matrix exponential function.* Consider a later time $t_d = t_c + h$, where h is understood to be a small increment in time. Then, by using the *trapezoidal rule* for

numerical integration, (2-35) can be approximately evaluated at time t_d as

$$y(t_d) = e^{hD}y(t_c) + \tfrac{1}{2}h\left[w(t_d) + e^{hD}w(t_c)\right] + O(h^3) \tag{2-36}$$

Using the transformation given by (2-33) and the expression for w from (2-34), (2-36) may in turn be used to approximately evaluate $z(t_d)$ as

$$z(t_d) = Te^{hD}T^{-1}z(t_c) + \tfrac{1}{2}h\left[f(t_d) + Te^{hD}T^{-1}f(t_c)\right] + O(h^3) \tag{2-37}$$

where $f \equiv B^u u + B^v v$. Recalling the series expansion for $e^{(\bullet)}$, and rearranging some of the terms, (2-37) may be expressed as

$$z(t_d) = z(t_c) + h\dot{z}(t_c) + \tfrac{1}{2}h^2 A\dot{z}(t_c) + \tfrac{1}{2}h^2\left[\frac{f(t_d) - f(t_c)}{h}\right] + O(h^3) \tag{2-38}$$

If $\dot{f}(t_c)$ is approximated by

$$\dot{f}(t_c) = \frac{f(t_d) - f(t_c)}{h} + O(h^2) \tag{2-39}$$

then it should be evident that the result in (2-38) could just as well be expressed as

$$z(t_d) = z(t_c) + h\dot{z}(t_c) + \tfrac{1}{2}h^2\ddot{z}(t_c) + O(h^3) \tag{2-40}$$

which is simply a *Taylor series expansion* for $z(t_d)$ in terms of quantities evaluated at t_c. The result in (2-40) clearly indicates that a restriction to linear systems, upon which the development in [9] is based, is not necessary.

The objective is to optimize the time-dependent performance index $J(t_d)$, as given in (2-32). In order to achieve this objective, a constraint relation between $z(t_d)$ and $u(t_d)$ is needed. This relation is obtained by dropping the terms of order $O(h^3)$ in (2-38) and regarding the expression for $z(t_d)$ as *exact*. Hence, it is apparent that the optimization of $J(t_d)$ is accomplished only in an approximate sense, and it should be recognized that this procedure is equivalent to assuming that $u(t)$ and $v(t)$ vary *linearly* with t.

The optimization of $J(t_d)$ is facilitated by forming the Hamiltonian $H(t_d)$ as

$$H(t_d) = \lambda^{\mathsf{T}}(t_d)\left[\left\{z(t_c) + h\dot{z}(t_c) + \tfrac{1}{2}h^2\left[A\dot{z}(t_c) + \dot{f}(t_c)\right]\right\} - z(t_d)\right] + J(t_d) \tag{2-41}$$

where $\lambda(t_d)$ is a vector Lagrange multiplier. According to the optimization theory of

Lagrange, the necessary conditions for minimizing $J(t_d)$ subject to the constraint (2-38) are obtained by requiring $H(t_d)$ to be *stationary* with respect to arbitrary infinitesimal changes in $\lambda(t_d)$, $z(t_d)$, and $\boldsymbol{u}(t_d)$; that is

$$\frac{\partial H(t_d)}{\partial \lambda(t_d)} = 0, \quad \frac{\partial H(t_d)}{\partial z(t_d)} = 0, \quad \frac{\partial H(t_d)}{\partial \boldsymbol{u}(t_d)} = 0 \tag{2-42}$$

where it is assumed that $\boldsymbol{v}(t_c)$, $\boldsymbol{u}(t_c)$, $z(t_c)$, and $\boldsymbol{v}(t_d)$ are fixed and known. The resulting necessary conditions are the constraint relation given in (2-38), neglecting the terms of order $O(h^3)$, and

$$Qz(t_d) + \lambda(t_d) = 0, \quad R\boldsymbol{u}(t_d) - \tfrac{1}{2} h B^{u\mathsf{T}} \lambda(t_d) = 0 \tag{2-43}$$

Thus,

$$\boldsymbol{u}(t_d) = -\tfrac{1}{2} h R^{-1} B^{u\mathsf{T}} Q z(t_d) \tag{2-44}$$

Substituting (2-44) into (2-38) and rearranging terms yields

$$\boldsymbol{u}(t_d) = -\tfrac{1}{2} h \left[I + \tfrac{1}{4} h^2 R^{-1} B^{u\mathsf{T}} Q B^{u} \right]^{-1} R^{-1} B^{u\mathsf{T}} Q \bar{z} \tag{2-45}$$

(assuming the indicated inverse exists), where

$$\bar{z} = z(t_c) + h\left[I + \tfrac{1}{2} h A \right] \dot{z}(t_c) - \tfrac{1}{2} h \left\{ B^{u} \boldsymbol{u}(t_c) - B^{v} \left[\boldsymbol{v}(t_d) - \boldsymbol{v}(t_c) \right] \right\} \tag{2-46}$$

There are two troublesome features of this result which must be pointed out. First, it is noticed that $\boldsymbol{u}(t_d) \to 0$ as $h \to 0$, which is inconsistent with the previous assumption that $\boldsymbol{u}(t)$ varies linearly with t, from which it would be expected that $\boldsymbol{u}(t_d) \to \boldsymbol{u}(t_c)$ as $h \to 0$. The difficulty may be traced to the definition of the performance index given in (2-32). Clearly, $J(t_d) \to J(t_c)$ as $h \to 0$. But upon examining (2-32) and realizing that $z(t_c)$ is fixed for the analysis, and therefore independent of $\boldsymbol{u}(t_d)$, the obvious choice for $\boldsymbol{u}(t_d)$ to minimize $J(t_d)$ is zero in the limit as $h \to 0$. Thus, the form given in (2-32) is not acceptable for use with this instantaneous optimal control method.

Next, the manner in which the control input is physically implemented has not been addressed. In particular, $\boldsymbol{u}(t)$ is *ramped* in a linear fashion from $\boldsymbol{u}(t_c)$ at time t_c to $\boldsymbol{u}(t_d)$

at time t_d. To accomplish this process, the determination of $\boldsymbol{u}(t_d)$ must be completed by time t_c in order to establish the rate at which $\boldsymbol{u}(t)$ changes with t. However, $\boldsymbol{v}(t_d)$ is not known until time t_d. Hence, $\boldsymbol{u}(t_d)$ cannot be calculated according to (2-45) at time t_c. Thus, this particular method violates causality. Perhaps this fact was overlooked by the investigators because their study was based upon numerical simulations for which a complete excitation record was available in advance.

An Alternative Instantaneous Optimal Control Method

The analysis for the control method outlined above involves a single representative short time interval for which the calculations used to determine $\boldsymbol{u}$ are uncoupled from all other segments in time. It is conceivable that some of the difficulties with this approach might be eliminated if a performance index which accounted for a series of consecutive short time intervals were used instead. This approach is briefly explored below.

Consider again a linear dynamical system governed by (2-27). Then

$$z(t_{k+1}) = z(t_k) + h\left[A z(t_k) + B^u \boldsymbol{u}(t_k) + B^v \boldsymbol{v}(t_k)\right] + O(h^2) \tag{2-47}$$

where

$$t_k = t_a + (k-1)h, \quad h = \frac{t_b - t_a}{m-1}; \quad k \in \{1, \ldots, m\} \tag{2-48}$$

and m is an integer, with

$$z(t_1) = z_a, \quad z(t_m) = z_b; \quad z_a,\ t_a,\ t_b,\ P_b \text{ specified} \tag{2-49}$$

Suppose the following performance index is selected

$$J(m) = \tfrac{1}{2} z_b^{\mathsf{T}} P_b z_b + \sum_{k=1}^{m-1} c_k \tfrac{1}{2}\left[z^{\mathsf{T}}(t_{k+1}) Q z(t_{k+1}) + \boldsymbol{u}^{\mathsf{T}}(t_k) R \boldsymbol{u}(t_k)\right] \tag{2-50}$$

where P_b, Q, and R are all as previously defined in Section 2.4, and c_k represents some appropriately chosen weighting factor. Using (2-47) as a constraint relation between the values of $z(t_k)$, $\boldsymbol{u}(t_k)$, and $z(t_{k+1})$, the optimal values for $\boldsymbol{u}(t_k)$ which minimize $J(m)$ are to be found.

As before, the optimization theory of Lagrange asserts that the solution for the

constrained minimization of $J(m)$ is equivalent to the solution for the unconstrained minimization of $H(m)$, where

$$H(m) = \sum_{k=1}^{m-1} \lambda^{\mathsf{T}}(t_k)\left[z(t_k) + h\,g(t_k) - z(t_{k+1}) + O(h^2)\right] + J(m) \tag{2-51}$$

and $g \equiv Az + B^u u + B^v v$. The necessary conditions for the unconstrained minimization of $H(m)$, where $\lambda(t_k)$ is now regarded as an independent vector variable, are

$$\frac{\partial H(m)}{\partial \lambda(t_l)} = 0, \quad \frac{\partial H(m)}{\partial z(t_{l+1})} = 0, \quad \frac{\partial H(m)}{\partial u(t_l)} = 0 \tag{2-52}$$

with $l \in \{1, \ldots, m-1\}$. Upon letting $c_l = h$ (this choice will be explained momentarily), and dropping the terms of order $O(h^2)$, the relations in (2-52) become

$$z(t_{l+1}) = z(t_l) + h\left[Az(t_l) + B^u u(t_l) + B^v v(t_l)\right] \qquad l \in \{1, \ldots, m-1\} \tag{2-53}$$

$$\lambda(t_l) = \lambda(t_{l+1}) + h\left[Qz(t_{l+1}) + A^{\mathsf{T}}\lambda(t_{l+1})\right] \qquad l \in \{1, \ldots, m-2\} \tag{2-54}$$

$$u(t_l) = -R^{-1}B^{u\mathsf{T}}\lambda(t_l) \qquad l \in \{1, \ldots, m-1\} \tag{2-55}$$

subject to the boundary condition

$$\lambda(t_{m-1}) = \left(P_b + hQ\right)z(t_m) \tag{2-56}$$

Equation (2-54) represents a relation between $\lambda(t_l)$ and $\lambda(t_{l+1})$ which develops backward in time, with a boundary condition specified for $\lambda(t_{m-1})$. Since $\lambda(t_l)$ depends directly upon $z(t_{l+1})$, which in turn depends upon $v(t_l)$, it is not possible to determine an optimal solution for $u(t_l)$ unless the values of $v(t_l)$ are *a priori* known. Hence, although otherwise analytically sound, this method is not appropriate for applications involving seismic excitations or any physical phenomenon for which a complete excitation record is not available in advance.

It is interesting to observe the behavior of these necessary conditions in the limit as $m \to \infty$. Upon rearrangement and letting $m \to \infty$ (in which case $h \to 0$, $t_{l+1} \to t_l$, and the discrete variable t_l becomes the continuous variable t), (2-53) through (2-55) become

$$\dot{z} = Az + B^u u + B^v v, \quad -\dot{\lambda} = Qz + A^T \lambda, \quad u = -R^{-1} B^{uT} \lambda; \quad \forall t \in [t_a, t_b] \tag{2-57}$$

with the accompanying boundary conditions

$$\lambda(t_b) = P_b z_b; \quad z_a, t_a, t_b, P_b \text{ specified} \tag{2-58}$$

These results are identical to the necessary conditions obtained for the inhomogeneous LQR problem discussed in Section 2.3, for which a solution can be found by using the relations given in (2-25), (2-28), and (2-29) if $v(t)$ is known in its entirety. The reason for selecting $c_k = h$ now becomes apparent: this choice ensures that the series in (2-50) and (2-51) converge as $m \to \infty$ (since $h \to 0$ as $m \to \infty$).

The Suggested Instantaneous Optimal Control Method

Attention is now turned toward a control method which provides what may be more accurately described as an instantaneous optimal control method for linear dynamical systems subject to unpredictable external excitations. The key idea behind the proposed approach is based upon a method attributed in [10] to Bass. Before proceeding with the development of this approach, it is first worth revisiting the homogeneous LQR problem examined in Section 2.4 so that a remarkable property associated with the optimal control process can be demonstrated. This property is directly related to the proposed approach.

Consider the quadratic function

$$V(z, t) = \tfrac{1}{2} z^T S(t) z \tag{2-59}$$

and define the matrix $S(t)$ to be governed by the relation

$$-\dot{S} = A^T S + SA - SBR^{-1}B^T S + Q; \quad \forall t \in [t_a, t_b], \quad S(t_b) = S_b \tag{2-60}$$

where S_b is symmetric and nonnegative definite. It can be easily verified that S is also symmetric and nonnegative definite. Using (2-59), the expression for $\dot{V}$ evaluated along trajectories obeying (2-15) is given by

$$\dot{V} = \tfrac{1}{2} z^T \left[A^T S + \dot{S} + SA \right] z + (Sz)^T Bu \tag{2-61}$$

where, upon using (2-60), (2-61) becomes

$$\dot{V} = (Sz)^{\mathsf{T}} Bu - \tfrac{1}{2} z^{\mathsf{T}} \left[SBR^{-1}B^{\mathsf{T}}S + Q \right] z \tag{2-62}$$

Now suppose that the control strategy is to minimize $\dot{V}$ — to cause $\dot{V}$ to become as negative as possible — along system trajectories at *every* instant in time (the motivation for selecting this strategy is discussed below). Clearly, the choice for $\boldsymbol{u}$ which minimizes $\dot{V}$ along trajectories obeying (2-15) is $\boldsymbol{u} \to -\infty$, $\forall t \in [t_a, t_b]$, which is neither physically possible nor desirable. Indeed, a better choice for $\boldsymbol{u}$ would be one that yields the "best" performance for the system while simultaneously conserving the control effort. If the control input were also constrained to belong to some set of admissible functions (*i.e.*, restricted to some reasonable range of values), then this procedure would be acceptable. In the case of the homogenous LQR problem, there are no explicit restrictions on $\boldsymbol{u}$; rather, $\boldsymbol{u}$ is chosen to optimize the performance index given in (2-16), which assigns a direct penalty for the "size" of $\boldsymbol{u}$ in the last quadratic term of the integrand. Based upon this observation, an alternative procedure is proposed for the case in which the control input is unconstrained: the modified control strategy is to minimize the *sum* of $\dot{V}$ and a positive definite function of $\boldsymbol{u}$, such as $\frac{1}{2}\boldsymbol{u}^{\mathsf{T}} R \boldsymbol{u}$, where R is as previously defined.

By using (2-62), it can be shown that along trajectories obeying (2-15)

$$\dot{V} + \tfrac{1}{2}\boldsymbol{u}^{\mathsf{T}} R \boldsymbol{u} = \tfrac{1}{2} \left\| \boldsymbol{u} + R^{-1}B^{u\mathsf{T}} S z \right\|_R^2 - \tfrac{1}{2} z^{\mathsf{T}} Q z \tag{2-63}$$

where

$$\| \cdot \|_R^2 \equiv (\,\cdot\,)^{\mathsf{T}} R (\,\cdot\,) \tag{2-64}$$

Since the system state is uniquely defined at each instant in time, the control input which minimizes $\dot{V} + \frac{1}{2}\boldsymbol{u}^{\mathsf{T}} R \boldsymbol{u}$ at every instant in time is given by

$$\boldsymbol{u} = -R^{-1}B^{u\mathsf{T}} S z \tag{2-65}$$

where S is the solution to (2-60). This solution for $\boldsymbol{u}$ is exactly the same as the solution previously obtained in Section 2.4 when $S_b = P_b$. The precise equivalence of the two

solutions is now further demonstrated.

In order to verify the true optimality of the proposed control strategy, consider the *generalized performance index*

$$J[z,\ t;\ t_b,\ \boldsymbol{u}(\bar{t})] = \tfrac{1}{2} z_b^{\mathsf{T}} S_b\, z_b + \int_t^{t_b} \tfrac{1}{2}\left[z^{\mathsf{T}}(\bar{t}) Q z(\bar{t}) + \boldsymbol{u}^{\mathsf{T}}(\bar{t})\, R \boldsymbol{u}(\bar{t})\right] d\bar{t} \tag{2-66}$$

where $z(\bar{t})$ denotes a trajectory obeying (2-15), $t \le \bar{t} \le t_b$. For a given initial state z at an arbitrary initial time t, but fixed final time t_b and prescribed $\boldsymbol{u}(\bar{t})$, it is shown in [11] (see Appendix B) that

$$-\frac{d}{dt}\left[\frac{\partial J}{\partial z}\right] = \frac{\partial L}{\partial z} + \frac{\partial \boldsymbol{g}^{\mathsf{T}}}{\partial z}\,\frac{\partial J}{\partial z} \tag{2-67}$$

where L and $\boldsymbol{g}$ are the same objects as defined in Section 2.2. Ordinarily, (2-67) only represents an intermediate result that is used in the development of the *Hamilton-Jacobi-Bellman equation*, which forms the basis of another method by which solutions to optimal control problems may be obtained. It is used for a different purpose here. In the present context, (2-67) becomes

$$-\frac{d}{dt}\left[\frac{\partial J}{\partial z}\right] = Qz + A^{\mathsf{T}}\frac{\partial J}{\partial z} \tag{2-68}$$

By comparison with the second necessary condition in (2-18), (2-68) reveals that

$$\lambda = \frac{\partial J}{\partial z} \tag{2-69}$$

when the optimal $\boldsymbol{u}(\bar{t})$ is used. Using (2-63), it may be shown that along trajectories obeying (2-15), (2-66) becomes

$$J[z,\ t;\ t_b,\ \boldsymbol{u}(\bar{t})] = \tfrac{1}{2} z^{\mathsf{T}} S z + \int_t^{t_b} \tfrac{1}{2}\left\| \boldsymbol{u}(\bar{t}) + R^{-1} B^{u\mathsf{T}} S(\bar{t}) z(\bar{t}) \right\|_R^2 d\bar{t} \tag{2-70}$$

If the control input is selected according to (2-65), (2-70) is simply given by

$$J[z,\ t;\ t_b,\ \boldsymbol{u}(\bar{t})] = \tfrac{1}{2} z^{\mathsf{T}} S z \tag{2-71}$$

in which case $\lambda = Sz$, by (2-69) and (2-71). Letting $S_b = P_b$, it is clear that this is the same result as obtained earlier, since $S(t) = P(t),\ \forall t \in [t_a,\ t_b]$, from (2-25) and (2-60). Hence, this class of optimal control problems has the property that the control strategy of

selecting $\boldsymbol{u}$ to minimize $\dot{V}+\frac{1}{2}\boldsymbol{u}^{\mathsf{T}}R\boldsymbol{u}$ along system trajectories at every instant in time produces an optimal control process as defined in Section 2.2.

The question then naturally arises as to the significance of using $\dot{V}$ evaluated along trajectories obeying (2-15). This question can be answered by recalling the *second* or *direct method of Liapunov* [12], which is typically useful for stability analyses of general dynamical systems. The basic idea is that if a positive definite function of the system state can be found whose total time derivative is always negative when evaluated along system trajectories, the system is asymptotically stable: $|z| \to 0$ as $t \to \infty$. In the case of the homogeneous LQR problem, V, as given by (2-59), would be a candidate Liapunov function if *stronger* conditions are imposed on Q and S_b, requiring them to be positive definite instead of merely nonnegative definite. Under these conditions, it is easy to show that $\dot{V}$, as given by (2-62), is negative definite when the control input prescribed by (2-65) is used. Thus, the control strategy has the following physical interpretation: it ensures that the state of the controlled system will eventually be driven to zero in an optimal manner by selecting the control input given in (2-65).

It was indicated in Section 2.4 that as $t_b - t_a \to \infty$, a steady-state solution $S = \bar{S}$ to (2-60) might exist. Actually, it can be shown [13] that even with the relaxed conditions on Q and S_b, $\bar{S}$ exists and is positive definite whenever the matrix pair (A, B) is *stabilizable* and the matrix pair (C, A) is *detectable*. The pair (A, B) is said to be stabilizable if a constant matrix L exists such that $A - BL$ is stable. Since $Q^{\mathsf{T}} = Q$ by hypothesis, Q can be decomposed as $Q = C^{\mathsf{T}}C$, and the pair (C, A) is said to be detectable if a constant matrix M exists such that $A - MC$ is stable. If $\dot{V}$ is evaluated by using the control input given in (2-65), with $S = \bar{S}$, it is nonpositive definite. However, a generalization of the Liapunov direct method, proved by Barbasin and Krasovskii [14], states that if $\dot{V}$ is nonpositive definite along every nontrivial system trajectory, but not identically zero $\forall t \in [t_a, t_b]$ for arbitrary t_a, the system is asymptotically stable. It can be shown that these requirements are satisfied with the relaxed conditions on Q and S_b

when the pair $(A,\ B)$ is stabilizable and the pair $(C,\ A)$ is detectable.

Of course, deducing that (2-60) should govern the time evolution of S would have been nearly impossible apart from the hindsight afforded in Section 2.4. But the principle of the suggested control approach is still valid, especially in light of the desirable stability properties discussed above. These asymptotic stability properties imply that the measure used for the response of the system, given by equation (2-59), is being driven to zero in a monotonically nonincreasing fashion. This is certainly an attractive type of behavior for controlling the system response.

In view of the foregoing results, the following approach is suggested for the control of linear dynamical systems subjected to external excitations for which information is not available in advance. This control approach constitutes an instantaneous optimal control method (*i.e.*, optimal in a *local-time* sense but certainly suboptimal in a *global-time* sense as delineated by (2-4), (2-9), and (2-10) in Section 2.2).

Consider again the linear dynamical system described by (2-27), where A, B^u, and B^v are time-invariant, and A is assumed to be stable. Let

$$V(z,\ t) = \tfrac{1}{2} z^{\mathsf{T}} S(t) z \tag{2-72}$$

be a Liapunov function for the system trajectories described by (2-27) with $\boldsymbol{u}$ and $\boldsymbol{v}$ *identically zero*. $S(t)$ is then evaluated from a matrix *differential Liapunov equation*

$$-\dot{S} = A^{\mathsf{T}} S + S A + Q,\ \ \forall t \in [t_a,\ t_b];\ \ S(t_b) = S_b \tag{2-73}$$

where Q is any symmetric, positive definite matrix. The solution to (2-73) is given by

$$S(t) = e^{(t_b - t)A^{\mathsf{T}}} S_b\, e^{(t_b - t)A} + \int_t^{t_b} e^{(t_b - \bar{t})A^{\mathsf{T}}} Q\, e^{(t_b - \bar{t})A}\, d\bar{t} \tag{2-74}$$

which can be directly verified by *Leibnitz's rule* for differentiation of an integral. Now, for the case in which $\boldsymbol{u}$ and $\boldsymbol{v}$ are not zero, the control strategy is to select $\boldsymbol{u}$ so as to instantaneously minimize $\dot{V}$ or $\dot{V} + \frac{1}{2}\boldsymbol{u}^{\mathsf{T}} R \boldsymbol{u}$ along trajectories obeying (2-27), depending on whether $\boldsymbol{u}$ is constrained or unconstrained to belong to $\Omega \subset R^r$, respectively, where

$$\dot{V} = (Sz)^{\mathsf{T}}\left(B^{u}\boldsymbol{u} + B^{v}\boldsymbol{v}\right) - \tfrac{1}{2}z^{\mathsf{T}}Qz \tag{2-75}$$

Note: Henceforth, the analysis will be carried out for the case in which the control input is unconstrained, with the understanding that when the constrained control input case is being considered, the terms which contain R should be dropped from the resulting expressions or relations.

Now, consider a performance index of the form

$$J = \tfrac{1}{2}z_b^{\mathsf{T}}S_b z_b + \int_{t_a}^{t_b} \tfrac{1}{2}\left[z^{\mathsf{T}}Qz + \boldsymbol{u}^{\mathsf{T}}R\boldsymbol{u}\right]dt \tag{2-76}$$

where Q and R are no longer arbitrary as for the standard LQR problem but correspond to the matrix parameters indicated above. S_b should be a symmetric, positive definite matrix but otherwise arbitrary. Using (2-75), (2-76) becomes

$$J = \tfrac{1}{2}z_a^{\mathsf{T}}S(t_a)z_a + \int_{t_a}^{t_b}\left[(Sz)^{\mathsf{T}}B^{u}\boldsymbol{u} + \tfrac{1}{2}\boldsymbol{u}^{\mathsf{T}}R\boldsymbol{u}\right]dt + \int_{t_a}^{t_b}(Sz)^{\mathsf{T}}B^{v}\boldsymbol{v}\,dt \tag{2-77}$$

It is recognized that the integrand in the first integral of (2-77) possesses the same combination of terms involving $\boldsymbol{u}$ as the expression $\dot{V} + \tfrac{1}{2}\boldsymbol{u}^{\mathsf{T}}R\boldsymbol{u}$, in which $\dot{V}$ is evaluated from (2-75). In fact, this structure will always be present as long as the positive definite function of $\boldsymbol{u}$ appearing in the performance index matches that which is appended to $\dot{V}$. Therefore, a minimization of the expression $\dot{V} + \tfrac{1}{2}\boldsymbol{u}^{\mathsf{T}}R\boldsymbol{u}$ corresponds to a minimization of the integrand in the first integral in (2-77).

Thus, in addition to the previous discussion based upon stability considerations, it is apparent that the suggested control strategy has an alternate interpretation. For the case where both $\boldsymbol{u}$ and $\boldsymbol{v}$ are identically zero, the matrix $S(t_a)$, as evaluated from (2-74), and the initial state z_a determine the *zero input cost*, $\tfrac{1}{2}z_a^{\mathsf{T}}S(t_a)z_a$, which is the value of the performance index when the dynamical inputs are absent. When $\boldsymbol{u}$ and $\boldsymbol{v}$ are not zero, the effect of the control strategy is to instantaneously minimize the integrand of the first integral in (2-77), which represents the rate of accumulation of J contributed by the control input. However, the rate of accumulation of J contributed by the excitation

input, represented by the last integral in (2-77), cannot be directly altered in an instantaneous sense, since $\boldsymbol{v}$ is externally imposed and the value of z is fixed at the current instant in time.

Some additional comments are now in order. First, although the final time t_b has been regarded as fixed in the analysis, its value is generally unknown. This is because t_a along with t_b are taken to define a segment of time during which the external excitation affects the system to be controlled. But as mentioned before, information concerning the excitation is not available in advance. Thus, it is reasonable to treat the problem simply as if $t_b - t_a \to \infty$. This approach has the added benefit of enabling S to be determined, since the solution for $S(t)$ cannot be obtained from (2-74), even when S_b is specified, if t_b is not known. But the solution in (2-74) reveals that as $t_b - t_a \to \infty$, $S(t) \to \bar{S}$, a steady-state value that is given by

$$\bar{S} = \int_0^\infty e^{\bar{t}A^\mathsf{T}} Q e^{\bar{t}A} \, d\bar{t} \tag{2-78}$$

In practice though, $\bar{S}$ can be more easily evaluated by using its steady-state property in (2-73), requiring it to satisfy a matrix *algebraic Liapunov equation*

$$A^\mathsf{T}\bar{S} + \bar{S}A = -Q \tag{2-79}$$

which may be readily solved for $\bar{S}$ (also, the need to specify S_b is eliminated). Thus, this instantaneous optimal control method depends only on the parameter matrices A, B^u, Q, and possibly R (if the unconstrained control input case is considered).

Of interest is the case for which the control input is unconstrained. In this case, the instantaneous optimal control method yields

$$\boldsymbol{u} = -R^{-1}B^{u\mathsf{T}}\bar{S}z \tag{2-80}$$

In the absence of external excitations, $\dot{V}$ will be negative definite when the value given for $\boldsymbol{u}$ in (2-80) is used, indicating the unforced system will be asymptotically stable under the effect of the control strategy. Incidentally, it is apparent that the control method

method outlined above may alternatively be described as a procedure to minimize the total time derivative of the *augmented* Liapunov function

$$\bar{V}(z,\, t) = V(z,\, t) - \int_t^{t_b} \tfrac{1}{2}\boldsymbol{u}^{\mathsf{T}}(\bar{t})\boldsymbol{R}\boldsymbol{u}(\bar{t})\,d\bar{t} \tag{2-81}$$

along trajectories obeying (2-27), although the geometric interpretation of $\bar{V}(z,\, t)$ is no longer apparent. In addition, there are no explicit restrictions on the particular functional form selected for the integrand in (2-81), other than it is taken to be a positive definite function of $\boldsymbol{u}$. Forms other than the quadratic type used above will generally lead to a nonlinear functional dependence of $\boldsymbol{u}$ upon z, in contrast to (2-80).

2.6 Incremental Optimal Control Methods

In real applications, it may not be feasible to measure or estimate the system state at *every* instant in time, as is required when using an instantaneous optimal control method. Instead, it might be acceptable to determine a suitably optimized value for the control input which may be applied during a short interval in time by using a zero-order hold (*i.e.*, a step function input). This procedure could then be repeated for the next short time interval immediately following the current interval, and by continuing in this manner, the control input is incrementally adjusted for each successive short time interval. This approach is referred to as an *incremental* optimal control method.

Suppose that the entire interval $[t_a,\, t_b]$ is uniformly partitioned into a set of short intervals, and consider some *representative* interval from this set with an initial time t_c and a final time t_d. Again, let $h \equiv t_d - t_c$ be small in comparison to some characteristic time for the linear dynamical system described by (2-27). Define a performance index for the representative interval as

$$\Delta J = \sum_{k=1}^{m-1} c_k \left[\dot{V}_k + \tfrac{1}{2}\boldsymbol{u}^{\mathsf{T}}(t_k)\boldsymbol{R}\boldsymbol{u}(t_k)\right] \tag{2-82}$$

where c_k is an appropriately chosen weighting factor, $\dot{V}_k$ is the value of $\dot{V}$ at time t_k, as given by (2-75), with

$$t_k = t_c + \frac{(k-1)}{(m-1)}h, \;\; t_1 = t_c, \;\; t_m = t_d; \;\; k \in \{1, \ldots, m\} \tag{2-83}$$

and m is an integer. The motivation for selecting a performance index of this form is now explained.

The control strategy associated with an instantaneous optimal control method seeks to minimize an expression of the kind appearing in the summand of (2-82) at every instant in time. Consider the modified objective of seeking to minimize a collection of terms associated with the representative interval, each term being this expression evaluated at a particular time t_k belonging to the short interval $[t_c, t_d]$. So ΔJ is the series obtained by adding together all of the terms in this collection. However, the minimization is accomplished only in an *approximate* sense — the evaluation of the expression at each t_k is *estimated* on the basis of its value at t_c. Thus, the procedure used for the incremental optimal control method consists of a sequence of minimizations at particular points in time (represented by t_c) belonging to the entire interval $[t_a, t_b]$, each minimization effort reflecting an approximate optimization of ΔJ for a particular short interval (represented by $[t_c, t_d]$).

Before proceeding further, it is convenient to let $m \to \infty$, and thereby increase without limit the number of terms in the series forming ΔJ. However, the series will generally diverge unless $c_k \to 0$ as $m \to \infty$. To avoid this difficulty, c_k is set equal to $h/(m-1)$, whereby (2-82) becomes

$$\Delta J = \int_{t_c}^{t_d} \left[\dot{V} + \tfrac{1}{2} \boldsymbol{u}^{\mathsf{T}} R \boldsymbol{u} \right] dt \tag{2-84}$$

As in Section 2.5, the particular form of V considered is

$$V = \tfrac{1}{2} z^{\mathsf{T}} S z \;\; \Rightarrow \;\; \dot{V} = (Sz)^{\mathsf{T}} \dot{z} \tag{2-85}$$

where S is now understood to be time-invariant and specified according to (2-79) (in which Q should be positive definite). Thus, (2-84) becomes

$$\Delta J = \int_{t_c}^{t_d} \left[(Sz)^{\mathsf{T}} \dot{z} + \tfrac{1}{2} \boldsymbol{u}^{\mathsf{T}} R \boldsymbol{u} \right] dt \tag{2-86}$$

As given by (2-86), ΔJ is to be minimized subject to the constraint relation (2-27), and were it not for the fact that the excitation input is presumed unknown beyond the time t_c, the necessary conditions given in (2-11) through (2-14) could be used to obtain an optimal solution for $\boldsymbol{u}$ during the interval $[t_c, t_d]$. The approach adopted to develop an incremental optimal control method is to demand that these necessary conditions be satisfied in an approximate sense, one which is based only upon information available at time t_c.

To this end, it is clear that the value of any dynamic quantity associated with the system at t_d may be expressed in terms of its value and higher order derivatives at t_c by using a Taylor series expansion involving powers of h, for example

$$z(t_d) = z(t_c) + \dot{z}(t_c)(h) + O(h^2) \tag{2-87}$$

and

$$\lambda(t_d) = \lambda(t_c) + \dot{\lambda}(t_c)(h) + O(h^2) \tag{2-88}$$

Since h is fixed and t_c is assumed to be known, t_d will also be fixed, and therefore the last boundary condition in (2-12) is automatically satisfied. In general, $z(t_d)$ is not fixed but will depend upon $\boldsymbol{u}(t_c)$ and $\boldsymbol{v}(t_c)$ — only $\boldsymbol{u}(t_c)$ may be specified. From (2-12), the first boundary condition which should be satisfied in order for the control process to be optimal is

$$\left[\frac{\partial H}{\partial \dot{z}} - \lambda\right]\Bigg|_{t_d} = 0 \tag{2-89}$$

In addition, the first term appearing in (2-89) can be expanded in powers of h to give

$$\frac{\partial H}{\partial \dot{z}}\Bigg|_{t_d} = \frac{\partial H}{\partial \dot{z}}\Bigg|_{t_c} + \frac{d}{dt}\left[\frac{\partial H}{\partial \dot{z}}\right]\Bigg|_{t_c}(h) + O(h^2) \tag{2-90}$$

Evaluating (2-11) at t_c and using relations (2-87) through (2-90), the following equations are obtained after dropping the terms of order $O(h^2)$

$$z(t_d) = z(t_c) + \boldsymbol{g}\big|_{t_c}(h) \tag{2-91}$$

$$\lambda(t_c) = \left.\frac{\partial H}{\partial \dot{z}}\right|_{t_c} + \left.\frac{\partial H}{\partial z}\right|_{t_c} (h) \tag{2-92}$$

$$\left.\frac{\partial H}{\partial \boldsymbol{u}}\right|_{t_c} = 0 \tag{2-93}$$

in the case where the control input is unconstrained. In the case where the control input is constrained to belong to some specified set of admissible functions; $\boldsymbol{u} \in \Omega$, with $\Omega \subset R^r$; (2-14) is evaluated at t_c and (2-93) is replaced by

$$H(\lambda, \dot{z}, z, \boldsymbol{u}, t)\big|_{t_c} \leq H(\lambda, \dot{z}, z, \bar{\boldsymbol{u}}, t)\big|_{t_c}; \quad \forall \bar{\boldsymbol{u}} \in \Omega \tag{2-94}$$

By using the initial condition provided for the system at time t_a, (2-92) is used along with (2-93) or (2-94) to obtain $\lambda(t_c)$ and $\boldsymbol{u}(t_c)$ for the first short time interval. Then, equation (2-91) can be used to integrate the system state to obtain $z(t_d)$. This is subsequently used as the initial condition $z(t_c)$ for the next short time interval, and by continuing in this manner, the process may be repeated for each successive short time interval in the set comprising the entire interval $[t_a, t_b]$.

A knowledge of the external excitation beyond the current instant in time is never needed to determine the control input. This feature obeys the principle of causality, and so the method is suitable for applications involving seismically-excited systems. In actual practice though, (2-91) is not used, and $z(t_d)$ is obtained either by measurement or estimation in the case of physical applications or by a more sophisticated integration scheme than (2-91) in the case of numerical simulations. This algorithm represents a closed-loop control method.

Finally, in the case where the control input is unconstrained, the expression for $\boldsymbol{u}$ obtained from the incremental optimal control method is given by

$$\boldsymbol{u} = -\left[I + hR^{-1}B^{u\mathsf{T}}SB^{u}\right]^{-1} R^{-1}B^{u\mathsf{T}}\left[Sz + hS\left(Az + B^{v}v\right)\right] \tag{2-95}$$

(assuming the indicated inverse exists). Several additional remarks are in order. First, if $B^{u\mathsf{T}}SB^{u}$ is invertible, then it can be shown (see Appendix B) that

$$\left[I + hR^{-1}B^{u\mathsf{T}}SB^{u}\right]^{-1} = I - hR^{-1}B^{u\mathsf{T}}SB^{u} + O(h^2) \tag{2-96}$$

In the analysis that lead to (2-95), the terms of order $O(h^2)$ were ignored. If this same level of approximation is maintained, then (2-95) becomes

$$\boldsymbol{u} = -R^{-1}B^{u\mathsf{T}}\left\{\left[I - hSB^{u}R^{-1}B^{u\mathsf{T}}\right]Sz + hS\left(Az + B^{v}v\right)\right\} \tag{2-97}$$

Also, it is observed that as $h \to 0$, the result given in (2-97) approaches the result given in (2-80), which was obtained by using the instantaneous optimal control method. This sort of behavior for $\boldsymbol{u}$ is both reasonable and expected.

Dynamic Controllers

At all stages in the foregoing development, it has been assumed that, other than the requirement for piecewise continuity, the control input may be arbitrarily prescribed to instantaneously become any member belonging to Ω. This assumption corresponds to the idealization of a *nondynamic* (sometimes referred to as *inertialess*) controller, where the value of $\boldsymbol{u}$ can jump from one point to another in Ω. Such an assumption is justified if the "level" of control input is not excessive and the dynamic response of the controlled system varies slowly in comparison to the dynamic response of the physical controller — which depends upon the amount of time required for sensing, processing, and sending signals, along with that necessary for the actuators to mechanically respond.

A variation on the previous results obtained by using incremental optimal control methods is now presented for cases in which the dynamics of the controller are to be explicitly taken into account. Only the case for which the control input is unconstrained (*i.e.*, $\Omega \equiv R^r$) will be considered. This extension is based upon a discussion in [15].

Consider again a linear dynamical system governed by (2-27). Suppose that the performance index is now selected to have the form

$$\Delta J = \int_{t_c}^{t_d}\left[(Sz)^{\mathsf{T}}\dot{z} + \tfrac{1}{2}\dot{\boldsymbol{u}}^{\mathsf{T}}\hat{R}\dot{\boldsymbol{u}} + \tfrac{1}{2}\boldsymbol{u}^{\mathsf{T}}R\boldsymbol{u}\right]dt \tag{2-98}$$

which assigns a direct penalty on the "size" of $\dot{\boldsymbol{u}}$ and thereby limits the extent of dynamic performance expected from the physical controller. Also, assume that the control input obeys a dynamical relation of the form

$$\dot{\boldsymbol{u}} = \boldsymbol{h}(\boldsymbol{u}, \boldsymbol{z}, \boldsymbol{c}) \tag{2-99}$$

where $\boldsymbol{c}$ is a vector of appropriate dimension whose components represent a set of control variables which may be directly specified. It is assumed *a priori* that (2-99) may be inverted to obtain a functional relationship for $\boldsymbol{c}$, expressible as

$$\boldsymbol{c} = \hat{\boldsymbol{h}}(\dot{\boldsymbol{u}}, \boldsymbol{u}, \boldsymbol{z}) \tag{2-100}$$

Furthermore, assume that the initial values of the system state $\boldsymbol{z}(t_c)$ and control input $\boldsymbol{u}(t_c)$ are known. Next, define the new vector variables

$$\hat{\boldsymbol{z}} \equiv \begin{Bmatrix} \boldsymbol{z} \\ \boldsymbol{u} \end{Bmatrix}, \quad \hat{\boldsymbol{u}} \equiv \dot{\boldsymbol{u}}, \quad \hat{\boldsymbol{v}} \equiv \boldsymbol{v}; \quad \hat{\boldsymbol{z}}(t_c) = \begin{Bmatrix} \boldsymbol{z}(t_c) \\ \boldsymbol{u}(t_c) \end{Bmatrix} \tag{2-101}$$

Then, (2-27) and (2-98) can be recast in terms of these quantities as

$$\dot{\hat{\boldsymbol{z}}} = \hat{\boldsymbol{A}}\hat{\boldsymbol{z}} + \hat{\boldsymbol{B}}^{u}\hat{\boldsymbol{u}} + \hat{\boldsymbol{B}}^{v}\hat{\boldsymbol{v}} \tag{2-102}$$

and

$$\Delta J = \int_{t_c}^{t_d} \left[\left(\hat{\boldsymbol{S}}\hat{\boldsymbol{z}} \right)^{\mathsf{T}} \dot{\hat{\boldsymbol{z}}} + \tfrac{1}{2}\hat{\boldsymbol{u}}^{\mathsf{T}}\hat{\boldsymbol{R}}\hat{\boldsymbol{u}} \right] dt \tag{2-103}$$

where the new parameter matrices are given by

$$\hat{\boldsymbol{A}} = \begin{bmatrix} \boldsymbol{A} & \boldsymbol{B}^{u} \\ \boldsymbol{0} & \boldsymbol{0} \end{bmatrix}, \quad \hat{\boldsymbol{B}}^{u} = \begin{bmatrix} \boldsymbol{0} \\ \boldsymbol{I} \end{bmatrix}, \quad \hat{\boldsymbol{B}}^{v} = \boldsymbol{B}^{v}, \quad \hat{\boldsymbol{S}} = \begin{bmatrix} \boldsymbol{S} & \boldsymbol{0} \\ \boldsymbol{0} & \boldsymbol{R} \end{bmatrix} \tag{2-104}$$

The augmented system governed by the dynamical equation in (2-102) and the performance index as expressed in (2-103) are now in a form suitable for application of the incremental optimal control method outlined above. Applying a zero-order hold on $\hat{\boldsymbol{u}}$ (*i.e.*, $\hat{\boldsymbol{u}}$ is a step function) for the augmented system, which has a nondynamic controller, carries over to applying a first-order hold on $\boldsymbol{u}$ (*i.e.*, $\boldsymbol{u}$ is a ramp function) for the original system, obeying the dynamical expression

$$\boldsymbol{u}(t) = \boldsymbol{u}(t_c) + \hat{\boldsymbol{u}}(t_c)(t - t_c); \quad t_c \le t \le t_d \tag{2-105}$$

where $\hat{\boldsymbol{u}}(t_c)$ is evaluated from (2-97) by replacing R by $\hat{R}$, S by $\hat{S}$, *etc.* Also, if the same level of approximation is maintained as was used in the foregoing analysis, then

$$z(t) = z(t_c) + g(t_c)(t - t_c); \quad t_c \le t \le t_d \tag{2-106}$$

where $g(t_c)$ is evaluated from the right-hand side of (2-27). Hence, (2-100) becomes

$$c(t) = \hat{h}(\hat{u}(t_c), u(t), z(t)); \quad t_c \le t \le t_d \tag{2-107}$$

Thus, the specifications for the operation of the dynamic controller according to the incremental optimal control method are complete.

2.7 Summary

The material introduced and developed in this chapter has focused on linear time-invariant dynamical systems described by a discrete set of state variables. It was shown that the equations of motion for the structural systems of interest may be expressed in terms of such variables. Definitions were given for an optimal control process, and a standard optimal control problem known as the linear quadratic regulator (LQR) was formulated and solved for both the externally-forced and unforced cases. It was pointed out that the solution for the externally-forced case is only possible when the excitation is *a priori* known. Thus, other control approaches must be considered for applications that involve seismic excitations or any physical phenomenon for which a complete excitation record is not available in advance.

This state of affairs motivated the development of instantaneous and incremental optimal control methods as alternatives for coping with the difficulties which arise when the external excitation is unpredictable. It is believed that some of the results obtained might prove effective in the response control of structural systems subjected to seismic excitations.

The developments presented in this chapter are not immediately applicable to the proposed control method discussed in Chapter 1, which is based upon a semi-active control approach. However, it is hoped that these results will be useful for further studies in the field of structural control, specifically, those utilizing fully-active control systems.

References for Chapter 2

1. R. E. Kalman, "Mathematical Description of Linear Dynamical Systems," *Jour. of SIAM*, Ser. A: Control, Vol. 1, No. 2, 1963, pp. 152–192.
2. K. Ogata, *State Space Analysis of Control Systems*, Series in Instrumentation and Controls, Englewood Cliffs, N.J.: Prentice-Hall, Inc., 1967, Chap. 1 and 4.
3. L. K. Timothy and B. E. Bona, *State Space Analysis: An Introduction*, Series in Electronic Systems, New York: McGraw-Hill, Inc., 1968, Chap. 1 and 4.
4. I. M. Gelfand and S. V. Fomin, *Calculus of Variations*, trans. and ed. by R. A. Silverman, Englewood Cliffs, N.J.: Prentice-Hall, Inc., 1963, Appx. B.
5. L. S. Pontryagin, V. G. Boltyanskii, R. V. Gamkrelidze, and E. F. Mishchenko, *The Mathematical Theory of Optimal Processes*, trans. by K. N. Trirogoff and ed. by L. W. Neustadt, New York: John Wiley and Sons, Inc., 1962, Chap. 1–2.
6. A. E. Bryson and Y.-C. Ho, *Applied Optimal Control*, Waltham, Mass.: Ginn and Co. (Publishers), 1969, Chap. 5.
7. R. E. Kalman, "Contributions to the Theory of Optimal Control," *Boletin de la Sociedad Matematica Mexicana*, Vol. 5, Part 2, No. 1, Apr. 1960, pp. 102–119.
8. B. D. O. Anderson and J. B. Moore, *Linear Optimal Control*, Network Series, Englewood Cliffs, N.J.: Prentice-Hall, Inc., 1971, Chap. 3.
9. J. N. Yang, A. Akbarpour, and P. Ghaemmaghami, "New Optimal Control Algorithms for Structural Control," *Jour. of Engrg. Mech.*, Vol. 113, No. 9, Sep. 1987, pp. 1369–1386.
10. R. E. Kalman and J. E. Bertram, "Control System Analysis and Design via the Second Method of Lyapunov, Part I: Continuous-Time Systems," *Jour. of Basic Engrg., Trans. of ASME*, Vol. 82, Ser. D, No. 2, June 1960, pp. 371–393.
11. D. G. Schultz and J. L. Melsa, *State Functions and Linear Control Systems*, Series in Electronic Systems, New York: McGraw-Hill, Inc., 1967, Chap. 7.
12. J. LaSalle and S. Lefschetz, *Stability by Liapunov's Direct Method With Applications*, Mathematics in Science and Engineering Series, New York: Academic Press, Inc., 1961, Chap. 3.
13. J. L. Casti, *Dynamical Systems and Their Applications — Linear Theory*,

Mathematics in Science and Engineering Series, New York: Academic Press, Inc., 1977, Chap. 8.

14. N. N. Krasovskii, *Stability of Motion — Applications of Lyapunov's Second Method to Differential Systems and Equations With Delay*, trans. and ed. by J. L. Brenner, Stanford: Stanford University Press, 1963, Chap. 3.

15. B. D. O. Anderson and J. B. Moore, *Linear Optimal Control*, Network Series, Englewood Cliffs, N.J.: Prentice-Hall, Inc., 1971, Chap. 10.

Chapter 3

Response Control of Linear SDOF Systems Using Active Interface Damping

3.1 Introduction

When investigating the application of new technological principles and methods to physical systems of interest, it is usually advantageous to begin by considering simple idealizations of the actual systems. Thus, the present study focuses on two interacting SDOF systems that are subjected to base acceleration, the source of which is seismically-generated horizontal ground motion. One of these systems is designated the primary system and the other is referred to as the auxiliary system. The two SDOF systems are understood to be models for either two interacting structures or a single structure and a control device which facilitates interaction of the structure with its base.

The control objective is to reduce the resonance buildup in the response of the primary system that is produced by an external excitation. The strategy employed to achieve this objective is to remove energy associated with relative vibration from the primary system through interaction with the auxiliary system. A control algorithm is used to determine when interactions between the systems should occur. Interactions are permitted only when their anticipated effect is favorable to the control strategy. The interactions consist of reaction forces that are developed within and transmitted through a single interaction element that is located between the systems. The mechanical properties of this interaction element can be altered in real time by a control signal and are discussed later for each of the control cases considered.

Since the control objective is concerned with the response of the primary system, it becomes necessary to specify those aspects of the system behavior that are to be controlled. Typical response features of interest for an actual structure are the relative

displacements of certain points on the structure from their equilibrium positions, as well as the absolute accelerations of these points. In the present study, the control effort is directed at reducing the relative displacements which are caused by the excitation. The stresses induced in the structure are directly proportional to these displacements when deformations are within the linear-elastic range of the material comprising the structure.

3.2 Problem Formulation

The following conditions are assumed to hold in this study: 1) the primary system and the auxiliary system are subjected to the same base acceleration and respond linearly; 2) the interaction element functions passively, is considered to be massless, and responds instantaneously to control signals (*i.e.*, its mechanical properties may be instantaneously altered); 3) the system states are completely observable, and all system parameters have been identified in advance; and 4) only current values of the base acceleration and system state variables are available to determine the control input.

Under these conditions, the equations of motion for the primary and auxiliary systems are expressible as

$$\ddot{x}_i + 2\zeta_i\omega_i\dot{x}_i + \omega_i^2 x_i = \bar{f}_i - \ddot{y} \tag{3-1}$$

where $i \in \{1,\ 2\}$, with the parameter definitions

$$\omega_i \equiv \sqrt{\frac{k_i}{m_i}},\quad \zeta_i \equiv \frac{c_i}{2\sqrt{m_i k_i}},\quad \bar{f}_i \equiv \frac{f_i}{m_i} \tag{3-2}$$

where m_i, k_i, c_i, and x_i represent the mass, stiffness, damping, and relative displacement (as measured from the base) of the ith system. f_i is the control force applied to the ith system by the interaction element, and y is the absolute displacement of the base of each system. The subscripts 1 and 2 are used to denote the primary and auxiliary systems, respectively. For the purposes of later discussion, let u be the reaction force developed within the interaction element, which is subsequently referred to as the *control input*, and let $v \equiv \ddot{y}$, which is subsequently referred to as the *excitation input*. u is assumed to be

positive when the interaction element is in tension. Because the element is treated to be massless, a relationship exists between the control force acting on the ith system and the control input, which is given by

$$f_i = -l_i u \tag{3-3}$$

where $l_1 = 1 = -l_2$ for the assumed configuration of the systems. A schematic illustration of the systems is provided in Figure 3.1.

Occasionally, it is convenient to recast (3-1) into the modified form

$$\dot{z}_i = A_i z_i + \boldsymbol{b}_i^u u + \boldsymbol{b}^v v \tag{3-4}$$

where

$$z_i \equiv \begin{Bmatrix} x_i \\ \dot{x}_i \end{Bmatrix}; \quad A_i = \begin{bmatrix} 0 & 1 \\ -\omega_i^2 & -2\zeta_i\omega_i \end{bmatrix}, \quad \boldsymbol{b}_i^u = \begin{Bmatrix} 0 \\ -l_i/m_i \end{Bmatrix}, \quad \boldsymbol{b}^v = \begin{Bmatrix} 0 \\ -1 \end{Bmatrix} \tag{3-5}$$

The equations represented by (3-4) are the *state space* form for the equations represented by (3-1). It is evident that both u and v are *dynamical inputs* to the equations governing the systems. The scalar pair $(x_i, \dot{x}_i)$, which comprise the vector z_i, is referred to as the *state* of the ith dynamical system. The state of a dynamical system is an embodiment of the minimum amount of information at a particular point in time which, along with the equation governing the dynamic behavior of the system, is sufficient to determine the state of the system at all future points in time. Loosely speaking, the state of a system consists of a certain set of defining conditions associated with that system.

3.3 Control Strategy

In much of modern control theory, the framework used to formulate problems is founded upon the assumption that the control input may be arbitrarily prescribed and, hence, no explicit restrictions regarding admissibility of a control input need be taken into account during the solution procedure. In contrast though, the control approach under investigation here utilizes control forces which are reactive in nature and, thus, cannot be

arbitrarily prescribed. However, the objective of the control effort for the applications of interest is response stabilization or reduction rather than more sophisticated goals, such as regulation or tracking, in which a precise type of behavior is desired for the controlled system. This simple control objective renders the proposed control approach extremely attractive, especially in view of the following feature: successful operation of the control system may be ensured without the demand for a significant supply of external power.

Due to its inherent simplicity and accompanying restrictions on admissible control forces, the proposed control approach is only capable of directly controlling dynamical quantities that are more primitive than the state. Of particular interest is a type of energy associated with the controlled system. As indicated above, the control input is related to the control forces which enter directly into the equations of motion. But the energy of a system is related to a first integral of the equation of motion for that system. Hence, by differentiating an appropriate expression for the energy of the system, the rate at which this energy changes is directly related to the control input. Furthermore, it is shown below that this energy is a positive definite function of the system state. Thus, if the system energy can be limited in some fashion, then the system state is bounded. In turn, each of the components of the system state is bounded. This logic constitutes the control strategy proposed below.

Consider some time interval $[t_a, t_b]$ during which control of the primary system is to be accomplished (*e.g.*, the duration of the external excitation). The *relative vibrational energy* of the primary system, E_1, is defined as

$$E_1 \equiv \tfrac{1}{2} m_1 \dot{x}_1^2 + \tfrac{1}{2} k_1 x_1^2 \tag{3-6}$$

or, in terms of the system state,

$$E_1 = \tfrac{1}{2} z_1^{\mathsf{T}} S_1 z_1; \;\; S_1 = \begin{bmatrix} k_1 & 0 \\ 0 & m_1 \end{bmatrix} = \begin{bmatrix} m_1 & 0 \\ 0 & m_1 \end{bmatrix} \begin{bmatrix} \omega_1^2 & 0 \\ 0 & 1 \end{bmatrix} \tag{3-7}$$

The response control objective is to reduce the *maximum absolute value* of the primary system *relative displacement*, $|x_1|_{max}$, that occurs during this interval of time. Since

$\frac{1}{2}m_1\dot{x}_1^2 \geq 0$ at any instant in time, a least upper bound for $|x_1|$, denoted by $|x_1|_{sup}$, can be established at every instant in time. The greatest of these upper bounds then serves as a bound for $|x_1|_{max}$, that is

$$|x_1| \leq |x_1|_{sup}, \quad \forall t \in [t_a, t_b]; \quad |x_1|_{sup} \equiv \sqrt{\frac{2E_1}{m_1\omega_1^2}} \tag{3-8}$$

in which case

$$|x_1|_{max} \leq \max_{t_a \leq t \leq t_b} |x_1|_{sup} \tag{3-9}$$

Thus, E_1 provides a measure which bounds $|x_1|$ at every instant in time. Hence, $|x_1|_{max}$ may be controlled by controlling E_1 during the time interval $[t_a, t_b]$.

When $u = u(t)$ and $v = v(t)$ are prescribed $\forall t \in [t_a, t_b]$, the state of the primary system evolves according to (3-4) along a definite dynamical path in the state space, $z_1 = z_1(t)$, which then determines $E_1 = E_1(t)$. The control strategy is to remove relative vibrational energy from the system to the extent allowed by the constraints on the control input values, and thereby drive E_1 as close to zero as possible at all intermediate times t. Since v is seismically generated, and therefore unpredictable, the values of u used to construct any portion of such a path during a time interval $[t_a, \bar{t}]$ must not depend upon any values of v for $t > \bar{t}$.

A control process which produces a succession of system states that should approximate the desired dynamical path is proposed as follows: First, let $[t_a, t_b]$ be uniformly partitioned into a set of suitably short time intervals, each of duration h and referred to as a *control algorithm sampling period.* Next, consider a representative short time interval, the kth sampling period, defined by $t_k \leq t \leq t_k + h$. At time t_k, v and z_1 are measured or estimated. A control processor then uses this information to ascertain an appropriate operating state for the interaction element: *activated* or *deactivated.* In the activated state, interactions between the systems are enabled. In the deactivated state, interactions between the systems are disabled. This determination may initiate a switching event by which changes in the mechanical properties of the interaction element

are accomplished. These mechanical properties dictate the physical nature of the interactions and subsequently the control input values used for the sampling period duration. Interactions are permitted during the kth sampling period only when their anticipated effect is favorable to the control strategy. The system then responds to the values of u resulting from these interactions until the beginning of the $(k+1)$th sampling period is reached, when an appropriate operating state is determined again. This procedure is repeated for each successive sampling period.

For the purposes of both implementing the control strategy and formulating control algorithms, efforts are directed toward minimizing the change in E_1 for the representative sampling period, denoted as ΔE_1^k, or even causing this change to be as negative as possible. By differentiating (3-6) and using (3-1), $\dot{E}_1$ may be evaluated as

$$\dot{E}_1 = m_1\left(\ddot{x}_1 + \omega_1^2 x_1\right)\dot{x}_1 = \left[f_1 - m_1\left(\ddot{y} + 2\zeta_1\omega_1\dot{x}_1\right)\right]\dot{x}_1 \tag{3-10}$$

which then yields

$$\Delta E_1^k = \int_{t_k}^{t_k+h}\left[f_1 - m_1\left(\ddot{y} + 2\zeta_1\omega_1\dot{x}_1\right)\right]\dot{x}_1\,dt \tag{3-11}$$

Two methods are considered to achieve this goal. For each of these methods, let $f_1(t)$ be the functional form for f_1, the value of the control force applied to the primary system by the interaction element. Such a form depends upon the type of interaction element used and its current operating state (*i.e.*, activated or deactivated).

Method 1:

Let $f_1(t)$ be the functional form for a *finite* control force resulting from continuous operation of the interaction element during the sampling period. It is assumed that the interaction element remains in one of its admissible operating states for the entire sampling period. Using (3-11), and assuming further that $f_1(t)$ is a continuous function of t, a series expansion may be obtained for ΔE_1^k as

$$\Delta E_1^k = \left[f_1(t)\dot{x}_1\right]\Big|_{t_k}(h) - m_1\left[\left(\ddot{y} + 2\zeta_1\omega_1\dot{x}_1\right)\dot{x}_1\right]\Big|_{t_k}(h) + O(h^2) \tag{3-12}$$

If the sampling period is small in comparison to some characteristic time for the primary system, the terms of order $O(h^2)$ may effectively be ignored. In addition, the quantities multiplying h in the second term of (3-12) are fixed irrespective of the operating state selected for the interaction element. Thus, the contribution of this term to ΔE_1^k cannot be changed. Hence, to the degree of approximation considered, the difference in values for ΔE_1^k obtained by selecting different operating states depends solely on the first term in (3-12).

If the value of $f_1(t) = -l_1 u(t)$ at t_k, corresponding to the activated state, yields a negative value for the first term in (3-12), then the resulting value for ΔE_1^k will be less than the value obtained by using $f_1(t) = 0$, corresponding to the deactivated state.

Method 2:

Let $f_1(t)$ be the functional form for a *pulse-like* control force that is localized to the time t_k. Such a control force could be produced by a sudden impact between the systems occurring at the beginning of the sampling period. To idealize this phenomenon, suppose that $f_1(t) = I_1(t_k)\delta(t - t_k)$, where $I_1(t_k)$ is the impulse imparted to the primary system as a result of the impact, and $\delta(t - t_k)$ is a *Dirac delta function*. Using (3-11), and by again considering a series expansion for $\Delta E_{1,k}$, it may be shown that

$$\Delta E_{1,k} = \tfrac{1}{2}\left[\dot{x}_1(t_k^+) + \dot{x}_1(t_k^-)\right] I_1(t_k) - m_1\left[\left(\ddot{y} + 2\zeta_1\omega_1\dot{x}_1\right)\dot{x}_1\right]\Big|_{t_k^+}(h) + O(h^2) \qquad (3\text{-}13)$$

where the symbols – and + denote times immediately before and after the impulsive interaction, which is modelled to happen instantaneously. If a sudden impact is initiated at time t_k such that the first term in (3-13) is sufficiently negative, then E_1 will decrease immediately following time t_k and the resulting value of ΔE_1^k for the controlled system will be less than that for the uncontrolled system. In contrast to Method 1, some of the quantities multiplying h in the second term of (3-13) (*i.e.*, $\dot{x}_1$) may change if such an impulsive interaction occurs.

3.4 Interaction Elements

In order to facilitate the implementation of the control strategy by the two methods discussed in the previous section, several interaction elements are considered. For the control cases which utilize Method 1, three types of interaction elements are separately used to examine the effectiveness of the control approach. Each of these elements may be described as *nondynamic* and *memoryless* (these qualifiers are discussed in more detail in Chapter 4). The first type consists of a member that is capable of providing a rigid connection between the two systems when activated. In the case for which the auxiliary system consists of a linear elastic element, it is assumed that, upon deactivation, the interaction element may be instantaneously slipped to reduce the reaction force to zero. The second type consists of a member that is capable of providing a viscously-damped reaction force between the two systems when activated. The third type consists of a member that is capable of providing a Coulomb-damped reaction force between the two systems when activated. For each type of interaction element, the activated state corresponds to the enabling or presence of an interaction between the systems, while the deactivated state corresponds to the disabling or absence of an interaction between the systems. The relation between the reaction force and the primary and auxiliary system displacements and their derivatives is given below for each type of interaction element in the activated operating state:

- Rigidly-Connected / Instantaneously-Slipped Member

$$u = \tfrac{1}{2} m_1 \left[(\beta - 1)\ddot{x}_1 + 2(\gamma - 1)\zeta_1 \omega_1 \dot{x}_1 + \omega_1^2 (\alpha x_2 - x_1) + (\beta - 1)\ddot{y} \right] \tag{3-14}$$

($\ddot{x}_1$ must be obtained iteratively from the equation of motion for the primary system, since that equation is expressed in terms of u.)

- Viscously-Damped Member

$$u = 2 m_1 \delta \zeta_1 \omega_1 (\dot{x}_1 - \dot{x}_2); \quad \delta \equiv \frac{c_{int}}{c_1} \tag{3-15}$$

- Coulomb-Damped Member
  - $\dot{x}_2 \neq \dot{x}_1$ (slipping phase)

$$u = m_1 \varepsilon_s g_o \operatorname{sgn}(\dot{x}_1 - \dot{x}_2); \quad \varepsilon_s \equiv \frac{f_s}{m_1 g_o} \tag{3-16}$$

- $\dot{x}_2 = \dot{x}_1$ (sticking phase)

$$u = m_1 \varepsilon_s g_o \operatorname{sgn}(u_{rig}) \ , \ |u_{rig}| > m_1 \varepsilon_s g_o \tag{3-17}$$

$$u = u_{rig} \ , \ |u_{rig}| \leq m_1 \varepsilon_s g_o$$

(u_{rig} is the value of u as given by (3-14). f_s is the slip force level normally associated with a stick-slip element.)

The parameters α, β, and γ are defined in the next section. Each of these element types is schematically illustrated in Figure 3.3. The configuration of the primary and auxiliary systems is indicated in Figure 3.3. The systems are shown to be connected by a generic interaction element, which could represent any one of the three types discussed above.

It is not necessary to specify the precise physical nature of the interaction element for the control cases which utilize Method 2 since the activation-deactivation process is modelled to happen instantaneously. However, the phenomenon is assumed to be equivalent to a perfectly-plastic impact between the two systems. The energy changes associated with this process could be effected, for example, either by rapid conversion of mechanical energy to thermal energy within the interaction element or through deformation of some of the material comprising the interaction element. The pertinent quantities associated with this process are the impulse transferred to and the final velocity acquired by the primary system immediately following the impact. These quantities are given below for an instantaneous interaction assumed to occur at time t_k:

- Impulsively-Generated Perfectly-Plastic Impact

$$I_1(t_k) = \frac{m_1 \beta}{\beta + 1}\left[\dot{x}_2(t_k^-) - \dot{x}_1(t_k^-)\right], \quad \dot{x}_1(t_k^+) = \frac{1}{\beta + 1}\left[\beta \dot{x}_2(t_k^-) + \dot{x}_1(t_k^-)\right] \tag{3-18}$$

3.5 Numerical Study

A deterministic analysis is conducted through numerical simulations. An explicit Runge-Kutta method with fourth-order truncation error is employed to numerically

integrate the equations given in (3-1). The numerical simulations are performed for a series of control cases using horizontal ground accelerations from an ensemble of earthquake time histories as excitation input. This ensemble is comprised of the 1940 Imperial Valley (El Centro) S00E, 1952 Kern County (Taft Lincoln School Tunnel) S69E, and 1971 San Fernando (Holiday Inn) N00W earthquake records. Subsequently, these earthquake records are denoted herein by the symbols ELC, TAF, and HOL, respectively, following the convention used in [1].

The accelerograms from these events were normalized to an effective peak ground acceleration of $0.40g$ according to the procedure described in [1]. Each of the recorded acceleration values was divided by a characteristic acceleration value computed for that particular event and then multiplied by $0.40g$. The purpose of this scaling operation was to reduce the statistical variance of the peak response of a SDOF oscillator subjected to each of the excitation records; it is meant to produce equal spectral intensities. The normalized accelerograms are shown in Figure 3.4, and the amplitudes of the Fourier Spectra for these records are shown in Figure 3.5. In contrast to one another, these records exhibit and possess very different time-domain behavior and frequency-domain content. They have been thoroughly analyzed and are widely accepted for use as excitation input to simulate the response of structural systems to the strong ground motion brought about by seismic disturbances.

For prescribed u and v, the dynamical behavior of the primary system is fully characterized by specifying the fraction of critical damping ζ_1 and the undamped natural frequency $\omega_1/2\pi$. In all of the control cases examined in this study, $\zeta_1 = 0.02$. Values ranging between 0.10 and 10.0 Hz are used for $\omega_1/2\pi$ to construct response spectra. In turn, the dynamical behavior of the auxiliary system is fully characterized by specifying the dimensionless parameters

$$\alpha \equiv \frac{k_2}{k_1}, \quad \beta \equiv \frac{m_2}{m_1}, \quad \gamma \equiv \frac{c_2}{c_1} \tag{3-19}$$

which, when inserted into (3-2) and used with (3-3), yield

$$\omega_2 = \sqrt{\frac{\alpha}{\beta}}\,\omega_1, \quad \zeta_2 = \frac{\gamma}{\sqrt{\alpha\beta}}\zeta_1, \quad \bar{f}_2 = -\frac{1}{\beta}\bar{f}_1 \tag{3-20}$$

In the case of $i = 2$, (3-20) permits an alternative expression for (3-1)

$$\beta\,\ddot{x}_2 + 2\,\gamma\,\zeta_1\omega_1\dot{x}_2 + \alpha\,\omega_1^2 x_2 = -\bar{f}_1 - \beta\,\ddot{y} \tag{3-21}$$

It is convenient to group the control cases to be examined into nine *control categories*, which are distinguished by the method of control strategy implementation, the number of possible operating states for the interaction element, the physical nature of the interactions (which corresponds to the type of interaction element used), and the values considered for the parameters that characterize the dynamical behavior of the auxiliary system. A listing of these control categories is provided in Table 3.1. For most of them, the interaction element has the capability to function in either one of two operating states. However, this capability is restricted by the additional limitation that the element may be activated or deactivated only at the beginning of a sampling period, and that it must remain in the selected operating state for the duration of the sampling period. For all of these control cases, a fundamental criterion which is based upon the control strategy is used in the determination of the appropriate operating state. This criterion is discussed in the next section.

For the cases in Categories 1 through 5, the interaction element is capable of two operating states: an activated state and a deactivated state. In Categories 1 through 3, the first type of interaction element described is used, which provides a rigid connection between the systems when activated and provides no interaction between the systems when deactivated. In Categories 4 and 5, an interaction element which is capable of producing an instantaneous effect that results in a perfectly-plastic impact between the systems is used (*e.g.*, some kind of robust impact damper which reduces the relative velocity between the systems to zero in an instant of time).

In Categories 6 and 7, the second type of interaction element described is used,

which provides a viscously-damped interaction between the systems when activated. In Categories 8 and 9, the third type of interaction element described is used, which provides a Coulomb-damped interaction between the systems when activated. However, for the cases in Categories 7 and 9, the interaction element possesses only a single operating state (the activated state), whereas for the cases in Categories 6 and 8, the interaction element is capable of two operating states (the activated and deactivated states).

The cases in Category 1 involve an auxiliary system that consists only of a linear elastic element. As the interaction element is deactivated, it is assumed that the rigid connecting member may be instantaneously slipped in a manner by which the strain energy stored in the auxiliary system is suddenly dissipated. The mechanism for this dissipation depends upon the actual hardware used to produce the interaction but could be achieved by the viscosity of a working fluid or sliding friction at a solid-solid interface. Now, let $\dot{U}_1$ be defined as the rate at which potential energy is stored in the elastic element of the primary system (or, $U_1 \equiv \frac{1}{2}k_1x_1^2$; $\dot{U}_1 = k_1\dot{x}_1x_1$, $k_1 > 0$). For exactly half of the cases considered in this category, interactions are prohibited whenever $\dot{U}_1 < 0$, whereas interactions are permitted for any value of $\dot{U}_1$ (but will occur only as directed by the control algorithm) in the remaining cases. *Note:* Special reasons exist for choosing to consider these two particular sets of cases, and these reasons are discussed in the last section of this chapter.

In addition to the fundamental criterion, which is used to determine whether or not an interaction may be initiated and/or maintained, the cases in Categories 2 and 3 utilize another criterion to determine whether or not an interaction may be initiated (from a deactivated operating state). This additional criterion is necessary because impulsive forces will generally develop between the systems at the moment when an interaction commences if the velocities of the systems are dissimilar and both systems possess mass. The criterion requires the relative velocity between the systems to be nearly zero in order

to initiate an interaction, as explained in the next section. It is recognized that such a criterion is unnecessary for the cases in Category 1 because the auxiliary system is treated to be massless in those cases (*i.e.*, $\beta = 0$).

For the cases in Categories 4 and 5, the interactions occur impulsively at strategic instants in time through an *attachment-and-release process*. During such a process, the systems are forced by means of a perfectly-plastic impact to instantaneously attach to each other so that they acquire the same velocity, as described earlier. The connection created is then immediately terminated, allowing the systems to move independently for the duration of the sampling period. Such interactions generally occur intermittently.

Regarding the cases in Categories 8 and 9, an effective damping coefficient, c_{eff}, may be obtained for a Coulomb damper by considering a linear viscous damper with actual damping coefficient c_{eff} and requiring each element to dissipate the same amount of energy per cycle when subjected to a sinusoidal deformation process of amplitude A and frequency ω. This method of equivalent damping is discussed in [2] and leads to a relation between the slip force level f_s of the Coulomb damper and the effective damping coefficient c_{eff}, given by

$$f_s = \frac{\pi}{4} c_{eff}\, \omega A \tag{3-22}$$

For the purposes of comparison, the values used for the parameter ε_s associated with the cases in Categories 8 and 9 are selected by requiring the values of c_{eff} to match the values of c_{int} used for the corresponding cases in Categories 6 and 7. By assuming that $A = |x_1|_{max}$ and $\omega = \omega_1$, and using the defining expressions for δ and ε_s in (3-15) and (3-16), (3-22) becomes

$$\varepsilon_s = \frac{\pi}{2 g_o} \delta \zeta_1 \omega_1 \left[\omega_1 |x_1|_{max}\right] \tag{3-23}$$

It is recognized that the last term in (3-23) is the *pseudo-velocity* of the primary system response. Several intermediate values were obtained for this quantity from the response of the *uncontrolled* primary system (for given values of δ and ω_1) when subjected to

each of the excitation records. These intermediate values were then averaged over the excitation records to obtain a final value for each combination of δ and ω_1. This final value is used in (3-23) to determine ε_s for the cases involving the *controlled* primary system. The range of values used for ε_s for the cases in Categories 8 and 9 are reflected in Table 3.1 by the effective values used for δ to compute ε_s according to (3-23).

The sets of parameter values used to characterize the auxiliary system and some of the particular features associated with specific control cases are listed in Tables 3.2 through 3.7. The values considered for the parameters indicated in Tables 3.2, 3.3, 3.4, 3.5, 3.6, and 3.7 are used for the cases belonging to Categories 1, 2, 3, 4, 5, and 6 through 9, respectively.

3.6 Control Algorithms

Before discussing control algorithms in detail, it is necessary to call attention to some matters concerning the additional criterion that is used to determine whether or not an interaction may be initiated for the cases in Categories 2 and 3. These matters are related to some of the principles involved in the control algorithm used for cases in Categories 4 and 5, and so it is prudent to discuss them now.

Attachment Criterion

For the cases in Categories 2 and 3, the purpose of the interaction is to transfer energy from the primary system to the auxiliary system without dissipating any energy within the interaction element, which consists of a rigidly connected member when activated. In order for such an interaction to commence, it is necessary for the velocities of the two systems to be brought into coincidence; this process is referred to as an *attachment* and is modelled to happen instantaneously. Since the velocities of the systems are generally dissimilar before an interaction commences, and because each system typically has mass associated with it, an impulsive force is required during the attachment process to cause the systems to acquire the same velocity, $\dot{x}_2(t_k^+) = \dot{x}_1(t_k^+)$. As

indicated below, this process always results in a loss of the combined relative energy of the two systems. It can be shown that the change in the combined relative energy of the systems associated with the attachment process, assumed to occur at time t_k, is given by

$$\Delta E_{tot}(t_k) \equiv \Delta\left[E_1(t_k) + E_2(t_k)\right] = -\frac{1}{2}\frac{m_1\beta}{\beta+1}\left[\dot{x}_1(t_k^-) - \dot{x}_2(t_k^-)\right]^2 \tag{3-24}$$

while the accompanying change in relative energy of the primary system is given by

$$\Delta E_1(t_k) = -\frac{1}{2}\frac{m_1\beta}{\beta+1}\left[\dot{x}_1(t_k^-) - \dot{x}_2(t_k^-)\right]\left[\dot{x}_1(t_k^-) + \dot{x}_1(t_k^+)\right] \tag{3-25}$$

In all of the control cases other than those in Categories 4 and 5, the intention of the control effort is to achieve a favorable control effect on the primary system by the transfer or dissipation of energy through continuously-applied, nonimpulsive interactions but not by sudden changes in E_1 through instantaneously-applied, impulsive interactions. This objective may be ensured for the cases in Categories 2 and 3 if the attachment process is delayed until an instant in time when $\dot{x}_2(t_k^-) = \dot{x}_1(t_k^-)$. Under these conditions, $\Delta E_{tot}(t_k)$ and $\Delta E_1(t_k)$ are both zero, and the impulsive force vanishes as well (confer with (3-18)). However, this restriction is unnecessarily prohibitive and would cause many opportunities for interaction to be missed. So it becomes desirable to determine practical conditions under which an attachment process can be accomplished, even when $\dot{x}_2(t_k^-) \neq \dot{x}_1(t_k^-)$, but which limit the adverse effects.

The additional criterion used to determine whether or not an attachment process should be permitted at some representative time t_k is expressible as

$$0 \leq \frac{\left|\Delta\left|x_1(t_k)\right|_{sup}\right|}{\left|x_1(t_k^-)\right|_{sup}} \ll 1 \tag{3-26}$$

where

$$\Delta\left|x_1(t_k)\right|_{sup} \equiv \left|x_1(t_k^+)\right|_{sup} - \left|x_1(t_k^-)\right|_{sup} \tag{3-27}$$

The condition expressed by (3-26) has been chosen because $|x_1|_{sup}$, which is directly related to E_1, is left relatively unchanged following the attachment process, after which it

can be changed only through the interaction effects brought about by continuously-applied forces. It is relatively straightforward to show (see Appendix B) that

$$\frac{|\Delta E_1(t_k)|}{E_1(t_k^-)} = 2\left(\frac{\left|\Delta|x_1(t_k)|_{sup}\right|}{|x_1(t_k^-)|_{sup}}\right) + \left(\frac{\left|\Delta|x_1(t_k)|_{sup}\right|}{|x_1(t_k^-)|_{sup}}\right)^2 \tag{3-28}$$

and also that

$$\frac{\left|\Delta|x_1(t_k)|_{sup}\right|}{|x_1(t_k^-)|_{sup}} < \frac{1}{2}\frac{|\Delta E_1(t_k)|}{E_1(t_k^-)}, \quad \text{if} \quad \frac{|\Delta E_1(t_k)|}{E_1(t_k^-)} < 1 \tag{3-29}$$

Hence, if it is required that $|\Delta E_1(t_k)| < \varepsilon_E E_1(t_k^-)$, with $\varepsilon_E \ll 1$, then

$$\frac{\left|\Delta|x_1(t_k)|_{sup}\right|}{|x_1(t_k^-)|_{sup}} < \frac{\varepsilon_E}{2} \tag{3-30}$$

and it is evident that (3-26) will be satisfied.

Upon further inspection of (3-24) and (3-25), it is apparent that in some instances $|\Delta E_1(t_k)| < |\Delta E_{tot}(t_k)|$, while in other instances $|\Delta E_{tot}(t_k)| < |\Delta E_1(t_k)|$, depending on the particular values of $\dot{x}_1(t_k^-)$, $\dot{x}_2(t_k^-)$, and β. If it is stipulated that

$$|\Delta E_{tot}(t_k)| < \varepsilon_E E_1(t_k^-) \tag{3-31}$$

whenever $|\Delta E_1(t_k)| < |\Delta E_{tot}(t_k)|$, then (3-26) will certainly be satisfied. Alternatively, if it is stipulated that

$$|\Delta E_1(t_k)| < \varepsilon_E E_1(t_k^-) \tag{3-32}$$

whenever $|\Delta E_{tot}(t_k)| < |\Delta E_1(t_k)|$, then (3-26) will certainly be satisfied. Thus, by using the appropriate condition stipulated in either (3-31) or (3-32), $\Delta E_{tot}(t_k)$ is kept "small" while simultaneously satisfying (3-26). This is an attractive feature since it is reasonable to interpret $\Delta E_{tot}(t_k)$ as a measure of the potential for damage to the systems that is associated with an abrupt attachment process. In addition, by using (3-18) and (3-24), the following relation holds

$$|I_1(t_k)| = \sqrt{2\frac{m_1\beta}{\beta+1}|\Delta E_{tot}(t_k)|} \tag{3-33}$$

Therefore, requiring $\Delta E_{tot}(t_k)$ to be small also ensures that $I_1(t_k)$ will be small. This has important physical consequences because, in reality, the attachment process will require some small yet finite amount of time to transpire. An effective force during the impulsive interaction may then be determined by dividing the impulse by this small amount of time. By ensuring that $I_1(t_k)$ is small, this effective force is kept small. It is of anecdotal interest to note that the criterion is automatically satisfied for all cases in Category 1, since $\beta = 0$.

Fundamental Criterion

As discussed previously, two methods are considered to implement the control strategy: continuously-applied, nonimpulsive interactions; and instantaneously-applied, impulsive interactions. The control algorithm corresponding to Method 1 is described first. At the beginning of each sampling period, the states of the primary and auxiliary systems are measured or estimated. These states are used to determine the control forces that would be produced by an interaction. Then, the control processor evaluates the rate at which relative vibrational energy is added to the primary system as a result of the interaction (given by the term multiplying h in (3-12)). When this quantity is less than or equal to zero, then either: (*a*) an interaction is initiated and maintained for the sampling period duration, or (*b*) the interaction is maintained, if already in effect, for the sampling period duration. Otherwise, either: (*a*) an interaction is not initiated, or (*b*) the interaction is terminated, if already in effect. The conditional tests in this algorithm comprise what is referred to as the *fundamental criterion* for Method 1, and represent the logic used by the control processor to determine whether or not an interaction may be initiated and/or maintained.

There are a few caveats to the decision process outlined above that must be further explained. First, for the cases in Category 1 (excluding those cases for which interactions are prohibited when $\dot{U}_1 < 0$), the auxiliary system consists only of a linear elastic element, and upon deactivation, the interaction element may be instantaneously slipped to

reduce the reaction force to zero. Hence, the interaction element may always be immediately reactivated in accordance with the fundamental criterion. Thus, for these particular cases, the interaction element remains activated at all times with the exception of certain discrete points in time at which this deactivation-reactivation process occurs. Also, for the cases in Categories 2 and 3, the initiation of an interaction is only permitted when both the conditions of the fundamental criterion and those of the additional criterion related to the attachment process are satisfied.

The control algorithm corresponding to Method 2 is described next. As with the algorithm for Method 1, the states of the primary and auxiliary systems are measured or estimated at the beginning of each sampling period. These states are used by the control processor to compute the value of $\Delta E_1(t_k)$, according to (3-25), that would result from an impulsive interaction. When the value of $\Delta E_1(t_k)$ has reached a local (but negative) minimum in time, an attachment-and-release process is initiated (without regard for the attachment criterion). This local minimum is determined by monitoring the computed value for $\Delta E_1(t_k)$ at the beginning of each sampling period and identifying the lowest (but negative) value attained before it begins to increase for subsequent sampling periods. Then, to ensure that a true minimum has been reached, the control processor postpones initiation of the attachment-and-release process until the value of $\Delta E_1(t_k)$ is observed to monotonically increase from the identified minimum for n_P consecutive sampling periods, where n_P is a parameter. The conditional tests in this algorithm comprise what is referred to as the *fundamental criterion* for Method 2, and represent the logic used by the control processor to determine whether or not an attachment-and-release process may be initiated.

3.7 Results

The simulation results are compiled in the form of response spectra, which plot the pseudo-velocity of the primary system response, $\omega_1 |x_1|_{max}$, versus the undamped natural

frequency of the primary system, $\omega_1/2\pi$, for the range of values considered. Response spectra have historically been used by engineers for design purposes [3]. However, when several curves representing the response of various control cases are plotted along with the curve representing the uncontrolled case, this graphical construct becomes a useful tool for judging the effectiveness of the proposed control approach. Results are now summarized for the control cases belonging to each of the previously described control categories.

Category 1:

The response spectra for the controlled cases in which interactions are permitted for any value of $\dot{U}_1$ are significantly reduced in comparison to the response spectrum for the uncontrolled case for each of the excitation records considered. A trend of decrease in the response spectrum is nearly always observed as the value of α is increased. The spectra for all of the cases are shown in Figure 3.6 for each of the excitation records.

The response spectra for the controlled cases in which interactions are prohibited when $\dot{U}_1 < 0$ are generally reduced in comparison to the response spectrum for the uncontrolled case for each of the excitation records considered. A trend of decrease in the response spectrum is nearly always observed as the value of α is increased. The spectra for all of the cases are shown in Figure 3.7 for each of the excitation records.

Category 2:

The response spectra for the controlled cases are generally not reduced in comparison to the response spectrum for the uncontrolled case for each of the excitation records considered. The spectra for all of the cases are shown in Figure 3.8 for each of the excitation records.

Category 3:

The response spectra for the controlled cases are moderately but not consistently reduced in comparison to the response spectrum for the uncontrolled case for each of the excitation records considered. The spectra for all of the cases are shown in Figures 3.9

and 3.10 for each of the excitation records.

Category 4:

The response spectra for the controlled cases are generally reduced in comparison to the response spectrum for the uncontrolled case for each of the excitation records considered. A trend of decrease in the response spectrum is usually observed as the value of β is increased at all but the higher frequencies. The spectra for all of the cases are shown in Figure 3.11 for each of the excitation records.

Category 5:

The response spectra for the controlled cases are generally reduced in comparison to the response spectrum for the uncontrolled case for each of the excitation records considered. A trend of decrease in the response spectrum is generally observed as the value of α is increased while using the smallest value of β, and the opposite trend is usually observed as α is increased while using the largest value of β. The spectra for all of the cases are shown in Figures 3.12 and 3.13 for each of the excitation records.

Category 6:

The response spectra for the controlled cases in this category, which is included in the study primarily for the purposes of comparison with Category 7, are shown in Figures 3.14 through 3.18 for each of the excitation records. For all of the controlled cases in this category, the interaction element is permanently locked in the activated operating state. The performance exhibited by the controlled cases in Category 7 at least equal, and usually surpass, that in this category.

Category 7:

The response spectra for the controlled cases are moderately but generally reduced in comparison to the response spectrum for the uncontrolled case for each of the excitation records considered. A trend of decrease in the response spectrum is generally observed as the value of δ is increased. The spectra for all of the cases are shown in Figures 3.19 through 3.23 for each of the excitation records.

Category 8:

The response spectra for the controlled cases in this category, which is included in the study primarily for the purposes of comparison with Category 9, are shown in Figures 3.24 through 3.28 for each of the excitation records. For all of the controlled cases in this category, the interaction element is permanently locked in the activated operating state. The performance exhibited by the controlled cases in Category 9 at least equal, and usually surpass, that in this category.

Category 9:

The response spectra for the controlled cases are significantly and generally reduced in comparison to the response spectrum for the uncontrolled case for each of the excitation records considered. A trend of decrease in the response spectrum is generally observed as the value of δ is increased. The spectra for all of the cases are shown in Figures 3.29 through 3.33 for each of the excitation records.

3.8 Discussion

In the last column of Table 3.1, a qualitative assessment of the control effectiveness or performance achieved is assigned for typical cases in each of the control categories. Such factors as the extent of response reduction attained for the controlled system, and the consistency of the results obtained by using different excitation records for a given case are taken into account to arrive at these assessments. It is evident from the results previously discussed that the cases belonging to Category 1 are by far the most effective with regard to the response control objective. The response control effort is generally ineffective for the cases belonging to Categories 2 and 3.

The cases in Categories 4 and 5, which are the only ones that use the Method 2 form of the control strategy implementation, are also very effective. But the consequences of allowing impulsive forces to act upon the systems, and thereby modify their response, have not been adequately addressed. Also, some questions remain concerning the details

of how such impulsive interactions might be physically achieved. As was pointed out earlier, the interactions for the cases in these categories correspond to perfectly-plastic impacts which are assumed to occur instantaneously, and so it was not necessary to specify the actual devices used to accomplish this idealized phenomenon. For these reasons, the cases utilizing Method 2 are not pursued further in the follow-on study.

The cases in Categories 7 and 9 are also effective, with the results indicating that the cases in Category 9 are generally more effective than those in Category 7. However, this superior effectiveness might be related to the approximations used to determine the value of ε_s for the cases in Category 9, resulting in effective values for δ that are greater than they are supposed to have been. In fact, because of the difficulties associated with establishing the appropriate slip force level, as well as concerns about the power requirements to generate the normal forces necessary for the proper functioning of the stick-slip device, the third type of interaction element will not be pursued further in the follow-on study.

The results of those cases in Categories 6 and 8 which differ noticeably from the results of their corresponding cases in Categories 7 and 9 indicate that the switching process associated with altering the mechanical properties of the interaction element generally leads to improved control effectiveness.

Additional Observations

Of special interest are the cases in Category 1 for which interactions are prohibited when $\dot{U}_1 < 0$. Physically, this restriction means that when the elastic element of the primary system is in the process of unloading (*i.e.*, the system mass is moving back toward its equilibrium position), interactions with the auxiliary system are not permitted. In essence, these cases involve the same kind of auxiliary system and control algorithm as that employed by the Kajima Corporation of Japan for the Active Variable Stiffness (AVS) control method, as discussed in [4]. Thus, for the purposes of the present study, this control algorithm will be referred to as the Kajima AVS control algorithm. Figures

3.6 and 3.7 indicate that if an actual system can be made to respond like the auxiliary system used in this category, then the control algorithm which permits interactions for any value of $\dot{U}_1$ (*i.e.*, the proposed control algorithm) yields a substantial improvement in control effectiveness than the control algorithm which prohibits interactions when $\dot{U}_1 < 0$ (*i.e.*, the Kajima AVS control algorithm). Of course, this conclusion is valid only for the ensemble of excitation records considered.

Consider now the response characteristics of an externally-unforced SDOF primary system that interacts with a SDOF auxiliary system of the type used in Category 1 and is controlled by the two kinds of algorithms discussed above. It is assumed that at the initial time t_o, $x(t_o) = x_o$ and $\dot{x}(t_o) = 0$. Upon doing some simple analysis, further insight may be gained. The following results are obtained for the amplitude ratio, period of vibration, and energy change associated with one cycle of oscillation for an undamped system of mass m and natural frequency $\omega/2\pi$ (since in this case all quantities of interest except α refer to the primary system, the subscript denoting the primary system is suppressed for convenience and clarity):

- Proposed Control Algorithm –

$$\frac{x(t_o+\Delta t)}{x_o} = \frac{(1-\alpha)^2}{(1+\alpha)^2}, \quad \frac{\Delta t}{T} = \frac{1}{\sqrt{1+\alpha}}, \quad \frac{\Delta E}{E_o} = -\frac{8\alpha(1+\alpha^2)}{(1+\alpha)^4} \tag{3-34}$$

- Kajima AVS Control Algorithm –

$$\frac{x(t_o+\Delta t)}{x_o} = \frac{1}{(1+\alpha)}, \quad \frac{\Delta t}{T} = \frac{1+\sqrt{1+\alpha}}{2\sqrt{1+\alpha}}, \quad \frac{\Delta E}{E_o} = -\frac{\alpha(2+\alpha)}{(1+\alpha)^2} \tag{3-35}$$

For both of these algorithms, $T \equiv 2\pi/\omega$ and $E_o \equiv \frac{1}{2} m \omega^2 x_o^2$.

Figures 3.34 and 3.35 show a portion of the force-displacement time-history which develops within the interaction element for the two kinds of algorithms discussed above, respectively, for $\alpha = 0.25$. In both of these cases, the primary system is given an initial displacement of x_o and then released. The hysteresis loops which appear in the diagrams represent the energy dissipated per cycle by the interaction element. It is evident that more energy is dissipated per cycle for the case using the proposed control algorithm than

for the case using the Kajima AVS control algorithm; this conclusion can also be reached upon examining (3-34) and (3-35) when $\alpha < 3$. These results may offer a partial explanation for the observed behavior in the externally-forced case.

For the case in which the primary system is harmonically forced at a frequency of $\overline{\omega}/2\pi$ in a steady-state manner, it is simple to show that

- Proposed Control Algorithm –

$$\frac{x(t_o + \Delta t)}{x_o} = 1, \quad \frac{\Delta t}{\overline{T}} = 1, \quad \frac{\Delta E}{E_o} = -8\alpha \tag{3-36}$$

- Kajima AVS Control Algorithm –

$$\frac{x(t_o + \Delta t)}{x_o} = 1, \quad \frac{\Delta t}{\overline{T}} = 1, \quad \frac{\Delta E}{E_o} = -2\alpha \tag{3-37}$$

where $\overline{T} \equiv 2\pi/\overline{\omega}$. The force-displacement time-histories for this case would be similar to the diagrams shown in Figures 3.34 and 3.35, except that the displacement oscillates between positive and negative x_o, and each curve would return to the initial point at the end of each cycle of oscillation, yielding closed hysteresis loops.

In seeking to compare the performance achieved by these two control algorithms, it is also helpful to examine the effective damping ratio for both the externally-unforced and harmonically-forced cases. The effective damping ratio is the damping ratio for an uncontrolled SDOF system that would yield the same amount of energy dissipation per cycle as is obtained for the controlled SDOF system. In the case for which the primary system is externally unforced, it may be shown that

$$\zeta_{eff} = \sqrt{\frac{c^2}{c^2 + 4\pi^2}}; \quad |c| = \tfrac{1}{2}\ln(1-b), \quad b \equiv \left|\frac{\Delta E}{E_o}\right| \tag{3-38}$$

Using (3-36), (3-37), (3-38), and $\alpha = 0.50$, the values of ζ_{eff} for the proposed control algorithm and the Kajima AVS control algorithm are 0.33 and 0.06, respectively. In the case for which the primary system is harmonically forced at $\overline{\omega} = \omega$, it may be shown that

$$\zeta_{eff} = \frac{b}{4\pi}\frac{\overline{\omega}}{\omega} = \frac{b}{4\pi}; \quad b \equiv \left|\frac{\Delta E}{E_o}\right| \tag{3-39}$$

Using (3-36), (3-37), (3-39), and $\alpha = 0.50$, the values of ζ_{eff} for the proposed control

algorithm and the Kajima AVS control algorithm are 0.32 and 0.08, respectively. Both the externally-forced and harmonically-forced cases demonstrate that much higher values for ζ_{eff} are achievable when using the proposed control algorithm.

It should be mentioned that the cases in Category 1 may be viewed in an entirely different manner than previously done. Consider a new interaction element consisting of the old interaction element used for these cases, which can be instantaneously slipped to a zero reaction force condition upon deactivation, placed in series with the linear elastic element that was formerly considered to be the auxiliary system. From this viewpoint, the cases in Category 1 may be described as those for which the new interaction element facilitates an interaction between the primary system and its base (*i.e.*, the ground). Such an interaction element, and a modified version of it, will form the basis for much of the follow-on study involving MDOF models of structural systems.

Chattering Phenomenon

In the theory of variable structure systems, or sliding mode control, usually the objective is to bring the state of a system to a singular hypersurface (often referred to as a *switching surface*) in the state space, and then to maintain the state on that surface while simultaneously driving it toward the origin. Because relay devices are utilized by the controller to achieve this desired behavior for the system, a chattering phenomenon will result. While in chatter, the state undergoes extremely fast, alternating excursions across the switching surface in an effort by the controller to maintain the state on the surface.

With regard to the Method 1 form of the control strategy implementation — which utilizes continuously-applied, nonimpulsive interactions to implement the control strategy — it is not desirable for such a phenomenon to occur. In the simulations conducted for the control cases in the present study, there was no evidence of a chattering behavior for the interaction elements during their operation. However, a simple example is now presented which indicates that this phenomenon can occur under certain conditions for the proposed control approach. It is prudent to mention that this example involves an

auxiliary system which, for the intended applications, is not very realistic, but it does serve to illustrate the phenomenon.

Consider again two interacting SDOF systems which are externally unforced. The primary system is characterized by a fraction of critical damping ζ of 0.02 and an undamped natural frequency $\omega/2\pi$ of 1.00 Hz. The auxiliary system is characterized by $\alpha = 0.00$ and $\beta = 5.00$. The interaction element is a semi-actively operated Coulomb-damped member, as previously used for control cases in Category 9, with $\varepsilon_s = 0.25$. Figure 3.36 shows the response time-history of the primary system, in which the auxiliary system is initially at rest and the primary system is given an initial displacement, for both the controlled and uncontrolled cases. The chattering phenomenon occurs during those portions of the response when the curve is relatively flat.

It may be of anecdotal interest to note that when an externally-unforced SDOF primary system that interacts with a SDOF auxiliary system of the type used in Category 1 (as described earlier) under conditions for which $\alpha \gg 1$ and the first control algorithm discussed is used, the displacement of the primary system does not oscillate. Rather, the response consists of a series of undulating decreases in the displacement, and as α becomes very large, chattering behavior results.

It would be advantageous to develop additional criteria that may be used to anticipate the occurrence of chattering behavior for the interaction elements and thereby prevent their operation, even if otherwise directed by the control algorithm, until such a time at which this phenomenon will not occur for a subsequent short interval of time.

Extension to MDOF Systems

In a later chapter, efforts are directed at extending the Active Interface Damping control approach investigated for two interacting SDOF systems to MDOF models of actual structural systems. This study will examine only linear MDOF systems, whose response can be decomposed into particular modes of vibration. The response control of one or several of these modes, each of which behaves like a SDOF system, is then sought.

References for Chapter 3

1. W. D. Iwan and N. C. Gates, "The Effective Period and Damping of a Class of Hysteretic Structures," *Earthquake Engrg. and Struct. Dynamics*, Vol. 7, No. 3, May-June 1979, pp. 199–211.

2. W. T. Thomson, *Theory of Vibration With Applications*, 2nd ed., Englewood Cliffs, N.J.: Prentice-Hall, Inc., 1981, Chap. 3.

3. G. W. Housner and P. C. Jennings, *Earthquake Design Criteria*, Engineering Monographs on Earthquake Criteria, Structural Design, and Strong Motion Records, Berkeley: Earthquake Engineering Research Institute, 1982, Engineering Design Criteria Sect.

4. T. Kobori and S. Kamagata, "Dynamic Intelligent Buildings — Active Seismic Response Control," *Intelligent Structures – 2: Monitoring and Control, Proc. of Intnl. Workshop on Intel. Systems*, ed. by Y. K. Wen, Perugia, Italy, 1991, London: Elsevier Science Pub. Ltd., 1992, pp. 279–292.

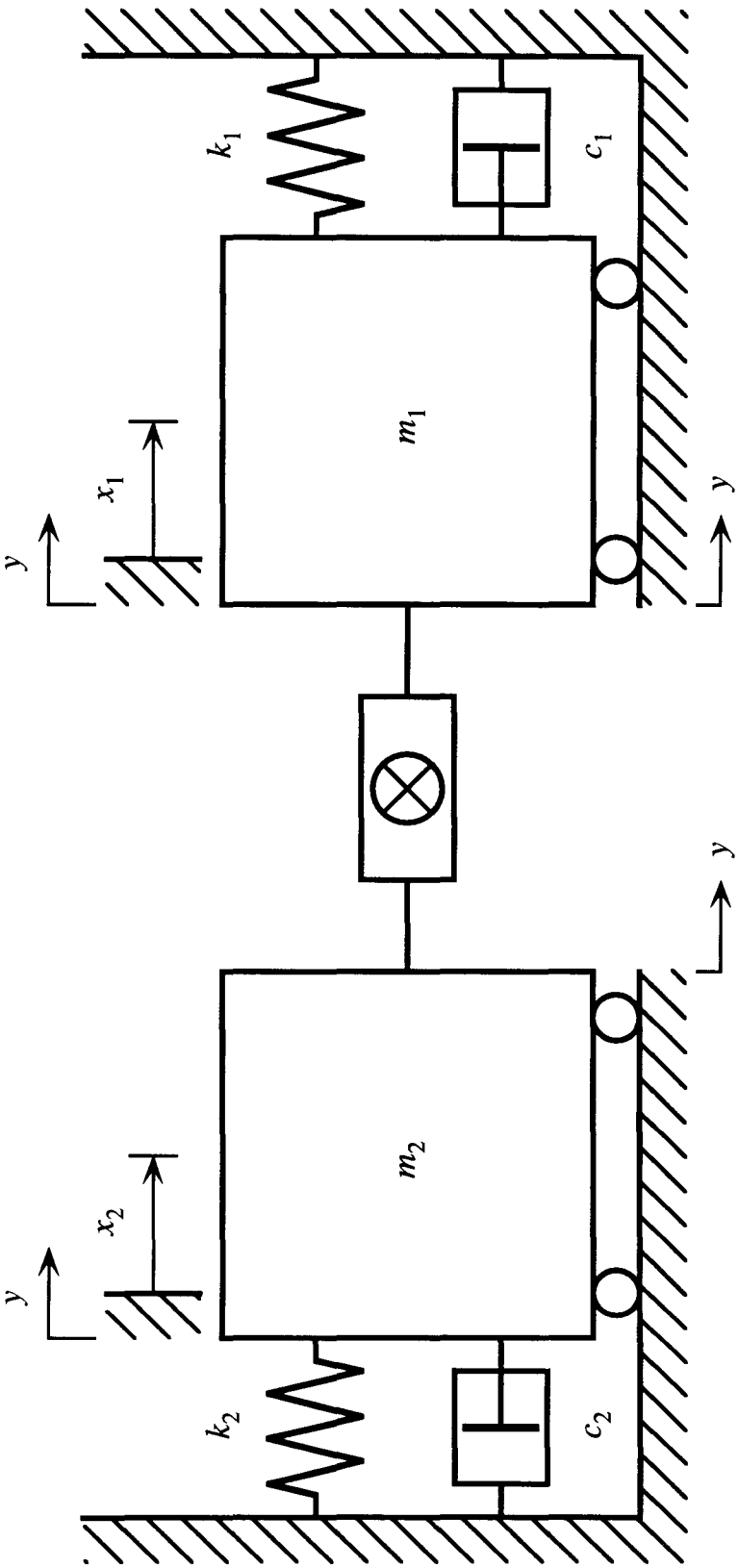

Figure 3.1. Schematic Representation of Two Interacting SDOF Systems. A generic interaction element is shown.

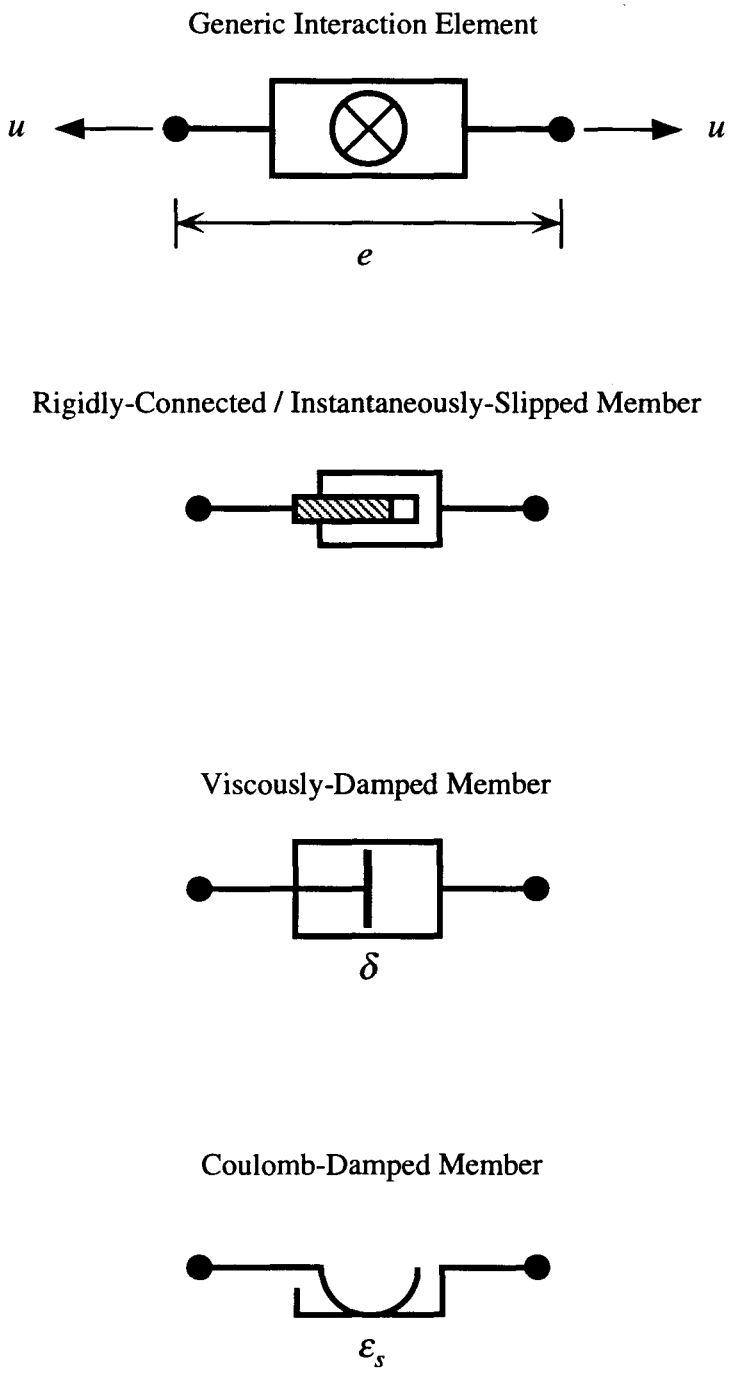

Figure 3.2. Schematic Representation of Interaction Elements Used for SDOF System Study.

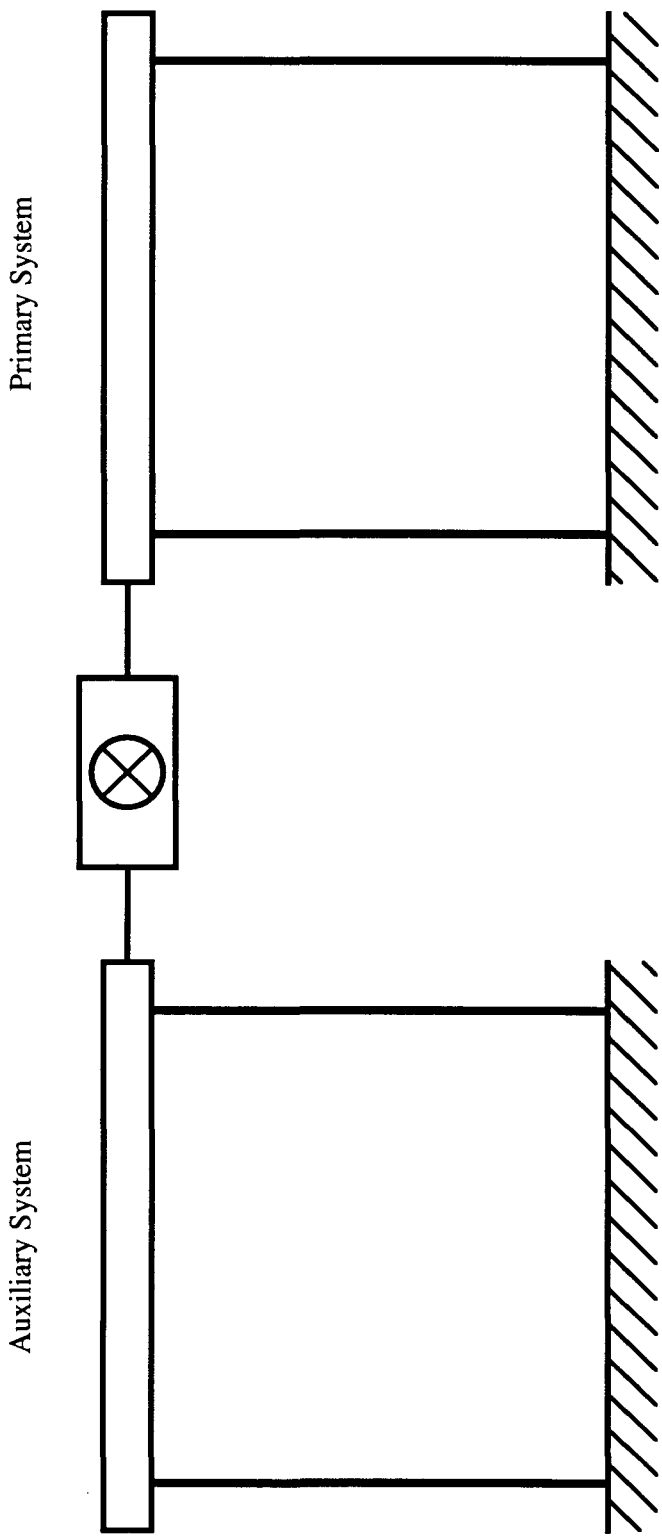

Figure 3.3. Primary-Auxiliary System Configuration for Control Cases in All Categories. A generic interaction element is shown.

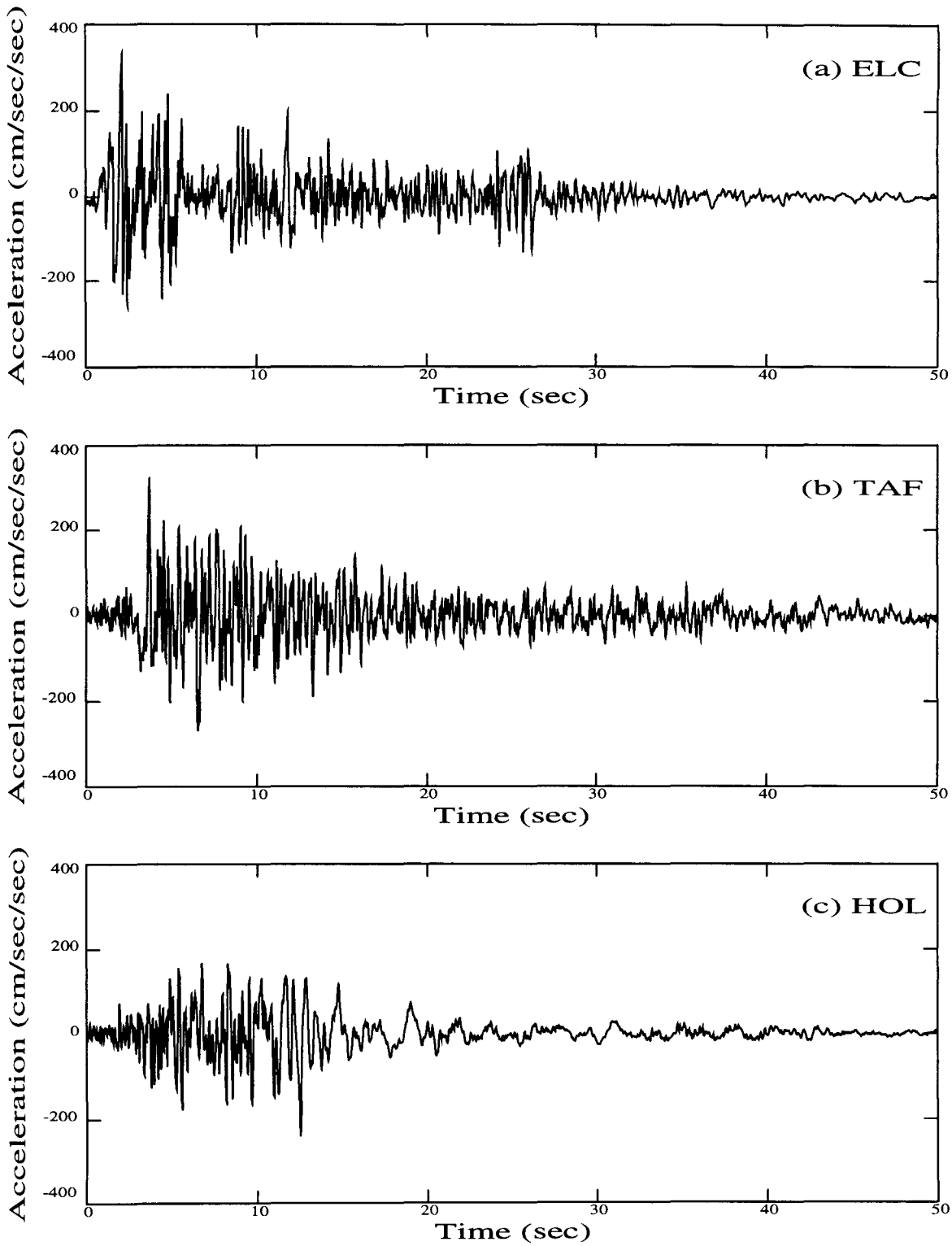

Figure 3.4. Normalized Accelerograms for the (a) 1940 Imperial Valley (El Centro) S00E, (b) 1952 Kern County (Taft Lincoln School Tunnel) S69E, and (c) 1971 San Fernando (Holiday Inn) N00W Earthquake Records.

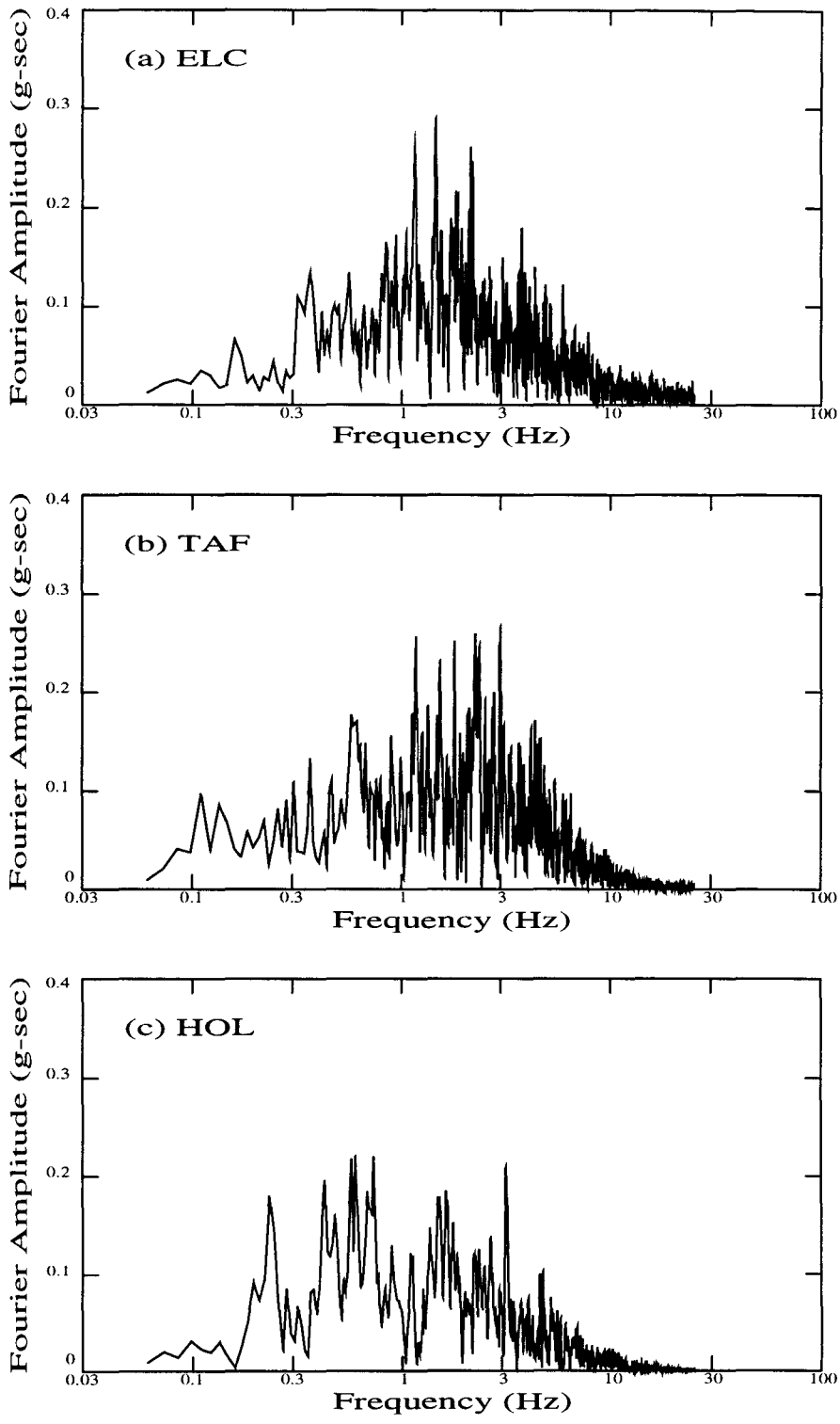

Figure 3.5. Fourier Spectra for the (a) 1940 Imperial Valley (El Centro) S00E, (b) 1952 Kern County (Taft Lincoln School Tunnel) S69E, and (c) 1971 San Fernando (Holiday Inn) N00W Earthquake Records.

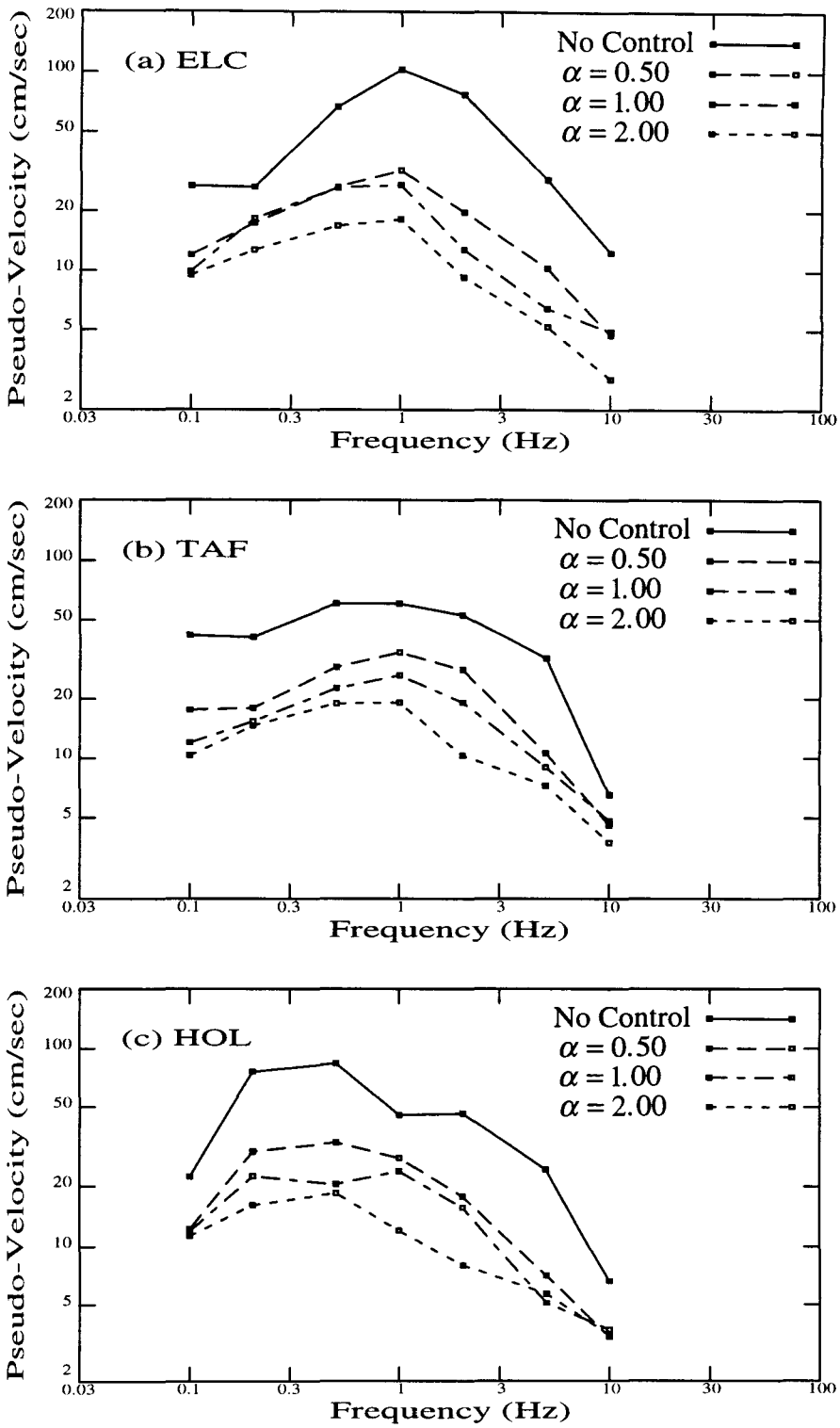

Figure 3.6. Response Spectra of Category 1 Controlled Cases for Various Values of α — with $\beta = 0$ and $\gamma = 0$ — for the (a) El Centro, (b) Taft Lincoln School Tunnel, and (c) Holiday Inn Excitation Records. Results are for primary system cases in which interactions are permitted for any value of $\dot{U}_1$.

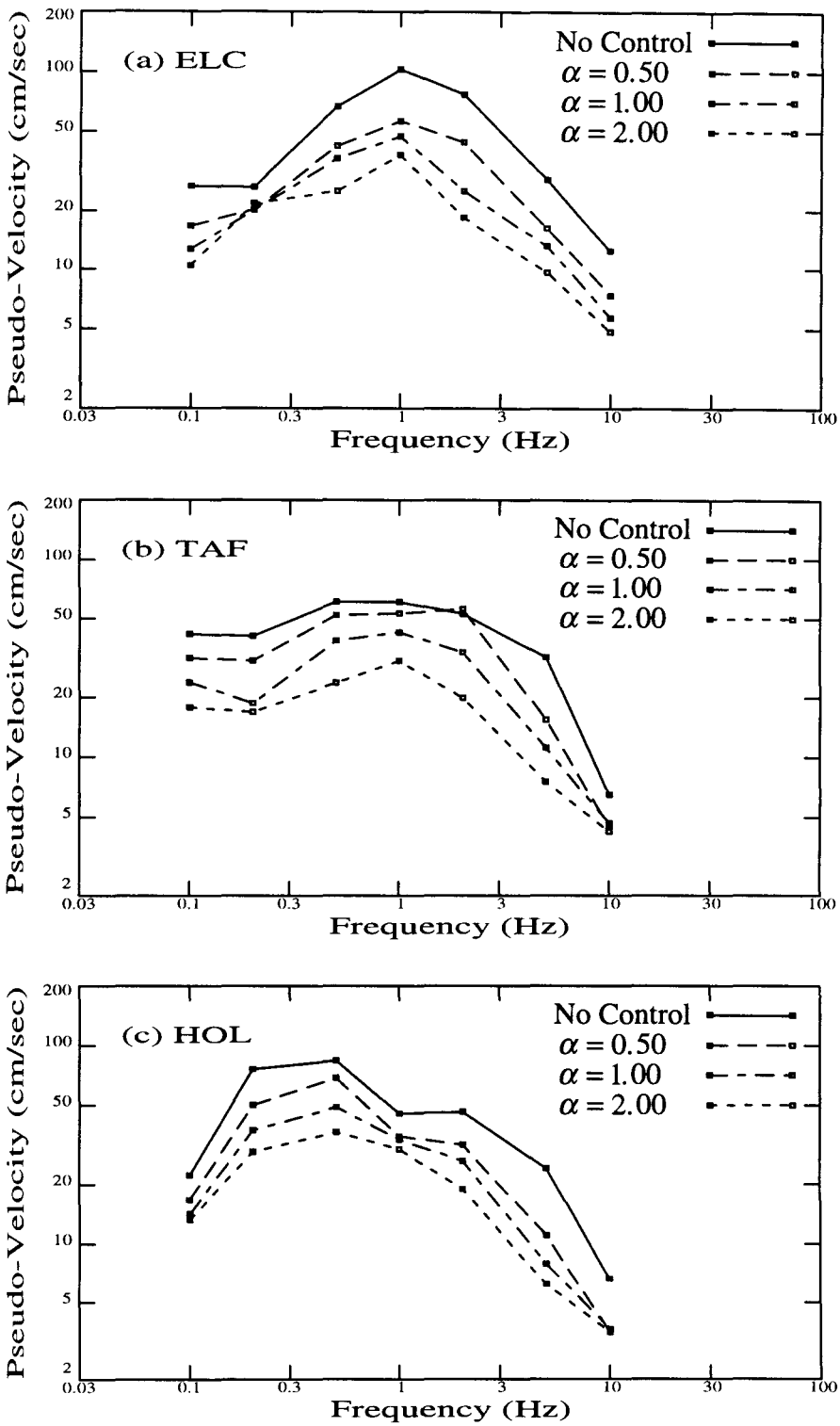

Figure 3.7. Response Spectra of Category 1 Controlled Cases for Various Values of α — with $\beta = 0$ and $\gamma = 0$ — for the (a) El Centro, (b) Taft Lincoln School Tunnel, and (c) Holiday Inn Excitation Records. Results are for primary system cases in which interactions are prohibited when $\dot{U}_1 < 0$.

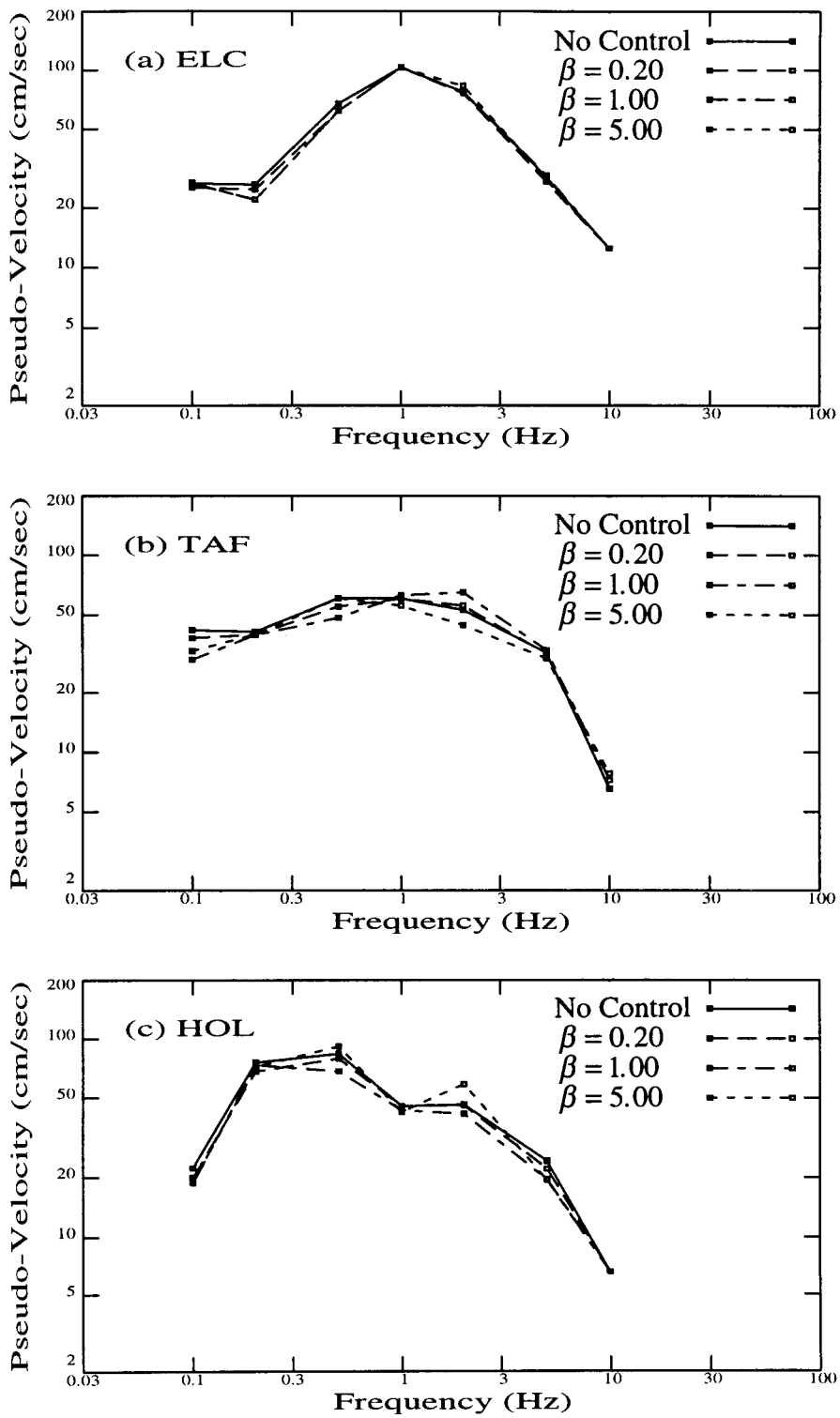

Figure 3.8. Response Spectra of Category 2 Controlled Cases for Various Values of β — with $\alpha = 0$ and $\gamma = 0$ — for the (a) El Centro, (b) Taft Lincoln School Tunnel, and (c) Holiday Inn Excitation Records. Results are for primary system.

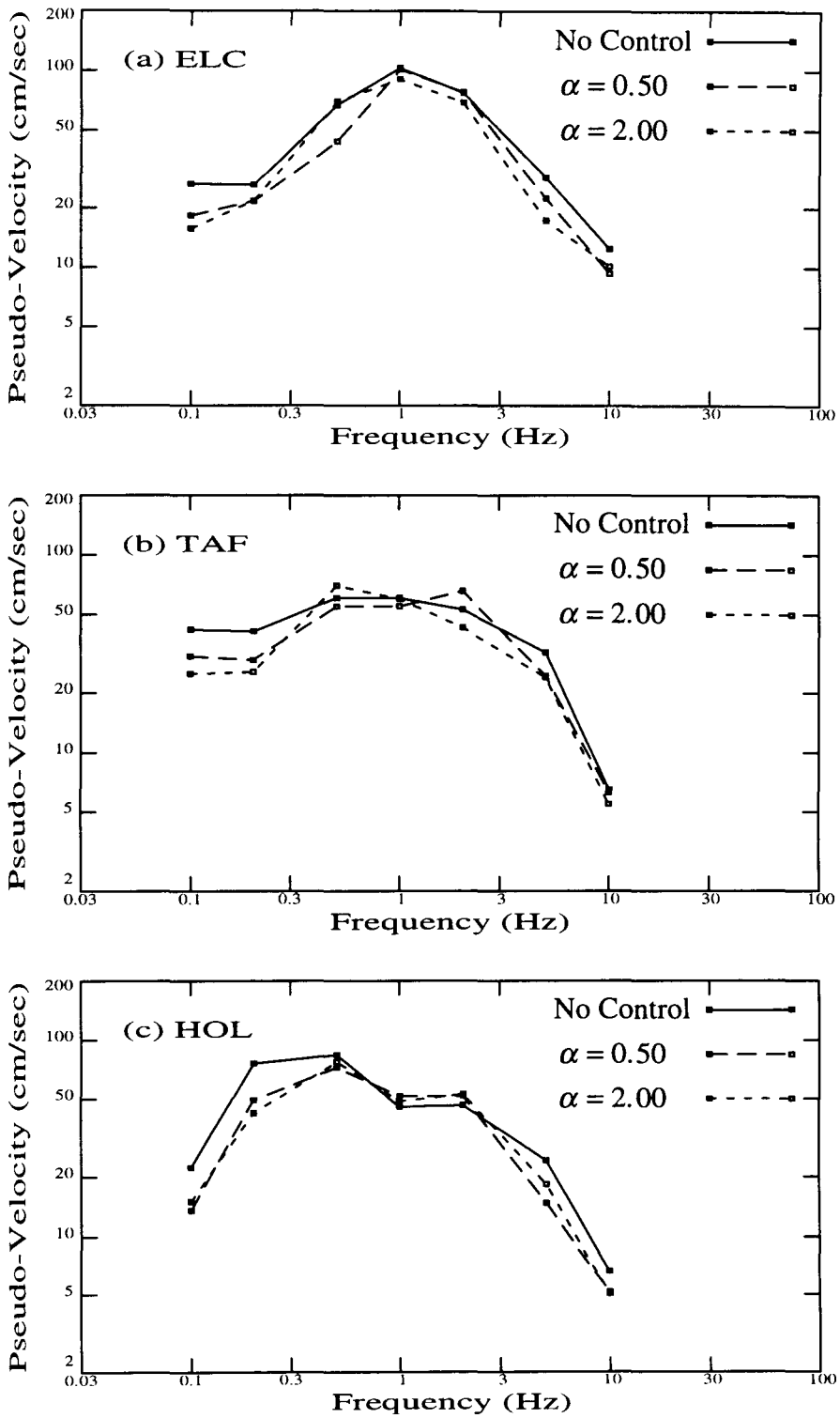

Figure 3.9. Response Spectra of Category 3 Controlled Cases for Various Values of α — with $\beta = 0.20$ and $\gamma = \sqrt{\alpha\beta}$ — for the (a) El Centro, (b) Taft Lincoln School Tunnel, and (c) Holiday Inn Excitation Records. Results are for primary system.

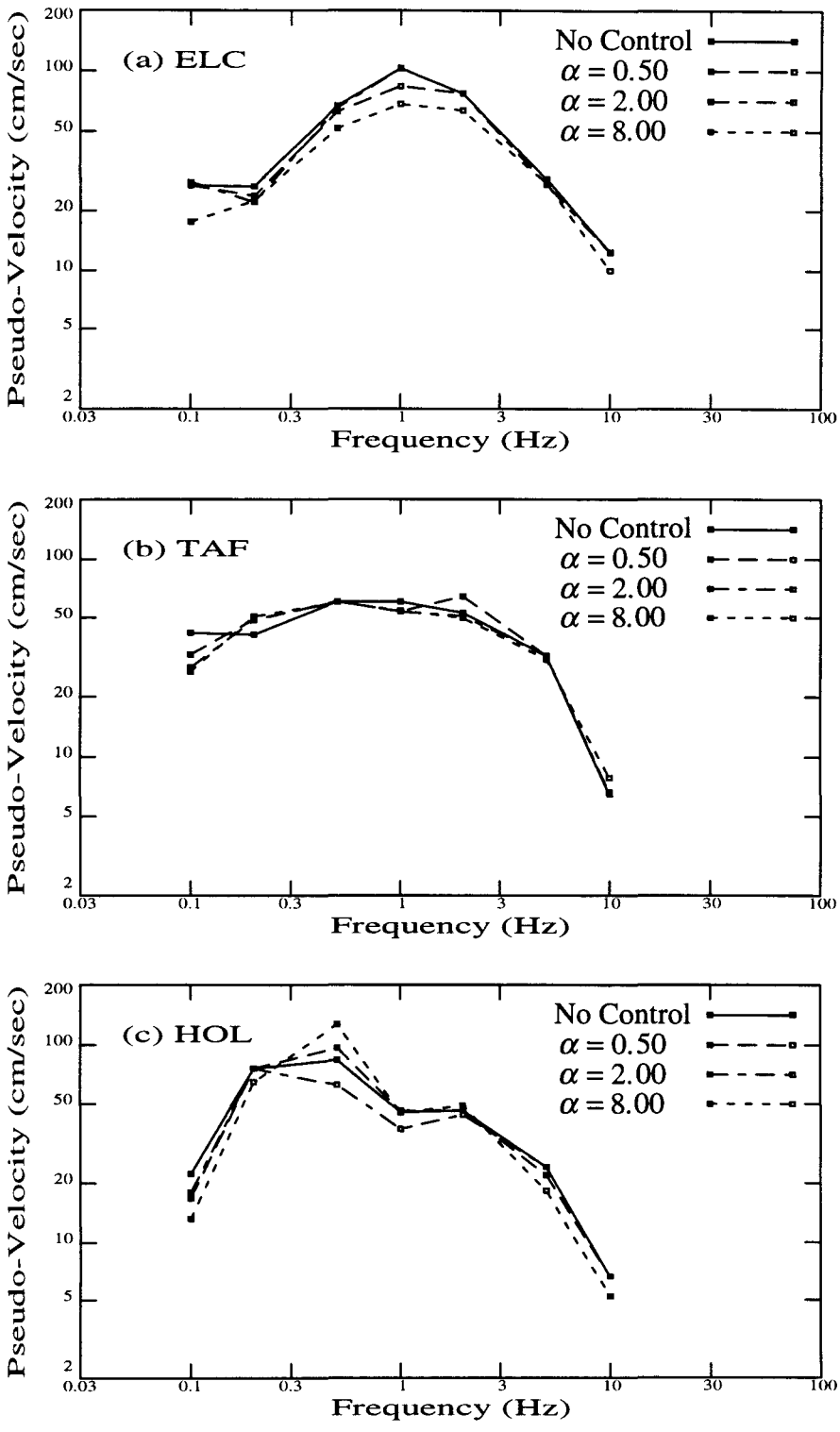

Figure 3.10. Response Spectra of Category 3 Controlled Cases for Various Values of α — with $\beta = 5.00$ and $\gamma = \sqrt{\alpha\beta}$ — for the (a) El Centro, (b) Taft Lincoln School Tunnel, and (c) Holiday Inn Excitation Records. Results are for primary system.

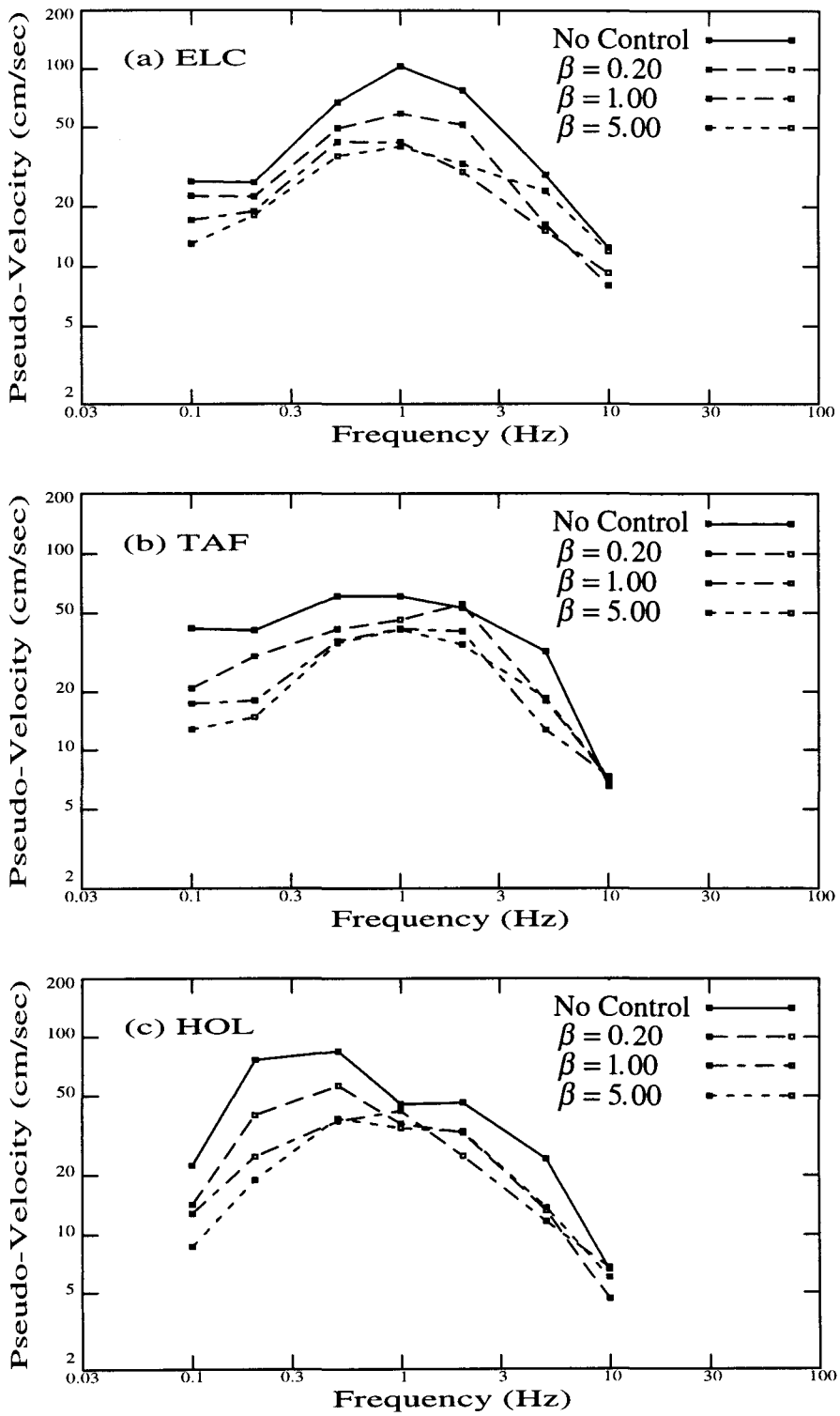

Figure 3.11. Response Spectra of Category 4 Controlled Cases for Various Values of β — with $\alpha = 0$ and $\gamma = 0$ — for the (a) El Centro, (b) Taft Lincoln School Tunnel, and (c) Holiday Inn Excitation Records. Results are for primary system.

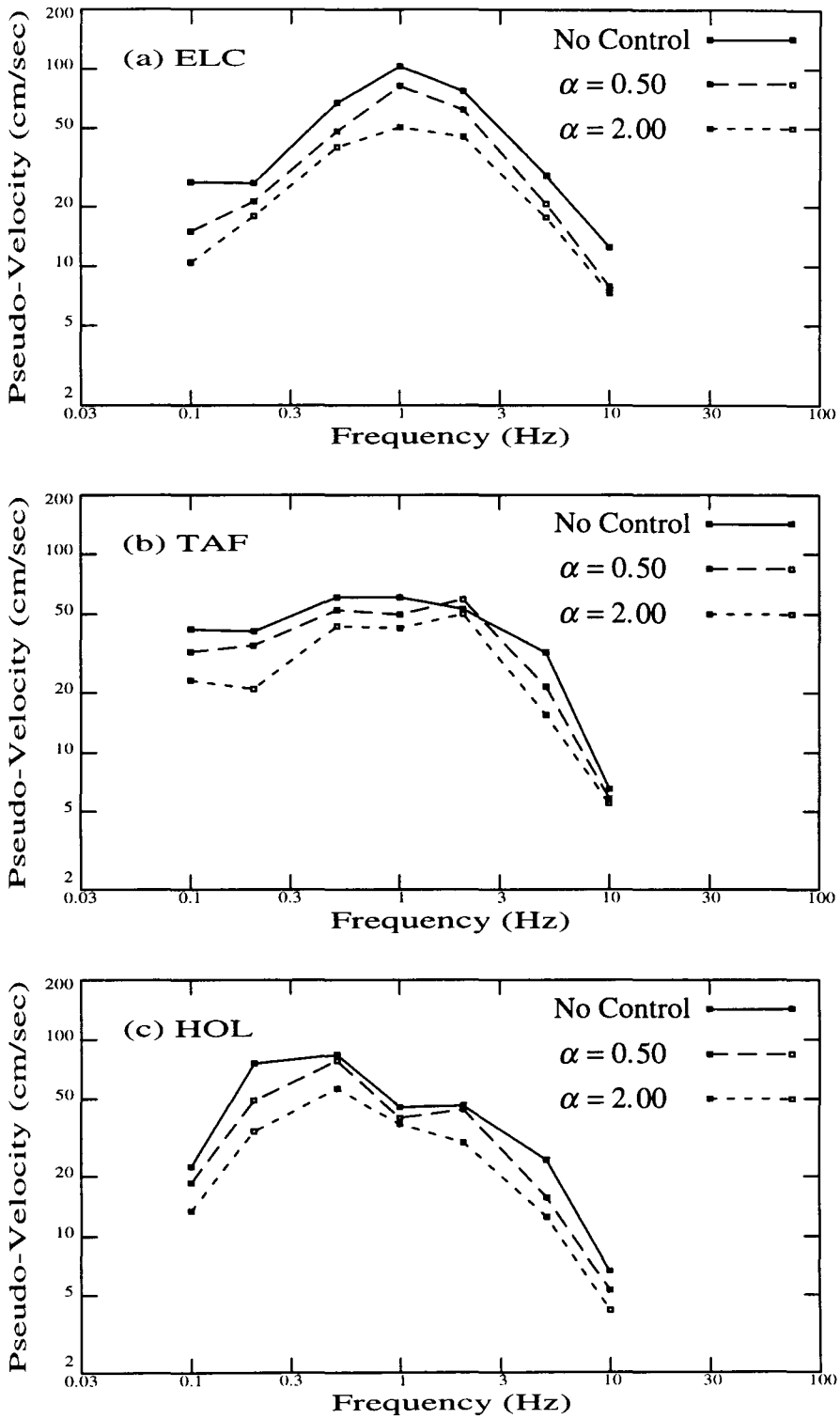

Figure 3.12. Response Spectra of Category 5 Controlled Cases for Various Values of α — with $\beta = 0.20$ and $\gamma = \sqrt{\alpha\beta}$ — for the (a) El Centro, (b) Taft Lincoln School Tunnel, and (c) Holiday Inn Excitation Records. Results are for primary system.

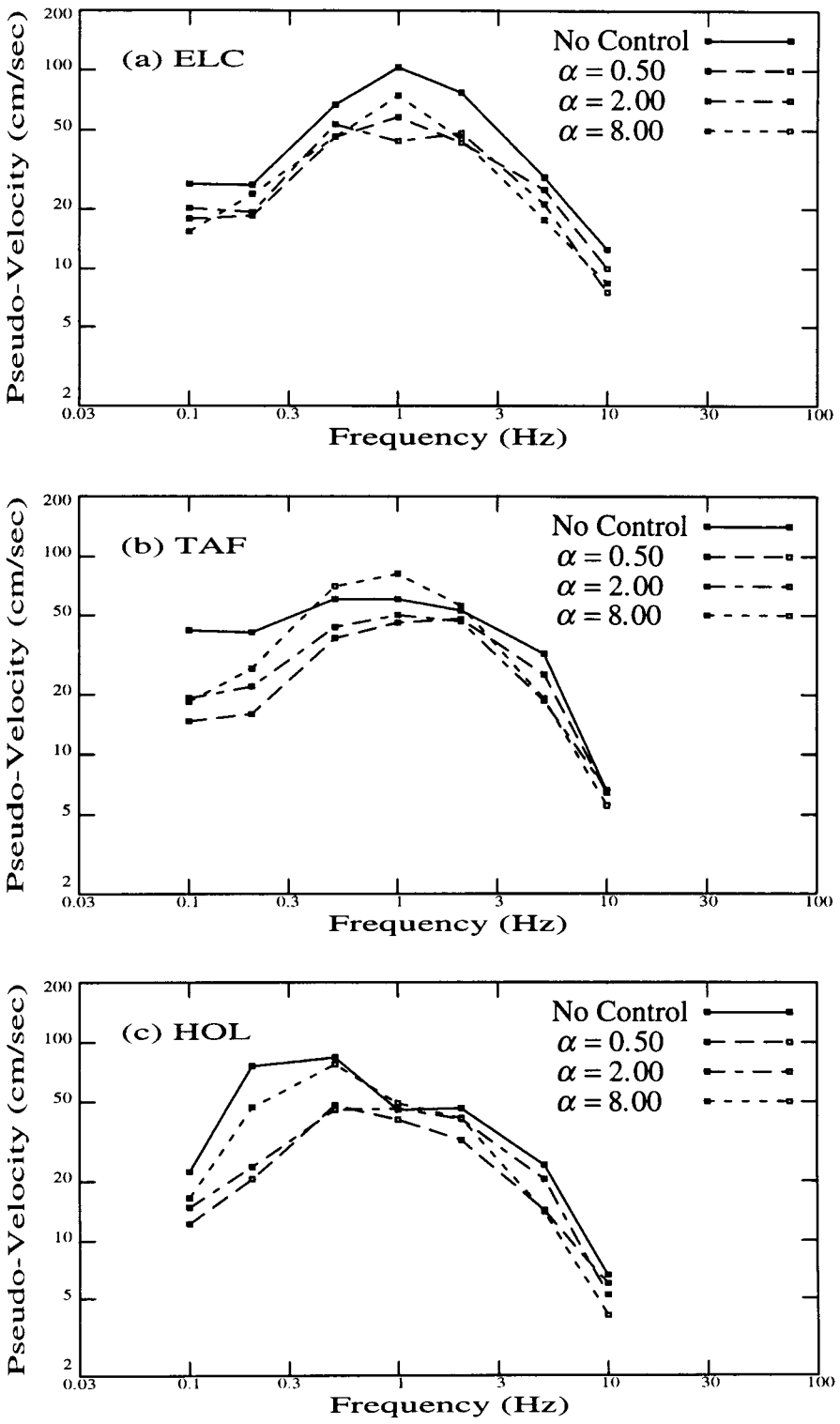

Figure 3.13. Response Spectra of Category 5 Controlled Cases for Various Values of α — with $\beta = 5.00$ and $\gamma = \sqrt{\alpha\beta}$ — for the (a) El Centro, (b) Taft Lincoln School Tunnel, and (c) Holiday Inn Excitation Records. Results are for primary system.

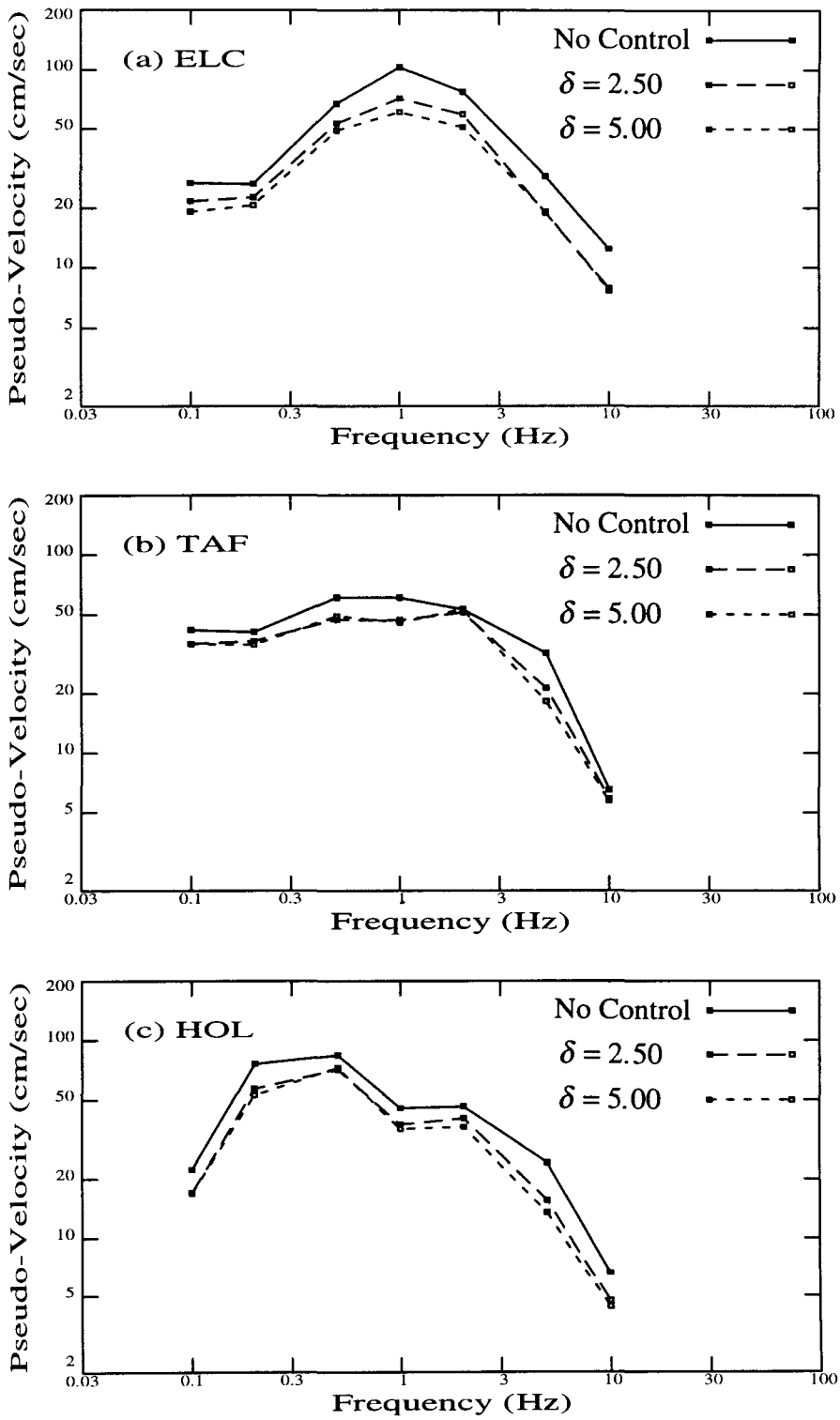

Figure 3.14. Response Spectra of Category 6 Controlled Cases for Various Values of δ — with $\alpha = 0.50$, $\beta = 0.20$, and $\gamma = \sqrt{\alpha\beta}$ — for the (a) El Centro, (b) Taft Lincoln School Tunnel, and (c) Holiday Inn Excitation Records. Results are for primary system.

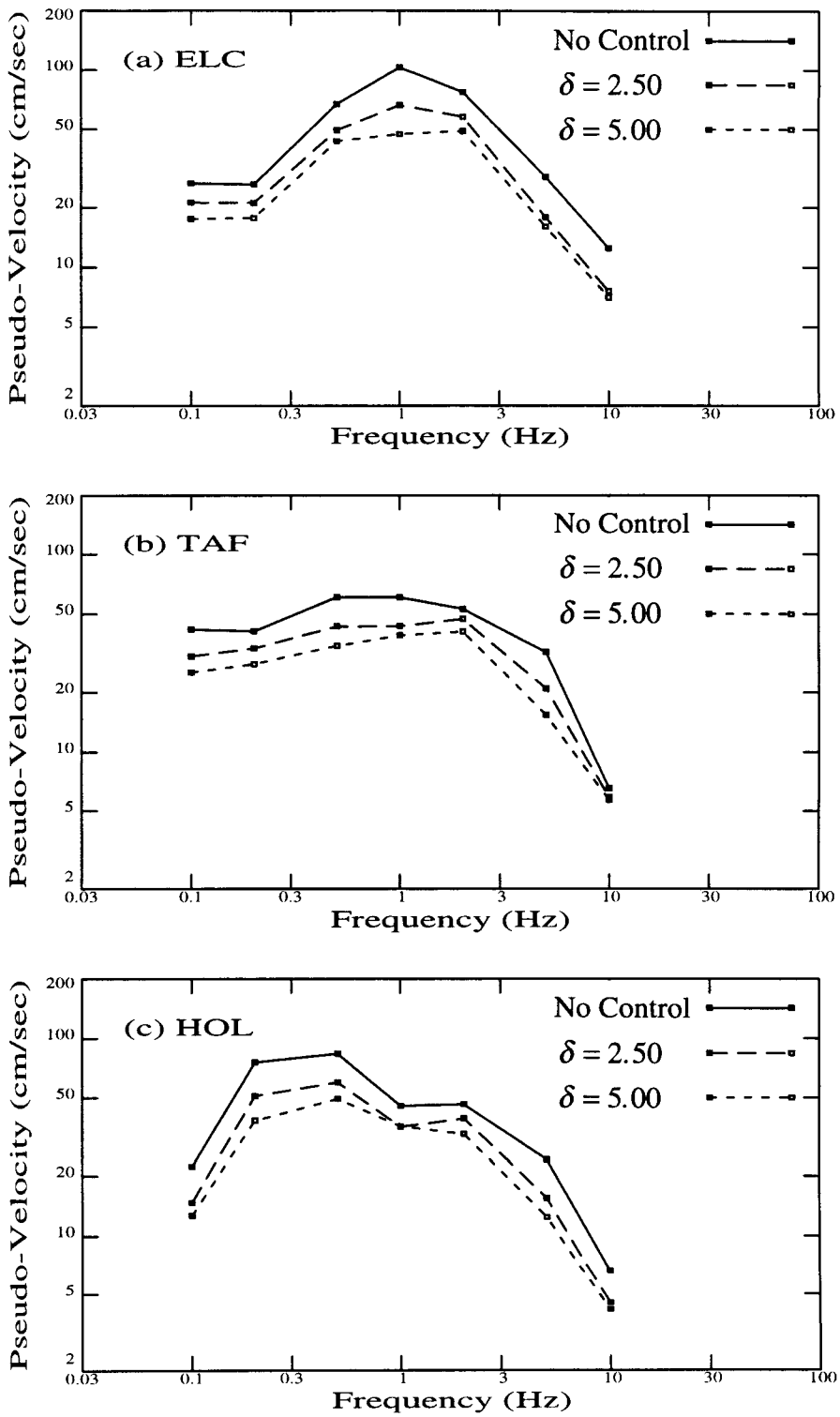

Figure 3.15. Response Spectra of Category 6 Controlled Cases for Various Values of δ — with $\alpha = 2.00$, $\beta = 0.20$, and $\gamma = \sqrt{\alpha\beta}$ — for the (a) El Centro, (b) Taft Lincoln School Tunnel, and (c) Holiday Inn Excitation Records. Results are for primary system.

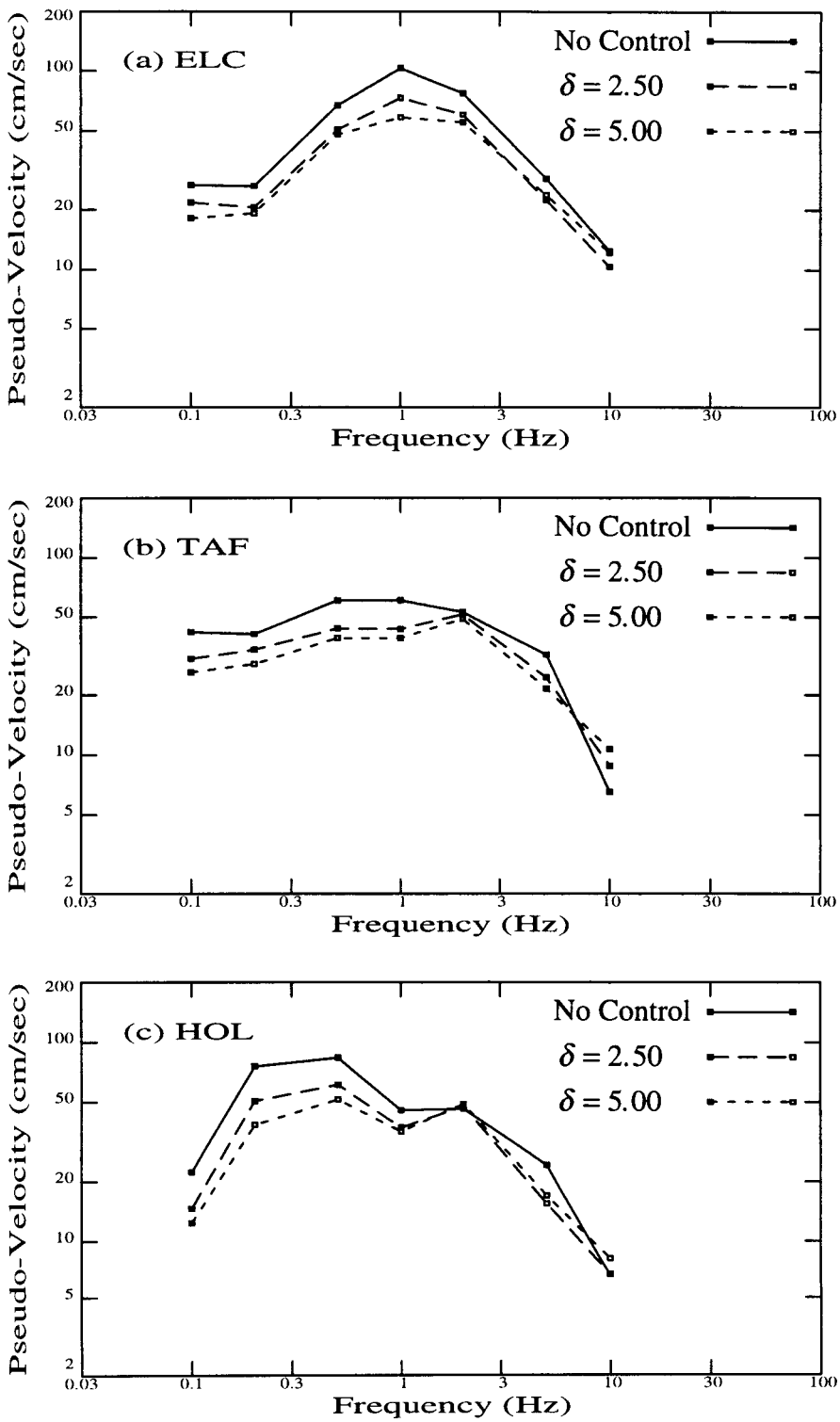

Figure 3.16. Response Spectra of Category 6 Controlled Cases for Various Values of δ — with $\alpha = 0.50$, $\beta = 5.00$, and $\gamma = \sqrt{\alpha\beta}$ — for the (a) El Centro, (b) Taft Lincoln School Tunnel, and (c) Holiday Inn Excitation Records. Results are for primary system.

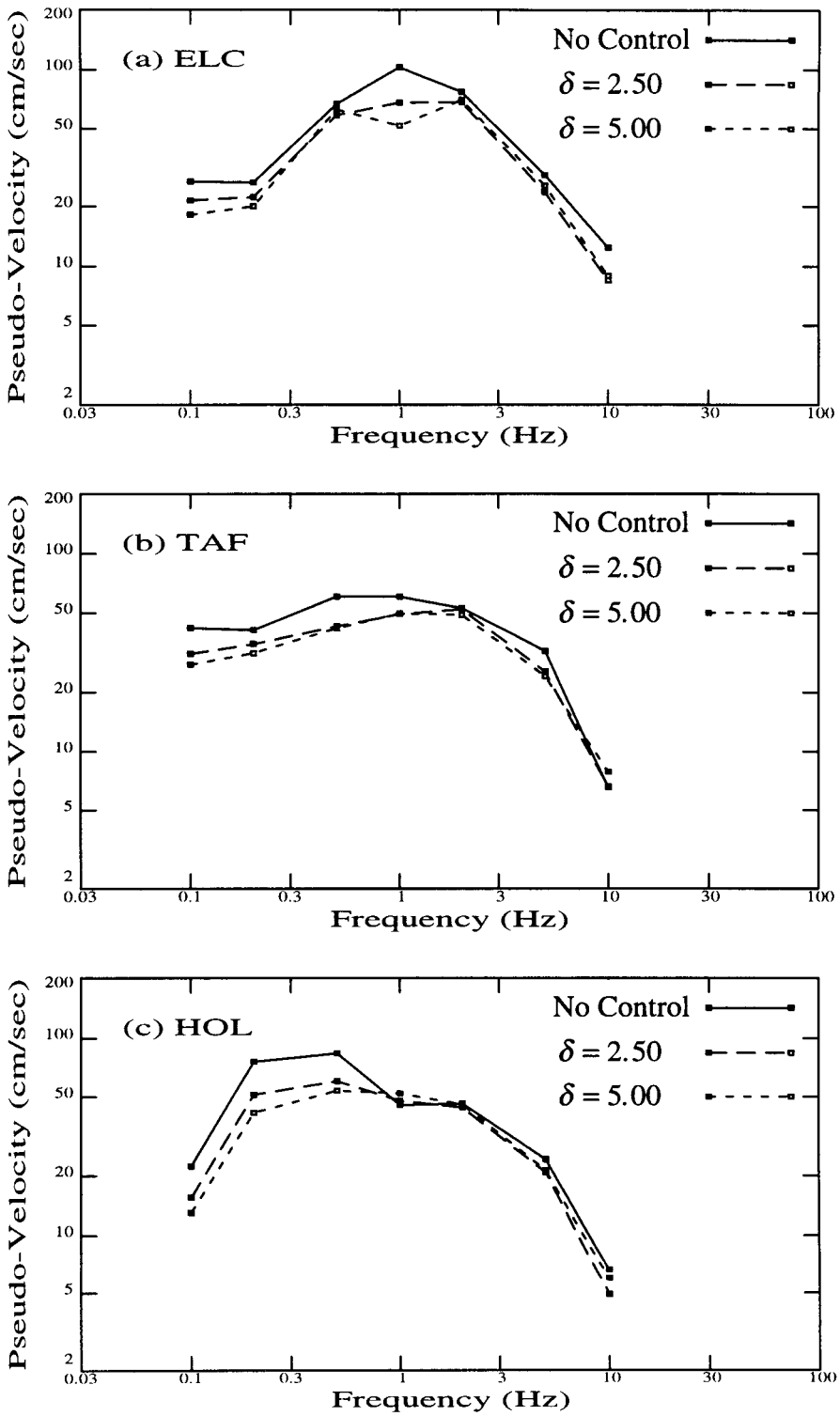

Figure 3.17. Response Spectra of Category 6 Controlled Cases for Various Values of δ — with $\alpha = 2.00$, $\beta = 5.00$, and $\gamma = \sqrt{\alpha\beta}$ — for the (a) El Centro, (b) Taft Lincoln School Tunnel, and (c) Holiday Inn Excitation Records. Results are for primary system.

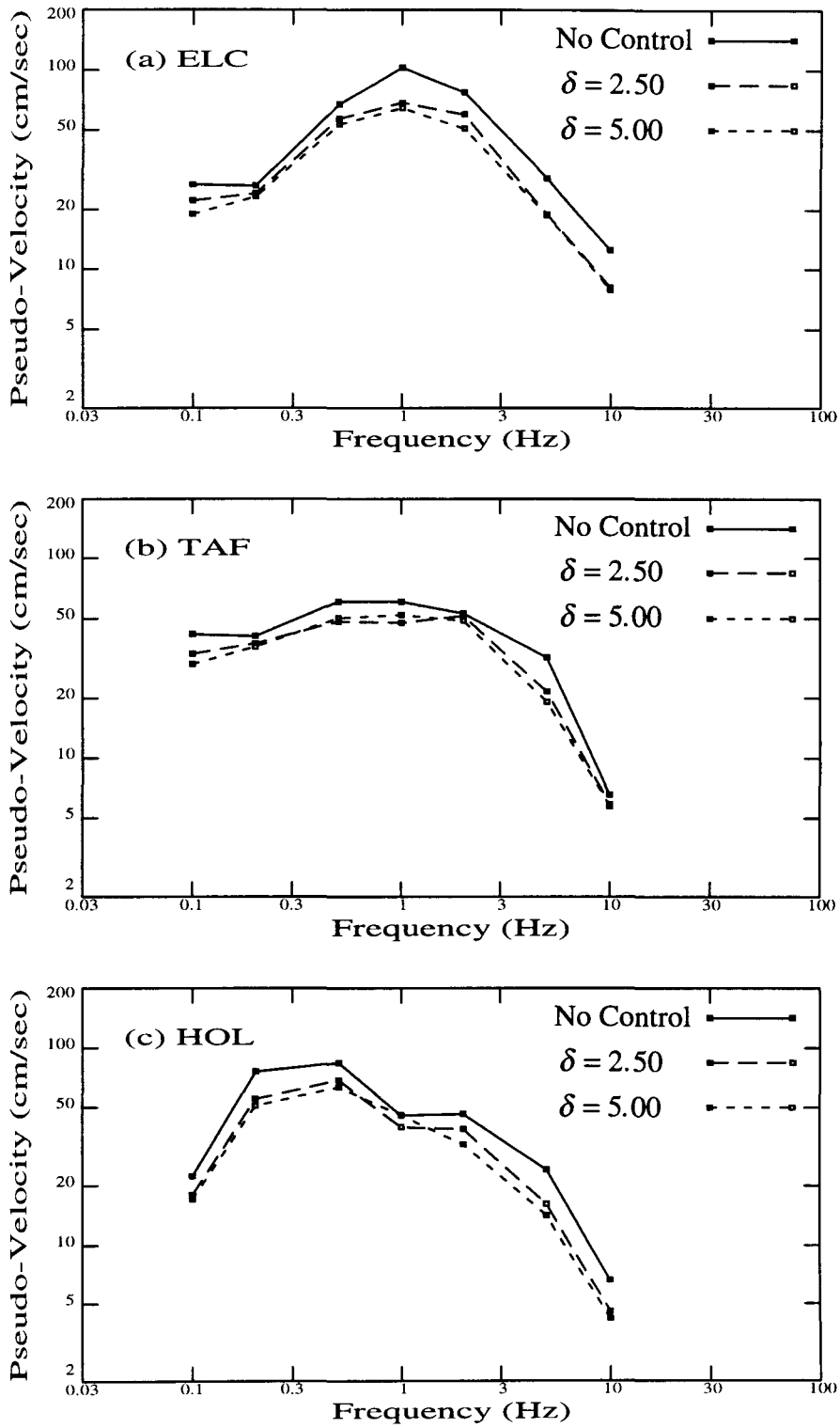

Figure 3.18. Response Spectra of Category 6 Controlled Cases for Various Values of δ — with $\alpha = 8.00$, $\beta = 5.00$, and $\gamma = \sqrt{\alpha\beta}$ — for the (a) El Centro, (b) Taft Lincoln School Tunnel, and (c) Holiday Inn Excitation Records. Results are for primary system.

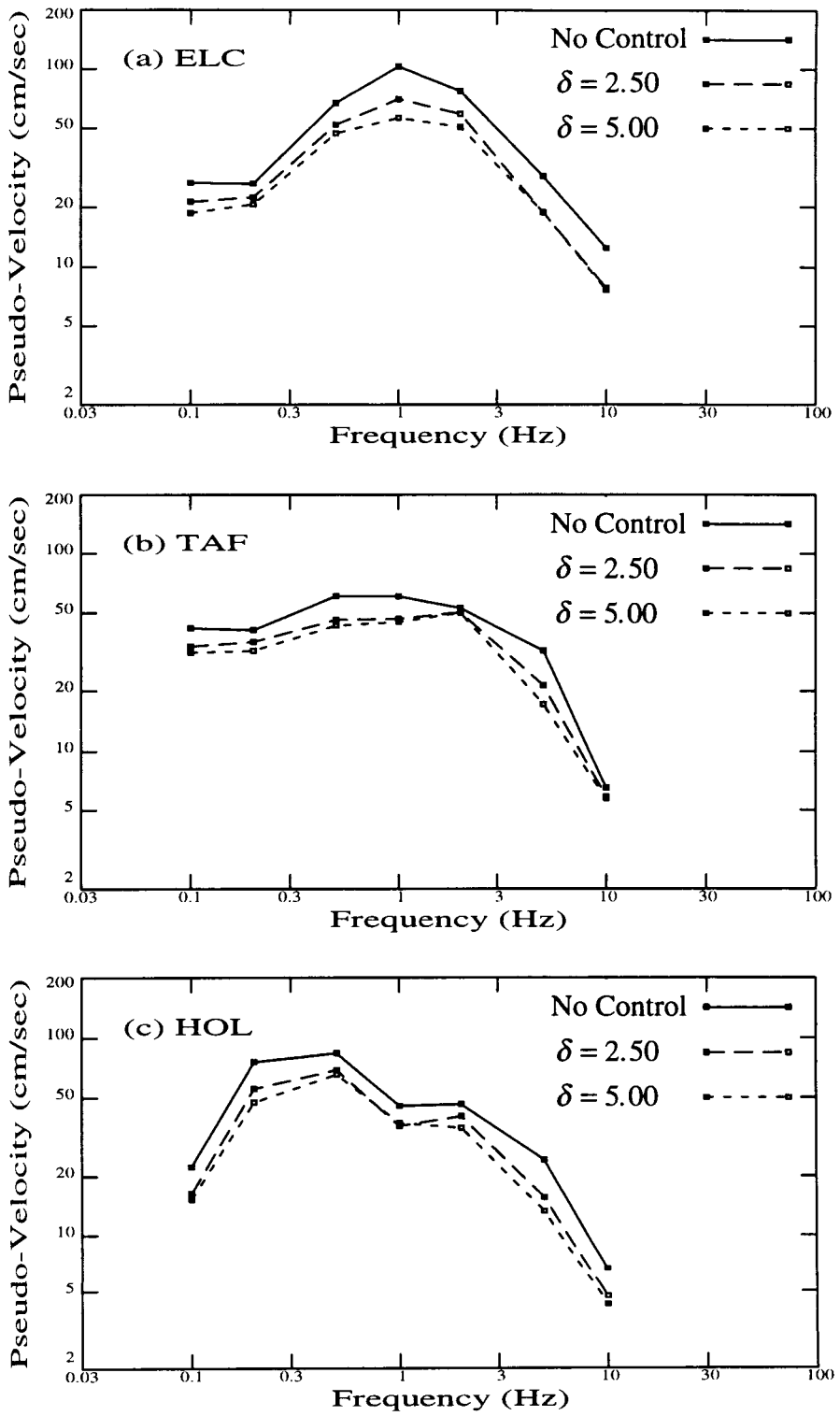

Figure 3.19. Response Spectra of Category 7 Controlled Cases for Various Values of δ — with $\alpha = 0.50$, $\beta = 0.20$, and $\gamma = \sqrt{\alpha\beta}$ — for the (a) El Centro, (b) Taft Lincoln School Tunnel, and (c) Holiday Inn Excitation Records. Results are for primary system.

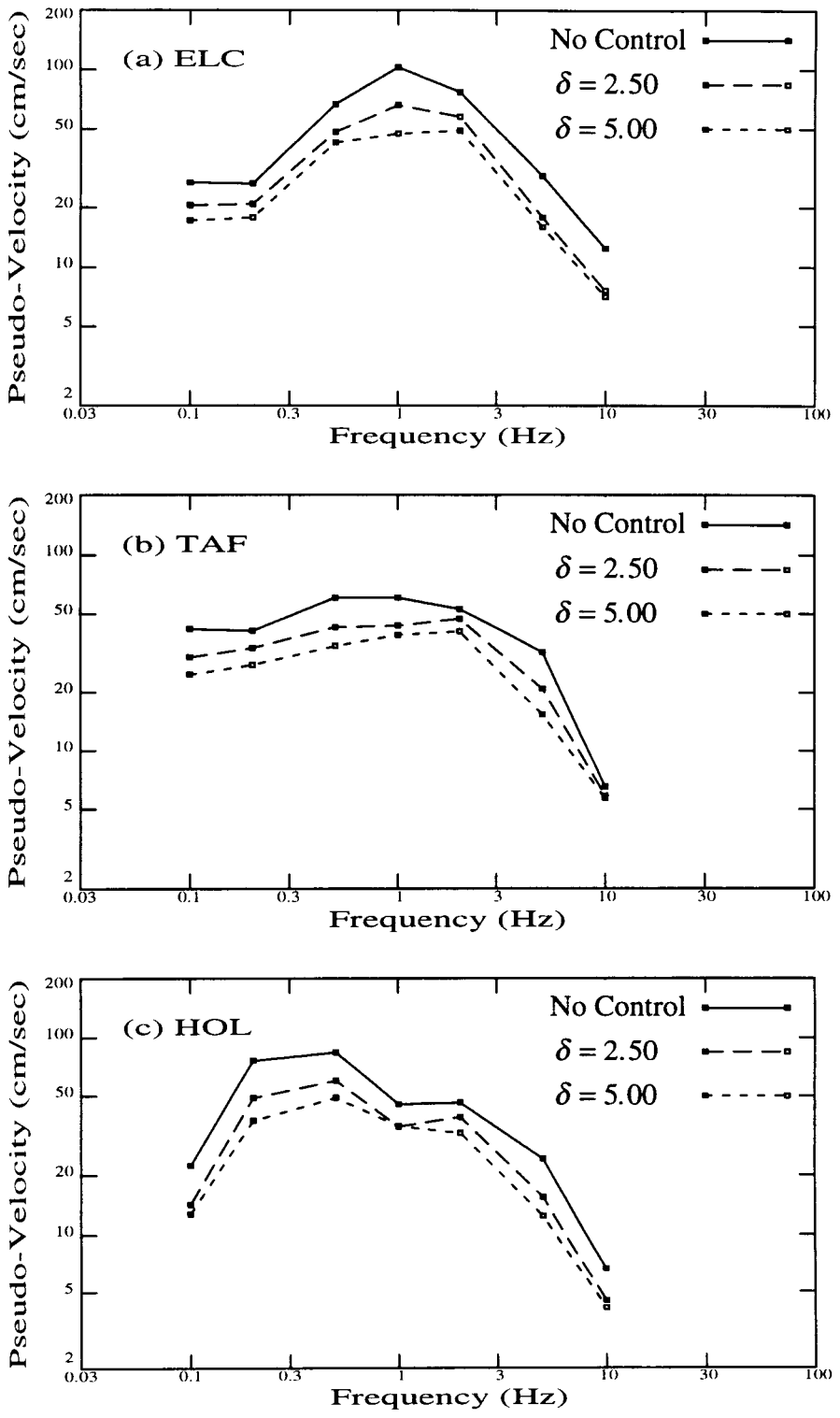

Figure 3.20. Response Spectra of Category 7 Controlled Cases for Various Values of δ — with $\alpha = 2.00$, $\beta = 0.20$, and $\gamma = \sqrt{\alpha\beta}$ — for the (a) El Centro, (b) Taft Lincoln School Tunnel, and (c) Holiday Inn Excitation Records. Results are for primary system.

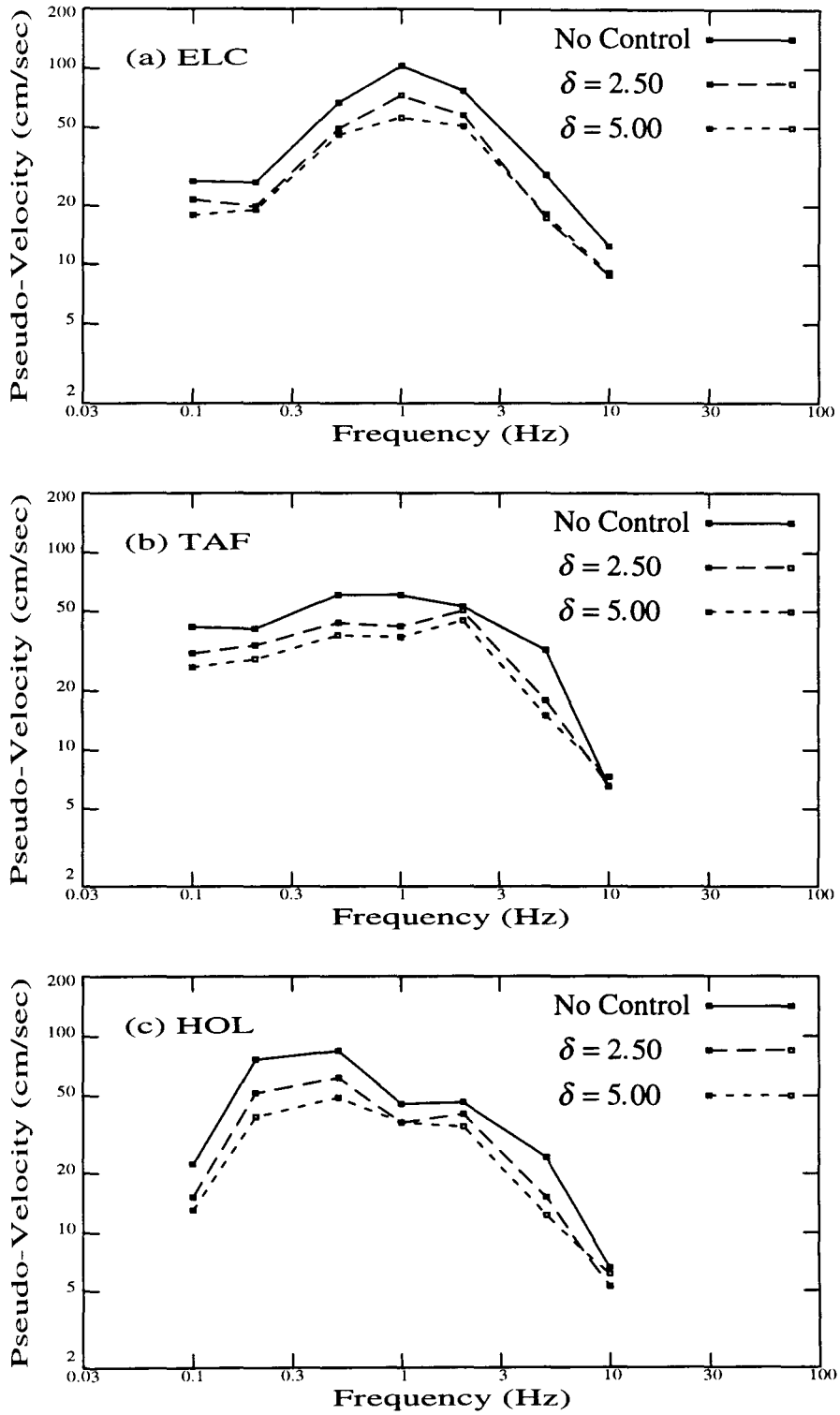

Figure 3.21. Response Spectra of Category 7 Controlled Cases for Various Values of δ — with $\alpha = 0.50$, $\beta = 5.00$, and $\gamma = \sqrt{\alpha\beta}$ — for the (a) El Centro, (b) Taft Lincoln School Tunnel, and (c) Holiday Inn Excitation Records. Results are for primary system.

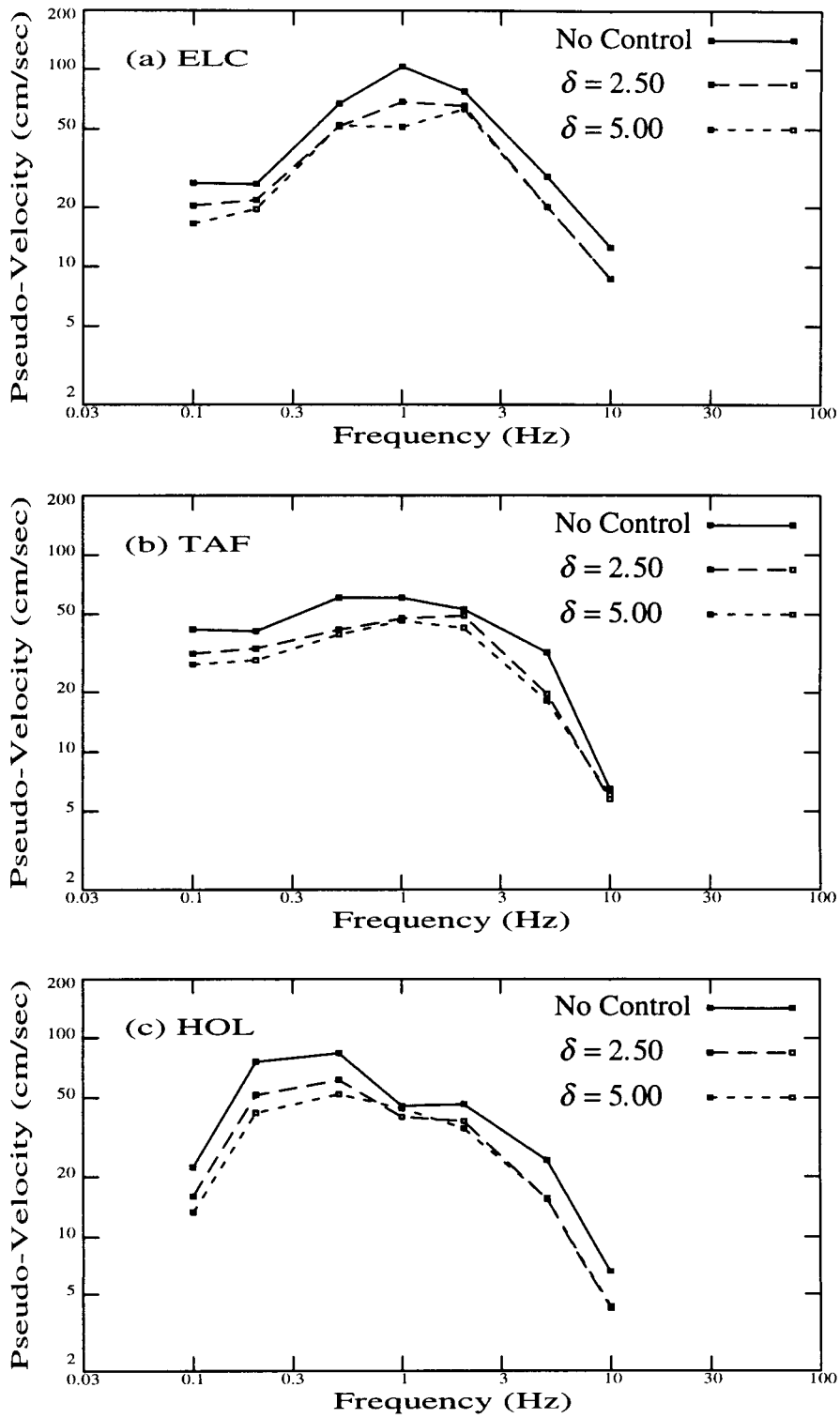

Figure 3.22. Response Spectra of Category 7 Controlled Cases for Various Values of δ — with $\alpha = 2.00$, $\beta = 5.00$, and $\gamma = \sqrt{\alpha\beta}$ — for the (a) El Centro, (b) Taft Lincoln School Tunnel, and (c) Holiday Inn Excitation Records. Results are for primary system.

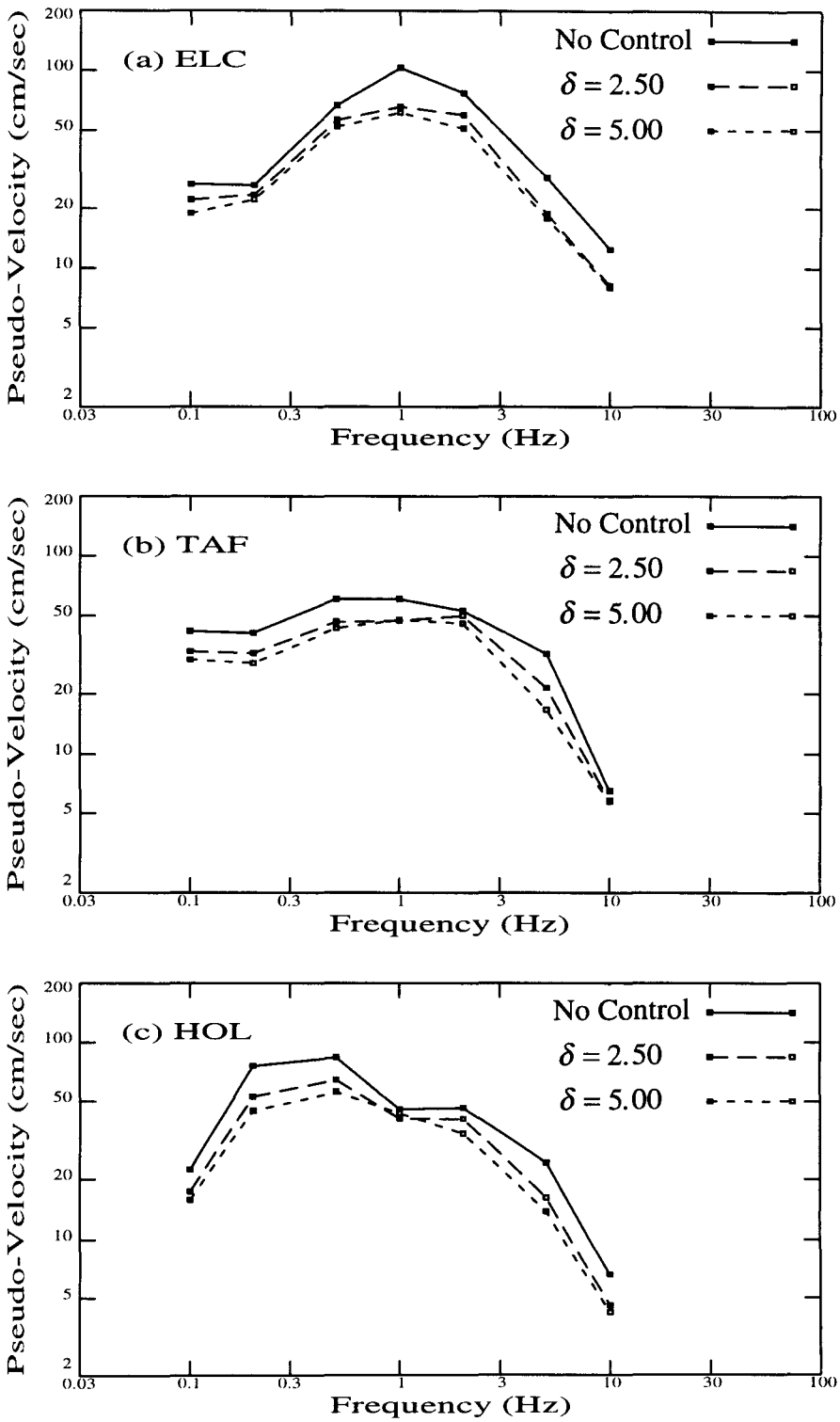

Figure 3.23. Response Spectra of Category 7 Controlled Cases for Various Values of δ — with $\alpha = 8.00$, $\beta = 5.00$, and $\gamma = \sqrt{\alpha\beta}$ — for the (a) El Centro, (b) Taft Lincoln School Tunnel, and (c) Holiday Inn Excitation Records. Results are for primary system.

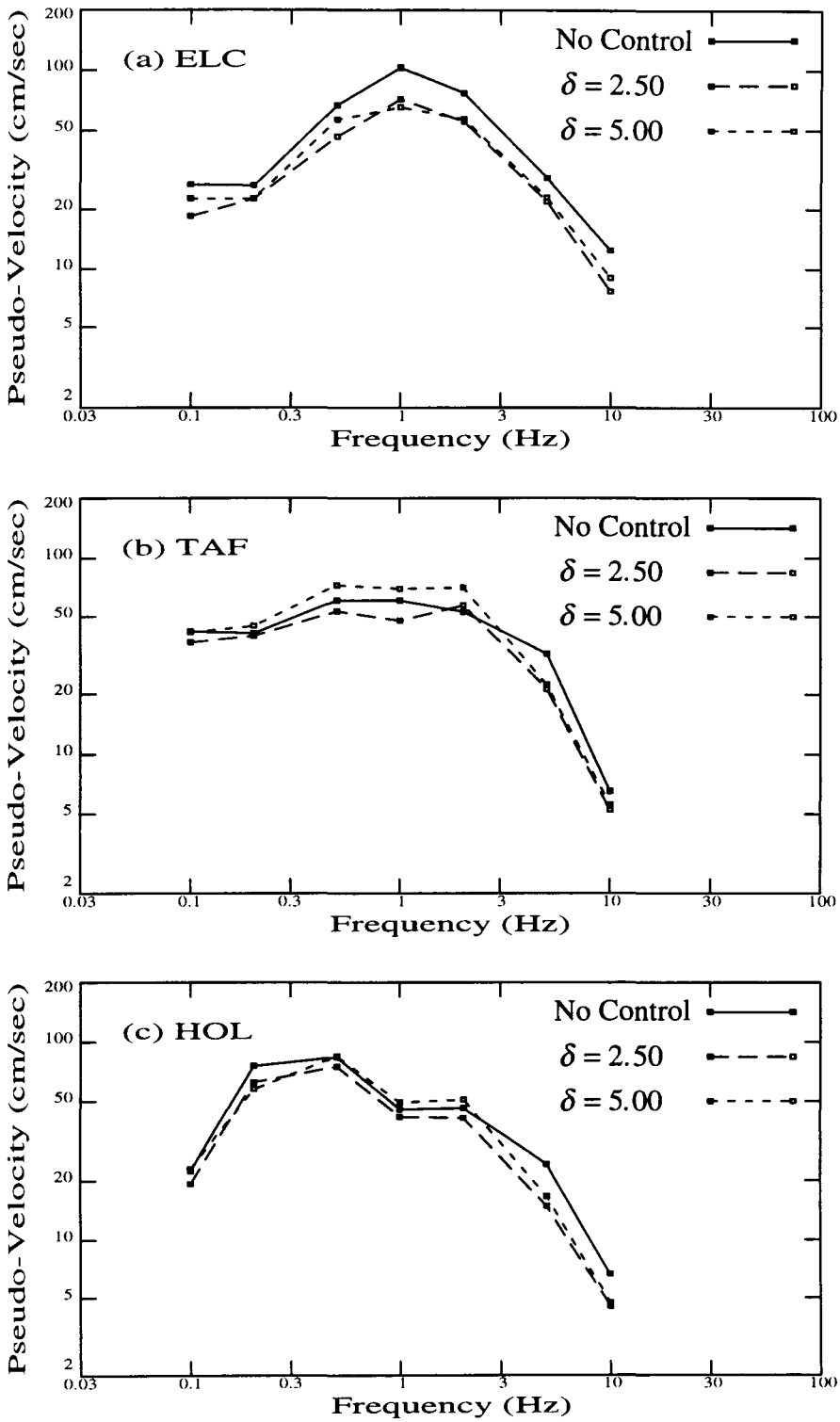

Figure 3.24. Response Spectra of Category 8 Controlled Cases for Various Values of δ — with $\alpha = 0.50$, $\beta = 0.20$, and $\gamma = \sqrt{\alpha\beta}$ — for the (a) El Centro, (b) Taft Lincoln School Tunnel, and (c) Holiday Inn Excitation Records. Results are for primary system.

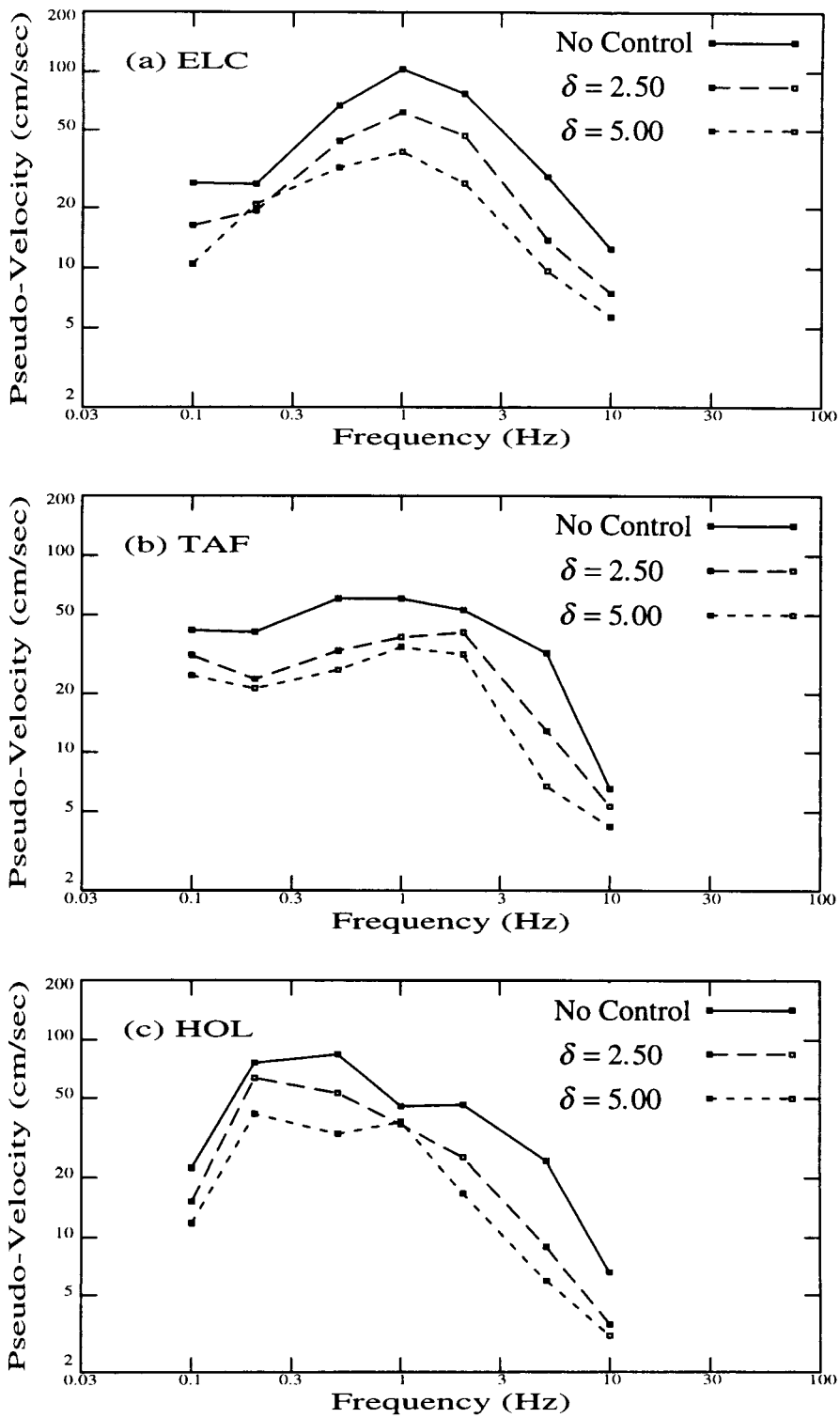

Figure 3.25. Response Spectra of Category 8 Controlled Cases for Various Values of δ — with $\alpha = 2.00$, $\beta = 0.20$, and $\gamma = \sqrt{\alpha\beta}$ — for the (a) El Centro, (b) Taft Lincoln School Tunnel, and (c) Holiday Inn Excitation Records. Results are for primary system.

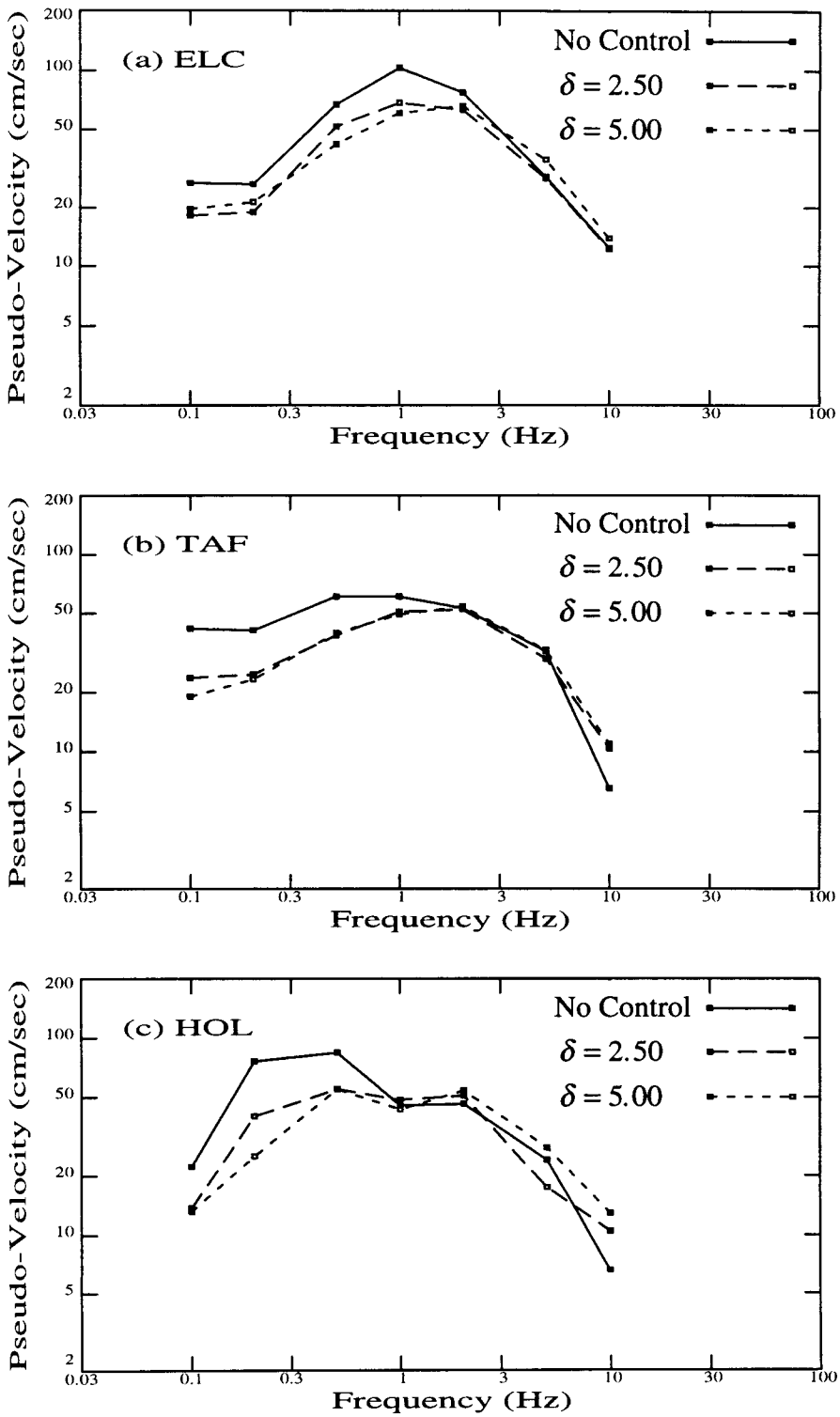

Figure 3.26. Response Spectra of Category 8 Controlled Cases for Various Values of δ — with $\alpha = 0.50$, $\beta = 5.00$, and $\gamma = \sqrt{\alpha\beta}$ — for the (a) El Centro, (b) Taft Lincoln School Tunnel, and (c) Holiday Inn Excitation Records. Results are for primary system.

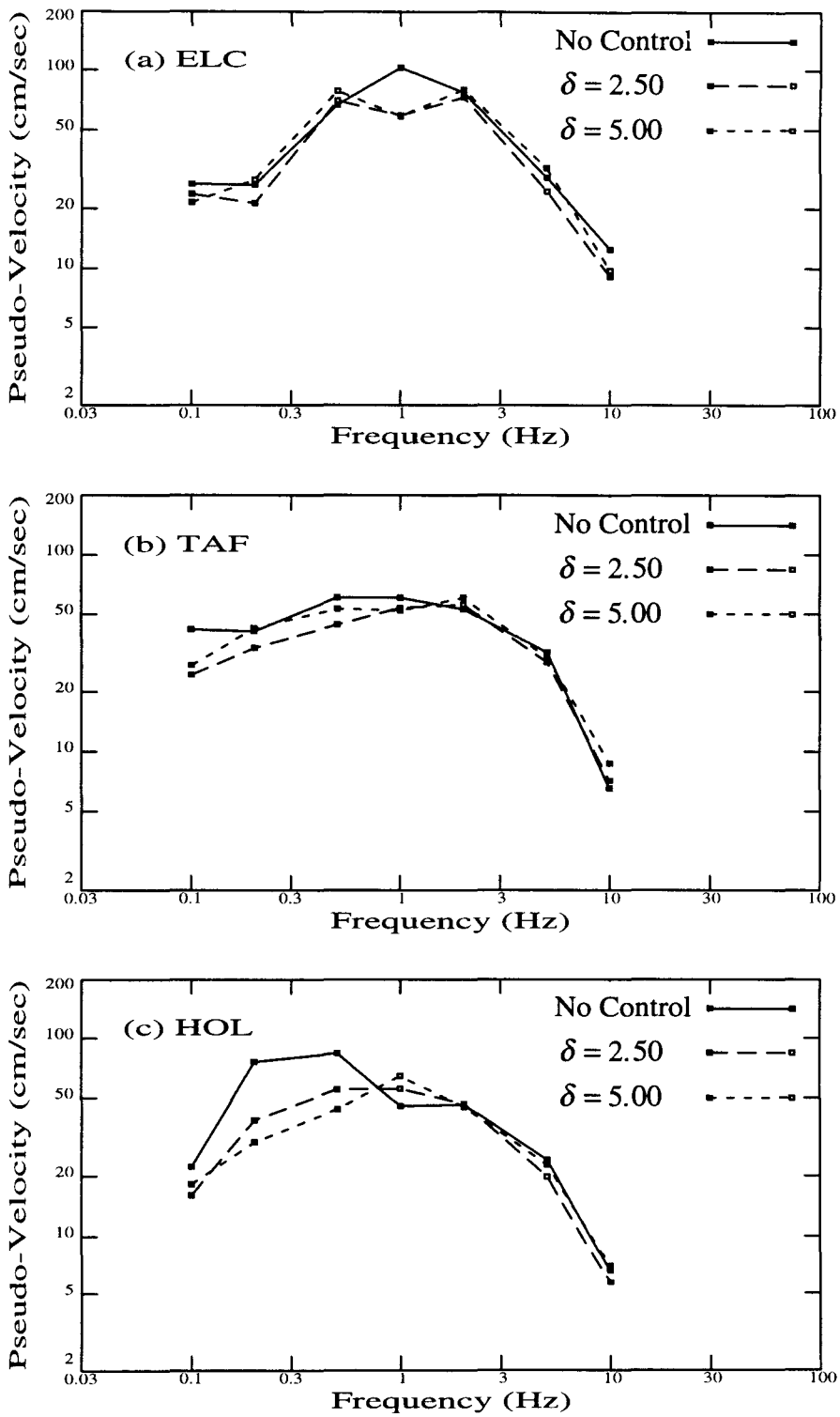

Figure 3.27. Response Spectra of Category 8 Controlled Cases for Various Values of δ — with $\alpha = 2.00$, $\beta = 5.00$, and $\gamma = \sqrt{\alpha\beta}$ — for the (a) El Centro, (b) Taft Lincoln School Tunnel, and (c) Holiday Inn Excitation Records. Results are for primary system.

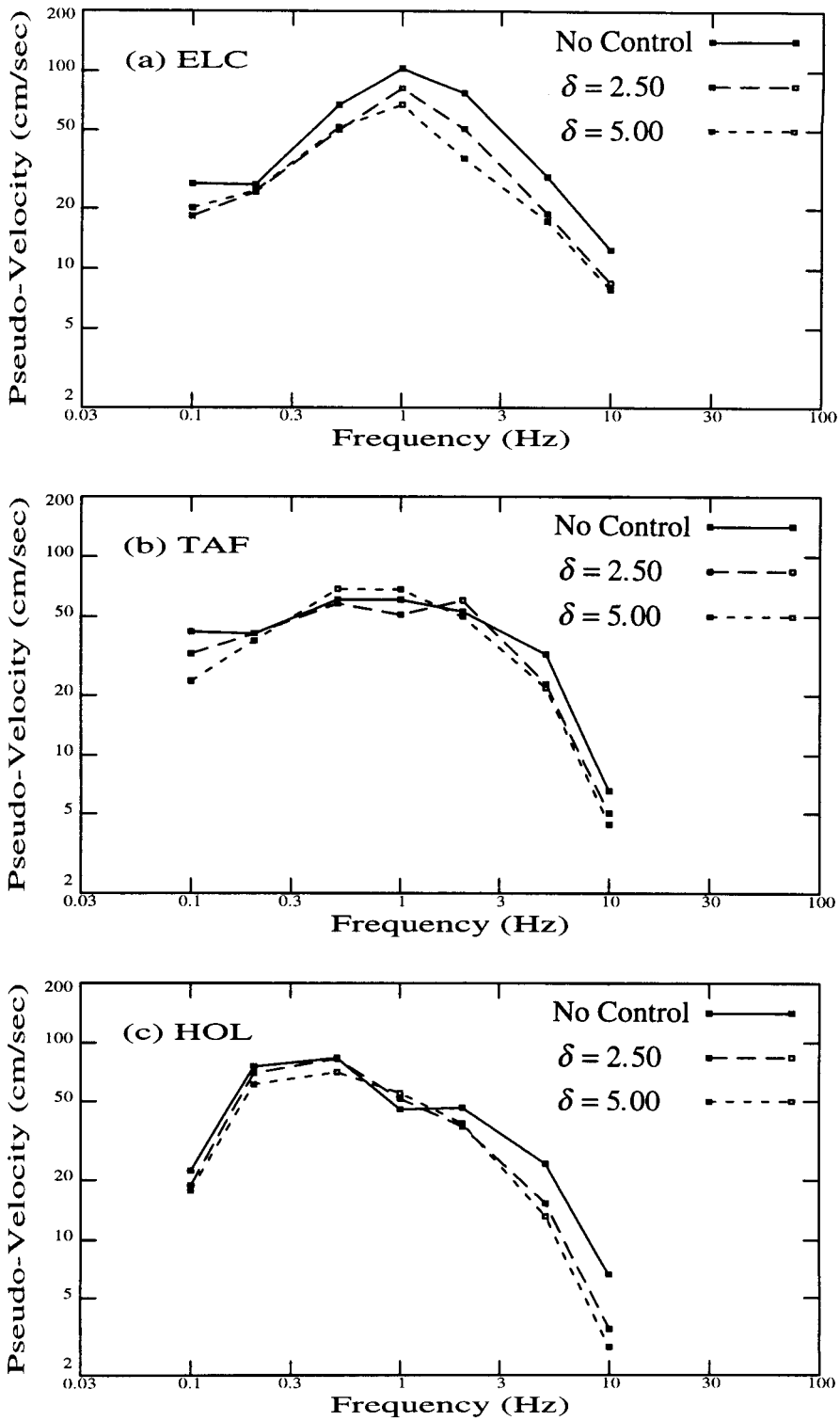

Figure 3.28. Response Spectra of Category 8 Controlled Cases for Various Values of δ — with $\alpha = 8.00$, $\beta = 5.00$, and $\gamma = \sqrt{\alpha\beta}$ — for the (a) El Centro, (b) Taft Lincoln School Tunnel, and (c) Holiday Inn Excitation Records. Results are for primary system.

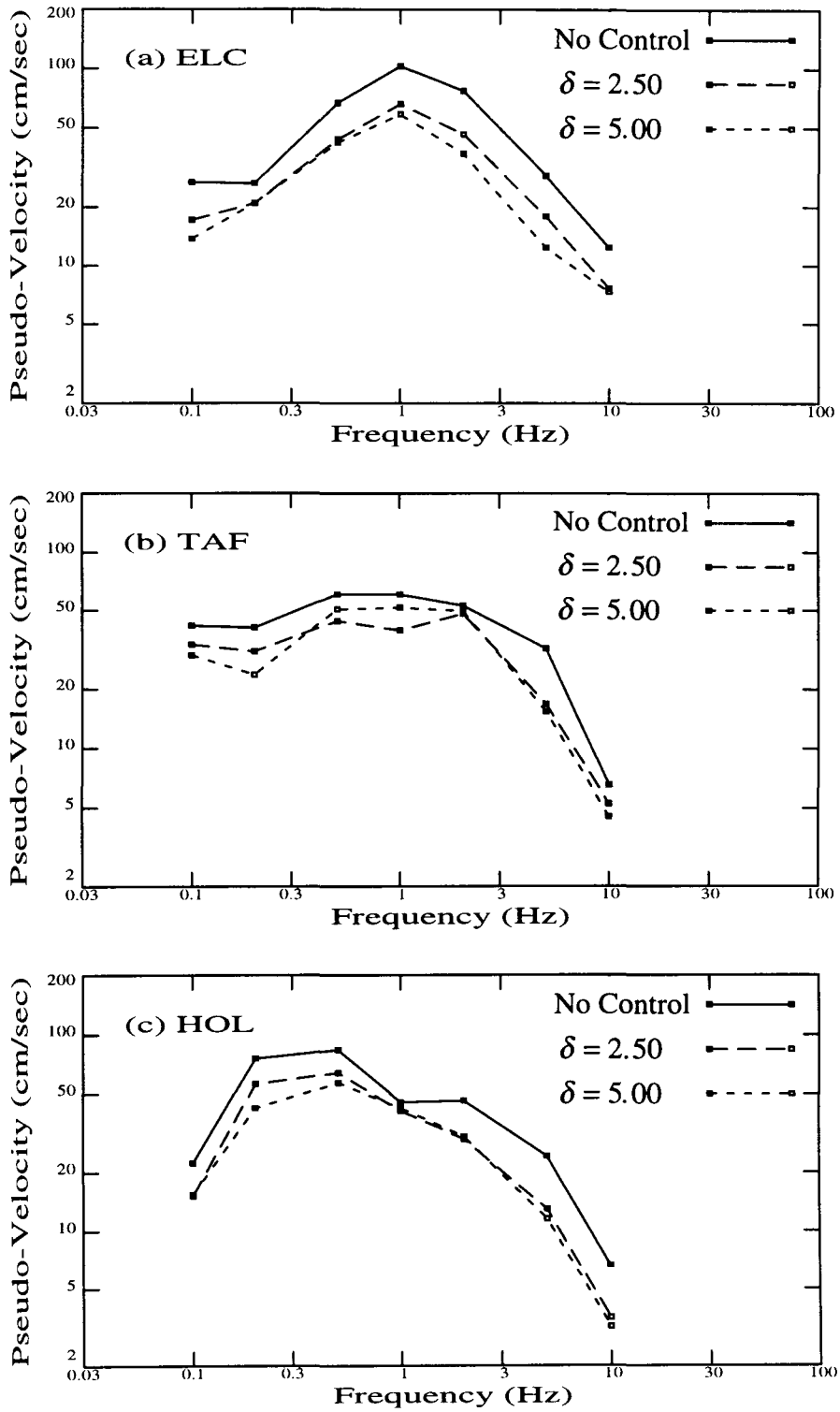

Figure 3.29. Response Spectra of Category 9 Controlled Cases for Various Values of δ — with $\alpha = 0.50$, $\beta = 0.20$, and $\gamma = \sqrt{\alpha\beta}$ — for the (a) El Centro, (b) Taft Lincoln School Tunnel, and (c) Holiday Inn Excitation Records. Results are for primary system.

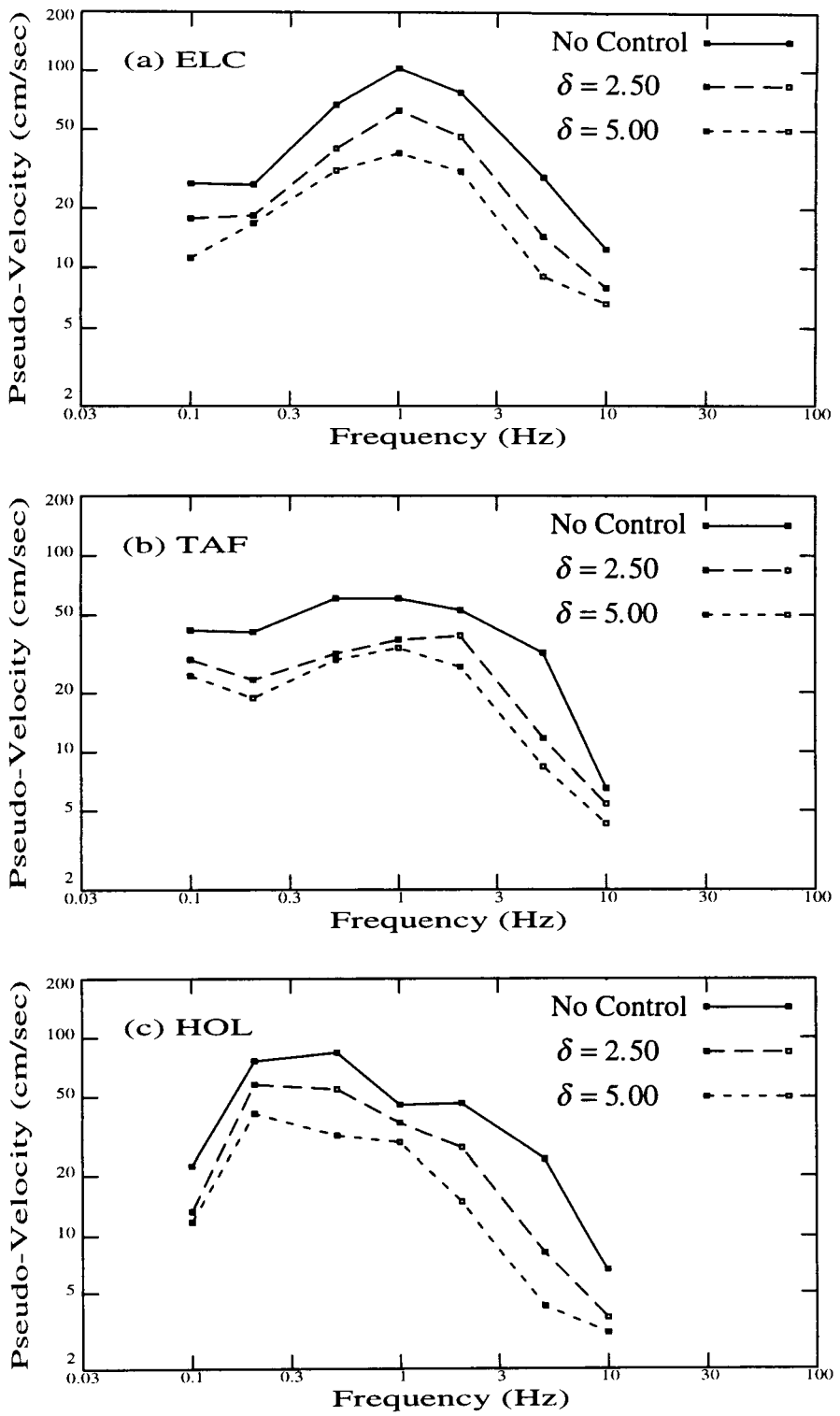

Figure 3.30. Response Spectra of Category 9 Controlled Cases for Various Values of δ — with $\alpha = 2.00$, $\beta = 0.20$, and $\gamma = \sqrt{\alpha\beta}$ — for the (a) El Centro, (b) Taft Lincoln School Tunnel, and (c) Holiday Inn Excitation Records. Results are for primary system.

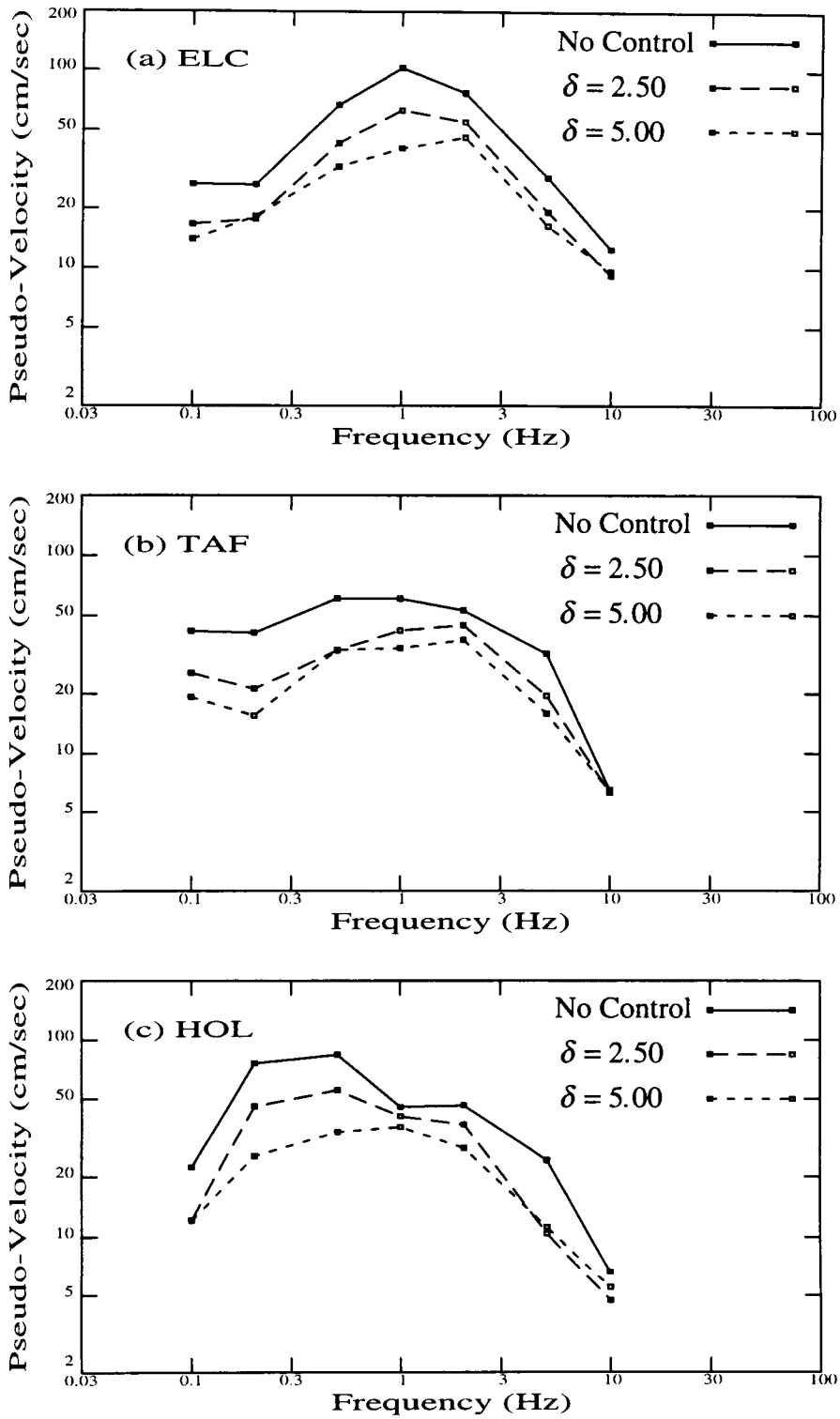

Figure 3.31. Response Spectra of Category 9 Controlled Cases for Various Values of δ — with $\alpha = 0.50$, $\beta = 5.00$, and $\gamma = \sqrt{\alpha\beta}$ — for the (a) El Centro, (b) Taft Lincoln School Tunnel, and (c) Holiday Inn Excitation Records. Results are for primary system.

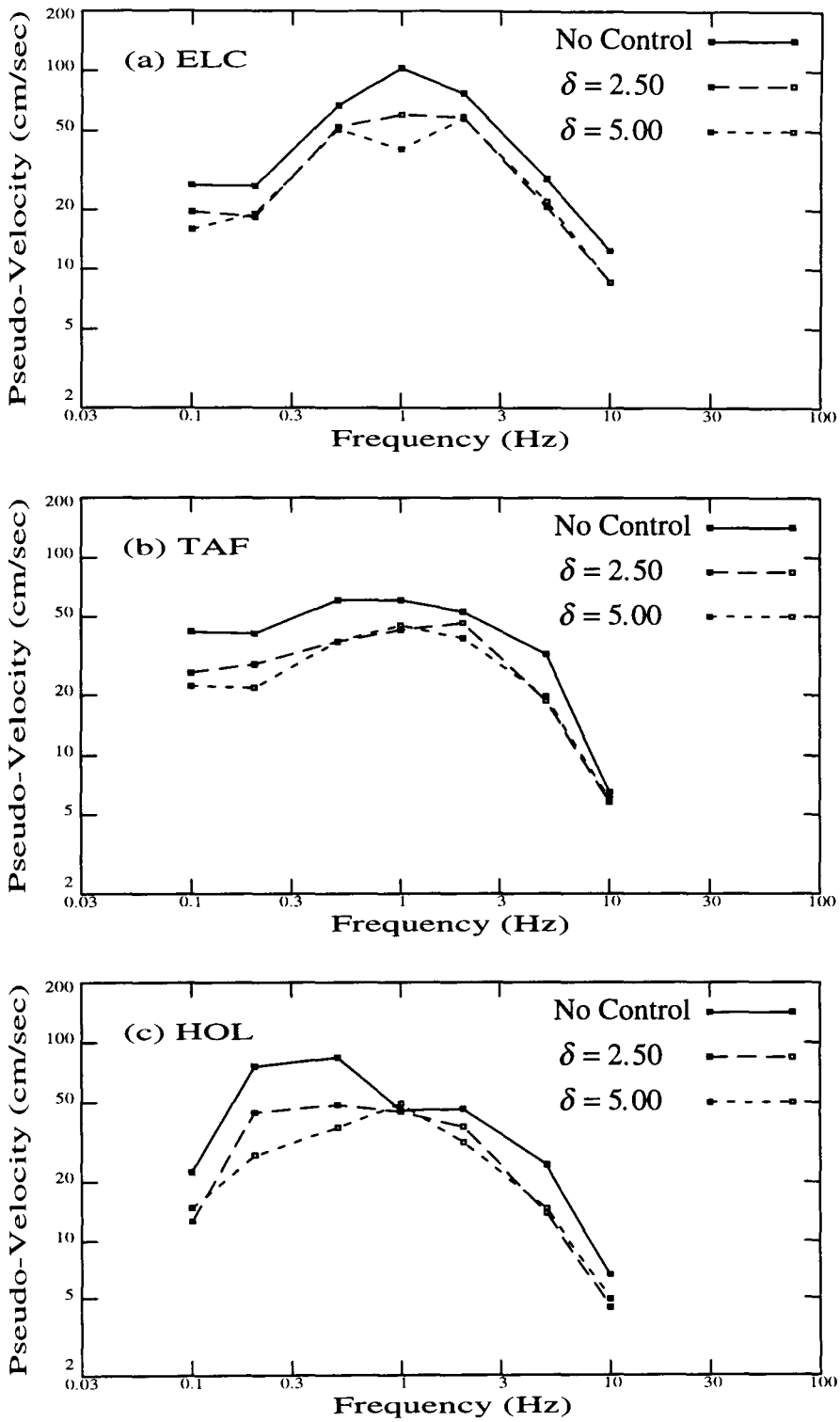

Figure 3.32. Response Spectra of Category 9 Controlled Cases for Various Values of δ — with $\alpha = 2.00$, $\beta = 5.00$, and $\gamma = \sqrt{\alpha\beta}$ — for the (a) El Centro, (b) Taft Lincoln School Tunnel, and (c) Holiday Inn Excitation Records. Results are for primary system.

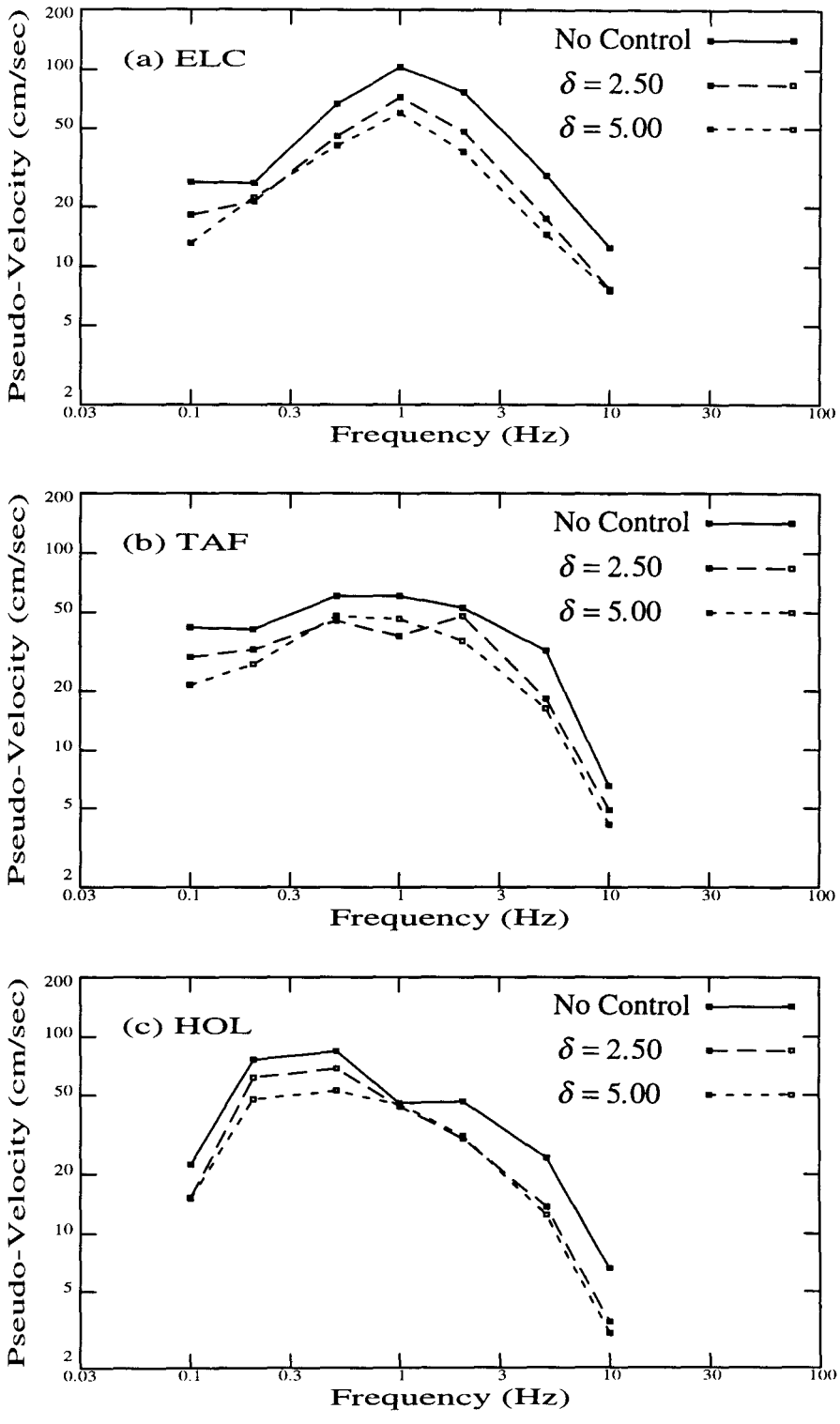

Figure 3.33. Response Spectra of Category 9 Controlled Cases for Various Values of δ — with $\alpha = 8.00$, $\beta = 5.00$, and $\gamma = \sqrt{\alpha\beta}$ — for the (a) El Centro, (b) Taft Lincoln School Tunnel, and (c) Holiday Inn Excitation Records. Results are for primary system.

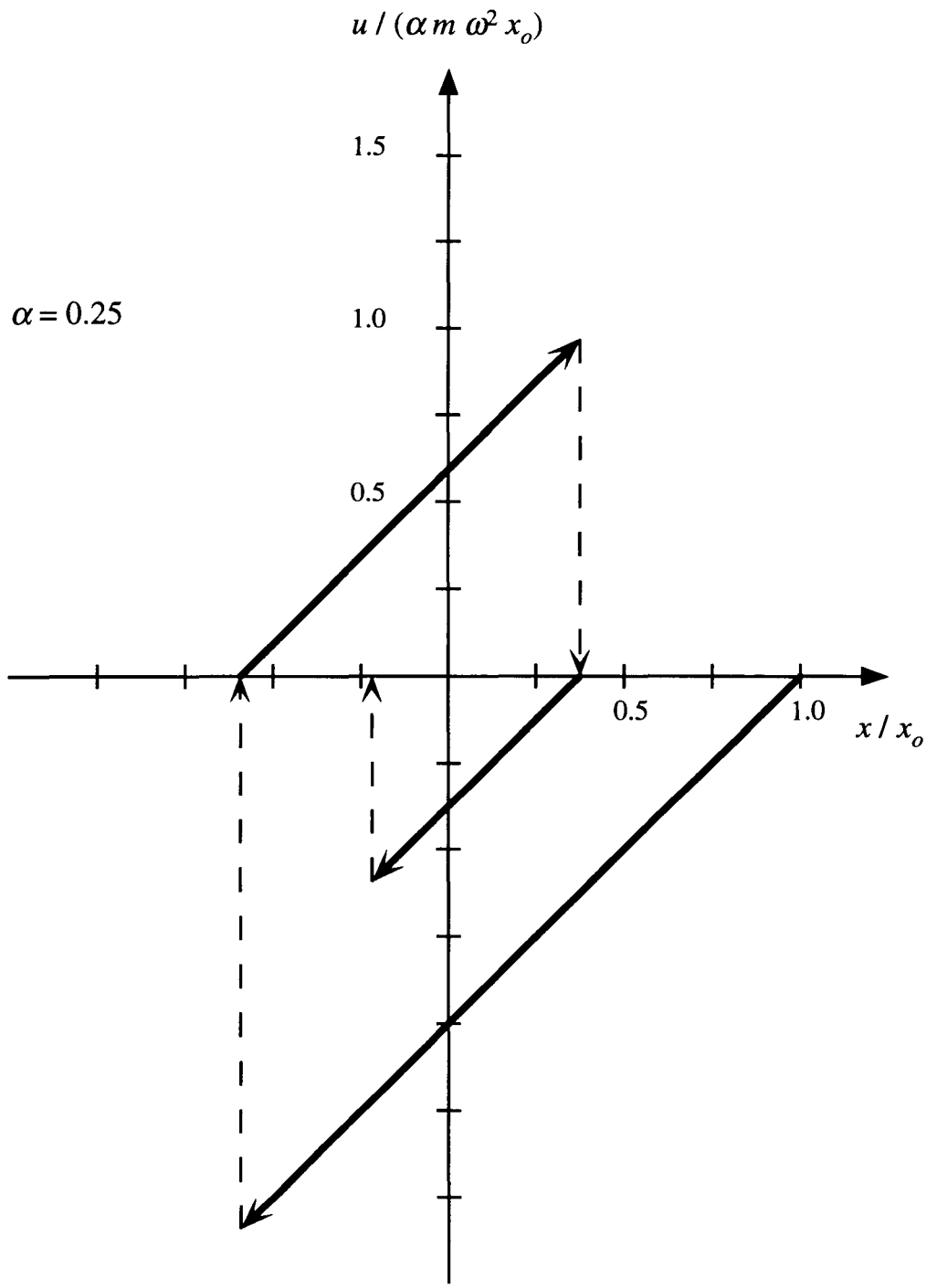

Figure 3.34. Force-Displacement Time-History According to Relations Given in (3-34).

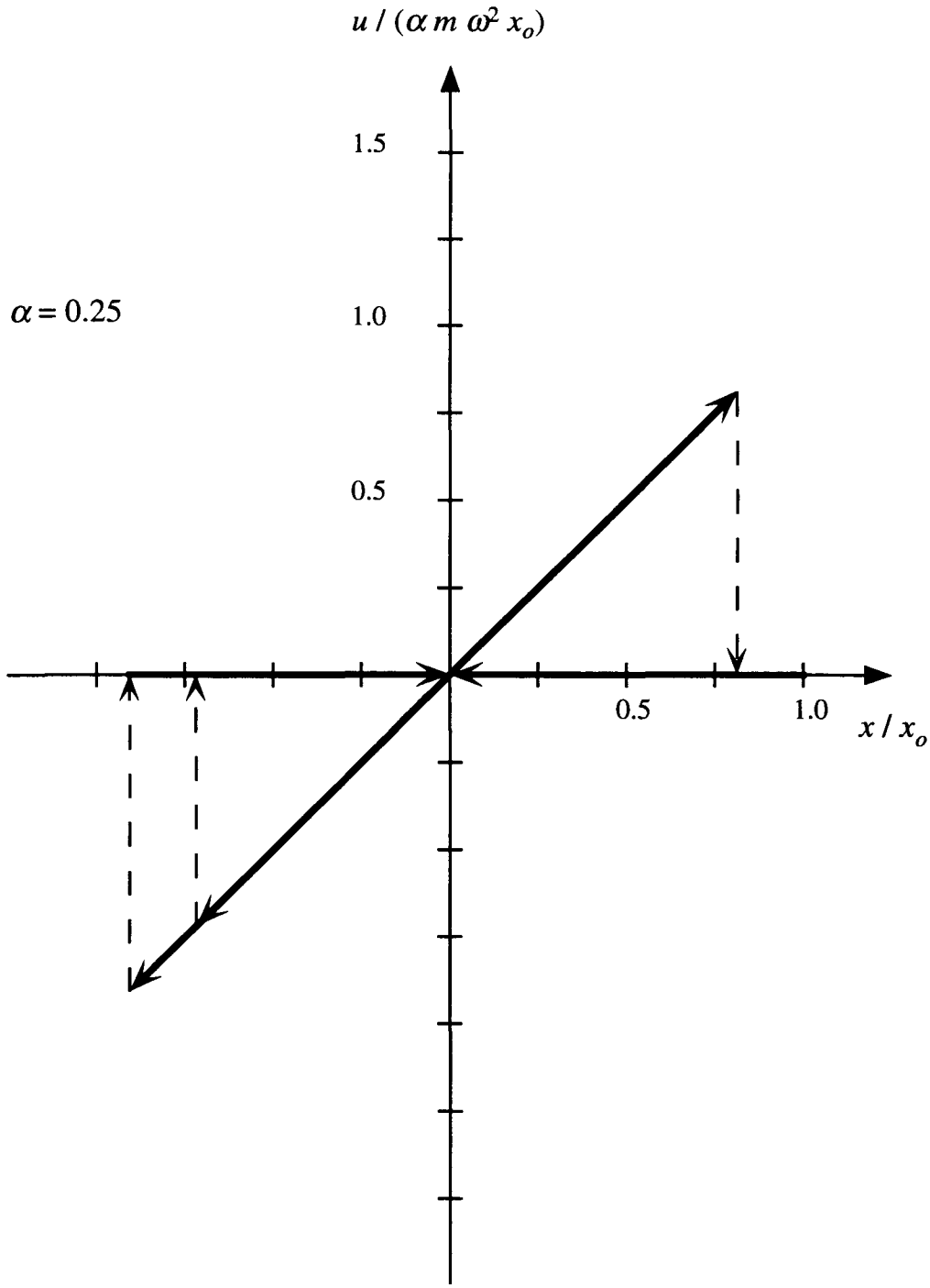

Figure 3.35. Force-Displacement Time-History According to Relations Given in (3-35).

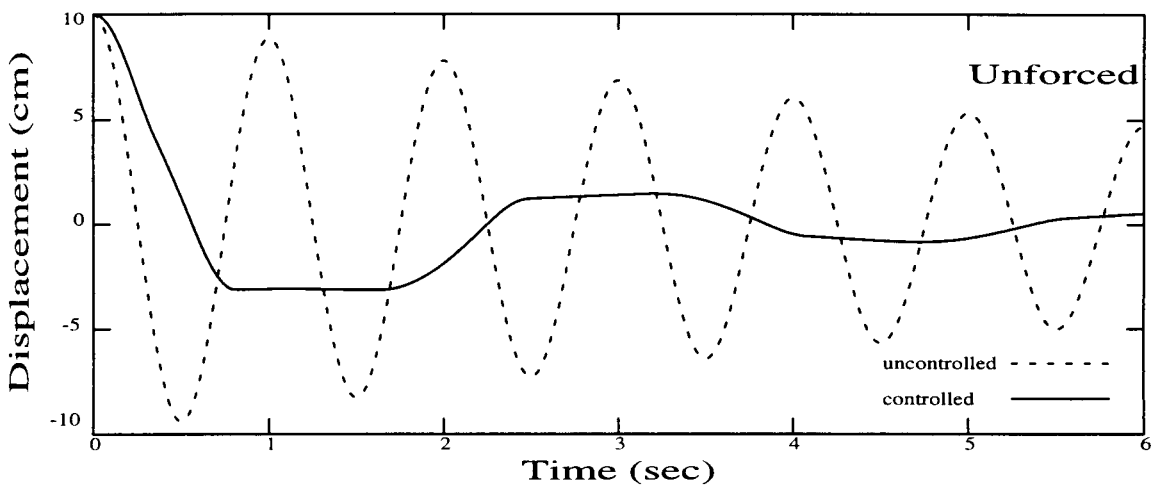

Figure 3.36. Response Time-History of Relative Displacement for a SDOF Category 9 Controlled Primary System which is Unforced, Initially at Rest, but Given an Initial Displacement. A semi-active Coulomb-damped member is used, with $\varepsilon_s = 0.25$. $\alpha = 0.00$ and $\beta = 5.00$.

Table 3.1. Descriptive Summary of Control Category Features for SDOF System Study.

Control Category	Control Strategy Implementation	Interaction Element Operation	Physical Nature of Interaction	$\alpha \equiv \frac{k_2}{k_1}$	$\beta \equiv \frac{m_2}{m_1}$	$\gamma \equiv \frac{c_2}{c_1}$	$\delta \equiv \frac{c_{int}}{c_1}$	Qualitative Performance Assessment
1	Method 1	2-state	Rigidly-Connected	0.5 – 2.0	0	0	—	E
2	Method 1	2-state	Rigidly-Connected	0	0.2 – 5.0	0	—	P
3	Method 1	2-state	Rigidly-Connected	0.5 – 8.0	0.2 – 5.0	$\sqrt{\alpha\beta}$	—	S to G
4	Method 2	2-state	Impulsive	0	0.2 – 5.0	0	—	G to E
5	Method 2	2-state	Impulsive	0.5 – 8.0	0.2 – 5.0	$\sqrt{\alpha\beta}$	—	G
6	Method 1	1-state	Viscously-Damped	0.5 – 8.0	0.2 – 5.0	$\sqrt{\alpha\beta}$	2.5, 5.0	S to G
7	Method 1	2-state	Viscously-Damped	0.5 – 8.0	0.2 – 5.0	$\sqrt{\alpha\beta}$	2.5, 5.0	G to E
8	Method 1	1-state	Coulomb-Damped	0.5 – 8.0	0.2 – 5.0	$\sqrt{\alpha\beta}$	2.5, 5.0	S to G
9	Method 1	2-state	Coulomb-Damped	0.5 – 8.0	0.2 – 5.0	$\sqrt{\alpha\beta}$	2.5, 5.0	G to E

Note: E = Excellent, G = Good, S = Satisfactory, P = Poor

Table 3.2. Parameter Sets Used for Category 1 Control Cases.

Parameter Set	$\alpha \equiv \frac{k_2}{k_1}$	$\beta \equiv \frac{m_2}{m_1}$	$\gamma \equiv \frac{c_2}{c_1}$	ε_E
1	0.5	0.0	0.0	—
2	1.0	0.0	0.0	—
3	2.0	0.0	0.0	—

Table 3.3. Parameter Sets Used for Category 2 Control Cases.

Parameter Set	$\alpha \equiv \frac{k_2}{k_1}$	$\beta \equiv \frac{m_2}{m_1}$	$\gamma \equiv \frac{c_2}{c_1}$	ε_E
1	0.0	0.2	0.0	0.01
2	0.0	1.0	0.0	0.01
3	0.0	5.0	0.0	0.01

Table 3.4. Parameter Sets Used for Category 3 Control Cases.

Parameter Set	$\alpha \equiv \frac{k_2}{k_1}$	$\beta \equiv \frac{m_2}{m_1}$	$\gamma \equiv \frac{c_2}{c_1}$	ε_E
1	0.5	0.2	$\sqrt{\alpha\beta}$	0.01
2	0.5	5.0	$\sqrt{\alpha\beta}$	0.01
3	2.0	0.2	$\sqrt{\alpha\beta}$	0.01
4	2.0	5.0	$\sqrt{\alpha\beta}$	0.01
5	8.0	5.0	$\sqrt{\alpha\beta}$	0.01

Table 3.5. Parameter Sets Used for Category 4 Control Cases.

Parameter Set	$\alpha \equiv \frac{k_2}{k_1}$	$\beta \equiv \frac{m_2}{m_1}$	$\gamma \equiv \frac{c_2}{c_1}$	n_P
1	0.0	0.2	0.0	2
2	0.0	1.0	0.0	2
3	0.0	5.0	0.0	2

Table 3.6. Parameter Sets Used for Category 5 Control Cases.

Parameter Set	$\alpha \equiv \frac{k_2}{k_1}$	$\beta \equiv \frac{m_2}{m_1}$	$\gamma \equiv \frac{c_2}{c_1}$	n_P
1	0.5	0.2	$\sqrt{\alpha\beta}$	2
2	0.5	5.0	$\sqrt{\alpha\beta}$	2
3	2.0	0.2	$\sqrt{\alpha\beta}$	2
4	2.0	5.0	$\sqrt{\alpha\beta}$	2
5	8.0	5.0	$\sqrt{\alpha\beta}$	2

Table 3.7. Parameter Sets Used for Categories 6 through 9 Control Cases.

Parameter Set	$\alpha \equiv \frac{k_2}{k_1}$	$\beta \equiv \frac{m_2}{m_1}$	$\gamma \equiv \frac{c_2}{c_1}$	$\delta \equiv \frac{c_{int}}{c_1}$
1	0.5	0.2	$\sqrt{\alpha\beta}$	2.5, 5.0
2	0.5	5.0	$\sqrt{\alpha\beta}$	2.5, 5.0
3	2.0	0.2	$\sqrt{\alpha\beta}$	2.5, 5.0
4	2.0	5.0	$\sqrt{\alpha\beta}$	2.5, 5.0
5	8.0	5.0	$\sqrt{\alpha\beta}$	2.5, 5.0

Chapter 4

Response Control of Linear MDOF Systems Using Active Interface Damping

4.1 Introduction

In Chapter 3, a preliminary study which examined various applications of the Active Interface Damping control approach to cases that involved two interacting SDOF systems was presented. This investigation was intended to be exploratory in nature but not exhaustive in extent. In this chapter, a follow-on study of the proposed control approach is presented. This investigation considers linear MDOF primary and auxiliary systems which are intended to represent actual structural systems. However, in some instances, the auxiliary system may represent an externally-situated resilient frame or a relatively small, unrestrained mass rather than a conventional structural system; in other instances, the auxiliary system is completely absent, and the interaction elements are merely attached between different components of the primary system. Using the results and insight obtained from the previous study, a reduced number of control cases are examined in the present study which include those deemed most effective and implementable.

As before, the control objective is to reduce the resonance buildup in the response of the primary system that is produced by an external excitation. The strategy employed to achieve this objective is to remove energy associated with one or several modes of vibration from the primary system through either interaction of the primary system with the auxiliary system or interaction of the primary system with itself and its base. A control algorithm is used to permit only those interactions which are anticipated to be favorable to the control strategy. Again, the interactions consist of reaction forces that are developed within and transmitted through interaction elements, whose mechanical

properties can be altered in real time by control signals.

4.2 Problem Formulation

The following conditions are assumed to hold in this study: 1) the primary system and the auxiliary system (when present) are subjected to the same base acceleration and respond linearly; 2) the systems are discrete models of multi-story structural systems, whose nodal masses are only capable of horizontal deformations from their equilibrium positions; 3) the systems possess classical normal response modes, and the damping matrix resulting from the discretization process is obtained by specifying values for the modal damping ratios; 4) the interaction elements function passively, are considered to be massless, and are characterized by parameters associated with their mechanical properties that may be instantaneously changed in real time by control signals; 5) the system states are completely observable, and all system parameters have been identified in advance; and 6) only current values of the base acceleration and system state variables are available to determine the control input.

The models used in this study represent two-dimensional uniformly-discretized structural systems, consisting of a series of identical stories formed by floor and roof slabs that are interconnected by elastic support columns which provide linear restoring forces. The mass of each slab is m_i, and the effective stiffness of all columns at each story is k_i, where $i \in \{1, 2\}$. The subscripts 1 and 2 are used to denote the primary and auxiliary systems, respectively. The equations used for the analysis of the systems are expressed in terms of the relative displacements of each slab from a vertically erected datum line which is fixed to the base of each system. A schematic illustration of a generic primary or auxiliary system is given in Figure 4.1.

Under these conditions, the equations of motion for the primary and auxiliary systems are expressible as

$$M_i \ddot{\boldsymbol{x}}_i + C_i \dot{\boldsymbol{x}}_i + K_i \boldsymbol{x}_i = \boldsymbol{f}_i - M_i \boldsymbol{v}_i \tag{4-1}$$

where the generally time-varying vectors $\boldsymbol{x}_i \in R^{n_i}$, $\boldsymbol{f}_i \in R^{n_i}$, and $\boldsymbol{v}_i \in R^{n_i}$ represent the relative displacements (as measured from the base), control forces, and excitation input associated with the ith system, respectively. The time-invariant matrices M_i, C_i, and K_i, assumed to be symmetric and positive definite, are directly related to the kinetic, dissipative, and elastic properties of the uncontrolled ith system, respectively.

For the purposes of later discussion, let the components of the time-varying vector $\boldsymbol{u} \in R^r$, referred to as the control input, represent the reaction forces developed within each of the interaction elements. Because each of the interaction elements is treated to be massless, a relationship exists between the control force acting on the ith system and the control input, which is given by

$$\boldsymbol{f}_i = -L_i \boldsymbol{u} \tag{4-2}$$

where the matrix L_i represents a mapping which relates the control forces applied to the ith system and its control input. The precise definition of L_i and the functional form for $\boldsymbol{u}$ depend upon the particular control case considered. The excitation input is defined as

$$\boldsymbol{v}_i \equiv \begin{Bmatrix} \ddot{y} \\ \vdots \\ \ddot{y} \end{Bmatrix} \tag{4-3}$$

where y is the absolute displacement of the base of each system.

Often, it is convenient to recast the equations in (4-1) into the state space form

$$\dot{\boldsymbol{z}}_i = A_i \boldsymbol{z}_i + B_i^u \boldsymbol{u} + B_i^v \boldsymbol{v}_i \tag{4-4}$$

where

$$\boldsymbol{z}_i \equiv \begin{Bmatrix} \boldsymbol{x}_i \\ \dot{\boldsymbol{x}}_i \end{Bmatrix}; \quad A_i = \begin{bmatrix} 0 & I \\ -M_i^{-1}K_i & -M_i^{-1}C_i \end{bmatrix}, \quad B_i^u = \begin{bmatrix} 0 \\ -M_i^{-1}L_i \end{bmatrix}, \quad B_i^v = \begin{bmatrix} 0 \\ -I \end{bmatrix} \tag{4-5}$$

0 and I represent null and identity matrices, respectively, of appropriate dimensions. The equations in (4-4) can be expressed in terms of *modal response coordinates*, the $\bar{x}_{i,j}$, with $j \in \{1, \ldots, n_i\}$, by using the transformation

$$\boldsymbol{x}_i \equiv \Phi_i \bar{\boldsymbol{x}}_i \;\Rightarrow\; \boldsymbol{z}_i \equiv T_i \bar{\boldsymbol{z}}_i, \quad T_i = \begin{bmatrix} \Phi_i & 0 \\ 0 & \Phi_i \end{bmatrix} \tag{4-6}$$

where Φ_i is an orthogonal matrix whose columns consist of the eigenvectors of $M_i^{-1}K_i$. Thus, as is well known, the response of a linear dynamical system may be decomposed into particular modes of vibration.

Since the models considered for the primary and auxiliary systems are *chain-like* systems, consisting of n_i repeated identical units, it can be shown [1] (see Appendix B) that the eigenvalues and eigenvectors of the ith system are given by

$$\omega_{i,j} = 2\sqrt{\frac{k_i}{m_i}}\sin\left[\frac{(2j-1)}{(2n_i+1)}\frac{\pi}{2}\right];\quad \eta_i^j = \begin{Bmatrix}\varphi_{i,1j}\\ \vdots \\ \varphi_{i,n_ij}\end{Bmatrix},\quad \varphi_{i,kj} = c_{i,j}\sin\left[\frac{(2j-1)}{(2n_i+1)}\pi k\right] \tag{4-7}$$

with $k \in \{1, \ldots, n_i\}$, where the $\varphi_{i,kj}$ are the entries of the matrix Φ_i. The coefficients of the orthogonal eigenvectors, the $c_{i,j}$, are obtained from the normalization condition

$$(\eta_i^j)^{\mathsf{T}}\eta_i^l = \delta_{jl} \tag{4-8}$$

with $l \in \{1, \ldots, n_i\}$, where δ_{jl} is the familiar *Kronecker delta symbol.* Substituting (4-6) into (4-4) and rearranging terms yields

$$\dot{\bar{z}}_i = \overline{A}_i\bar{z}_i + \overline{B}_i^u\boldsymbol{u} + \overline{B}_i^v\boldsymbol{v}_i \tag{4-9}$$

where

$$\overline{A}_i = \begin{bmatrix}0 & I\\ -\overline{D}_i^K & -\overline{D}_i^C\end{bmatrix},\quad \overline{B}_i^u = \begin{bmatrix}0\\ -\overline{P}_i^u\end{bmatrix},\quad \overline{B}_i^v = \begin{bmatrix}0\\ -\overline{P}_i^v\end{bmatrix} \tag{4-10}$$

with

$$\overline{D}_i^K \equiv \Phi_i^{\mathsf{T}}M_i^{-1}K_i\Phi_i,\quad \overline{D}_i^C \equiv \Phi_i^{\mathsf{T}}M_i^{-1}C_i\Phi_i,\quad \overline{P}_i^u \equiv \Phi_i^{\mathsf{T}}M_i^{-1}L_i,\quad \overline{P}_i^v \equiv \Phi_i^{\mathsf{T}} \tag{4-11}$$

In fact, $\overline{D}_i^K$ and $\overline{D}_i^C$ are diagonal matrices, given by

$$\overline{D}_i^K = \begin{bmatrix}\omega_{i,1}^2 & & 0\\ & \ddots & \\ 0 & & \omega_{i,n_i}^2\end{bmatrix},\quad \overline{D}_i^C = \begin{bmatrix}2\zeta_{i,1}\omega_{i,1} & & 0\\ & \ddots & \\ 0 & & 2\zeta_{i,n_i}\omega_{i,n_i}\end{bmatrix} \tag{4-12}$$

$\overline{D}_i^K$ is diagonal by virtue of the mathematical properties associated with Φ_i [2]. $\overline{D}_i^C$ is diagonal by definition; that is, $C_i \equiv M_i\Phi_i\overline{D}_i^C\Phi_i^{\mathsf{T}}$. This reflects the modelling assumption that the modal damping ratios may be specified, and it is further assumed that a single

value for the fraction of critical damping applies equally to all response modes (*i.e.*, $\zeta_{i,j} = \zeta_{i,o}$).

$\overline{P}_i^u$ and $\overline{P}_i^v$ are the *modal participation matrices* associated with the control and excitation inputs, respectively, and their entries, denoted by $\overline{p}_{i,jk}^u$ and $\overline{p}_{i,jl}^v$, are referred to as *modal participation factors*. In general, the concept of a modal participation factor is relevant whenever there are inhomogeneous forcing terms present in the coupled equations of motion for a linear dynamical system. From (4-12), it is apparent that the equations represented in (4-9), which govern the n_i response modes of the ith system, may be equivalently represented by a set of n_i uncoupled equations, where the jth equation is given by

$$\ddot{\overline{x}}_{i,j} + 2\zeta_{i,o}\omega_{i,j}\dot{\overline{x}}_{i,j} + \omega_{i,j}^2\overline{x}_{i,j} = -\sum_{k=1}^{r_i}\overline{p}_{i,jk}^u u_k - \sum_{l=1}^{n_i}\overline{p}_{i,jl}^v v_{i,l} \tag{4-13}$$

The equation in (4-13) indicates that the modal participation factors associated with the control and excitation inputs combine together the components of $\boldsymbol{u}$ and $\boldsymbol{v}_i$, respectively, to produce the effective control and excitation inputs for the response modes.

4.3 Control Strategy

In essence, the control strategy employed in the study for MDOF systems is the same as that employed in the study for SDOF systems. However, only the first method for implementing the control strategy, as described in Section 3.3, is used in the present study. As previously mentioned, the reason for this is that the effects on the systems caused by impulsively generated control forces have not been adequately addressed (though it may be possible to transmit these kinds of forces between the systems in a manner which does not incur damage to one or both of them).

As before, the control strategy is to remove relative vibrational energy from the primary system by transferring energy to the auxiliary system by means of interaction elements, dissipating energy directly in the interaction elements, or a combination of both

methods. In fact, attention will be focused on the relative vibrational energy present in the dominant response mode of the primary system. This is because in many practical situations for which a linear MDOF structural system is subjected to an external excitation, only a few (perhaps, a single) response modes are significantly affected. This kind of behavior depends upon two factors: 1) the dominant frequencies of the excitation; and 2) the participation factors for each response mode.

From the definitions of ν_i and $\overline{P}_i^{\nu}$ given in (4-3) and (4-11), the contribution of the excitation input to the jth response mode of the ith system is proportional to the sum of the entries in the jth column of Φ_i. Since these columns represent the eigenvectors of $M_i^{-1}K_i$, the extent to which the jth response mode is externally excited depends upon the nature of the eigenvectors of Φ_i. For the models used in this study, the sum of the components of the eigenvector associated with the fundamental frequency is greatest, as determined from (4-7), so it is expected that the fundamental response mode will be significantly excited. The contribution of the control input to the jth response mode of the ith system depends upon both the values prescribed for the u_k and the entries of the jth column of $\overline{P}_i^{u}$. If possible, the values of the u_k should be selected to achieve a desirable control effect for the ith system.

Note: Throughout the remainder of this section and following ones, attention is devoted exclusively to the primary system. For this reason, the leading subscript on the notation, which is used to distinguish between the primary and auxiliary systems, will be suppressed for convenience and clarity, with the understanding that the primary system is implied when this subscript is omitted. Elsewhere in the chapter, the subscript may be explicitly indicated when it is important to make this distinction.

Control Objective

Let the story drift vector of the primary system, denoted by $\boldsymbol{b}$, be defined in terms of its components

$$b_j \equiv x_j - x_{j-1};\ j \in \{1, \ldots, n\},\ x_0 \equiv 0 \tag{4-14}$$

This definition for the b_j then provides a relation between $\boldsymbol{b}$ and $\boldsymbol{x}$, given by

$$\boldsymbol{b} = G\boldsymbol{x} \tag{4-15}$$

where the entries of the matrix G are easily deduced from (4-14), and it may be shown that G is nonsingular. The response control objective is to reduce the *maximum absolute values* of the primary system *story drifts*, the $|b_j|$. Clearly,

$$|b_j|_{max} \le \|\boldsymbol{b}\|_{max} = \left[\sqrt{\boldsymbol{x}^{\mathsf{T}} G^{\mathsf{T}} G \boldsymbol{x}}\right]_{max} \tag{4-16}$$

Because G is nonsingular, the matrix $G^{\mathsf{T}}G$ will also be nonsingular. Moreover, $G^{\mathsf{T}}G$ is symmetric and positive definite, by construction.

A Useful Result

At this point, a brief digression is taken to develop a result that will be useful below. Let $\boldsymbol{w} \in R^m$ be an arbitrary vector and Q be a symmetric, positive definite, time-invariant matrix of appropriate dimensions. Suppose that $\boldsymbol{w}$ satisfies the relation

$$\boldsymbol{w}^{\mathsf{T}} Q \boldsymbol{w} \le \beta^2 \tag{4-17}$$

where $\beta > 0$ is a parameter used to establish an upper bound for the quadratic product $\boldsymbol{w}^{\mathsf{T}} Q \boldsymbol{w}$. Using the standard theory for normed linear vector spaces, it can be shown there exists a parameter $\alpha > 0$ such that

$$\|\boldsymbol{w}\| \le \alpha = \frac{\beta}{\lambda} \tag{4-18}$$

in order for (4-17) to hold, where $\lambda > 0$ is the smallest eigenvalue of Q. Furthermore, if (α_1, β_1) and (α_2, β_2) are two such pairs of corresponding parameters, then $\alpha_2 < \alpha_1$ whenever $\beta_2 < \beta_1$. The usefulness of this result may be qualitatively stated as follows.

Suppose that $\boldsymbol{w}$ varies with t during the time interval $[t_a, t_b]$, and $\|\boldsymbol{w}\|$ is to be maintained as small as possible $\forall t \in [t_a, t_b]$. If a time-dependent upper bound β^2 can be established for the quadratic product $\boldsymbol{w}^{\mathsf{T}} Q \boldsymbol{w}$, and if the value of this bound can be

controlled, then the value of $\|\boldsymbol{w}\|$ can likewise be controlled.

Control Strategy

Consider some time interval $[t_a,\ t_b]$ during which control of the primary system is to be accomplished (*e.g.*, the duration of the external excitation). In a manner similar to that considered for the SDOF system study, let the *relative vibrational energy* of the primary system, E, be defined as

$$E \equiv \tfrac{1}{2}\dot{\boldsymbol{x}}^{\mathsf{T}} M \dot{\boldsymbol{x}} + \tfrac{1}{2}\boldsymbol{x}^{\mathsf{T}} K \boldsymbol{x} \tag{4-19}$$

or, as expressed in state variable form,

$$E = \tfrac{1}{2}\boldsymbol{z}^{\mathsf{T}} S \boldsymbol{z};\ \ S = \begin{bmatrix} K & 0 \\ 0 & M \end{bmatrix} = \begin{bmatrix} M & 0 \\ 0 & M \end{bmatrix} \begin{bmatrix} M^{-1}K & 0 \\ 0 & I \end{bmatrix} \tag{4-20}$$

By using the result from above, it is possible to determine an upper bound for each of the $|b_j|$, based upon E. Since $\frac{1}{2}\dot{\boldsymbol{x}}^{\mathsf{T}} M \dot{\boldsymbol{x}} \geq 0$ at any instant in time,

$$\boldsymbol{x}^{\mathsf{T}} K \boldsymbol{x} \leq 2E \tag{4-21}$$

Applying the result from above, an upper bound for $\|\boldsymbol{x}\|$, denoted by α, can then be established at every instant in time

$$\|\boldsymbol{x}\| \leq \alpha \tag{4-22}$$

This implies that an upper bound, denoted by β^2, may be determined for $\boldsymbol{x}^{\mathsf{T}} G^{\mathsf{T}} G \boldsymbol{x}$

$$\boldsymbol{x}^{\mathsf{T}} G^{\mathsf{T}} G \boldsymbol{x} \leq \beta^2 \tag{4-23}$$

But from (4-15), (4-23) implies

$$|b_j| \leq \|\boldsymbol{b}\| \leq \beta \tag{4-24}$$

The greatest of these upper bounds then serves as a bound for $|b_j|_{max}$, that is

$$|b_j|_{max} \leq \max_{t_a \leq t \leq t_b} \beta \tag{4-25}$$

Thus, E indirectly provides a measure which bounds each $|b_j|$ at every instant in time. Hence, each $|b_j|_{max}$ may be controlled by controlling E during the time interval $[t_a,\ t_b]$.

Modal Decomposition of E

Attention is now directed to the fact that E can be decomposed in terms of modal energy components, as follows

$$E = \tfrac{1}{2}\bar{z}^{\mathsf{T}}\bar{S}\bar{z};\ \ \bar{S} = \begin{bmatrix} D^K & 0 \\ 0 & D^M \end{bmatrix} = \begin{bmatrix} D^M & 0 \\ 0 & D^M \end{bmatrix}\begin{bmatrix} \bar{D}^K & 0 \\ 0 & I \end{bmatrix} \tag{4-26}$$

where

$$D^K \equiv \Phi^{\mathsf{T}} K \Phi,\ \ D^M \equiv \Phi^{\mathsf{T}} M \Phi \tag{4-27}$$

are diagonal matrices [2], with $\bar{z}$ and $\bar{D}^K$ as defined in (4-6) and (4-11), respectively. A closer examination of (4-26) reveals that E may be expressed as

$$E = \sum_{j=1}^{n} E_j;\ \ E_j \equiv \tfrac{1}{2} d_j^M \left(\dot{\bar{x}}_j^2 + \omega_j^2 \bar{x}_j^2\right) \tag{4-28}$$

where d_j^M is the jth diagonal entry of D^M. From this decomposition, it is evident that

$$\left|\bar{x}_j\right| \le \left|\bar{x}_j\right|_{sup},\ \ \forall t \in [t_a,\, t_b];\ \ \left|\bar{x}_j\right|_{sup} \equiv \sqrt{\frac{2E_j}{d_j^M \omega_j^2}} \tag{4-29}$$

This result, applicable to a particular mode of vibration for the system, is analogous to condition (3-8) in Chapter 3. In addition, differentiating (4-28) and using (4-13) gives

$$\dot{E}_j = d_j^M \left(\ddot{\bar{x}}_j + \omega_j^2 \bar{x}_j\right)\dot{\bar{x}}_j = -d_j^M \left[\sum_{k=1}^{r} \bar{p}_{jk}^u u_k + \sum_{l=1}^{n} \bar{p}_{jl}^v v_l + 2\zeta_o \omega_j \dot{\bar{x}}_j\right]\dot{\bar{x}}_j \tag{4-30}$$

The control strategy is to remove relative vibrational energy from the dominant response mode — say, the sth response mode — to the extent allowed by the constraints on the control input. This is because the dominant response mode is expected to provide the largest contribution to E, which is the quantity to be directly controlled in order to achieve the control objective. Hence, the control effort is aimed at regulating E_s in order to maintain E as small as possible. This control approach is similar to some methods suggested for active control applications by Meirovitch and Öz [3] and Yang and Lin [4].

For the purposes of both implementing the control strategy and formulating control algorithms, efforts are directed toward minimizing the change in E_s for a representative

sampling period, denoted by ΔE_s^p, or even causing this change to be as negative as possible. Such a sampling period is exactly as described for the previous study involving two interacting SDOF systems. Upon integrating (4-30) over the sampling period, a series expansion for ΔE_s^p may be formed as

$$\Delta E_s^p = -d_s^M \left[\sum_{k=1}^{r} \overline{p}_{sk}^u u_k \right] \dot{\bar{x}}_s \Big|_{t_p} (h) - d_s^M \left[\sum_{l=1}^{n} \overline{p}_{sl}^v v_l + 2\zeta_o \omega_s \dot{\bar{x}}_s \right] \dot{\bar{x}}_s \Big|_{t_p} (h) + O(h^2) \quad (4\text{-}31)$$

Based upon this expression for ΔE_s^p, a control algorithm is used to determine the appropriate operating states for the interaction elements such that the control effort during a representative sampling period is anticipated to be favorable to the control strategy. If the sampling period is small in comparison to some characteristic time for the primary system (*e.g.*, the period of the sth response mode), the terms of order $O(h^2)$ may effectively be ignored. It is then recognized that the remaining terms which multiply h constitute $\dot{E}_s$. This forms the basis for the control algorithm. The specific details of this control algorithm are explained for two kinds of control cases in Section 4.6.

It should be mentioned that in seeking to control only the sth response mode, the values selected for the u_k could have an adverse effect upon the other response modes; that is, this choice for the u_k might serve to excite the other response modes. This effect is known as *spillover.*

4.4 Interaction Elements

One of the distinguishing features of the semi-active control approach proposed herein is that the interaction elements consist of devices whose mechanical properties can be discretely switched in real time according to the commands of a control processor but otherwise function passively. (*Note:* The class of control systems considered could be enlarged by allowing for the possibility of modulating some or all of the element mechanical properties in a continuous fashion). Such devices are attached between two distinct structural systems — or different components of a single structural system — in

order to facilitate interactions which are favorable to the control strategy.

Since the devices are reactive in nature, the control forces produced will develop in response to the motions of the points of attachment. These motions are determined by the dynamical behavior of each structural system involved, which is typically described by a set of nodal displacements associated with each degree of freedom for the system. Only *one-dimensional* interaction elements are considered herein, whose ends are connected to the points of attachment.

Dynamics and Memory

For the purposes of analysis, a mathematical model is constructed for each interaction element, which is generally characterized by a functional relation between the reactive force u developed within the element, the element deformation e, the rate of element deformation $\dot{e}$, and a set of parameters that represent the element mechanical properties, which form the components of a vector $\boldsymbol{p}$. u is assumed to be positive when the element is in tension, and e is assumed to be positive when the element ends are extended with respect to a given reference length. In addition, if the element behavior depends upon certain aspects of its deformation history (*i.e.*, if it possesses *memory*), then it is necessary to introduce *element state variables*, which form the components of a vector $\boldsymbol{q}$. The functional relation for the kth element is expressed as

$$u_k = g_k(\dot{e}_k,\ e_k,\ \boldsymbol{p}_k,\ \boldsymbol{q}_k) \tag{4-32}$$

Often, when the element possesses memory, $\boldsymbol{q}_k$ is governed by a relation of the form

$$\dot{\boldsymbol{q}}_k = \boldsymbol{h}_k(\boldsymbol{q}_k,\ \dot{e}_k,\ e_k,\ \boldsymbol{p}_k) \tag{4-33}$$

Hence, an element which is governed by the kinds of the relations appearing in (4-32) and (4-33) is said to be *memory-dependent.* If the relation given in (4-32) does not explicitly depend upon the $p_{k,l}$, with $l \in \{1, \ldots, m_k\}$, and if e_k and $\dot{e}_k$ are continuous functions of t, then the element is said to be *dynamic* as well. The continuity condition on e_k and $\dot{e}_k$ usually holds when the element ends are attached to dynamical systems whose state

variables are also continuous functions of t.

As examples, consider the *Maxwell* and *Kelvin viscoelastic elements.* A Maxwell element consists of a linear elastic element placed in series with a linear viscous element. A Kelvin element consists of a linear elastic element placed in parallel with a linear viscous element. In the descriptions which follow, let k denote the stiffness of the elastic constituent, and let c denote the damping coefficient of the viscous constituent. It is then easily shown that the force-deformation constitutive relation for a Maxwell element is given by

$$\dot{u} = k\dot{e} - \frac{u}{\tau}; \quad \tau \equiv \frac{c}{k} \tag{4-34}$$

Alternatively, equation (4-34) may be expressed as

$$u = g(\dot{e},\ e,\ k,\ \tau,\ q) = q \tag{4-35}$$

$$\dot{q} = h(q,\ \dot{e},\ e,\ k,\ \tau) = k\dot{e} - \frac{q}{\tau} \tag{4-36}$$

indicating that a Maxwell element is dynamic and memory-dependent. The well-known force-deformation constitutive relation for a Kelvin element is given by

$$u = g(\dot{e},\ e,\ c,\ k,\ q) = c\dot{e} + ke \tag{4-37}$$

indicating that a Kelvin element is nondynamic and memoryless.

Passivity Formalism

At this juncture, it is appropriate to provide a precise definition for the term *passive system.* This is because the semi-active control approach employed stipulates that only passive elements, whose mechanical properties may be altered in a discrete manner, are to be utilized. To facilitate the development of this definition, a *passivity formalism* [5] is first presented for general dynamical systems, which is then specialized for the case of mechanical systems. Attention will be confined to passive systems that interact with other dynamical systems only at a finite number of points along their boundaries.

Consider a dynamical system with arbitrary input $\boldsymbol{v}$ and a conjugate output $\boldsymbol{y}$, both

of which are generally time-varying. If the system obeys a relation of the form

$$\dot{V}(t) = \boldsymbol{v}^{\mathsf{T}}\boldsymbol{y} + g(t) \tag{4-38}$$

with $V(t)$ lower bounded and $g(t) \leq 0$, $\forall t \in [0, \infty)$, then the system is said to be *passive* (or, to represent a *passive mapping* between $\boldsymbol{v}$ and $\boldsymbol{y}$). Furthermore, a passive system is said to be *dissipative* whenever

$$\int_0^\infty \boldsymbol{v}^{\mathsf{T}}\boldsymbol{y}\, dt \neq 0 \;\Rightarrow\; \int_0^\infty g(t)\, dt < 0 \tag{4-39}$$

The quantities appearing in (4-38) may be interpreted as follows: $V(t)$ is a form of generalized energy stored by the system, $\boldsymbol{v}^{\mathsf{T}}\boldsymbol{y}$ is a form of generalized power externally supplied to the system, and $g(t)$ is a form of generalized power internally generated by the system (since $g(t) \leq 0$ for a passive system, the absolute value of $g(t)$ represents the generalized power internally dissipated by this kind of system). Thus, equation (4-38) represents a principle of generalized energy balance.

Integration and subsequent rearrangement of (4-38) yields

$$\int_0^\infty g(t)\, dt = \Delta V - \int_0^\infty \boldsymbol{v}^{\mathsf{T}}\boldsymbol{y}\, dt \tag{4-40}$$

where $\Delta V \equiv V(\infty) - V(0)$. If the implication in (4-39) is enforced, (4-40) indicates that the change in the generalized energy stored by system for all time is less than the net amount of generalized energy supplied to the system by the input. This result agrees nicely with the intuitive notion of a dissipative system. This formulation is now applied to a several mechanical devices, and in these cases, $V(t)$ is the mechanical energy stored by the device.

As examples, consider again the Maxwell and Kelvin viscoelastic elements. In the case of the Maxwell element, postmultiply (4-34) by u and rearrange terms to obtain

$$\frac{d}{dt}\left[\frac{1}{2}\frac{u^2}{k}\right] = \dot{e}u - \frac{u^2}{c} \tag{4-41}$$

Equation (4-41) represents a passive mapping between $\dot{e}$ and u for the Maxwell element, indicating that it is both passive and dissipative. In the case of the Kelvin element,

premultiply (4-37) with $\dot{e}$ and rearrange terms to obtain

$$\frac{d}{dt}\left[\frac{1}{2}ke^2\right] = \dot{e}u - c\dot{e}^2 \tag{4-42}$$

Equation (4-42) represents a passive mapping between $\dot{e}$ and u for the Kelvin element, indicating that it is both passive and dissipative. Note that (4-41) can be put into a form similar to (4-42) by recognizing that $u = ke_e$ and $u = c\dot{e}_v$ for a Maxwell element, where e_e and e_v are the individual deformations of the elastic and viscous constituents, respectively, and $e = e_e + e_v$. Using these expressions for u in (4-41) yields

$$\frac{d}{dt}\left[\frac{1}{2}ke_e^2\right] = \dot{e}u - c\dot{e}_v^2 \tag{4-43}$$

Reciprocity Relation

Another result that greatly facilitates the evaluation of the matrix L which is used to incorporate $\boldsymbol{u}$ into the equations of motion in (4-5) is the *reciprocity relation*. Consider a mechanical system that consists of the entire collection of interaction elements used in a given control case. Let the individual deformations of the one-dimensional elements constitute a vector $\boldsymbol{e} \in R^r$. It is assumed that the ends of these elements are permanently attached to either the nodal masses of the structural system or the base of this system. Then a mapping that relates the element deformations to the structural displacements which describe the configuration of the nodal masses may be found and is of the form

$$\boldsymbol{e} = L^T\boldsymbol{x} \tag{4-44}$$

where the components of the vector $\boldsymbol{x} \in R^n$ are the relative displacements. If several structural systems (to which the interaction elements are attached) are involved, then a relation of the form in (4-44) still may be found and can be generated by augmenting $\boldsymbol{x}$ such that it includes all of the displacements associated with the participating structures. The mapping in (4-44) physically represents certain kinematic constraints arising from the connections between the interaction elements and the structural system. For a passive system, the element deformations will be driven by the motions of the co-located nodal

masses of the structural system.

At the points of attachment, an interface exists between the mechanical system comprised by the interaction elements and the structural system. The *principle of virtual work* for a *dynamical system* [6] may be applied to the interface by considering the forces acting at the attachment points on either side of the interface. Because the interface is massless, the *D'Alembert forces* are not present, and the principle of virtual work becomes

$$\boldsymbol{f}^{\mathsf{T}}\delta\boldsymbol{x} + \boldsymbol{u}^{\mathsf{T}}\delta\boldsymbol{e} = 0 \;\Rightarrow\; \boldsymbol{f}^{\mathsf{T}}\delta\boldsymbol{x} = -\boldsymbol{u}^{\mathsf{T}}\delta\boldsymbol{e} \tag{4-45}$$

where the components of $\boldsymbol{f} \in R^n$ are the forces applied to the structural system, and the components of $\boldsymbol{u} \in R^r$ are the reaction forces that develop within the interaction elements. $\delta\boldsymbol{x}$ and $\delta\boldsymbol{e}$ represent virtual displacements from the particular values for the structural displacements and the element deformations, respectively, at a fixed point in time. For virtual displacements which are consistent with the kinematic constraints, (4-44) becomes

$$\delta\boldsymbol{e} = L^{\mathsf{T}}\delta\boldsymbol{x} \tag{4-46}$$

Substituting (4-46) into (4-45), it is then easily shown that $\boldsymbol{f}$ is *reciprocally related* to $\boldsymbol{u}$ (in view of the kinematic relation between $\boldsymbol{e}$ and $\boldsymbol{x}$) by

$$\boldsymbol{f} = -L\boldsymbol{u} \tag{4-47}$$

This result is especially useful, since it is usually a fairly simple matter to deduce L^{T} from the attachment geometry.

Element Types

Motivated by the performance achieved for some specific control cases considered in the previous study, only three types of interaction elements are proposed for use in the present study. One of these interaction elements (a Type 1 element) is idealized as a linear elastic element, of fixed stiffness k_{int}, that is assembled in series with a stick-slip device which may be either locked or unlocked. The parameter μ, defined below, is

used hereafter to specify the value of k_{int}, with

$$\mu \equiv \frac{k_{int}}{k_1} \tag{4-48}$$

When the stick-slip device is locked, the interaction element behaves simply as a linear elastic element. When the stick-slip device is unlocked, it is assumed to internally slip at an infinitely-fast rate, instantaneously dissipating the strain energy accumulated in the elastic element and thereby reducing the reaction force of the interaction element to zero.

Another of the interaction elements (a Type 2 element) is idealized as a Maxwell viscoelastic element whose damping coefficient c_{int} (or, alternatively, time constant τ) may be switched to either one of two fixed values: c_h, the *high* value of c_{int}; or c_l, the *low* value of c_{int}. The parameter δ, defined below, is used hereafter to specify the value of c_{int}, with

$$\delta \equiv \frac{c_{int}}{c_1} \tag{4-49}$$

where $c_1 \equiv 2 m_1 \zeta_{1,o} \omega_{1,1}$. Thus, δ_h and δ_l are used to represent c_h and c_l, respectively. The switching process is modelled to happen instantaneously. It is shown below that, with appropriate choices for δ_h and δ_l, the Type 2 element will behave in a manner very similar to that of the Type 1 element. In the case of a Type 2 element, it is occasionally useful to refer to τ instead of δ. The relationship between these two parameters is

$$\tau = \frac{2 \delta \zeta_{1,o} \omega_{1,1}}{\mu \omega_{1,o}^2} \tag{4-50}$$

where $\omega_{1,o}^2 \equiv k_1 / m_1$.

The remaining interaction element (a Type 3 element) is idealized as a linear viscous element whose damping coefficient c_{int} may be switched to either one of two fixed values: c_h or c_l. Again, the parameter δ, defined in (4-49), is used to specify the particular value for c_{int}. It is important to point out that although the same notation and terminology is used for their descriptions, the viscous constituents of the Type 2 and Type 3 interaction elements are considerably different with regard to their physical nature

and duty cycle. This will become evident in following sections of this chapter.

At points in time other than when a switching event occurs, each type of interaction element functions in either one of two possible *operating states*: an activated operating state and a deactivated operating state. In the activated state, the value of δ is δ_h; in the deactivated state, the value of δ is δ_l; where $\delta_h > \delta_l$. Also, each interaction element may be activated or deactivated only at the beginning of a sampling period, and once the operating state of an element is determined by the control processor, the value of δ associated with that element is fixed for the duration of the sampling period.

For the various control cases considered involving MDOF structural systems (hence, multiple interaction elements), it is worth emphasizing that the *same* element type is used for all of the interaction elements employed in a particular control case. Likewise, each element is characterized by the *same* set of possible parameter values (*i.e.*, δ_h, δ_l, and μ). However, when commanded by the control processor, each element may function in either one of the two admissible operating states *independently* of the others. Figure 4.2 shows schematic representations of all three types of interaction elements. A generic representation for either one of these element types, which is utilized in some of the subsequent diagrams, is shown at the top of this figure.

In view of the previous discussion, it is convenient to solve (4-34), which represents a Maxwell viscoelastic element, for the reactive force in terms of the element deformation history (in order to avoid notational confusion, let ε denote the element deformation, and let $e^{(\bullet)}$ denote the *scalar exponential function*)

$$u(t) = u(t_o)e^{-(t-t_o)/\tau} + k\int_{t_o}^{t} e^{-(t-\bar{t})/\tau}\,\varepsilon(\bar{t})\,d\bar{t} \tag{4-51}$$

As mentioned above, the Type 2 interaction element corresponds to a Maxwell element with a variable value for τ. Consider the case where $\varepsilon(\bar{t})$ is slowly-varying over a time interval that has a duration of several τ, which corresponds to slow motions of the element attachment points; then $u(t) \to 0$ as $\tau \to 0$. This feature permits the element to

suddenly dissipate energy that has been previously accumulated as strain energy in the elastic constituent. This behavior illustrates that when the interaction element is operated with $\tau \to 0$ in the deactivated state, it functions in virtually the same manner as does the Type 1 element upon deactivation. In fact, it is this kind of behavior which is sought.

There is an important difference in the application of the control strategy for the different types of interaction elements considered, which will necessitate a modification to the control algorithm, depending upon the element type that is utilized. For cases in which a Type 3 element is used, a high level of reaction force may be instantaneously produced upon activation by selecting $\delta = \delta_h$. Likewise, a low level of reaction force may be instantaneously produced upon deactivation by selecting $\delta = \delta_l$.

In contrast, for cases in which a Type 2 element is used, a new level of reaction force is not immediately produced by changing the value of δ. Indeed, the operating state of the element will change from an activated state to a deactivated state, or *vice versa*. But the reaction force developed within the device does not instantaneously jump from one value to another because the element is dynamic, in the sense described earlier, and the states of the dynamical systems with which the element interacts, which dictate the motion of the element attachment points, and hence ε, are bounded and continuous. Thus, the reaction force develops within the element over time according to (4-34), and it is a continuous function of t even when δ (and therefore τ) is a discontinuous function of t. For cases in which a Type 1 element is used, a zero value for the reaction force is instantaneously produced upon deactivation of the element (this value persists as long as the element remains deactivated), whereas a new level of reaction force is not immediately produced upon activation of the element. Thus, this element is nondynamic in the deactivated state but dynamic in the activated state.

Finally, it should be apparent that all of the element types considered are passive and dissipative because each may be described as special case of the Maxwell or Kelvin viscoelastic element with controllable parameters, representing the mechanical properties

of the element. The Type 3 element may be represented as a Kelvin element for which k is identically zero and c is intermittently switched to either one of two constant values. The Type 2 element may be represented as a Maxwell element for which k is fixed at a nominal value and τ is intermittently switched to either one of two constant values. The Type 1 element can be considered a special case of the Type 2 element, in which either $\tau \to \infty$ or $\tau \to 0$.

4.5 Numerical Study

As in the previous study involving two interacting SDOF systems, a deterministic analysis is conducted through numerical simulations. These are performed for a series of control cases using horizontal ground accelerations from an ensemble of earthquake time-histories as excitation input. The same numerical integration method and normalized earthquake records as were used in the previous study are used for the present study.

For prescribed $\boldsymbol{u}$ and ν_1, the dynamical behavior of the primary system is fully characterized upon specification of the undamped fundamental frequency of vibration $\omega_{1,1}/2\pi$, the modal damping ratio $\zeta_{1,o}$ (which is the same for all response modes), and the number of structural stories n_1. In all of the control cases examined, $\zeta_{1,o} = 0.01$. Most of the cases considered involve a 6-story primary system for which $\omega_{1,1}/2\pi$ is set to 1.00 Hz; a few cases involve a 3-story primary system for which $\omega_{1,1}/2\pi$ is set to 1.85 Hz. This is done to preserve the ratio of k_1/m_1 in all of the control cases so that primary systems of similar construction (though of differing heights) are compared. The selection of a 6-story primary system and its associated properties is based upon the previous work discussed in [7], which involved a full-scale experimental study of active structural control. For prescribed $\boldsymbol{u}$ and ν_2, the dynamical behavior of the auxiliary system (if present) is fully characterized upon specification of the parameters

$$\alpha \equiv \frac{k_2}{k_1}, \quad \beta \equiv \frac{m_2}{m_1}, \quad \zeta_{2,o}, \quad n_2 \tag{4-52}$$

In all of the control cases examined, $\zeta_{2,o} = 0.01$.

It is convenient to group the control cases examined into five control categories which are distinguished from one another by the type of interaction element employed, the range of parameters used to characterize both the auxiliary system (if present) and the interaction elements, as well as the location and attachment of the elements. A listing of the control categories is provided in Table 4.1.

For the cases in Categories 1, 3, and 5, Type 1 and 2 elements are utilized. For the cases in Category 4, a Type 3 element is utilized. In Category 2 cases, modified versions of the Type 1 and 2 elements are utilized. These modified versions are simply the regular versions without the elastic constituent, with the stick-slip device and viscous constituent operated exactly as for the ordinary versions of the Type 1 and 2 elements, respectively. This is because the auxiliary system in this category consists of an elastic frame that is treated to be massless, to which the modified elements are directly attached.

The physical nature and duty cycle of the viscous constituent used in the Type 2 element is considerably different from that used in the Type 3 element. In the case of a Type 2 element, $\delta_h \to \infty$, indicating complete lock-up of the viscous constituent during activation, such that it functions merely as a rigid connecting member, whereas δ_l takes on a finite, relatively small value. In the case of a Type 3 element, δ_h takes on a finite, relatively small value, whereas $\delta_l = 0$. Also, the Type 2 element is typically deactivated for only short time intervals (*i.e.*, an amount of time sufficient for the strain energy in the elastic constituent to be dissipated), whereas the Type 3 element may be deactivated for sustained periods of time. The range of values considered for δ_h and δ_l are indicated in Table 4.1 for each of the control categories.

In Category 1, the auxiliary system is absent and the interaction elements are attached between adjacent floor and roof slabs, as illustrated in Figure 4.3. In Category 2, the auxiliary system consists of a massless elastic frame that is externally-situated to the primary system. The interaction elements are attached between the primary and auxiliary

systems at corresponding vertical positions, as illustrated in Figure 4.4.

In Category 3, the auxiliary system represents a complete structural system that is adjacent to the primary system. However, there are two widely different applications considered for the control cases in this category. In one application (Category 3(a)), the auxiliary system is supposed to mimic the ideal elastic frame comprising the auxiliary system of Category 2. But unlike the cases in that category, a small but reasonable amount of mass is ascribed to the auxiliary system for the cases in this category, as would be physically expected for an actual elastic frame. In the other application (Category 3(b)), the auxiliary system is presumed to be much stronger and more massive than the primary system, as is reflected by the choice of values for α and β in Table 4.1. The interaction elements are attached between the primary and auxiliary systems to floor and roof slabs of corresponding height, as illustrated in Figure 4.5.

In Category 4, the auxiliary system again represents a complete structural system that is adjacent to the primary system. As is done for the cases in Category 3(b), all of the cases considered in this category presume that the auxiliary system is much stronger and more massive than the primary system. The attachment of the interaction elements is the same as that described for Category 3, as illustrated in Figure 4.5, but significantly different interaction elements are used. In Category 5, the auxiliary system consists of a relatively small mass located on top of the primary system, similar to the configuration used for a tuned mass damper or active mass driver. A single interaction element is attached between this small mass and the roof slab of the primary system, as illustrated in Figure 4.6.

Some further comments are in order. First, in addition to the control cases of main interest, several others may be considered within each control category by examining conditions under which all of the participating interaction elements are permanently locked in either their activated or deactivated states for the duration of the simulation. These additional cases could be included for comparison purposes to verify both the

efficacy of the switching process and the necessity of a control algorithm, and they are discussed further in Section 4.7.

Next, the control cases represented in Category 2 are highly idealized because the auxiliary system consists simply of an elastic frame which is treated to be massless. Because of these properties, the relative displacements of the auxiliary system are not directly affected by the base acceleration. And because the frame is massless, it is not possible to separate the dynamics of the interaction elements (*i.e.*, the modified versions of Type 1 and 2 elements) from the dynamics of the frame. In fact, a composite system consisting of the interaction elements and the elastic frame behaves in a manner similar to a collection of *coupled* interaction elements (*i.e.*, the regular versions of Type 1 and 2 elements), with the frame responding rapidly upon activation and deactivation of the interaction elements with which it is in contact.

Although the models for the structural systems considered in the present study are certainly more realistic than those dealt with in the previous study, the interaction elements described in Section 4.4 are still very idealized devices. It was already pointed out that the Type 1 element may be viewed as a more idealized version of the Type 2 element. However, the Type 2 and 3 elements could be physically realized by combining a hydraulic actuator — which utilizes a variable flow restriction in the fluid return line that connects the high-pressure and low-pressure compartments of the piston-cylinder mechanism — with other purely passive devices. Figure 4.7 (a) depicts a configuration of actual hardware to produce a Type 2 element. The hydraulic actuator is arranged in parallel with a viscous damper of fixed damping coefficient c_l. This unit is then placed in series with a strong helical coil of fixed stiffness k_{int}. Figure 4.7 (b) depicts a configuration of actual hardware to produce a Type 3 element. The hydraulic actuator is placed in series with a viscous damper of fixed damping coefficient c_h.

In each of these configurations, the desired functional behavior for the idealized interaction element, corresponding to the two admissible operating states, is achieved by

either completely opening or closing the flow control valve of the hydraulic actuator. Other than the stepwise changes commanded for the flow control valve, the actuator functions passively, with fixed mechanical properties, during piecewise continuous intervals of time.

4.6 Control Algorithms

The implementation of the control strategy is based upon the previous discussion surrounding equation (4-31). However, certain modifications must be introduced when dynamic interaction elements (Type 1 and 2 elements) are utilized. As described earlier, the control strategy is to maintain as small as possible the components of the primary system relative vibrational energy contributed by the dominant response modes. In the present study, the control effort is actually directed at the most dominant response mode. But before restricting attention to that particular case, the following development will consider the possibility of attempting the control of several response modes, whose effects are assumed to be relatively dominant in comparison to all others.

Let the jth mode be one such dominant mode. As indicated in Section 4.3, efforts are directed at minimizing the change in E_j for a representative sampling period. Following the argument used in that section, it was pointed out that the quantity which may be used to achieve this goal is $\dot{E}_j$. This is because the components of $\boldsymbol{u}$ enter directly into the expression for $\dot{E}_j$, as seen in (4-30). However, if the u_k are selected to be optimally effective in reducing the energy component corresponding to a particular mode, it is uncertain what the effect will be on another dominant mode. Hence, a compromise is struck by attempting to control the *sum* of the energy components associated with the dominant modes, which is a reasonable approach since this sum comprises the major portion of E, which is the quantity to be controlled.

Consider the *pseudo-Liapunov function*

$$V = \tfrac{1}{2}\bar{z}^{\mathsf{T}}\bar{T}\bar{z} \tag{4-53}$$

where $\overline{T}$ is defined as

$$\overline{T} \equiv \begin{bmatrix} \Theta & 0 \\ 0 & \Theta \end{bmatrix} \overline{S} = \begin{bmatrix} \Theta D^K & 0 \\ 0 & \Theta D^M \end{bmatrix} \tag{4-54}$$

and Θ is a *diagonal projection matrix* (*i.e.*, $\Theta^{\mathsf{T}} = \Theta$ and $\Theta^2 = \Theta$), defined as follows. Suppose that the jth response mode of the primary system is to be controlled. Then the entry appearing in the jth diagonal position of Θ should be unity. In turn, each controlled response mode should have this value in the associated diagonal position, depending upon its particular value of j, where $j \in \{1, \ldots, n\}$. All other entries along the diagonal of Θ should be zero. Therefore, the pseudo-Liapunov function consists of the sum of energy components contributed to E by the dominant response modes

$$V = \sum_j E_j; \;\; E_j = \tfrac{1}{2} d_j^M \left(\dot{\overline{x}}_j^2 + \omega_j^2 \overline{x}_j^2 \right) \tag{4-55}$$

Consider the first and second derivatives of V with respect to t, given by

$$\dot{V} = \left(\overline{T} \overline{z} \right)^{\mathsf{T}} \dot{\overline{z}} \tag{4-56}$$

and

$$\ddot{V} = \left(\overline{T} \overline{z} \right)^{\mathsf{T}} \ddot{\overline{z}} + \left(\overline{T} \dot{\overline{z}} \right)^{\mathsf{T}} \dot{\overline{z}} \tag{4-57}$$

By using (4-9) through (4-11), (4-56) and (4-57) become

$$\dot{V} = \dot{V}^z + \dot{V}^u + \dot{V}^v \tag{4-58}$$

and

$$\ddot{V} = \ddot{V}^z + \ddot{V}^u + \ddot{V}^v + \left(\overline{T} \dot{\overline{z}} \right)^{\mathsf{T}} \dot{\overline{z}} \tag{4-59}$$

with

$$\dot{V}^z = \overline{z}^{\mathsf{T}} \begin{bmatrix} 0 & \Theta D^K \\ -\Theta D^K & -\Theta D^C \end{bmatrix} \overline{z}, \;\; \dot{V}^u = \overline{z}^{\mathsf{T}} \begin{bmatrix} 0 \\ -\Theta P^u \end{bmatrix} \boldsymbol{u}, \;\; \dot{V}^v = \overline{z}^{\mathsf{T}} \begin{bmatrix} 0 \\ -\Theta P^v \end{bmatrix} \boldsymbol{v} \tag{4-60}$$

and

$$\ddot{V}^z = \dot{\overline{z}}^{\mathsf{T}} \begin{bmatrix} 0 & \Theta D^K \\ -\Theta D^K & -\Theta D^C \end{bmatrix} \dot{\overline{z}}, \;\; \ddot{V}^u = \dot{\overline{z}}^{\mathsf{T}} \begin{bmatrix} 0 \\ -\Theta P^u \end{bmatrix} \dot{\boldsymbol{u}}, \;\; \ddot{V}^v = \dot{\overline{z}}^{\mathsf{T}} \begin{bmatrix} 0 \\ -\Theta P^v \end{bmatrix} \dot{\boldsymbol{v}} \tag{4-61}$$

where

$$P^u \equiv \Phi^T L, \quad P^v \equiv \Phi^T M \tag{4-62}$$

The form for the last term comprising $\ddot{V}$ in (4-59) has not been expanded from that given in (4-57) because it will subsequently be demonstrated that this term may be dropped from consideration. Finally, it may be shown that

$$\dot{V}^z = -\sum_j 2 d_j^M \zeta_o \omega_j \dot{\bar{x}}_j \dot{\bar{x}}_j, \quad \dot{V}^u = \sum_{k=1}^{r} \dot{V}_k^u, \quad \dot{V}^v = \sum_{l=1}^{n} \dot{V}_l^v \tag{4-63}$$

and

$$\ddot{V}^z = -\sum_j 2 d_j^M \zeta_o \omega_j \ddot{\bar{x}}_j \ddot{\bar{x}}_j, \quad \ddot{V}^u = \sum_{k=1}^{r} \ddot{V}_k^u, \quad \ddot{V}^v = \sum_{l=1}^{n} \ddot{V}_l^v \tag{4-64}$$

with

$$\dot{V}_k^u = -\sum_j \dot{\bar{x}}_j p_{jk}^u u_k, \quad \dot{V}_l^v = -\sum_j \dot{\bar{x}}_j p_{jl}^v v_l \tag{4-65}$$

and

$$\ddot{V}_k^u = -\sum_j \ddot{\bar{x}}_j p_{jk}^u \dot{u}_k, \quad \ddot{V}_l^v = -\sum_j \ddot{\bar{x}}_j p_{jl}^v \dot{v}_l \tag{4-66}$$

The quantities of interest to the control algorithm are $\dot{V}$ and $\ddot{V}$. However, as will be explained momentarily, only $\dot{V}^u$ or $\ddot{V}^u$ can be directly affected. Hence, attention is focused on these quantities.

Since the control algorithm adopted for the control cases which utilize *nondynamic* interaction elements (Category 4) is the simplest, it will be described first. The control algorithm adopted for the control cases which utilize *dynamic* interaction elements (Categories 1, 2, 3, and 5) is somewhat more complicated, and it will be described next.

Control Algorithm for Nondynamic Elements

At the beginning of each sampling period, the states of the primary and auxiliary systems are either measured or estimated. These may be used to determine the values for each of the u_k in both the activated and deactivated operating states (which, in general, will be different). Then, because the operating state of each element may be selected independently of the other elements, the following conditions are used to determine the

appropriate operating state for the kth element, $\forall k \in \{1, \ldots, r\}$, during the sampling period.

- kth Element is Currently Activated:

$$\dot{V}_k^u(\delta_h) \leq \dot{V}_k^u(\delta_l) \;\Rightarrow\; \text{element remains activated} \tag{4-67}$$

$$\dot{V}_k^u(\delta_h) > \dot{V}_k^u(\delta_l) \;\Rightarrow\; \text{element is deactivated}$$

- kth Element is Currently Deactivated:

$$\dot{V}_k^u(\delta_h) \leq \dot{V}_k^u(\delta_l) \;\Rightarrow\; \text{element is activated} \tag{4-68}$$

$$\dot{V}_k^u(\delta_h) > \dot{V}_k^u(\delta_l) \;\Rightarrow\; \text{element remains deactivated}$$

Some further remarks are in order here. Of interest is the minimization of $\dot{V}$. Since $\bar{z}$ and v are fixed at any instant in time, $\dot{V}^z$ and $\dot{V}^v$ will also be fixed at that instant in time. Hence, an instantaneous change in $\dot{V}$ may only be effected by directly altering $\dot{V}^u$. This is accomplished by selecting a particular value for each of the u_k, which then determines each of the $\dot{V}_k^u$. Thus, the logic comprising the control algorithm proposed for nondynamic elements is justified.

Control Algorithm for Dynamic Elements

At the beginning of each sampling period, the states of the primary and auxiliary systems are either measured or estimated, as are the reaction forces in each element. Then, a two-step procedure is used to select the appropriate operating state for each of the elements. This procedure consists of: (*a*) determining which of the currently activated elements should be deactivated, and then immediately deactivating these elements; and (*b*) determining which of the currently deactivated elements should be activated, and then immediately activating these elements. The reason for employing such a procedure is that in cases for which Type 1 elements are utilized, it is possible for the element to be immediately reactivated following deactivation.

Since dynamic elements are utilized, the values for each of the u_k are fixed at a

given instant in time and cannot be changed, even if the element mechanical properties are instantaneously altered (except in the case of the deactivation of a Type 1 element). Thus, it is expected that certain modifications must be made to the control algorithm proposed for nondynamic elements. Then, because the operating state of each element may be selected independently of the other elements, the following conditions are used to determine the appropriate operating state for the kth element, $\forall k \in \{1, \ldots, r\}$, during the sampling period.

- kth Element is Currently Activated:

$$\dot{V}_k^u(u_k) \leq 0 \;\Rightarrow\; \text{element remains activated} \qquad (4\text{-}69)$$

$$\dot{V}_k^u(u_k) > 0 \;\Rightarrow\; \text{element is deactivated}$$

- kth Element is Currently Deactivated:

$$\ddot{V}_k^u(\delta_h) \leq \ddot{V}_k^u(\delta_l) \;\Rightarrow\; \text{element is activated} \qquad (4\text{-}70)$$

$$\ddot{V}_k^u(\delta_h) > \ddot{V}_k^u(\delta_l) \;\Rightarrow\; \text{element remains deactivated}$$

Some further remarks are in order here. Again, of interest is the minimization of $\dot{V}$. Since $\bar{z}$, $\boldsymbol{u}$, and $\boldsymbol{v}$ are fixed at any instant in time, $\dot{V}^z$, $\dot{V}^u$, and $\dot{V}^v$ will also be fixed at that instant in time, as will be $\dot{\bar{z}}$ from (4-9). Hence, an instantaneous change in $\dot{V}$ cannot be effected because $\dot{V}^z$, $\dot{V}^u$, and $\dot{V}^v$ cannot be directly altered (except in the case of the deactivation of a Type 1 element). However, an instantaneous change in $\ddot{V}$ can be effected by directly altering $\ddot{V}^u$. This is accomplished by selecting a particular value for each of the $\dot{u}_k$, which then determines each of the $\ddot{V}_k^u$. It should be recognized that the last term in (4-59) may be dropped from consideration by virtue of $\dot{\bar{z}}$ being fixed at a given instant in time.

When operated according to the specified control algorithm, the reaction force level within an element generally increases, in a gradual manner, for a period of time following activation. This gradual development of the reaction force is characteristic of a dynamic

element, since $\dot{u}_k$ must be finite. As long as the value of $\dot{V}_k^u$ is less than or equal to zero, the element should remain activated since the effect it provides upon $\dot{V}$ is anticipated to be favorable to the control strategy; the value of $\ddot{V}_k^u$ under these conditions is of no consequence. However, when the value of $\dot{V}_k^u$ is greater than zero, it is desirable to drive that value to zero as rapidly as possible. This is tantamount to requiring $\ddot{V}_k^u$ to be as negative as possible. Upon examining (4-65) and (4-66), it is evident that this may be accomplished by causing $\dot{u}_k$ and u_k to have opposite signs and requiring $\dot{u}_k$ to be as negative as possible. From (4-34), this will be accomplished if τ (or, equivalently, δ) is selected to be as small as possible. Since $\delta_l < \delta_h$, the deactivated operating state should be selected. If the value of δ_l has been carefully chosen, a process of rapid reduction in the reaction force level will be ensured upon deactivation under most conditions (in the case of a Type 1 element, it is instantaneous).

Once the element is in a deactivated operating state, the concerns are different. In this situation, the value of $\ddot{V}_k^u$ should be maintained as small as possible. This is true either because the value of $\dot{V}_k^u$ is still positive, and it is desired to drive that value to zero as rapidly as possible, or because $\dot{V}_k^u$ is nonpositive, and it desired to cause $\dot{V}_k^u$ to become more negative. Of course, once the element is reactivated, the criterion in (4-69) is used.

For cases in which Type 2 elements are used, u_k is generally nonzero in the deactivated state. Consider the sum which multiplies $\dot{u}_k$ in (4-66), which is the same sum as that which multiplies u_k in (4-65). By referring again to (4-34) and examining all of the combinations obtained by considering the possible signs for this sum and u_k, it may be shown that the criterion in (4-70) is consistent with the desired objectives. Moreover, when the criterion in (4-70) indicates that the element should be reactivated, the resulting operating state will never immediately conflict with the criterion in (4-69).

For cases in which Type 1 elements are used, u_k is always zero in the deactivated state. In addition, although it is not apparent from (4-34), $\dot{u}_k$ will be zero for $\delta = \delta_l$, while $\dot{u}_k$ will equal just the first term in (4-34) for $\delta = \delta_h$. This is a result of the singular

conditions associated with a Type 1 element: $\delta_l \to 0$ and $\delta_h \to \infty$. Hence, $\dot{V}_k^u$ is always zero in the deactivated state, and it is necessary to examine $\ddot{V}_k^u$ in order to determine the appropriate operating state.

4.7 Results

The simulation results are compiled in the form of response time-history diagrams, which plot the dominant modal response coordinates of the primary system, the $\bar{x}_j$, versus the time, t, for the first 30 seconds of each excitation input record. The modal response coordinates are of principal interest because the control effort is specifically directed at reducing the maximum absolute value of these quantities. As will be seen, the first or *fundamental* response mode of the uncontrolled primary system exhibits the most activity for the ensemble of excitation records considered. For this reason, only the fundamental response mode is specifically targeted for reduction in all cases.

In all of the time-history diagrams, solid and dashed lines are used to illustrate the response of a designated modal coordinate for a controlled and uncontrolled primary system, respectively, that is associated with a particular control case. Usually, three such diagrams, corresponding to the three excitation records, are shown on a single page. As previously discussed in Chapter 3, the symbols ELC, TAF, and HOL denote the 1940 El Centro, 1952 Taft Lincoln School Tunnel, and 1971 Holiday Inn excitation records.

The $\bar{x}_j$ are dimensionally expressed in centimeters. This is because the matrix Φ used for the mapping in (4-6) is taken to be dimensionless, and the relative displacements of the primary system nodal masses, the x_k, are computed in centimeters. Hence, the $\bar{x}_j$ may be interpreted in a physical manner by recognizing that the quantity $\varphi_{kj}\,\bar{x}_j$ represents the contribution, in centimeters, to the relative displacement of the kth nodal mass by the jth modal coordinate, where φ_{kj} is the entry in the kth row and jth column of Φ. The columns of Φ — given by the η^j in (4-7) and (4-8), and referred to as *mode shapes* — are indicated in Tables 4.2 and 4.3 for a 6-story and 3-story primary system, respectively.

These mode shapes are schematically illustrated in Figures 4.8 and 4.9.

Figures 4.10 through 4.12 and Figures 4.13 through 4.15 show the uncontrolled response of the first three modes for a 6-story and 3-story primary system, respectively. These structural systems possess fundamental frequencies of vibration of 1.00 Hz and 1.85 Hz. In the case of the 6-story primary system, the response of the higher modes is not shown because they exhibit no significant activity, relative to the lower modes, for all of the control cases examined.

In addition to time-history diagrams, tabular data is provided for most of the control cases examined, which consists of both peak and root-mean-square (RMS) nodal mass accelerations and story drifts for the primary system. Tables 4.4 and 4.5 give the nodal mass accelerations and story drifts, respectively, for the case of an uncontrolled 6-story primary system. Tables 4.6 and 4.7 give these same quantities for the case of an uncontrolled 3-story primary system.

In both these tables and the discussion below, a special notation is used to describe the control cases in Categories 2 through 4. If an n_1-story primary system interacts with an n_2-story auxiliary system, then this interaction arrangement is said to be characterized by an n_1–n_2 *primary-auxiliary system configuration.* Such a description is not applicable to the control cases in Categories 1 and 5, for obvious reasons.

For each of the categories, a class of special reference cases is considered as well, in which all of the interaction elements are permanently locked in the activated operating state for the duration of the simulation. As mentioned before, this is done to verify both the efficacy of the switching process and the necessity of a control algorithm for the class of proposed control cases. It is recognized that another class of reference cases could be considered, in which the interaction elements are permanently locked in the deactivated operating state. However, this class would apply only to control cases which utilize Type 2 elements. In fact, some of these latter reference cases were examined in this study, but it was observed that the system response did not significantly differ from that for the

uncontrolled cases. Therefore, no further attention is given to these latter reference cases.

Category 1:

The schematic illustration for the interaction arrangement associated with the cases in this category is given in Figure 4.3. Only a 6-story primary system is considered, and the auxiliary system is absent. These cases utilize either Type 1 or 2 elements, and control effectiveness is examined for $\mu = 0.50$ and 1.00. These values are considered to be physically realizable in view of the location and attachment of the elements.

Figures 4.16 and 4.17 show the response of Modes 1 and 2 for a case that uses Type 1 elements with $\mu = 0.50$, and for which all elements participate. Significant response reduction is achieved in the first mode for each of the excitation records. In addition, the second mode response is moderately suppressed as a result of the control effort, though it is not specifically targeted for reduction by the control algorithm. Figure 4.18 shows the response of Mode 1 for a case that uses Type 2 elements with $\mu = 0.50$ and $\delta_l = 5.00$, and for which all elements participate. Almost the same degree of response reduction is achieved as in the case utilizing Type 1 elements (the second mode response for this case is virtually the same as that shown in Figure 4.17).

Figure 4.19 shows the response of Mode 1 for the special reference case that corresponds to the control case used for Figure 4.16. Clearly, the response of Mode 1 is adversely affected in comparison to both that obtained by using the proposed control method and that which results from using no control for each of the excitation records.

Figures 4.20 and 4.21 show the response of Modes 1 and 2 for a case that corresponds to the control case used for Figures 4.16 and 4.17, but for which only the bottom three elements participate. Figure 4.20 indicates that nearly the same degree of response reduction is achieved in the first mode, while Figure 4.21 reveals that the second mode is significantly excited as a result of this control effort.

Finally, Figure 4.22 shows the response of Mode 1 for a case that corresponds to the control case used for Figure 4.16, but for which only the top three elements participate.

Clearly, the first mode response is degraded in comparison to that obtained by using the proposed control method.

Tables 4.8 through 4.11 give data on the peak and RMS nodal mass accelerations and story drifts for the cases corresponding to the proposed control method, which use either Type 1 or 2 elements, with the indicated element participation. These data indicate that both the acceleration levels and the drift levels are generally reduced in comparison to that which results by using no control. However, a trend of decrease in the drift levels is typically observed as μ is increased, while a trend of increase in the acceleration levels is generally observed as μ is increased.

Category 2:

The schematic illustration for the interaction arrangement associated with the cases in this category is given in Figure 4.4. Only a 6-story primary system is considered. These cases utilize either modified Type 1 or 2 elements, and control effectiveness is examined for $\alpha = 1.00$ and 2.00. These values are considered to be physically realizable in view of the character of the auxiliary system for this category.

Figures 4.23 and 4.24 show the response of Modes 1 and 2 for a case that uses $\alpha = 1.00$ and modified Type 1 elements, and which involves a 6–6 primary-auxiliary system configuration for which all elements participate. Significant response reduction is achieved in the first mode for each of the excitation records. In addition, the second mode response is moderately suppressed as a result of the control effort, though it is not specifically targeted for reduction by the control algorithm. Figure 4.25 shows the response of Mode 1 for a case that uses $\alpha = 1.00$ and modified Type 2 elements with $\delta_l = 5.00$, and which involves a 6–6 primary-auxiliary system configuration for which all elements participate. Almost the same degree of response reduction is achieved as in the case utilizing modified Type 1 elements (the second mode response for this case is virtually the same as that shown in Figure 4.24).

Figure 4.26 shows the response of Mode 1 for the special reference case that

corresponds to the control case used for Figure 4.23. Clearly, the response of Mode 1 is adversely affected in comparison to both that obtained by using the proposed control method and that which results from using no control for most of the excitation records.

Figures 4.27 and 4.28 show the response of Modes 1 and 2 for a case that corresponds to the control case used for Figures 4.23 and 4.24, but which involves a 6–3 primary-auxiliary system configuration for which only the bottom three elements participate. Figure 4.27 indicates that nearly the same degree of response reduction is achieved in the first mode, while Figure 4.26 reveals that the second mode is significantly excited as a result of the control effort.

Finally, Figure 4.29 shows the response of Mode 1 for a case that corresponds to the control case used for Figure 4.23, and which involves a 6–6 primary-auxiliary system configuration for which only the top three elements participate. Figure 4.29 indicates that the degree of response reduction is nearly the same as that in Figure 4.23 and slightly better than that in Figure 4.27 (the second mode response for this case is virtually the same as that which results from using no control).

Tables 4.12 through 4.15 give data on the peak and RMS nodal mass accelerations and story drifts for the cases corresponding to the proposed control method, which use either modified Type 1 or 2 elements and the 6–6 primary-auxiliary system configuration, with the indicated element participation. These data indicate that the drift levels are generally reduced in comparison to that which results by using no control. A trend of decrease in these levels is typically observed as α is increased. Consistent conclusions regarding the acceleration levels are not easily drawn. However, these levels are the same order of magnitude as those which result from using no control.

Category 3(*a*):

The schematic illustration for the interaction arrangement associated with the cases in this category is given in Figure 4.5. Only a 6-story primary system is considered. These cases utilize either Type 1 or 2 elements, and control effectiveness is examined for

$\alpha = 1.00$ and 2.00, $\beta = 0.15$ and 0.30, and $\mu = 1.00$ and 2.00, respectively. These values are considered to be physically realizable in view of the character of the auxiliary system for this category.

Figures 4.30 and 4.31 show the response of Modes 1 and 2 for a case that uses $\alpha = 1.00$, $\beta = 0.15$, and Type 1 elements with $\mu = 1.00$, and which involves a 6–6 primary-auxiliary system configuration for which all elements participate. Significant response reduction is achieved in the first mode for each of the excitation records. In addition, the second mode response is moderately suppressed as a result of the control effort, even though it is not specifically targeted for reduction by the control algorithm. Figure 4.32 shows the response of Mode 1 for a case that uses $\alpha = 1.00$, $\beta = 0.15$, and Type 2 elements with $\mu = 1.00$ and $\delta_l = 5.00$, and which involves a 6–6 primary-auxiliary system configuration for which all elements participate. Almost the same degree of response reduction is achieved as in the case utilizing Type 1 elements (the second mode response for this case is virtually the same as that shown in Figure 4.31).

Figure 4.33 shows the response of Mode 1 for the special reference case that corresponds to the control case used for Figure 4.30. Clearly, the response of Mode 1 is adversely affected in comparison to both that obtained by using the proposed control method and that which results from using no control for most of the excitation records.

Figures 4.34 and 4.35 show the response of Modes 1 and 2 for a case that corresponds to the control case used for Figures 4.30 and 4.31, but which involves a 6–3 primary-auxiliary system configuration for which only the bottom three elements participate. Figure 4.34 indicates that nearly the same degree of response reduction is achieved in the first mode, while Figure 4.35 reveals that the second mode is significantly excited as a result of the control effort.

Finally, Figure 4.36 shows the response of Mode 1 for a case that corresponds to the control case used for Figure 4.30, and which involves a 6–6 primary-auxiliary system configuration for which only the top three elements participate. Figure 4.36 indicates that

the degree of response reduction is nearly the same as that in Figure 4.30 and that in Figure 4.34 (the second mode response for this case is virtually the same as that which results from using no control).

Tables 4.16 through 4.19 give data on the peak and RMS nodal mass accelerations and story drifts for the cases corresponding to the proposed control method, which use either Type 1 or 2 elements and the 6–6 primary-auxiliary system configuration, with the indicated element participation. These data indicate that the drift levels are generally reduced in comparison to that which results by using no control. A trend of decrease in these levels is typically observed as α and μ are increased. However, the acceleration levels are much higher than those in previous categories. Also, it appears that for a given control case, the acceleration levels are typically lower when Type 2 elements are used as compared to when Type 1 elements are used.

Category 3(*b*):

The schematic illustration for the interaction arrangement associated with the cases in this category is given in Figure 4.5. Both 6-story and 3-story primary systems are considered. These cases utilize only Type 1 elements, and control effectiveness is examined for $\alpha = 6.50$, $\beta = 5.00$, and various values of μ. The values chosen for α and β reflect the assumption that the auxiliary system is presumed to be much stronger and more massive than the primary system. The value of α is selected to be 30 percent greater than the value of β because it is assumed that the primary system is of inherently weaker construction; otherwise, it might be expected that the stiffness and mass associated with each story of the auxiliary system should be scaled by the same factor, in which case α and β would be equal. The procedure by which the values selected for μ were obtained is now explained.

Initially, the following values of μ were considered for each primary-auxiliary system configuration: 0.50, 0.20, 0.10, 0.05, 0.02, and 0.01. Upon examining the first mode response of the primary system for each excitation record, it was observed that the

greatest response reduction is achieved for only one or two of these values, so it was concluded that an optimal value for μ might exist. However, this optimal value was not precisely determined. The two consecutive values for which the response reduction is greatest are reported with the tabular data. Because of space limitations, only one of these values is discussed below for each primary-auxiliary system configuration.

Figure 4.37 shows the response of Mode 1 for a case that uses $\mu = 0.05$, and which involves a 6–6 primary-auxiliary system configuration for which all elements participate. Only moderate response reduction is achieved in the first mode for each of the excitation records. Figure 4.38 shows the response of Mode 1 for the special reference case that corresponds to the control case used for Figure 4.37. Clearly, the first mode response is adversely affected in comparison to both that obtained by using the proposed control method and that which results from using no control for each of the excitation records.

Figure 4.39 shows the response of Mode 1 for a case that uses $\mu = 0.10$, and which involves a 6–3 primary-auxiliary system configuration for which only the bottom three elements participate. Significant response reduction is achieved in the first mode for each of the excitation records. However, Figure 4.40 reveals that the second mode is significantly excited as a result of the control effort. Figure 4.41 shows the response of Mode 1 for the special reference case that corresponds to the control case used for Figure 4.39. Clearly, the first mode response is adversely affected in comparison to both that obtained by using the proposed control method and that which results from using no control for each of the excitation records.

Figure 4.42 shows the response of Mode 1 for a case that uses $\mu = 0.05$, and which involves a 3–6 primary-auxiliary system configuration for which only the bottom three elements participate. Significant response reduction is achieved in the first mode for each of the excitation records. Also, the second mode response for this case is virtually the same as that which results from using no control. Figure 4.43 shows the response of Mode 1 for the special reference case that corresponds to the control case used for Figure

4.42. Clearly, the first mode response is adversely affected in comparison to both that obtained by using the proposed control method and that which results from using no control for most of the excitation records.

Tables 4.20 through 4.25 give data on the peak and RMS nodal mass accelerations and story drifts for the cases corresponding to the proposed control method, which use Type 1 elements and the 6–6, 6–3, and 3–6 primary-auxiliary system configurations, with the indicated element participation. These data indicate that the drift levels are generally reduced in comparison to that which results by using no control. In contrast, the acceleration levels are generally elevated in comparison to that which results by using no control. Only the acceleration levels associated with the 3–6 primary-auxiliary system configuration are generally reduced in comparison to that which results by using no control.

Category 4:

The schematic illustration for the interaction arrangement associated with the cases in this category is given in Figure 4.5. Both 6-story and 3-story primary systems are considered. These cases utilize only Type 3 elements, and control effectiveness is examined for $\alpha = 6.50$ and $\beta = 5.00$. The values chosen for α and β reflect the assumption that the auxiliary system is presumed to be much stronger and more massive than the primary system. The same reasons as are given for Category 3(b) apply to this category. For the cases involving a 6-story primary system, either $\delta_h = 5.00$ or 10.00; for the cases involving a 3-story primary system, either $\delta_h = 2.71$ or 5.42. These choices for δ_h ensure that the interaction elements used for the 3-story primary system are the same as those used for the 6-story primary system, owing to the manner in which δ_h is defined (confer with (4-49)). The values selected for δ_h are considered to be near the upper limit that could be physically realized by the actual devices which the Type 3 elements are supposed to represent.

Figure 4.44 shows the response of Mode 1 for a case that uses $\delta_h = 10.00$, and

which involves a 6–6 primary-auxiliary system configuration for which all elements participate. Only moderate response reduction is achieved in the first mode for each of the excitation records. Figure 4.45 shows the response of Mode 1 for the special reference case that corresponds to the control case used for Figure 4.44. It is evident that the degree of response reduction for the first mode is less than that for the proposed control method for each of the excitation records.

Figure 4.46 shows the response of Mode 1 for a case that uses $\delta_h = 10.00$, and which involves a 6–3 primary-auxiliary system configuration for which only the bottom three elements participate. Only moderate response reduction is achieved in the first mode for each of the excitation records. Also, the second mode response for this case is virtually the same as that which results from using no control. Figure 4.47 shows the response of Mode 1 for the special reference case that corresponds to the control case used for Figure 4.46. The difference between the degree of response reduction for the first mode in this case and that for the proposed control method is minimal for each of the excitation records.

Figure 4.48 shows the response of Mode 1 for a case that uses $\delta_h = 5.42$, and which involves a 3–6 primary-auxiliary system configuration for which only the bottom three elements participate. Significant response reduction is achieved in the first mode for each of the excitation records. Also, the second mode response for this case is virtually the same as that which results from using no control. Figure 4.49 shows the response of Mode 1 for the special reference case that corresponds to the control case used for Figure 4.48. The difference between the degree of response reduction for the first mode in this case and that for the proposed control method is minimal for each of the excitation records.

Tables 4.26 through 4.31 give data on the peak and RMS nodal mass accelerations and story drifts for the cases corresponding to the proposed control method, which use Type 3 elements and the 6–6, 6–3, and 3–6 primary-auxiliary system configurations, with

the indicated element participation. These data indicate that the drift levels are generally reduced in comparison to that which results by using no control. A trend of decrease in these levels is typically observed as δ_h is increased. The acceleration levels are generally reduced in comparison to that which results by using no control. A trend of decrease in these levels as δ_h is increased is observed only for the 3–6 primary-auxiliary system configuration.

Category 5:

The schematic illustration for the interaction arrangement associated with the cases in this category is given in Figure 4.6. Only a 6-story primary system is considered. These cases utilize only Type 1 elements, and control effectiveness is examined for $\alpha = 0.00$, $\beta = 0.06$ and 0.30, and various values of μ. The values chosen for α and β reflect the different character of the auxiliary system: a relatively small mass which is connected to the top nodal mass of the primary system by a single interaction element. The value of β is selected as either 1 or 5 percent of the total primary system mass, which is both reasonable and in conformity with the typical values used for structural control applications that involve tuned mass dampers and active mass drivers.

The values selected for μ were obtained in exactly the same manner as described for Category 3(*b*). However, the range of values initially considered for μ was different from that previously used: the values of μ considered in conjunction with $\beta = 0.06$ were 0.050, 0.020, 0.010, 0.005, 0.002, and 0.001; the values of μ considered in conjunction with $\beta = 0.30$ were 0.250, 0.100, 0.050, 0.025, 0.010, and 0.005.

Figure 4.50 shows the response of Mode 1 for a case in which $\beta = 0.06$ and $\mu = 0.005$. Moderate-to-significant response reduction is achieved in the first mode for each of the excitation records. Also, the second mode response for this case is virtually the same as that which results from using no control. Figure 4.51 shows the response of Mode 1 for the special reference case that corresponds to the control case used for Figure 4.50. The degree of response reduction for the first mode in this case is less than that

obtained by using the proposed control method but not very different from that which results from using no control for most of the excitation records.

Figure 4.52 shows the response of the first mode for a case in which $\beta = 0.30$ and $\mu = 0.025$. Significant response reduction is achieved in the first mode for each of the excitation records. Also, the second mode response for this case is virtually the same as that which results from using no control. Figure 4.53 shows the response of the first mode for the special reference case that corresponds to the control case used for Figure 4.52. Clearly, the first mode response is adversely affected in comparison to both that obtained by using the proposed control method and that which results from using no control for each of the excitation records.

Tables 4.32 through 4.35 give data on the peak and RMS nodal mass accelerations and story drifts for the cases corresponding to the proposed control method. These data indicate that the drift levels are generally reduced in comparison to that which results by using no control when the lower value of μ is used. A trend of decrease in these levels is generally observed as β is increased. The acceleration levels are generally reduced in comparison to that which results by using no control when the lower value of μ is used. A trend of decrease in these levels is generally observed as β is increased.

4.8 Discussion

In a manner similar to that done for the study involving two interacting SDOF systems, a qualitative assessment of the control effectiveness or performance achieved is assigned for typical cases in each of the control categories in Table 4.36. It is noted that assessments are made with respect to both story drift and nodal mass acceleration levels.

The results of the Category 1 control cases display excellent modal response reduction capability. In addition to the consistent reduction of drift levels, these results indicate that acceleration levels are generally reduced as well. These features make this specific control approach very attractive. The location and attachment scheme of the

interaction elements, along with the absence of an auxiliary system, render this particular interaction arrangement especially well-suited for the seismic upgrade and retrofit of existing structures.

The results of the Category 2 and 3(*a*) control cases display excellent modal response reduction capabilities as well. Actually, the more realistic cases considered in Category 3(*a*) exhibit nearly the same capability for response reduction as the corresponding more idealistic cases considered in Category 2. However, although consistent reduction of drift levels may be obtained, the acceleration levels are generally elevated. This effect is even more pronounced for the cases in Category 3(*a*), but the severity of the effect for these cases can be lessened if Type 2 elements are employed. If this increase in the acceleration levels can be tolerated, the interaction arrangement used for these categories suggests a suitability for incorporation into newly-built structures in zones of high seismic risk.

For all three of the categories mentioned above, it is demonstrated that some cases for which only a partial complement of the interaction elements is used are nearly as effective at response reduction as the corresponding cases for which the full complement of interaction elements is used. In the Category 1 cases, this partial complement would be the bottom three elements because the interaction elements are driven by the relative displacements between adjacent nodal masses. Upon examining the first mode shape of a 6-story primary system (refer to Table 4.2 and Figure 4.8), it is found that the relative displacements are greatest in the first three stories when the first mode response is dominant. Hence, it is expected that by placing the elements only at these positions, the response control effect would be comparable to that obtained when all of the elements are utilized.

In the Category 2 and 3(*a*) cases, this partial complement would be the top three elements because the interaction elements are now driven by the displacements of both the primary and auxiliary systems. Thus, it is more appropriate to view the elements as a

means of providing applied forces to the primary system. If it is assumed that the elements provide forces that are approximately equal to one another, then since the top three elements have the greatest participation factors (with respect to the first mode) associated with them, it is expected that by placing the elements only at these positions, the response control effect would be comparable to that obtained when all of the elements are utilized. For all three of the categories mentioned above, the response of the second mode is often excited because of the asymmetry in the loading conditions produced by the control forces associated with a partial complement of elements. By examining the second mode shape, it apparent why the loading conditions resulting from the utilization of only the bottom or top half of the available elements causes this excitation.

The control cases in Categories 3(*b*) and 4 correspond to situations involving the interaction of two existing structures. Hence, it is expected that the control approach of these categories is directed at applications involving protection of one of the structures from seismic hazards. For the cases in Category 4, the extent of response reduction is much less than that for the previous categories. This result is largely due to the nature of the interaction elements and the limitation imposed on the maximum value of δ_h. The position adopted in this study is that it would be overly-optimistic to expect that damping ratios greater than 10 percent (with respect to the fundamental mode of vibration) could be physically realized with conventional viscous dampers, and so this restriction is maintained for the semi-active control devices utilized.

Also, it appears that the interaction arrangement for two existing structures works best when structures of differing height are involved. This is probably because the act of coupling the dynamic behavior of the structures would be expected to have a more noticeable effect on either of the two systems when their respective mode shapes are significantly different, as will be true for uniformly-discretized structural systems with differing numbers of degrees of freedom. However, the results have shown (particularly for the cases in Category 3(*b*)) that a *low-high* primary-auxiliary system configuration is

preferable for response control of the primary system than is a *high-low* configuration. Again, this is due the fact that the participation factors associated with the low-high configuration are preferable for the first mode, while the high-low configuration induces significant excitation in the second mode as a result of asymmetric loading conditions.

Finally, the control cases in Category 5 show remarkable response reduction capability in view of the small size of the auxiliary system and the fact that only a single interaction element is employed. Although these cases are not as effective as some of the cases in earlier categories, such an interaction arrangement might prove useful for applications involving wind gust excitation, which have been previously considered for tuned mass dampers and active mass drivers.

Control of Higher Frequency and Several Dominant Modes

Some questions may be raised concerning the capability of the proposed control approach to reduce the response of higher frequency modes or even suppress the response which is due to several dominant modes. As previously mentioned, the ensemble of earthquake records considered significantly excite only the fundamental response mode of the 6-story and 3-story primary systems examined. For this reason, the fundamental mode was solely targeted for response reduction by the control algorithms used.

Some results are now presented in an effort to *suggest* that the control approach may be effective in both reducing the response of significantly-excited higher frequency modes and suppressing the response of several dominant modes. Results are given for a Category 1 controlled primary system, which utilizes Type 1 elements with $\mu = 0.50$, and only externally-unforced (*i.e.*, "free" vibration) response is considered, since the excitation input used for the MDOF system study does not significantly excite any of the modes other than the fundamental mode.

First, consider a 6-story primary system for which the initial conditions have been specified in order to produce dominant response activity in the second mode. Figures 4.54 and 4.55 show the results of the response control effort for cases in which: *only*

Mode 2 is targeted for reduction; and *both* Modes 1 and 2 are targeted for reduction; respectively.

Next, consider a 6-story primary system for which the initial conditions have been specified in order to produce equally-dominant response activity in the first and second modes (*i.e.*, $\bar{x}_2(0) = \bar{x}_1(0)$). Figures 4.56 through 4.58 show the results of the response control effort for cases in which: *only* Mode 1 is targeted for reduction; *only* Mode 2 is targeted for reduction; and *both* Modes 1 and 2 are targeted for reduction; respectively.

The results from these cases indicate that the proposed control approach appears to have the capability to both reduce the response of higher frequency modes and suppress the response of several dominant modes. From a comparison with Figures 4.56 and 4.57, Figure 4.58 strongly suggests that there is an advantage in controlling all dominant response modes when several modes exhibit nearly the same level of activity. In a future study, it would be desirable to consider a situation in which the combination of the structural system and the external excitation yields significant response activity in some higher frequency modes.

Existence of Modes for Category 1 Control Cases

Some important features associated with Category 1 control cases which utilize Type 1 interaction elements are now discussed. As described in Section 4.4, the control algorithm used for the cases that involve dynamic interaction elements hinges upon the quantities $\ddot{V}_k^u$, as given by (4-64), where the subscript refers to the kth element. Consider now a situation in which *all* of the elements are simultaneously either activated or deactivated. Under these conditions, it may be shown that

$$\dot{u} = k_{int}\,\dot{e} \quad , \quad \delta = \delta_h \tag{4-71}$$

$$\dot{u} = 0 \qquad , \quad \delta = \delta_l$$

Because all of the elements are in the same operating state at once, it is now more appropriate to examine $\ddot{V}^u$, as given by (4-61), rather than individually examine each $\ddot{V}_k^u$,

as given by (4-66). From (4-6) and (4-44),

$$\dot{e} = L^{\mathsf{T}}\dot{x} = L^{\mathsf{T}}\Phi\dot{\tilde{x}} \tag{4-72}$$

Hence, using (4-62), (4-71), and (4-72), (4-61) becomes

$$\ddot{V}^{u} = -k_{int}\dot{\tilde{x}}^{\mathsf{T}}\Theta\Phi^{\mathsf{T}}LL^{\mathsf{T}}\Phi\dot{\tilde{x}} \quad , \ \delta = \delta_h \tag{4-73}$$

$$\ddot{V}^{u} = 0 \qquad\qquad\qquad , \ \delta = \delta_l$$

But, as may be verified from the location and attachment of the elements,

$$LL^{\mathsf{T}} = \frac{1}{k}K \tag{4-74}$$

where k is the effective stiffness of all columns at each story and K is the stiffness matrix associated with the uncontrolled primary system. Thus, (4-73) becomes

$$\ddot{V}^{u} = -\sum_{j}\mu\, d_j^{M}\omega_j^2\dot{\tilde{x}}_j^2 \qquad , \ \delta = \delta_h \tag{4-75}$$

$$\ddot{V}^{u} = 0 \qquad\qquad\qquad , \ \delta = \delta_l$$

It is now clear from the control algorithm, as given by (4-69) and (4-70), that once the elements have been deactivated *en masse*, they should be immediately reactivated upon relaxation since the expression for $\ddot{V}^{u}$ in (4-75) is nonpositive definite when $\delta = \delta_h$. Under certain conditions, to be described below, this feature permits the existence and preservation of response modes even while under the effect of the control effort.

Based upon this scheme of collective element operation, (4-71) and (4-72) may be used to determine the reaction forces in the elements at any particular time as

$$\boldsymbol{u}(t) = k_{int}\,L^{\mathsf{T}}\big(\boldsymbol{x}(t) - \boldsymbol{x}(t_s)\big); \ \ t \geq t_s \tag{4-76}$$

where t_s denotes the *switching time*, the time at which the *most recent* deactivation-reactivation process occurred. Equation (4-76) is only valid because of the prescribed operation of the elements (*i.e.*, collective activation or deactivation), the stipulation that the parameter values which characterize the mechanical properties are the same for each

element in both the activated and deactivated operating states, and the assumption that the reaction force level drops immediately to zero upon deactivation (*i.e.*, instantaneous relaxation). Thus, in terms of the modal response coordinates, the equation of motion for primary system becomes

$$\ddot{\bar{x}} + \bar{D}^C \dot{\bar{x}} + (1+\mu)\bar{D}^K \bar{x} = \mu \bar{D}^K \bar{x}(t_s) \tag{4-77}$$

Now suppose that at the initial time t_o, only the jth mode is given nonzero initial conditions. In addition, assume that at t_o, $\bar{x}(t_s)$ is selected so that

$$\bar{x}_i(t_s) = 0; \;\; i \in \{1, \ldots, n\}, \;\; i \neq j \tag{4-78}$$

with arbitrary selection of $\bar{x}_j(t_s)$ (usually taken to be zero). Then the equations in (4-77) become

$$\ddot{\bar{x}}_i + 2\zeta_o \omega_i \dot{\bar{x}}_i + (1+\mu)\omega_i^2 \bar{x}_i = 0 \tag{4-79}$$

where $\dot{\bar{x}}_i(t_o) = 0$ and $\bar{x}_i(t_o) = 0$; $i \in \{1, \ldots, n\}$, $i \neq j$; and

$$\ddot{\bar{x}}_j + 2\zeta_o \omega_j \dot{\bar{x}}_j + (1+\mu)\omega_j^2 \bar{x}_j = \mu \omega_j^2 \bar{x}_j(t_s) \tag{4-80}$$

where $\dot{\bar{x}}_j(t_o)$ and $\bar{x}_j(t_o)$ are specified.

It is evident that dynamic activity will only be present in the jth mode for all $t \geq t_o$. Even as switching events occur, and the value of $\bar{x}_j(t_s)$ generally changes, the zero initial conditions and zero forcing function in the ith mode is maintained. Thus, vibration will only occur in the jth mode, and the undisturbed condition in the ith mode is preserved. Furthermore, it is apparent that the undamped frequency in the jth mode is increased by a factor of $\sqrt{1+\mu}$, and it is a simple matter to show even when $\zeta_o = 0$, the amplitude of response is decreased by a factor of $\left(\frac{1-\mu}{1+\mu}\right)^2$ for each cycle of modal oscillation when $\mu \leq 1$.

Although this result is valid only for systems which are not externally excited, it offers a partial explanation for the fact that significant spillover into other modes is not observed for many of the Category 1 control cases examined, which had full element

participation. This conclusion follows because the fundamental response mode generally experiences a gradual buildup at an oscillatory frequency near the resonant frequency, much like the situation for free vibration, for each of the excitation records considered.

References for Chapter 4

1. W. T. Thomson, *Theory of Vibration With Applications*, 2nd ed., Englewood Cliffs, N.J.: Prentice-Hall, Inc., 1981, Chap. 10.

2. G. Strang, *Linear Algebra and Its Applications*, 2nd ed., New York: Academic Press, Inc., 1980, Chap. 6.

3. L. Meirovitch and H. Öz, "Active Control of Structures by Modal Synthesis," *Structural Control, Proc. of Intnl. IUTAM Symposium on Struct. Control*, ed. by H. H. E. Leipholz, Ontario, Canada, 1979, Amsterdam: North-Holland Pub. Co., 1980, pp. 505–521.

4. J. N. Yang and M. J. Lin, "Optimal Critical-Mode Control of Building Under Seismic Load," *Jour. of Engrg. Mech., Proc. of ASCE*, Vol. 108, No. EM6, Dec. 1982, pp. 1167–1185.

5. J.-J. E. Slotine and W. Li, *Applied Nonlinear Control*, Englewood Cliffs, N.J.: Prentice-Hall, Inc., 1991, Chap. 4.

6. C. Lanczos, *The Variational Principles of Mechanics*, 4th ed., New York: Dover Publications, Inc., 1970, Chap. 3.

7. T. T. Soong and A. M. Reinhorn, "Full-Scale Implementation of Active Structural Control," *Intelligent Structures – 2: Monitoring and Control, Proc. of Intnl. Workshop on Intel. Systems*, ed. by Y. K. Wen, Perugia, Italy, 1991, London: Elsevier Science Pub. Ltd., 1992, pp. 252–263.

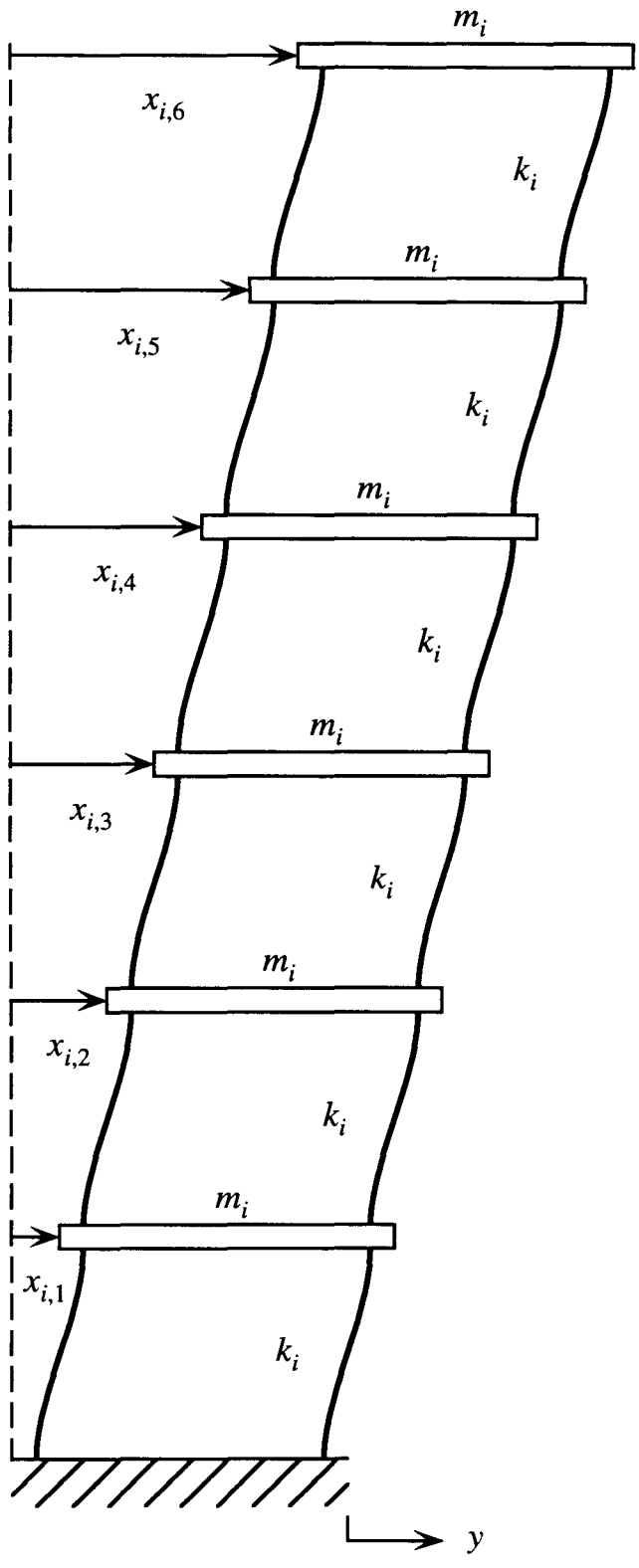

Figure 4.1. Schematic Representation of Generic Primary or Auxiliary System.

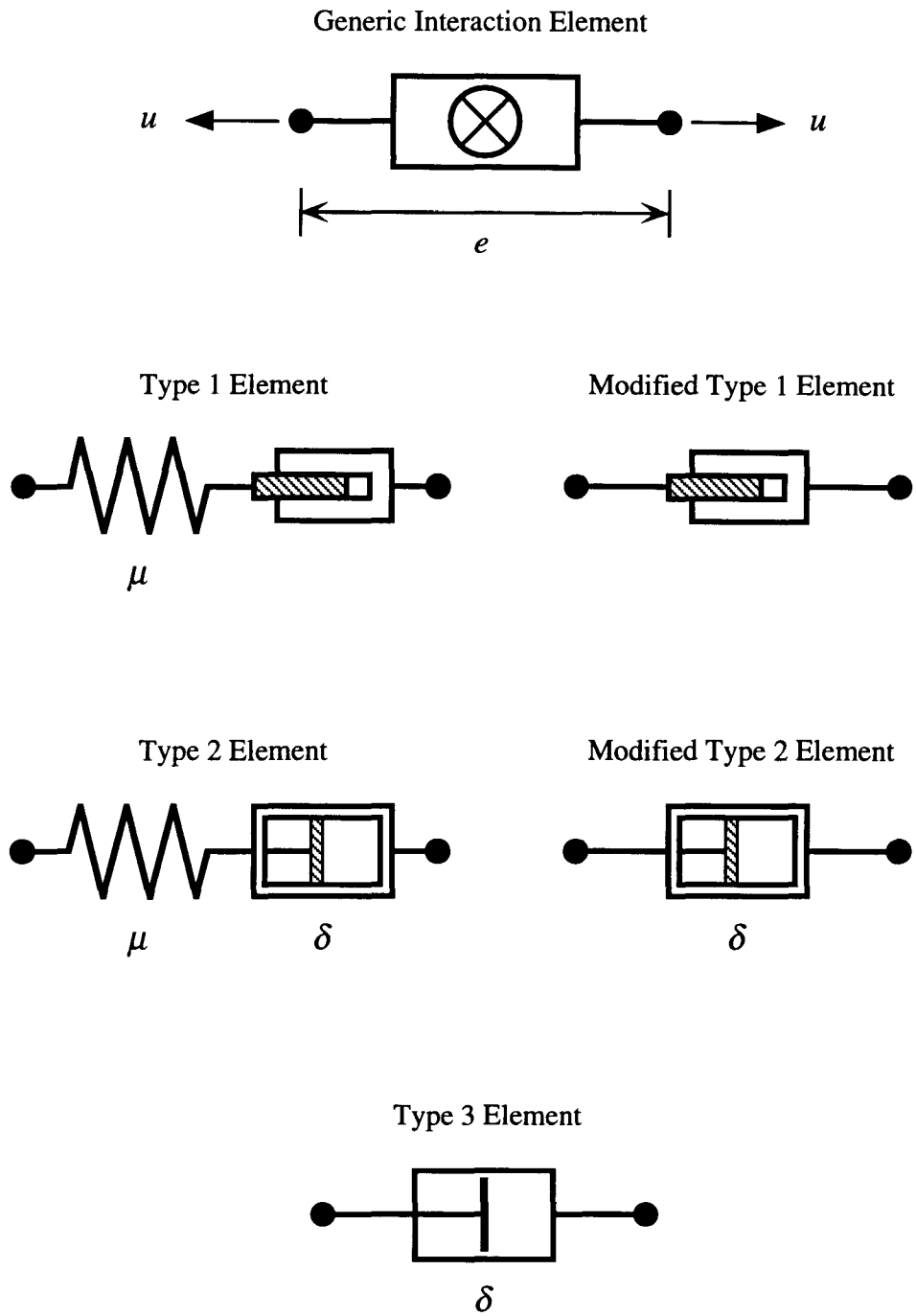

Figure 4.2. Schematic Representation of Interaction Elements Used for MDOF System Study.

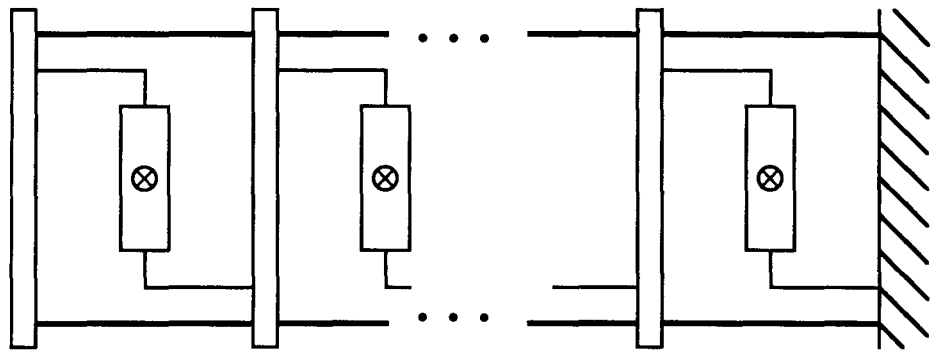

Figure 4.3. Configuration of Primary System for Category 1 Control Cases. Generic interaction elements are shown.

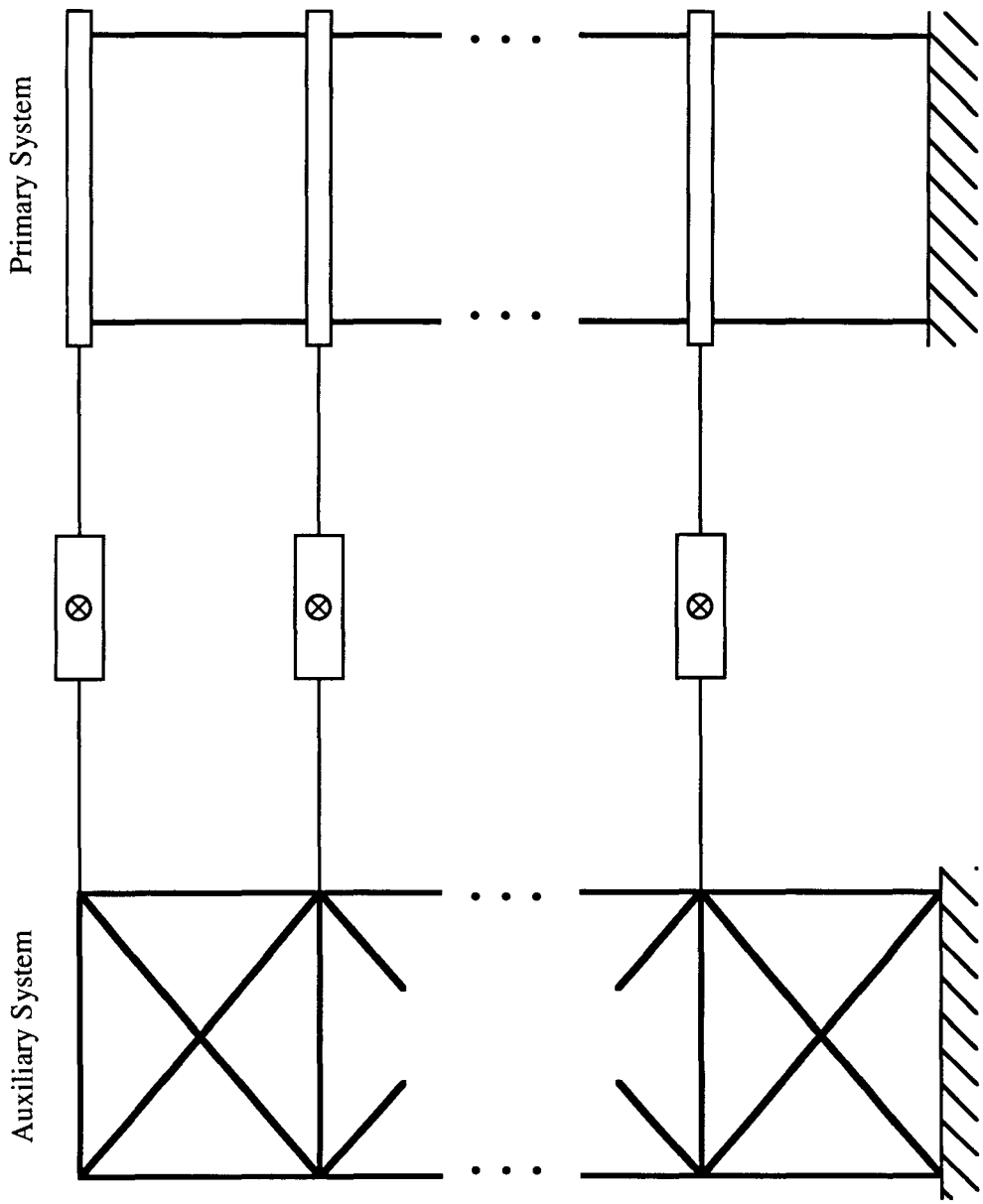

Figure 4.4. Primary-Auxiliary System Configuration for Category 2 Control Cases. Generic interaction elements are shown.

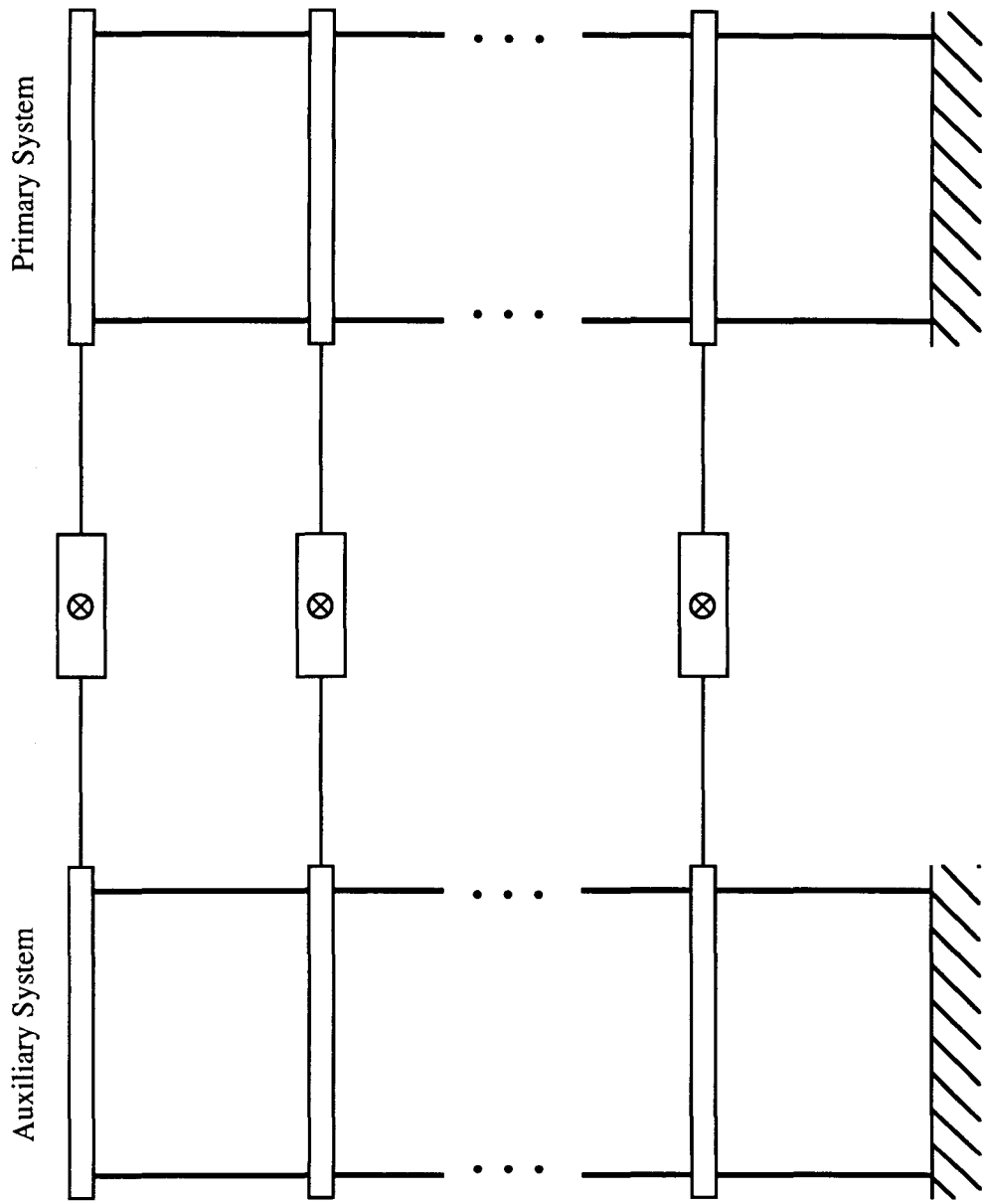

Figure 4.5. Primary-Auxiliary System Configuration for Category 3 and 4 Control Cases. Generic interaction elements are shown.

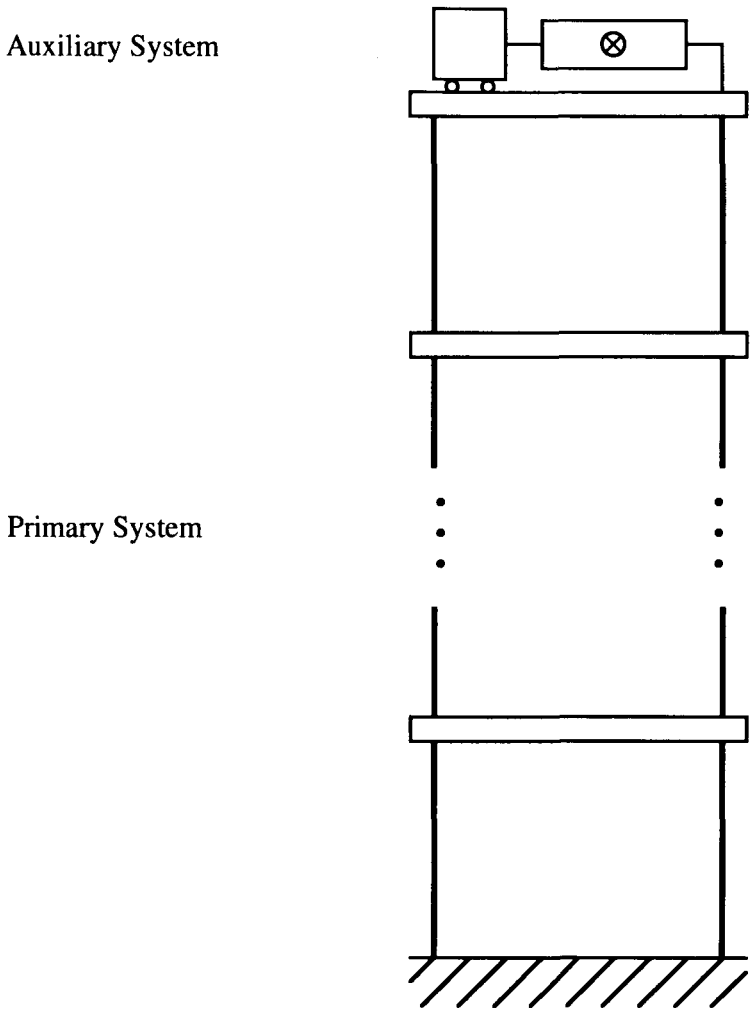

Figure 4.6. Primary-Auxiliary System Configuration for Category 5 Control Cases. A generic interaction element is shown.

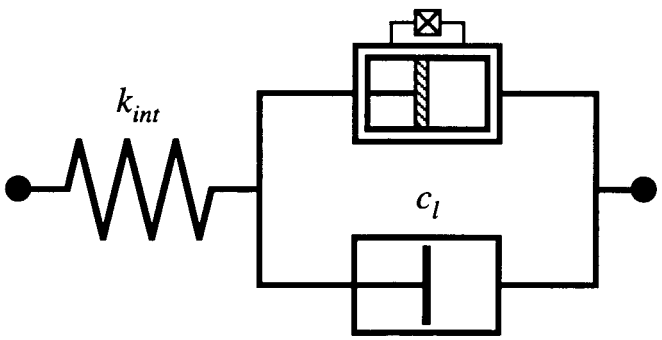

(a) Type 2 Element

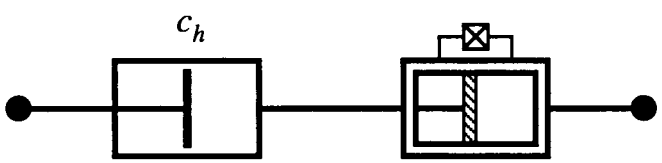

(b) Type 3 Element

Figure 4.7. Configuration of Actual Hardware to Produce (a) Type 2 or (b) Type 3 Elements.

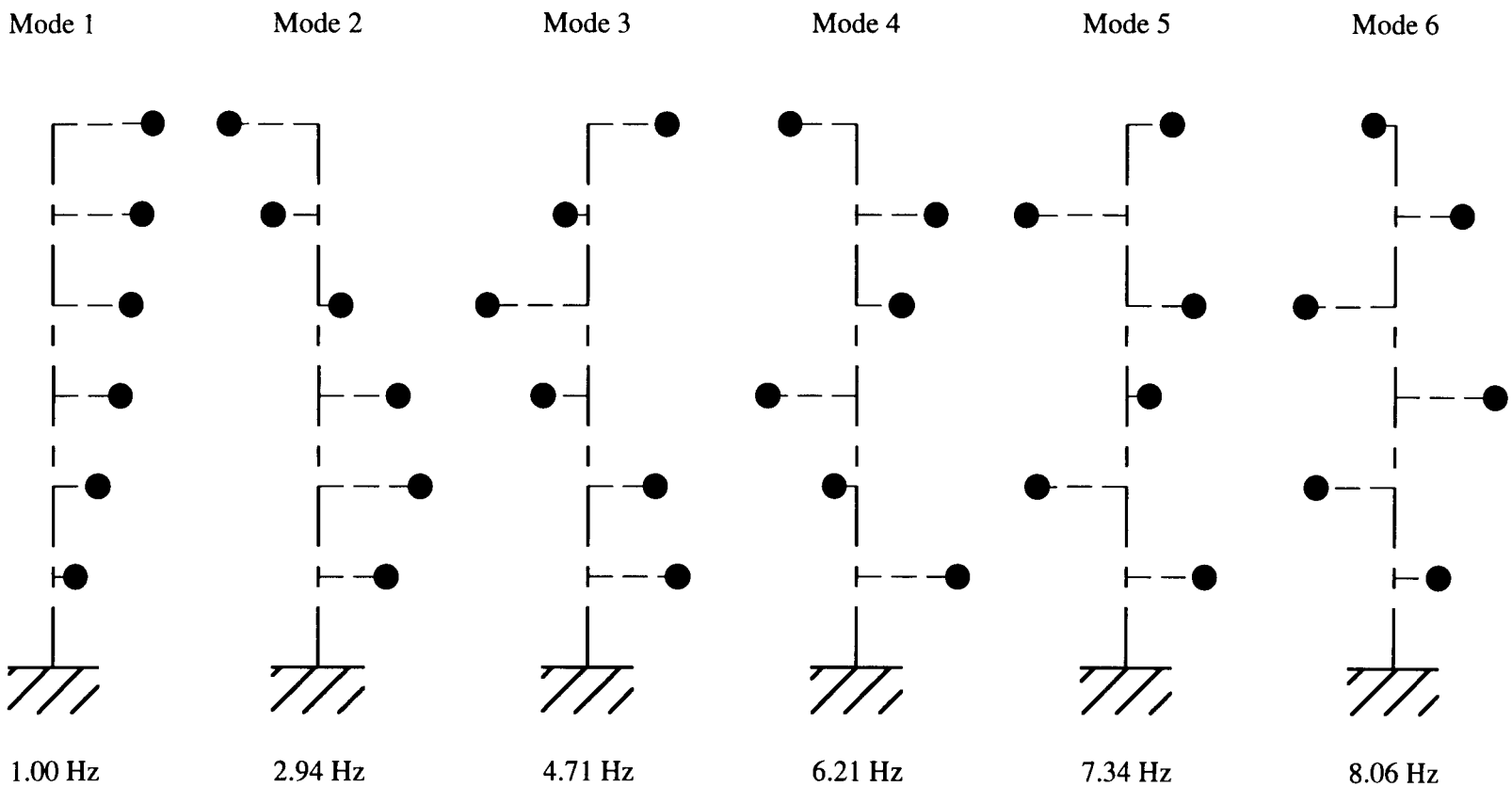

Figure 4.8. Graphical Depiction of Mode Shapes for a 6-Story Primary System. Vibrational frequencies are indicated for each mode.

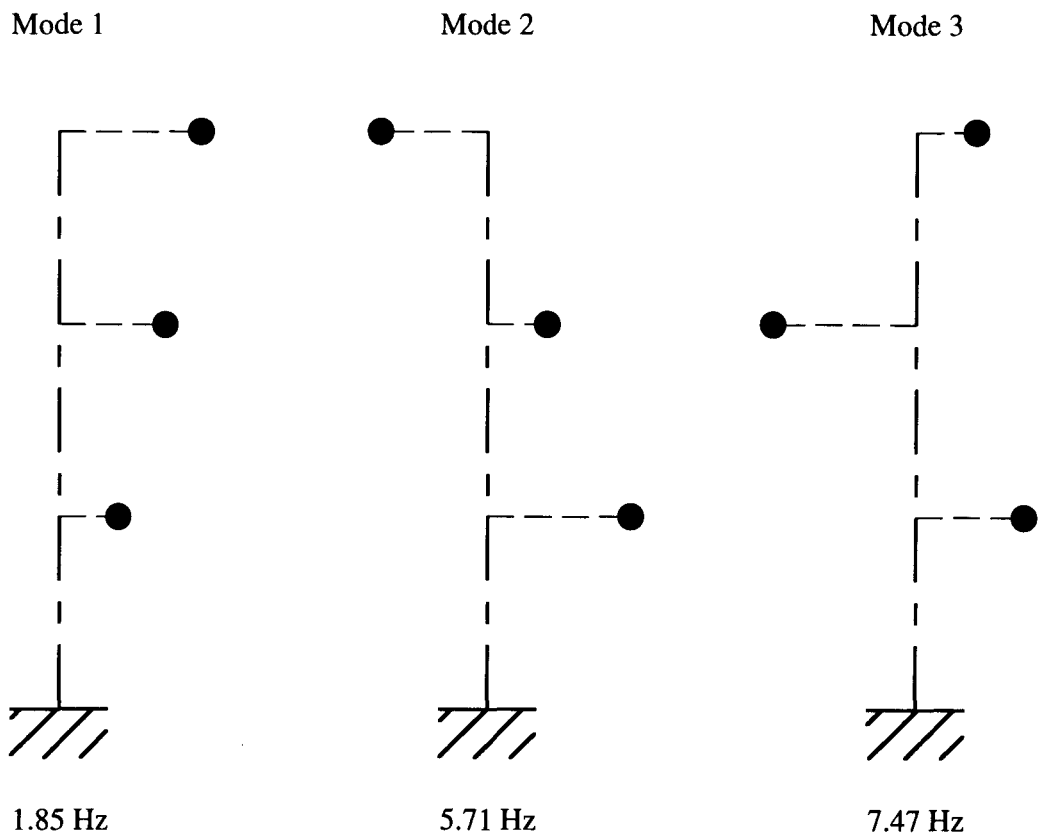

Figure 4.9. Graphical Depiction of Mode Shapes for a 3-Story Primary System. Vibrational frequencies are indicated for each mode.

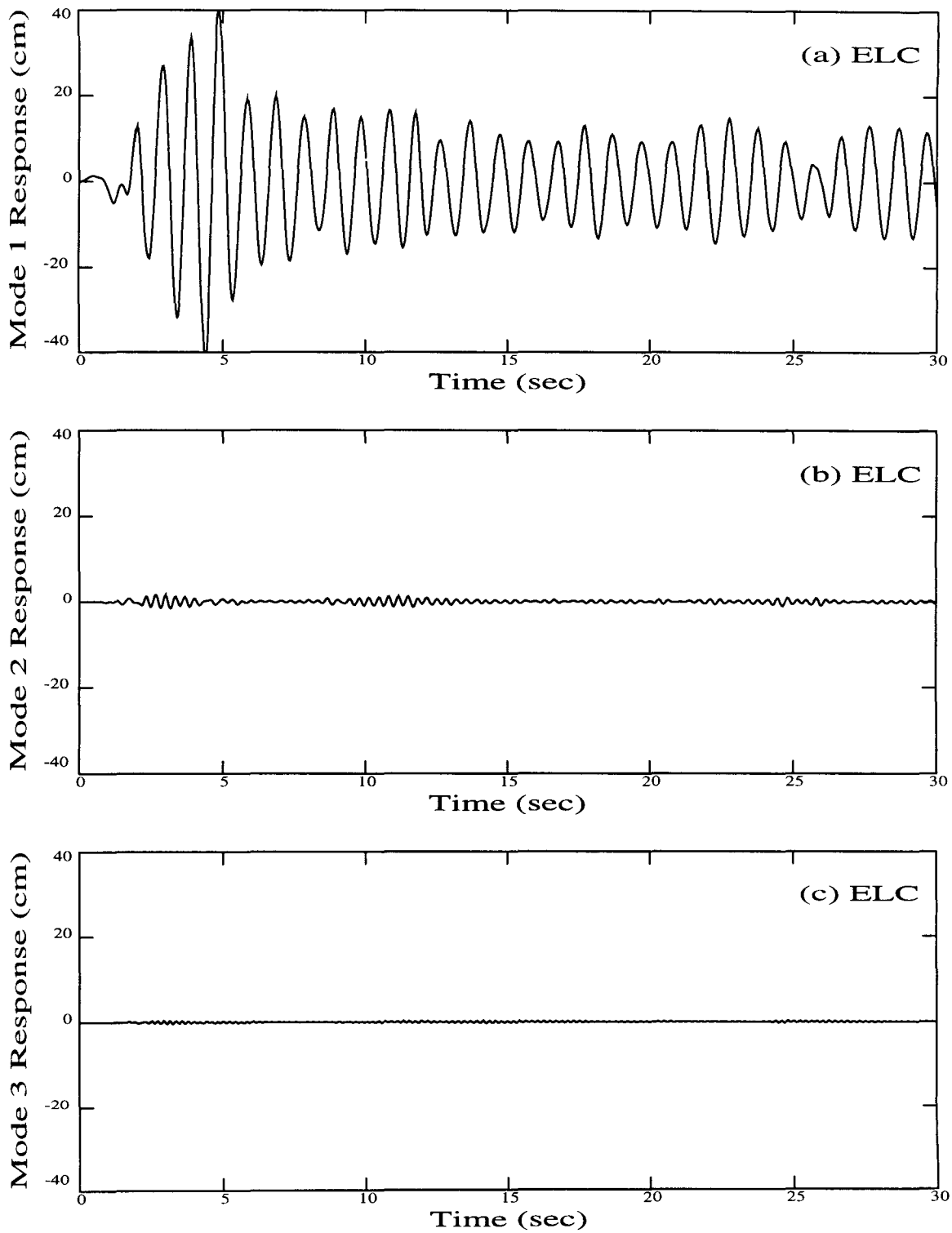

Figure 4.10. Response Time-History of (a) Mode 1, (b) Mode 2, and (c) Mode 3 for a 6-Story Uncontrolled Primary System Subjected to the El Centro Excitation Record.

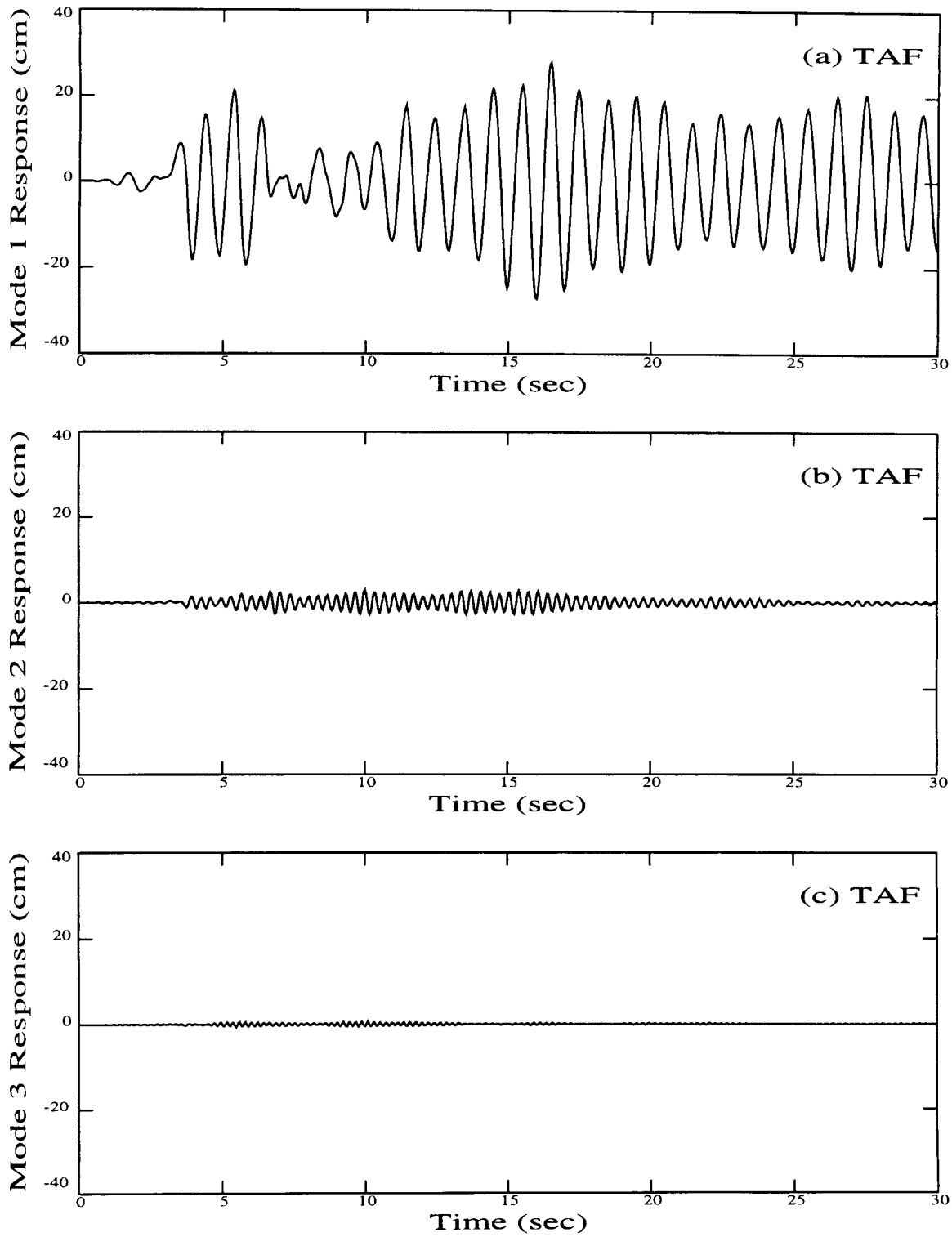

Figure 4.11. Response Time-History of (a) Mode 1, (b) Mode 2, and (c) Mode 3 for a 6-Story Uncontrolled Primary System Subjected to the Taft Lincoln School Tunnel Excitation Record.

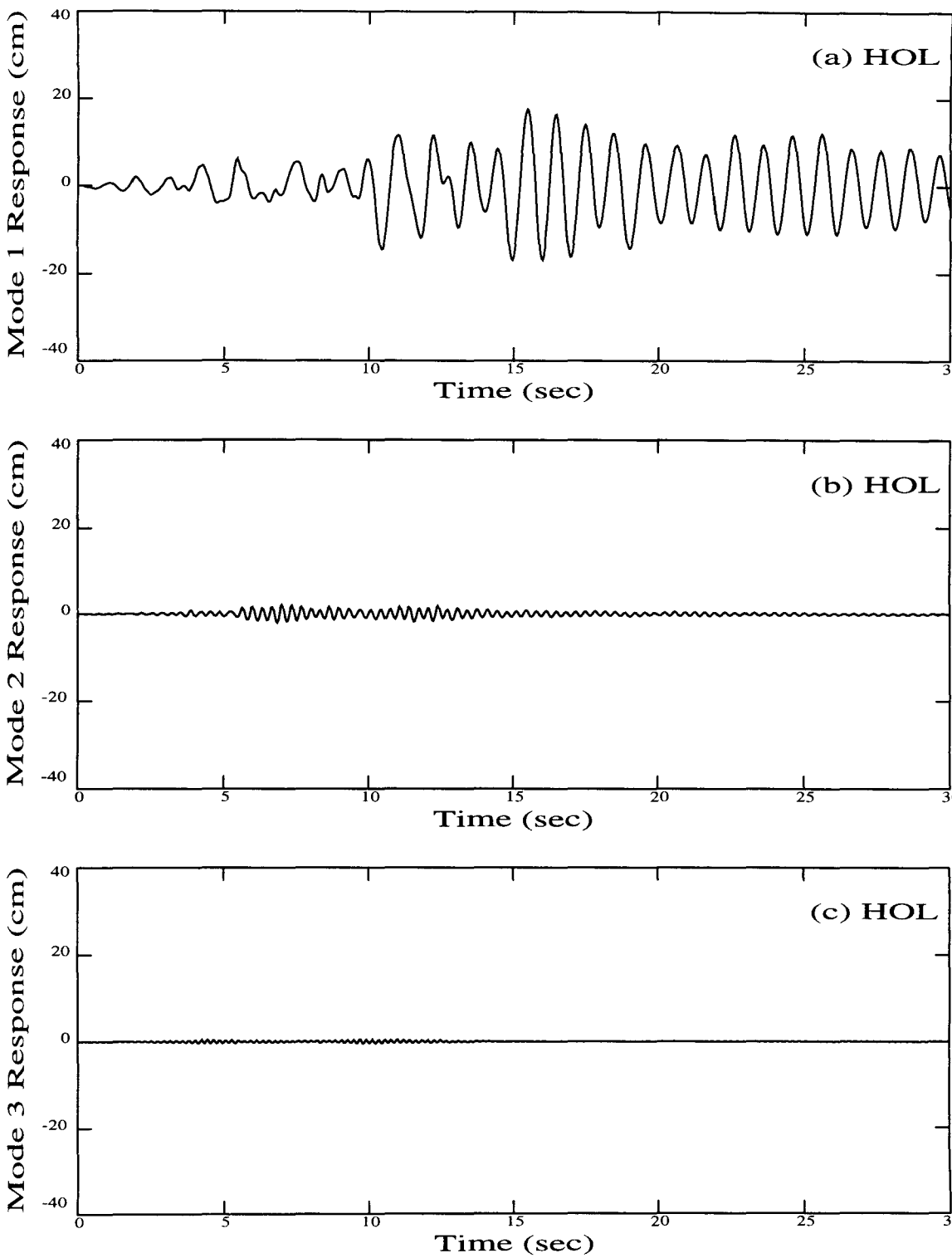

Figure 4.12. Response Time-History of (a) Mode 1, (b) Mode 2, and (c) Mode 3 for a 6-Story Uncontrolled Primary System Subjected to the Holiday Inn Excitation Record.

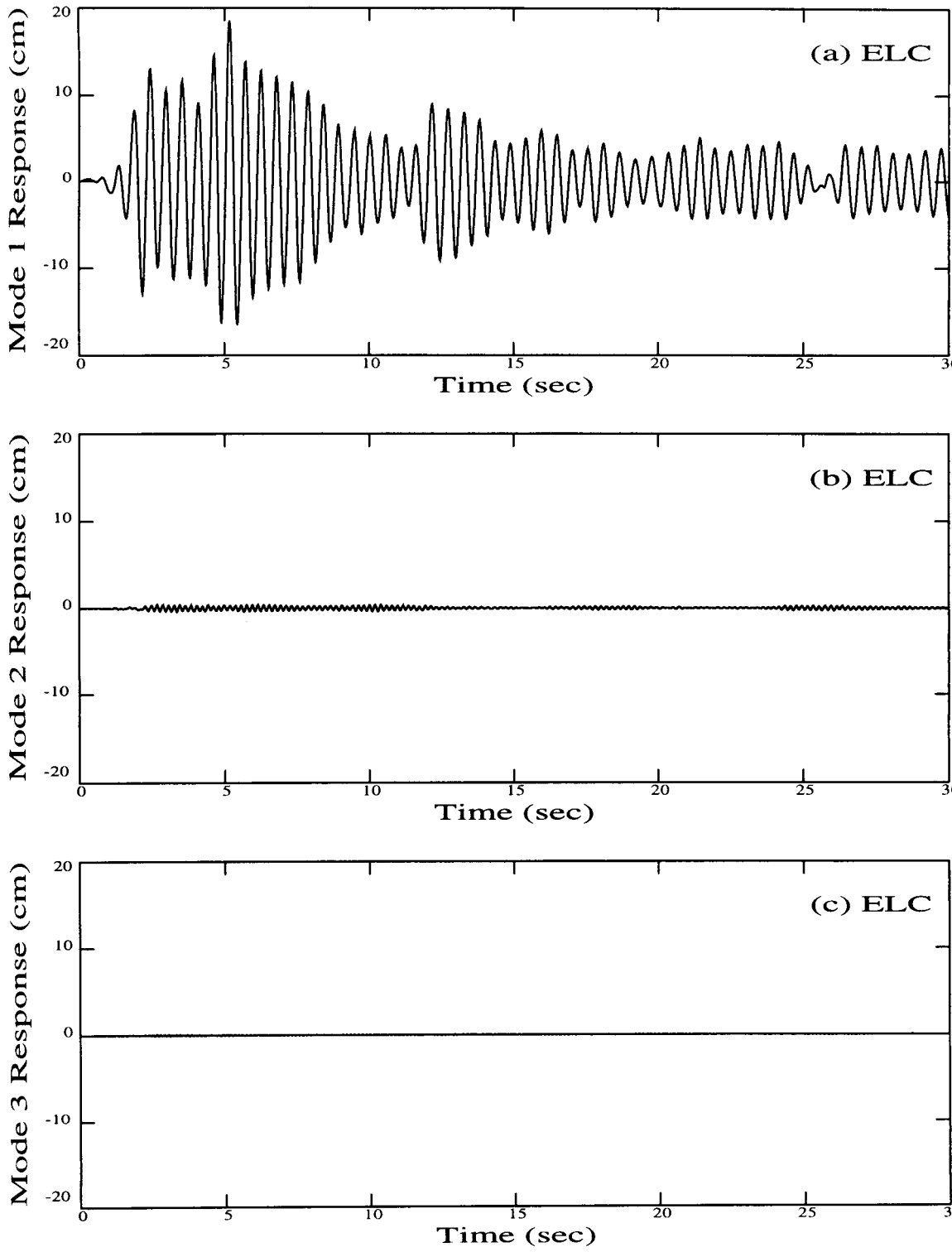

Figure 4.13. Response Time-History of (a) Mode 1, (b) Mode 2, and (c) Mode 3 for a 3-Story Uncontrolled Primary System Subjected to the El Centro Excitation Record.

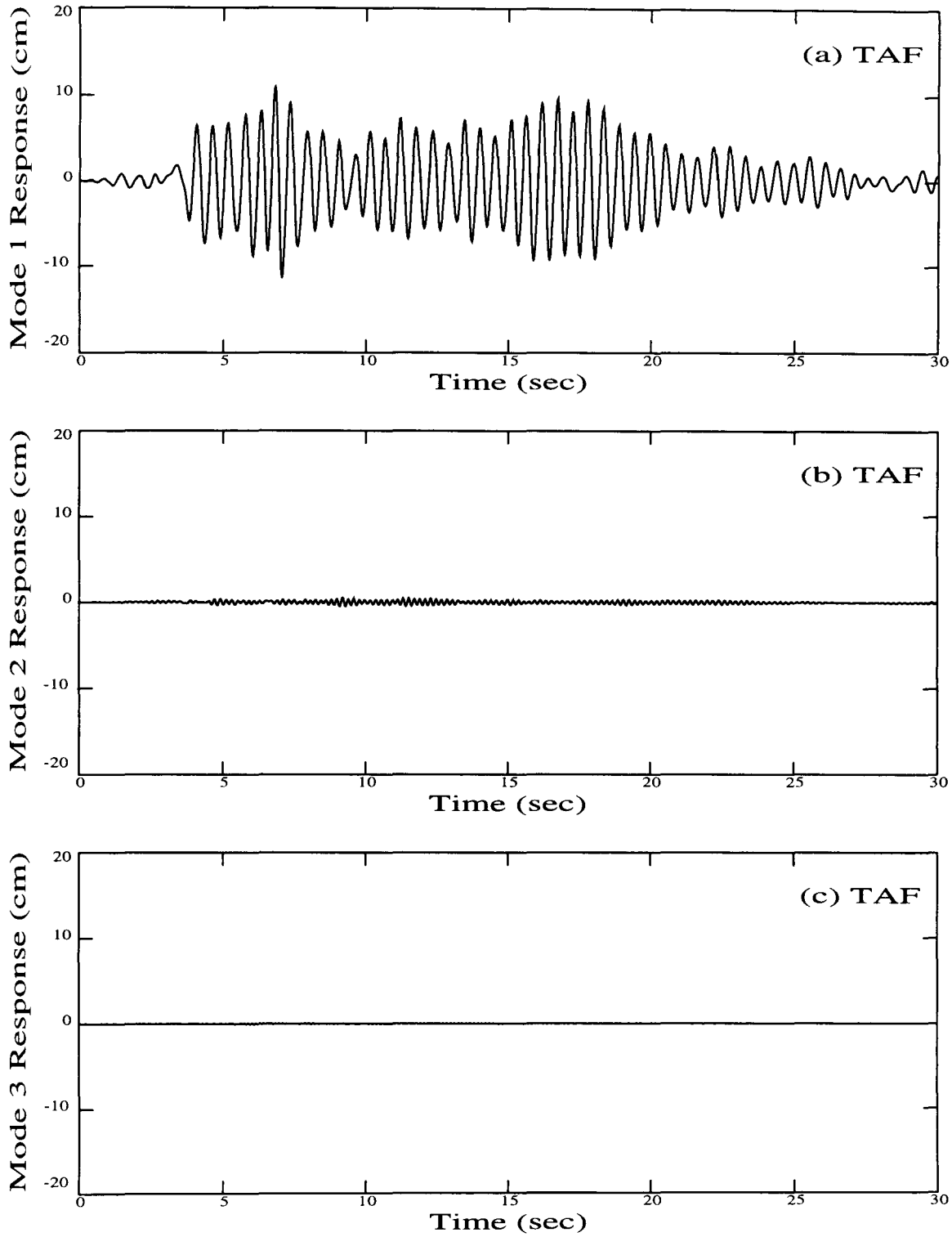

Figure 4.14. Response Time-History of (a) Mode 1, (b) Mode 2, and (c) Mode 3 for a 3-Story Uncontrolled Primary System Subjected to the Taft Lincoln School Tunnel Excitation Record.

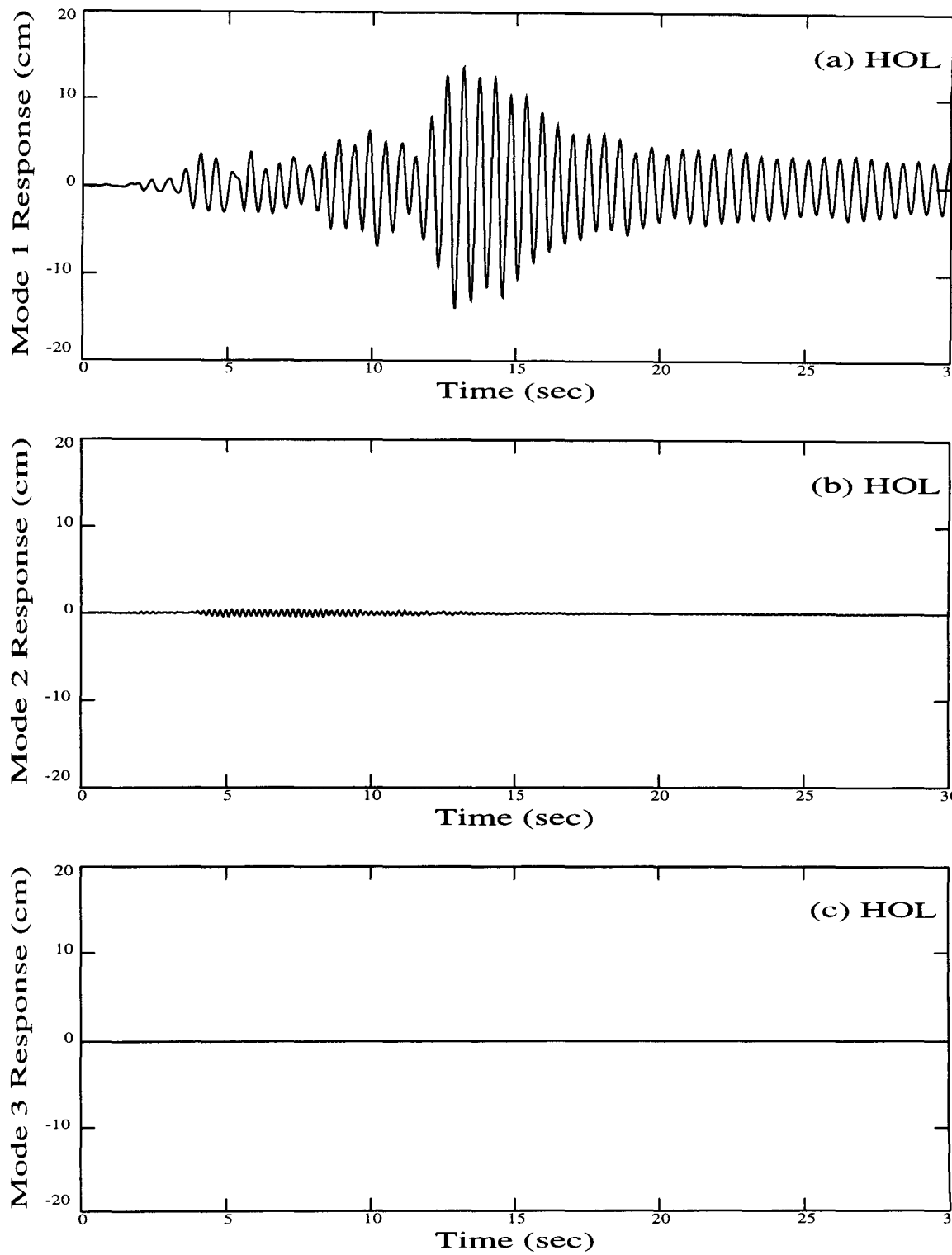

Figure 4.15. Response Time-History of (a) Mode 1, (b) Mode 2, and (c) Mode 3 for a 3-Story Uncontrolled Primary System Subjected to the Holiday Inn Excitation Record.

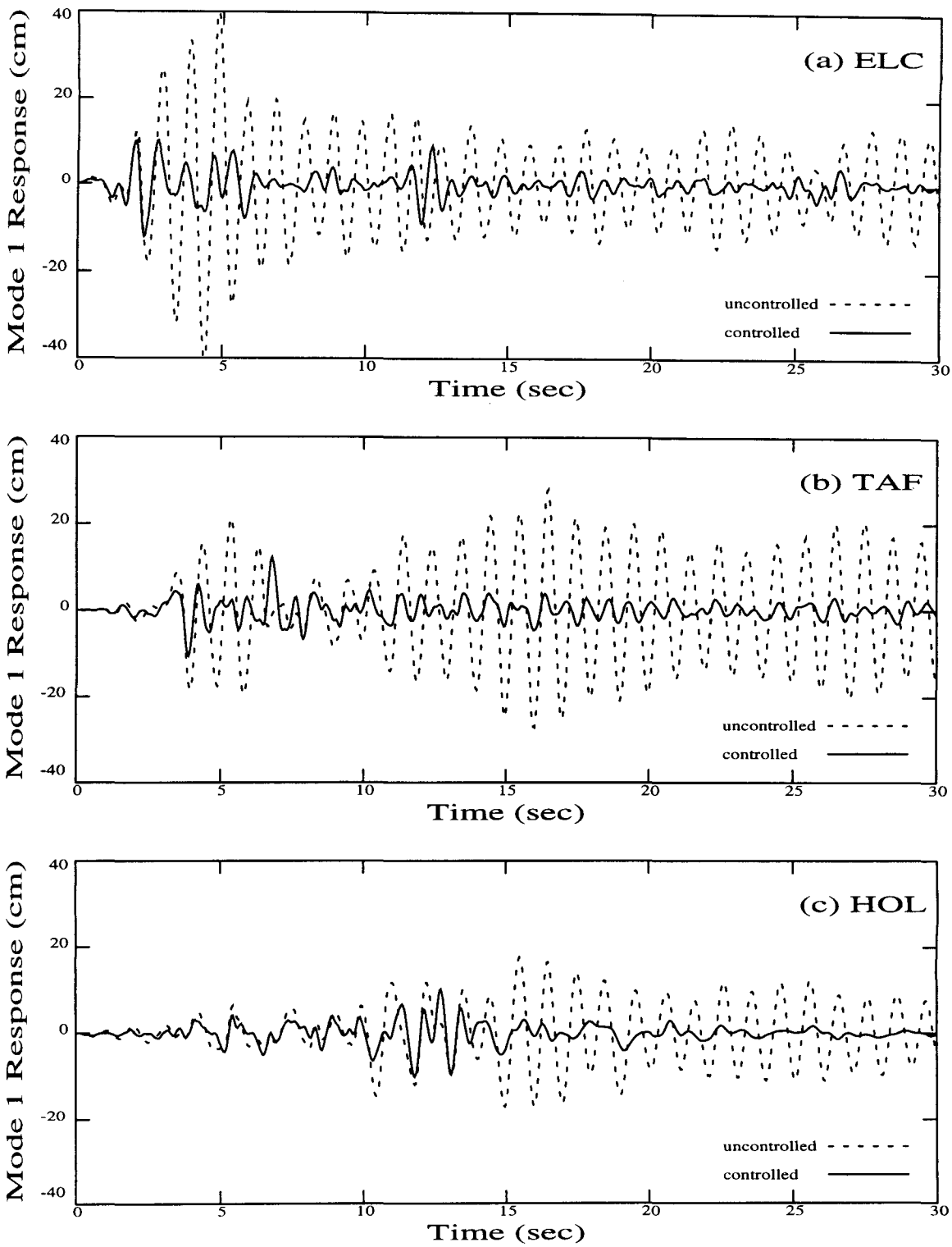

Figure 4.16. Response Time-History of Mode 1 for a 6-Story Category 1 Controlled Primary System Subjected to the (a) El Centro, (b) Taft Lincoln School Tunnel, and (c) Holiday Inn Excitation Records. Type 1 elements are used, with $\mu = 0.50$. All elements participate.

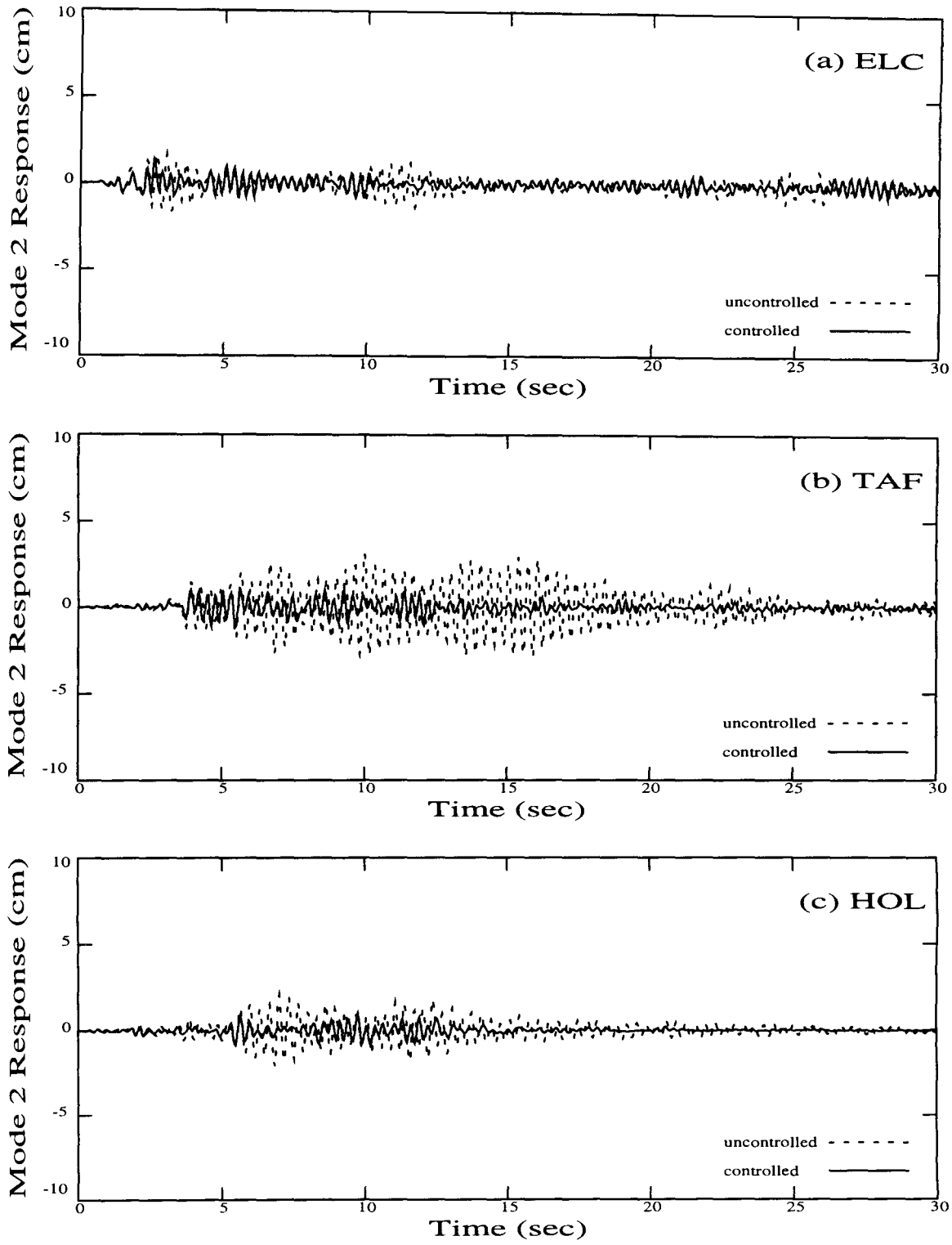

Figure 4.17. Response Time-History of Mode 2 for a 6-Story Category 1 Controlled Primary System Subjected to the (a) El Centro, (b) Taft Lincoln School Tunnel, and (c) Holiday Inn Excitation Records. Type 1 elements are used, with $\mu = 0.50$. All elements participate.

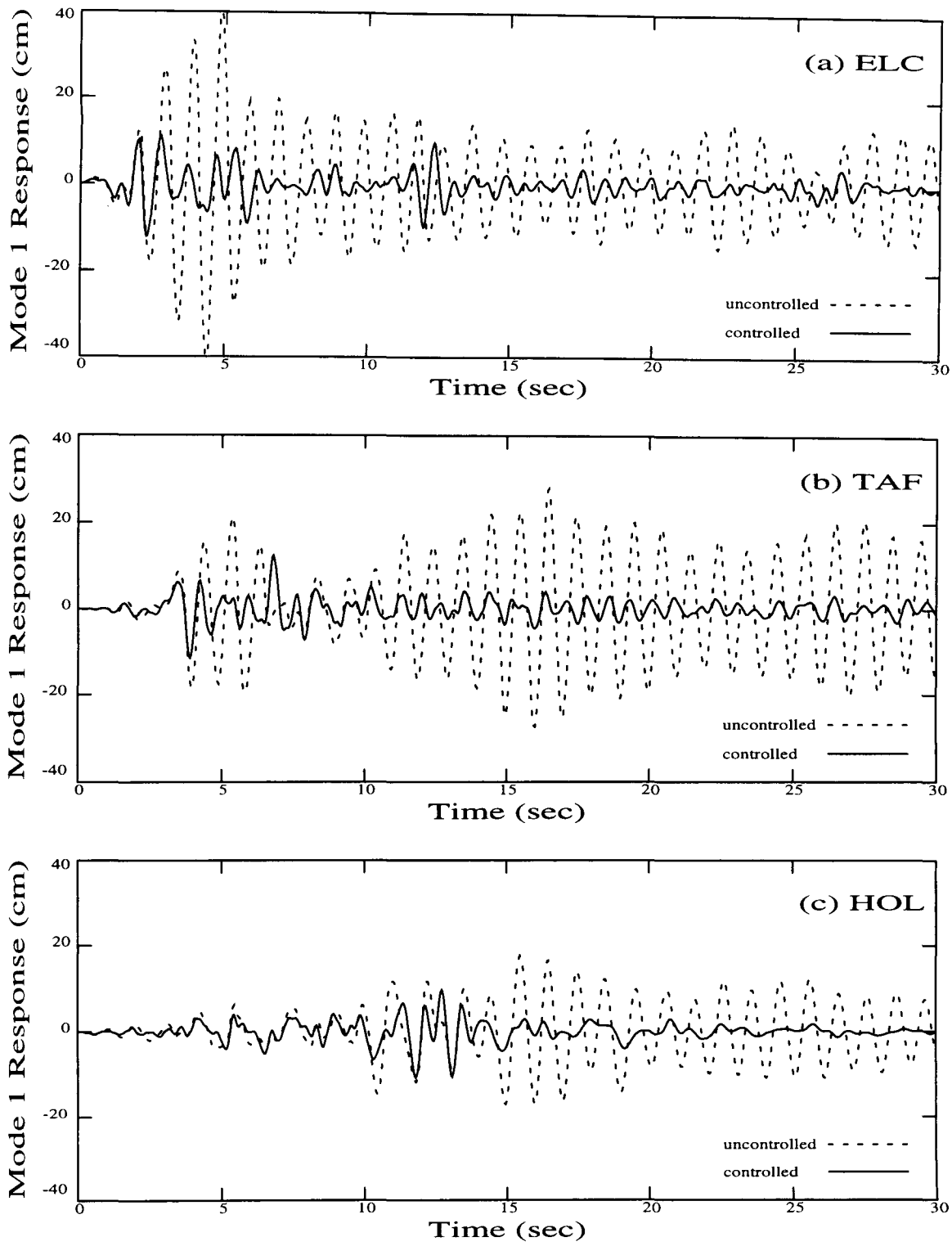

Figure 4.18. Response Time-History of Mode 1 for a 6-Story Category 1 Controlled Primary System Subjected to the (a) El Centro, (b) Taft Lincoln School Tunnel, and (c) Holiday Inn Excitation Records. Type 2 elements are used, with $\mu = 0.50$ and $\delta_l = 5.00$. All elements participate.

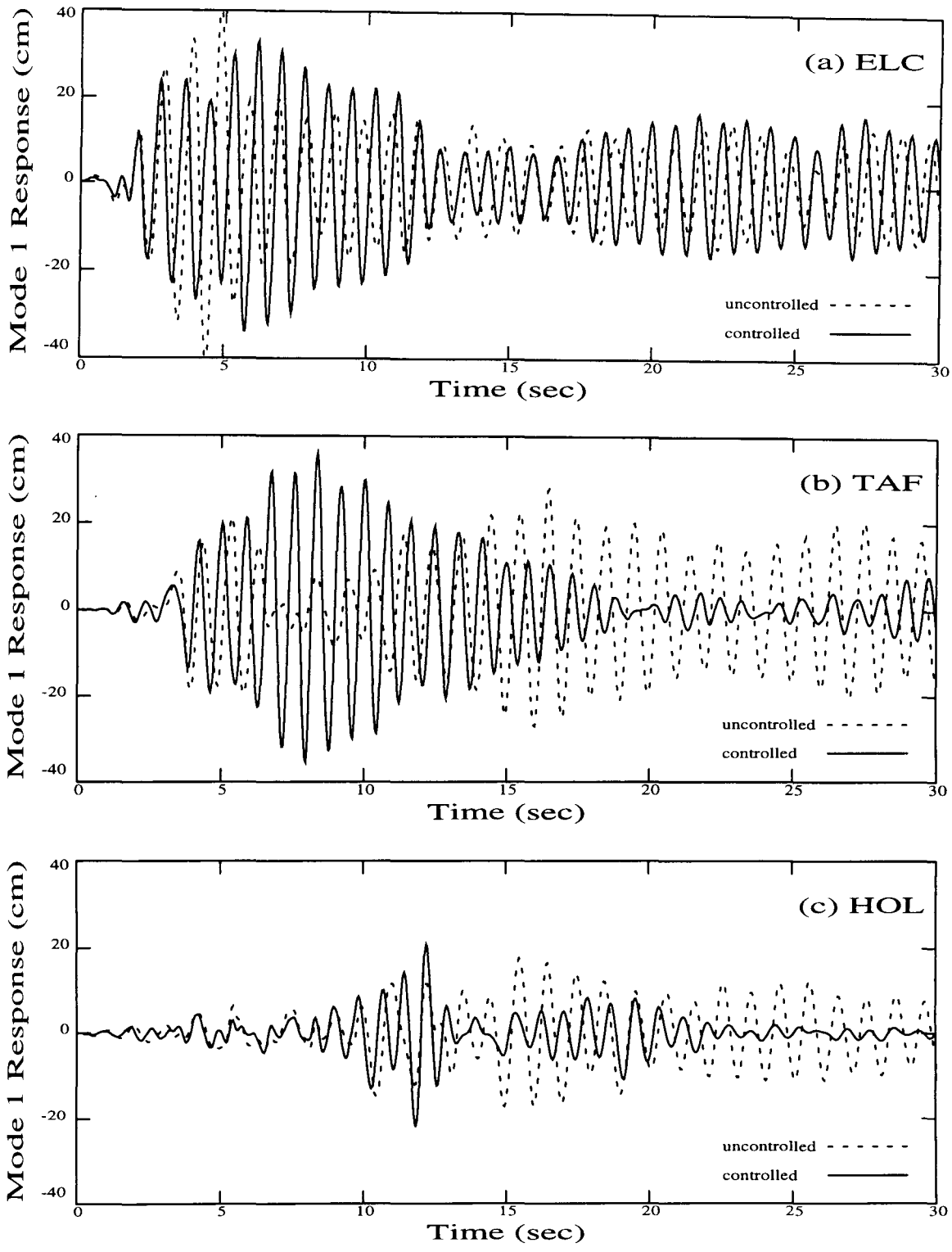

Figure 4.19. Response Time-History of Mode 1 for a 6-Story Category 1 Controlled Primary System Subjected to the (a) El Centro, (b) Taft Lincoln School Tunnel, and (c) Holiday Inn Excitation Records. Type 1 elements are used, with $\mu = 0.50$, and are locked in the activated state. All elements participate.

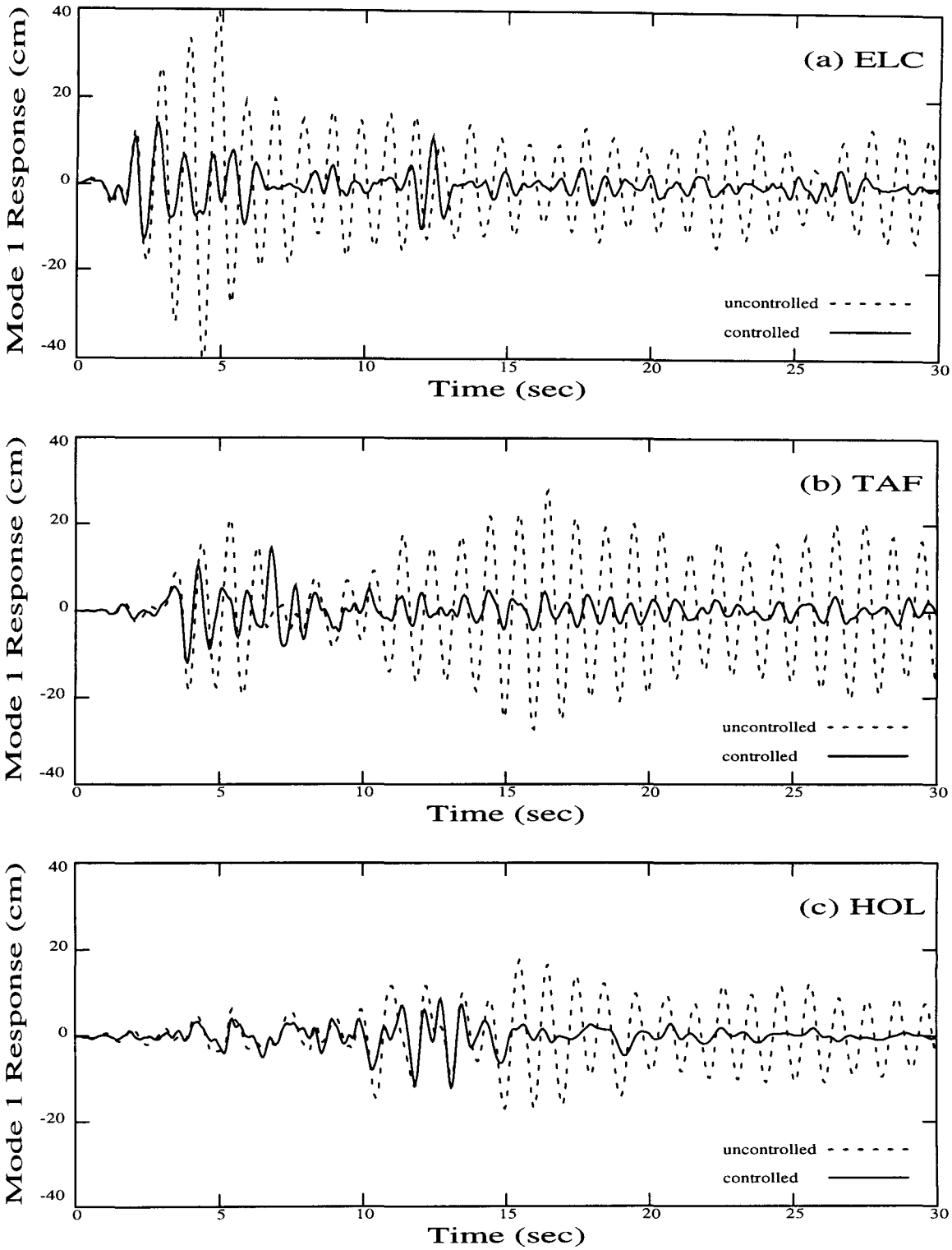

Figure 4.20. Response Time-History of Mode 1 for a 6-Story Category 1 Controlled Primary System Subjected to the (a) El Centro, (b) Taft Lincoln School Tunnel, and (c) Holiday Inn Excitation Records. Type 1 elements are used, with $\mu = 0.50$. Only bottom three elements participate.

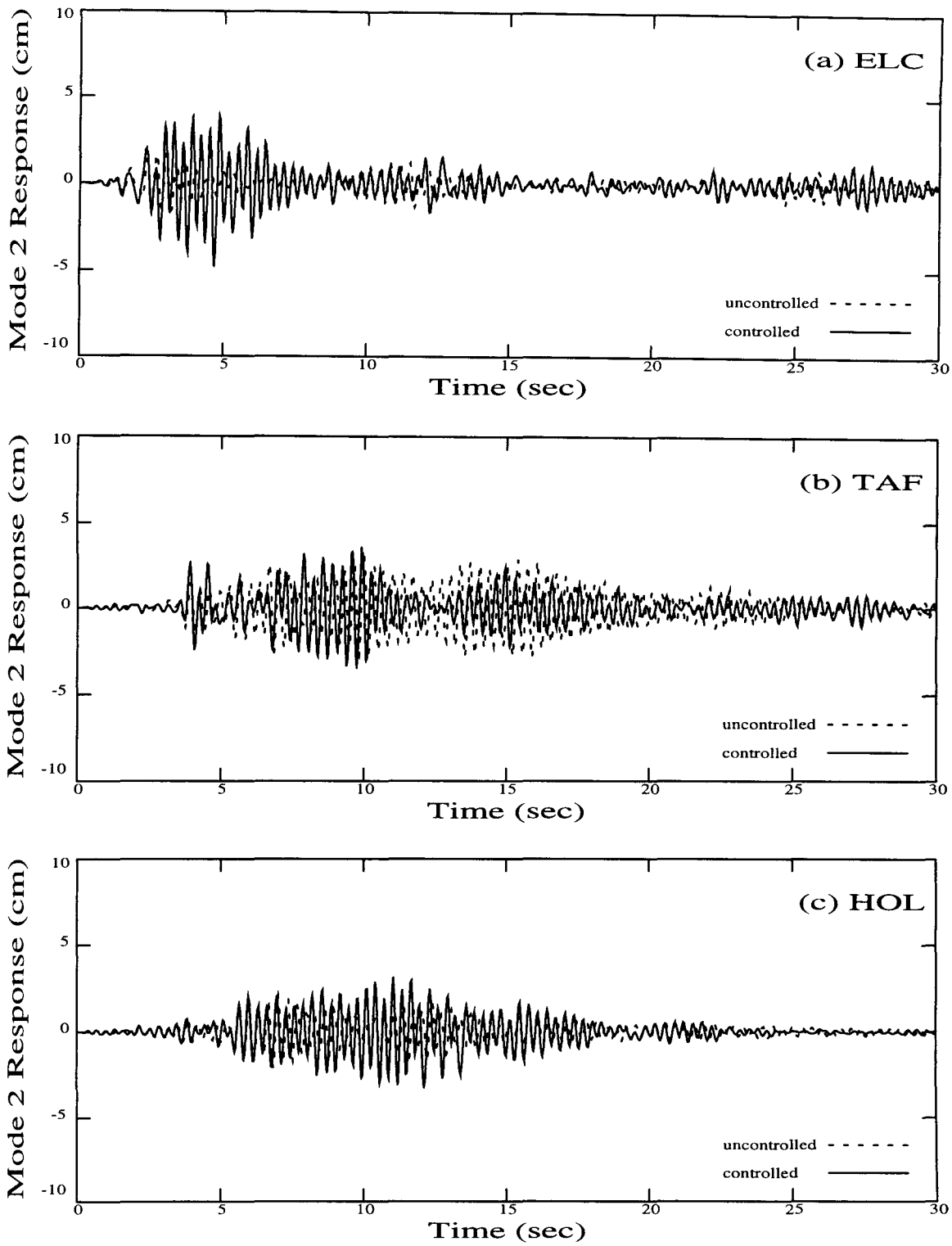

Figure 4.21. Response Time-History of Mode 2 for a 6-Story Category 1 Controlled Primary System Subjected to the (a) El Centro, (b) Taft Lincoln School Tunnel, and (c) Holiday Inn Excitation Records. Type 1 elements are used, with $\mu = 0.50$. Only bottom three elements participate.

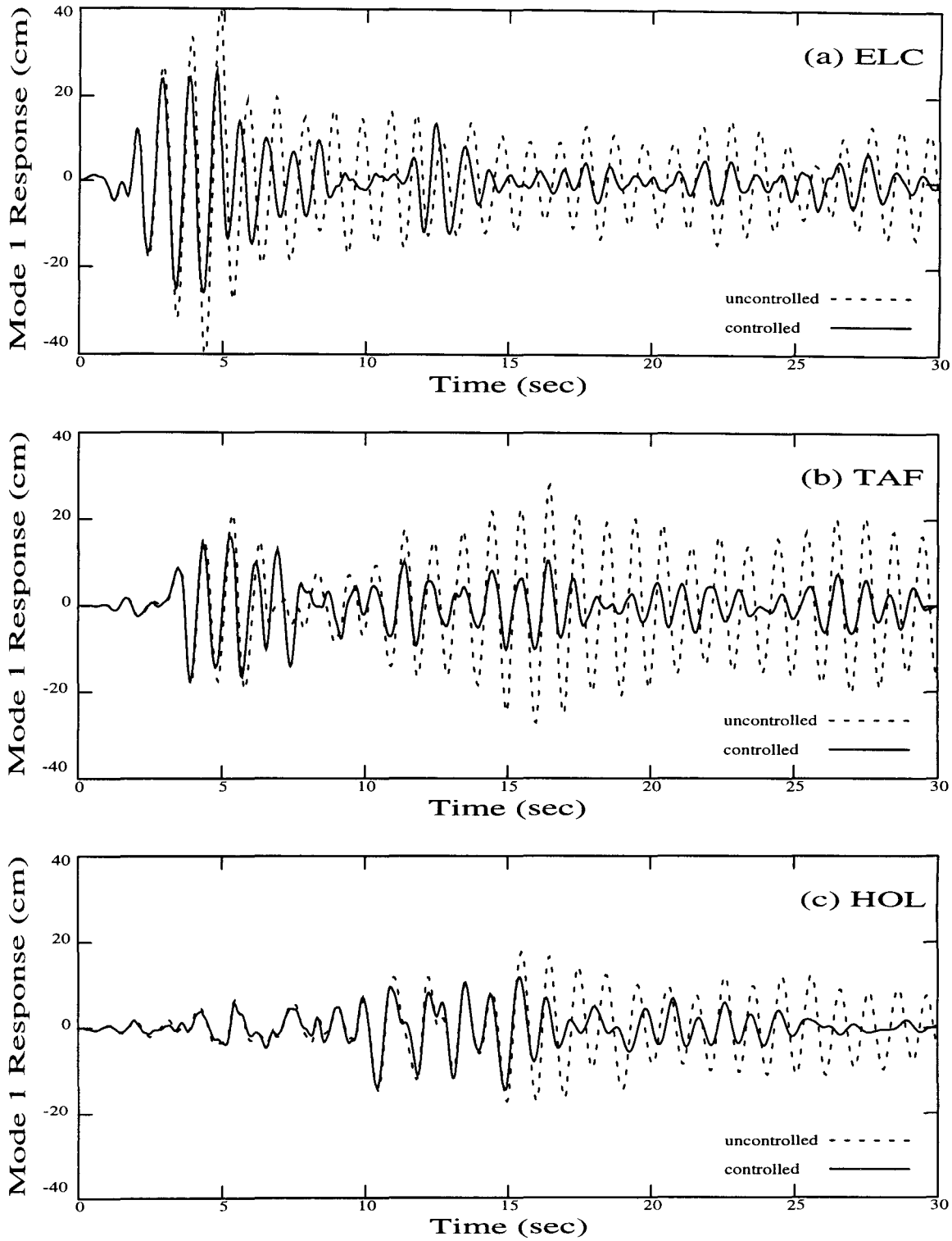

Figure 4.22. Response Time-History of Mode 1 for a 6-Story Category 1 Controlled Primary System Subjected to the (a) El Centro, (b) Taft Lincoln School Tunnel, and (c) Holiday Inn Excitation Records. Type 1 elements are used, with $\mu = 0.50$. Only top three elements participate.

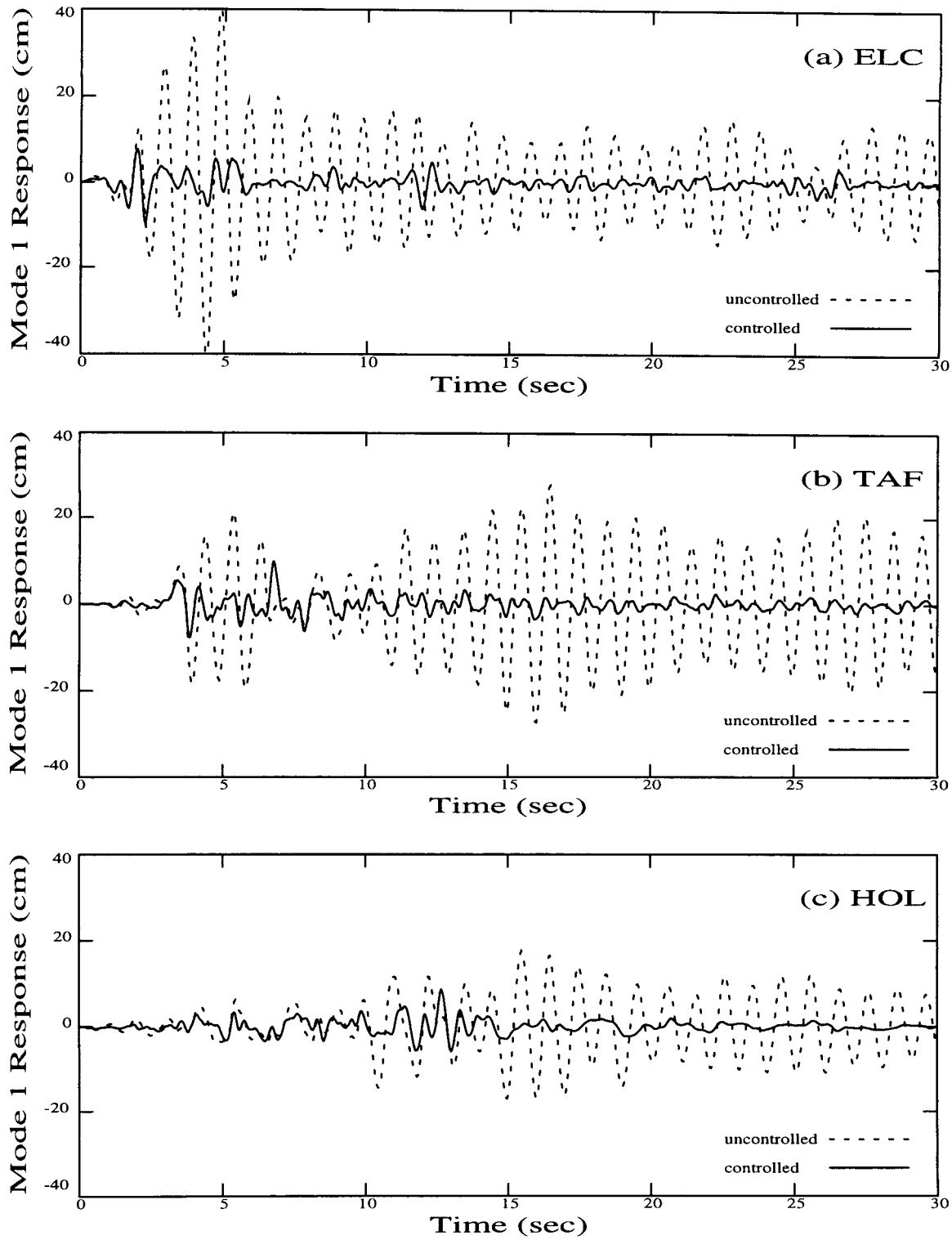

Figure 4.23. Response Time-History of Mode 1 for a 6-Story Category 2 Controlled Primary System Subjected to the (a) El Centro, (b) Taft Lincoln School Tunnel, and (c) Holiday Inn Excitation Records. Modified Type 1 elements are used. $\alpha = 1.00$. All elements participate. Primary-Auxiliary System Configuration: 6–6.

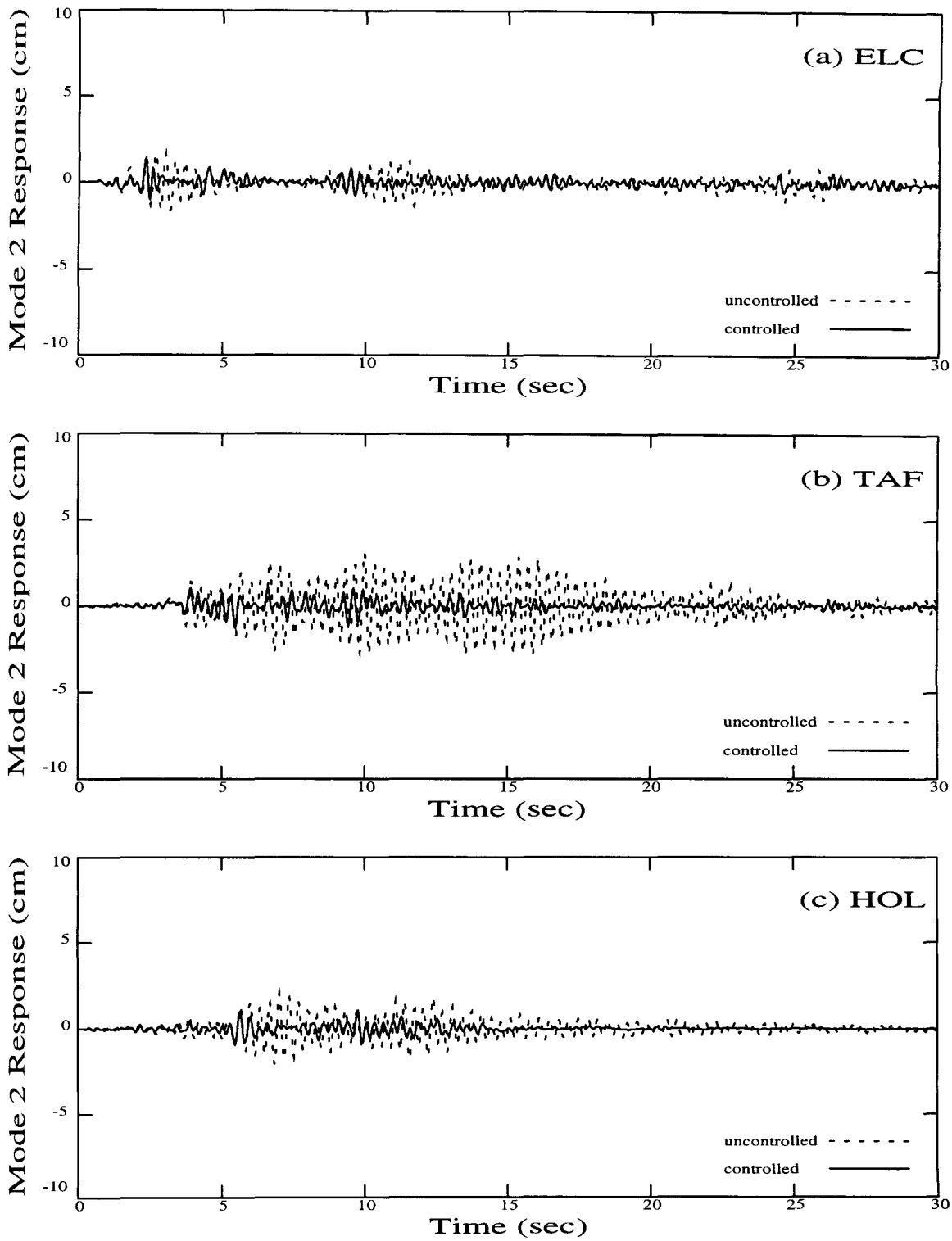

Figure 4.24. Response Time-History of Mode 2 for a 6-Story Category 2 Controlled Primary System Subjected to the (a) El Centro, (b) Taft Lincoln School Tunnel, and (c) Holiday Inn Excitation Records. Modified Type 1 elements are used. $\alpha = 1.00$. All elements participate. Primary-Auxiliary System Configuration: 6–6.

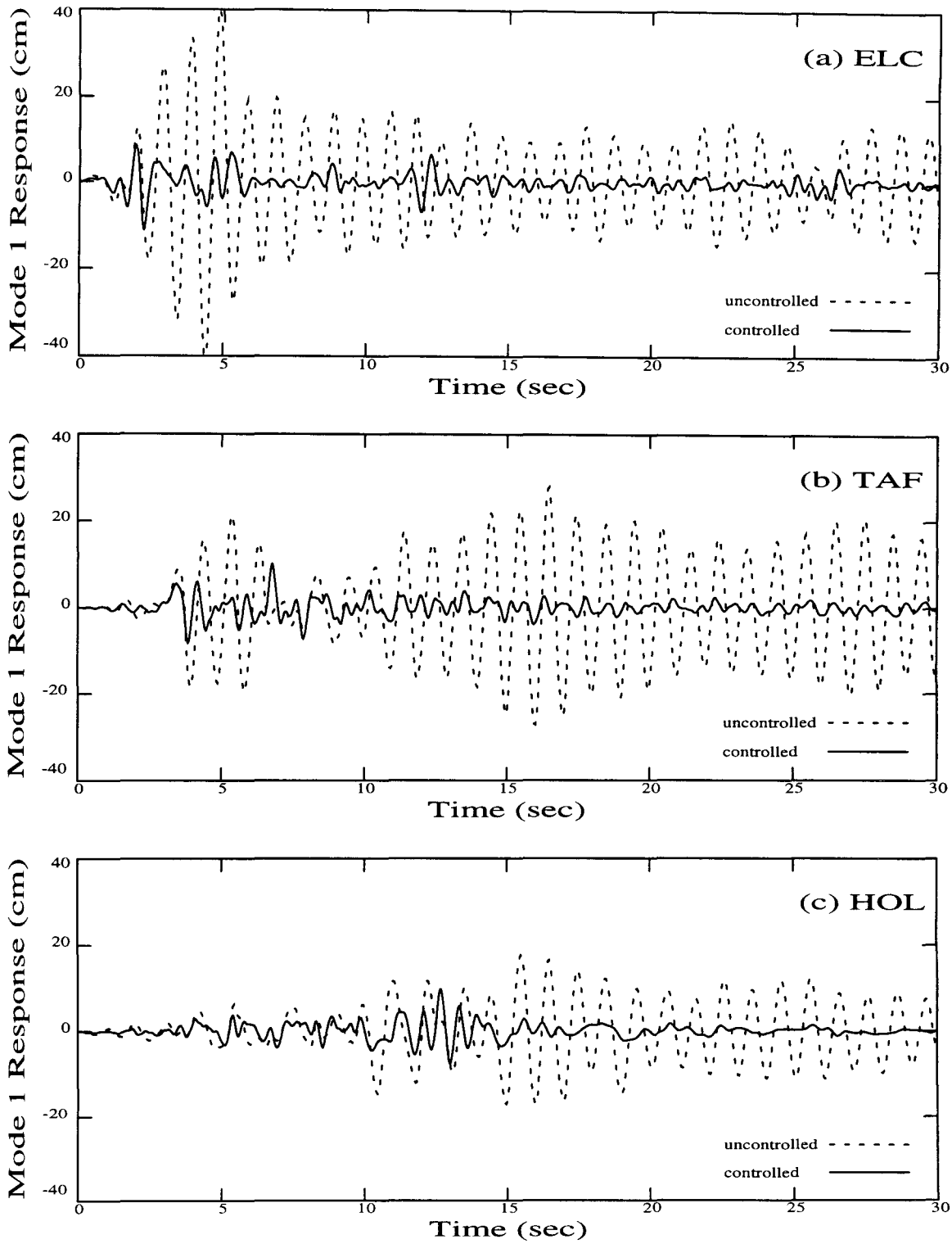

Figure 4.25. Response Time-History of Mode 1 for a 6-Story Category 2 Controlled Primary System Subjected to the (a) El Centro, (b) Taft Lincoln School Tunnel, and (c) Holiday Inn Excitation Records. Modified Type 2 elements are used, with $\delta_l = 5.00$. $\alpha = 1.00$. All elements participate. Primary-Auxiliary System Configuration: 6–6.

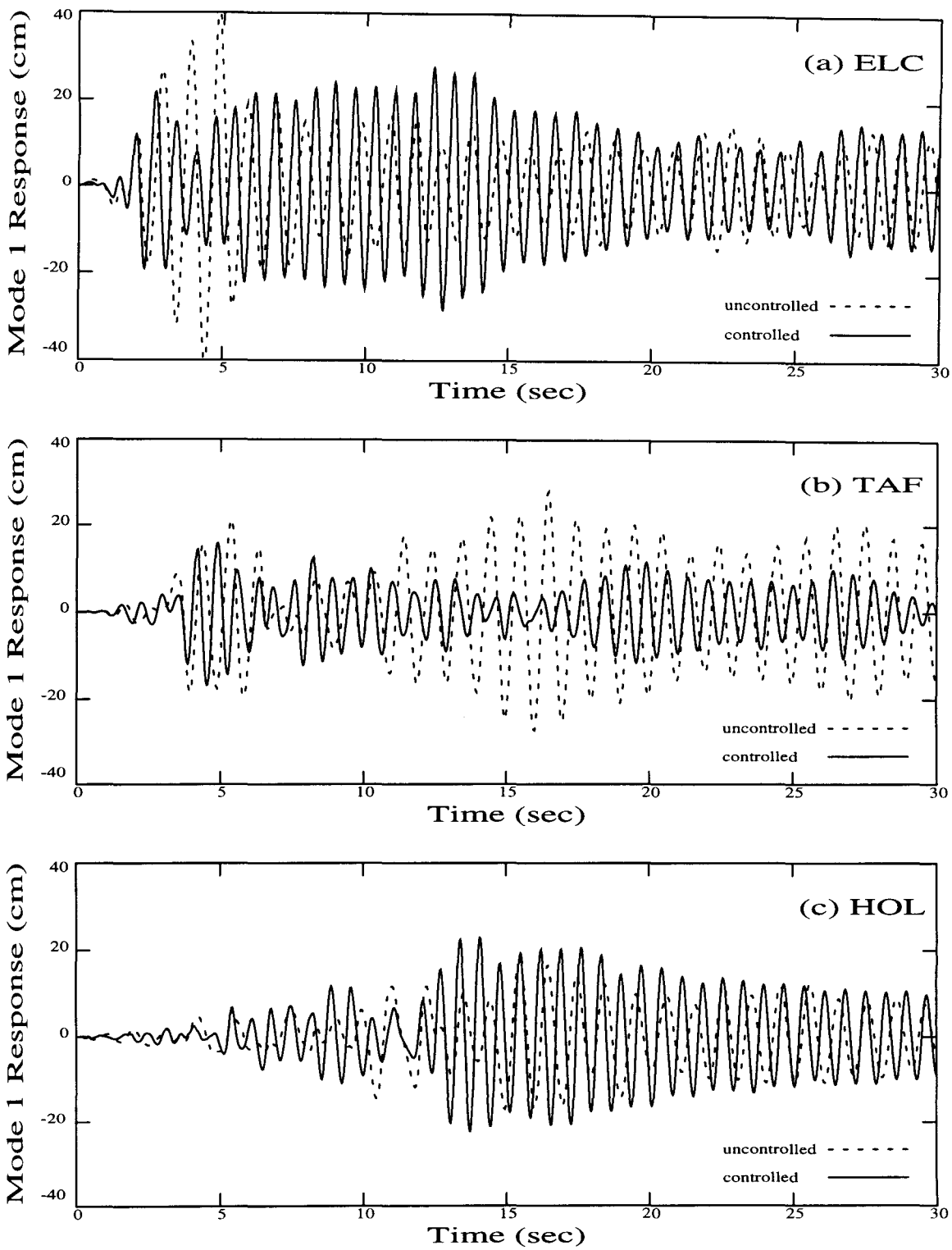

Figure 4.26. Response Time-History of Mode 1 for a 6-Story Category 2 Controlled Primary System Subjected to the (a) El Centro, (b) Taft Lincoln School Tunnel, and (c) Holiday Inn Excitation Records. Modified Type 1 elements are used, and are locked in the activated state. $\alpha = 1.00$. All elements participate. Primary-Auxiliary System Configuration: 6–6.

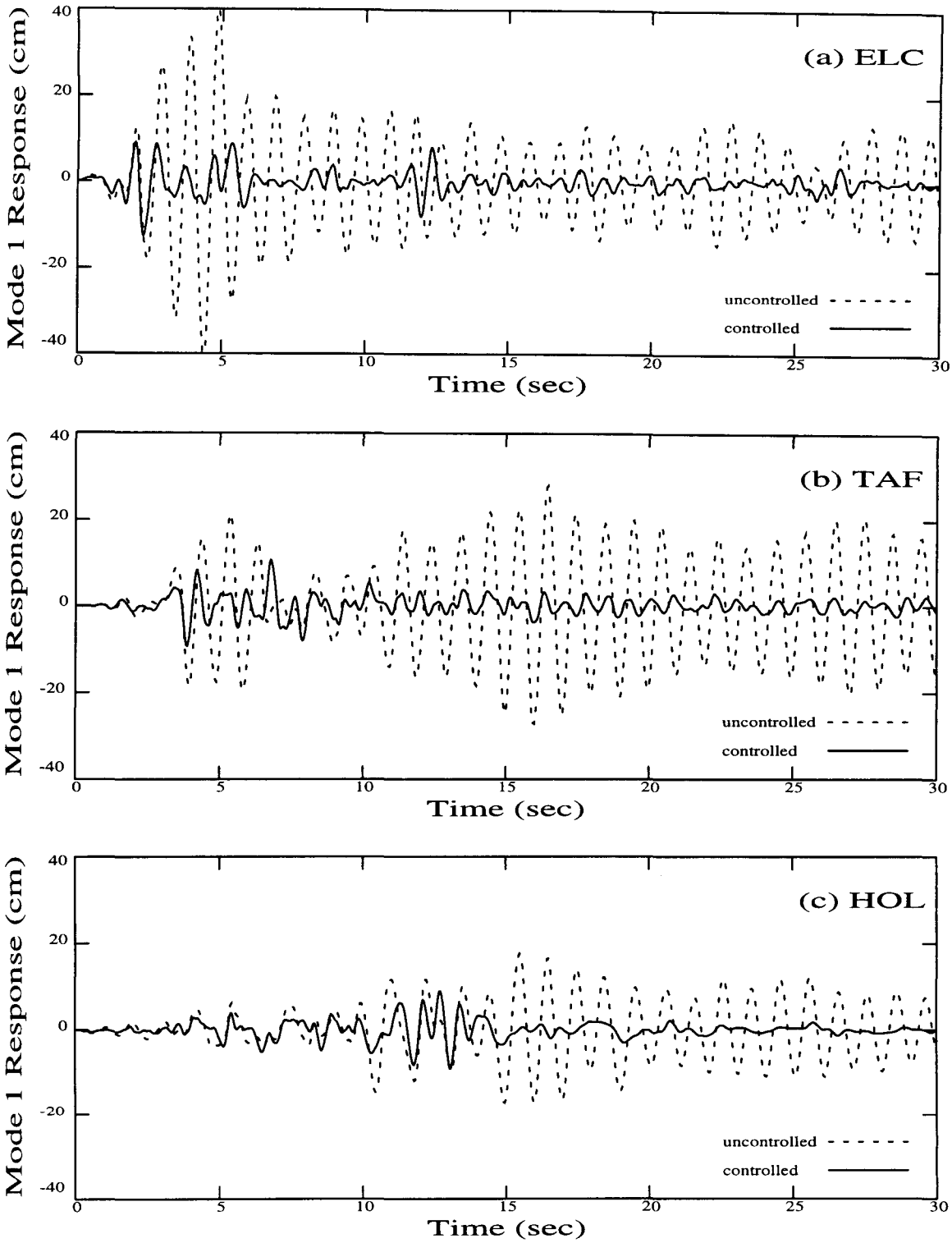

Figure 4.27. Response Time-History of Mode 1 for a 6-Story Category 2 Controlled Primary System Subjected to the (a) El Centro, (b) Taft Lincoln School Tunnel, and (c) Holiday Inn Excitation Records. Modified Type 1 elements are used. $\alpha = 1.00$. Only bottom three elements participate. Primary-Auxiliary System Configuration: 6–3.

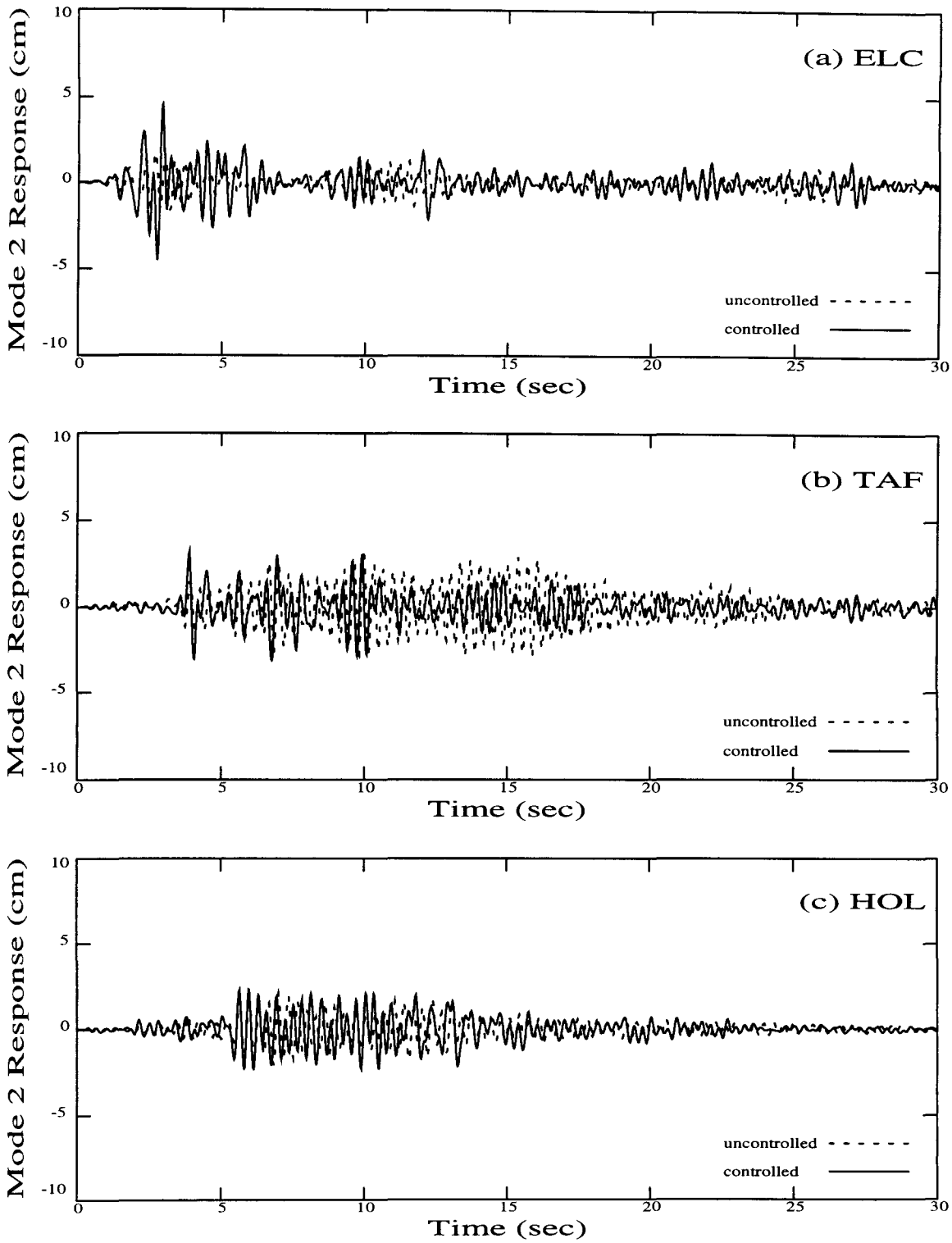

Figure 4.28. Response Time-History of Mode 2 for a 6-Story Category 2 Controlled Primary System Subjected to the (a) El Centro, (b) Taft Lincoln School Tunnel, and (c) Holiday Inn Excitation Records. Modified Type 1 elements are used. $\alpha = 1.00$. Only bottom three elements participate. Primary-Auxiliary System Configuration: 6–3.

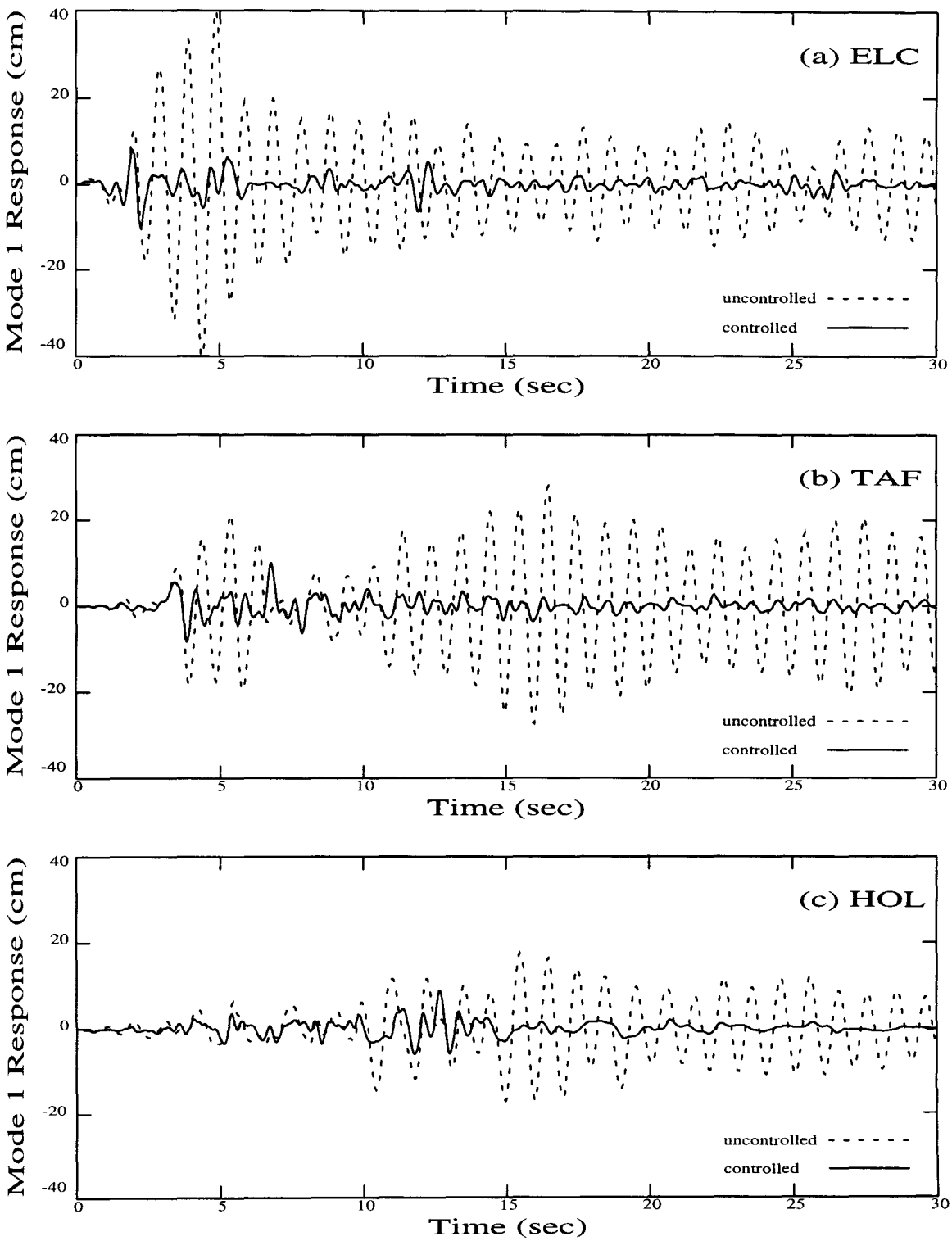

Figure 4.29. Response Time-History of Mode 1 for a 6-Story Category 2 Controlled Primary System Subjected to the (a) El Centro, (b) Taft Lincoln School Tunnel, and (c) Holiday Inn Excitation Records. Modified Type 1 elements are used. $\alpha = 1.00$. Only top three elements participate. Primary-Auxiliary System Configuration: 6–6.

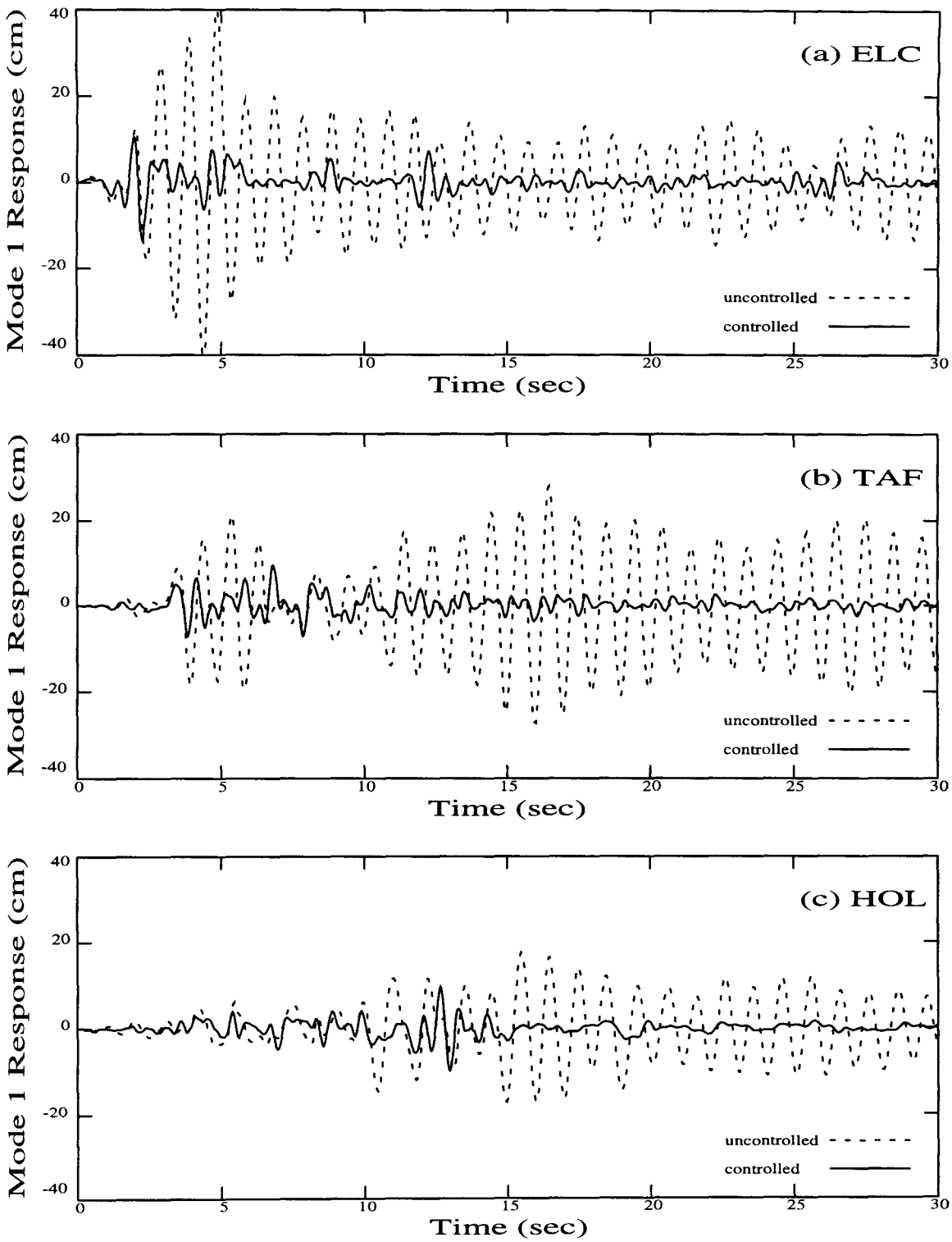

Figure 4.30. Response Time-History of Mode 1 for a 6-Story Category 3(a) Controlled Primary System Subjected to the (a) El Centro, (b) Taft Lincoln School Tunnel, and (c) Holiday Inn Excitation Records. Type 1 elements are used, with $\mu = 1.00$. $\alpha = 1.00$ and $\beta = 0.15$. All elements participate. Primary-Auxiliary System Configuration: 6–6.

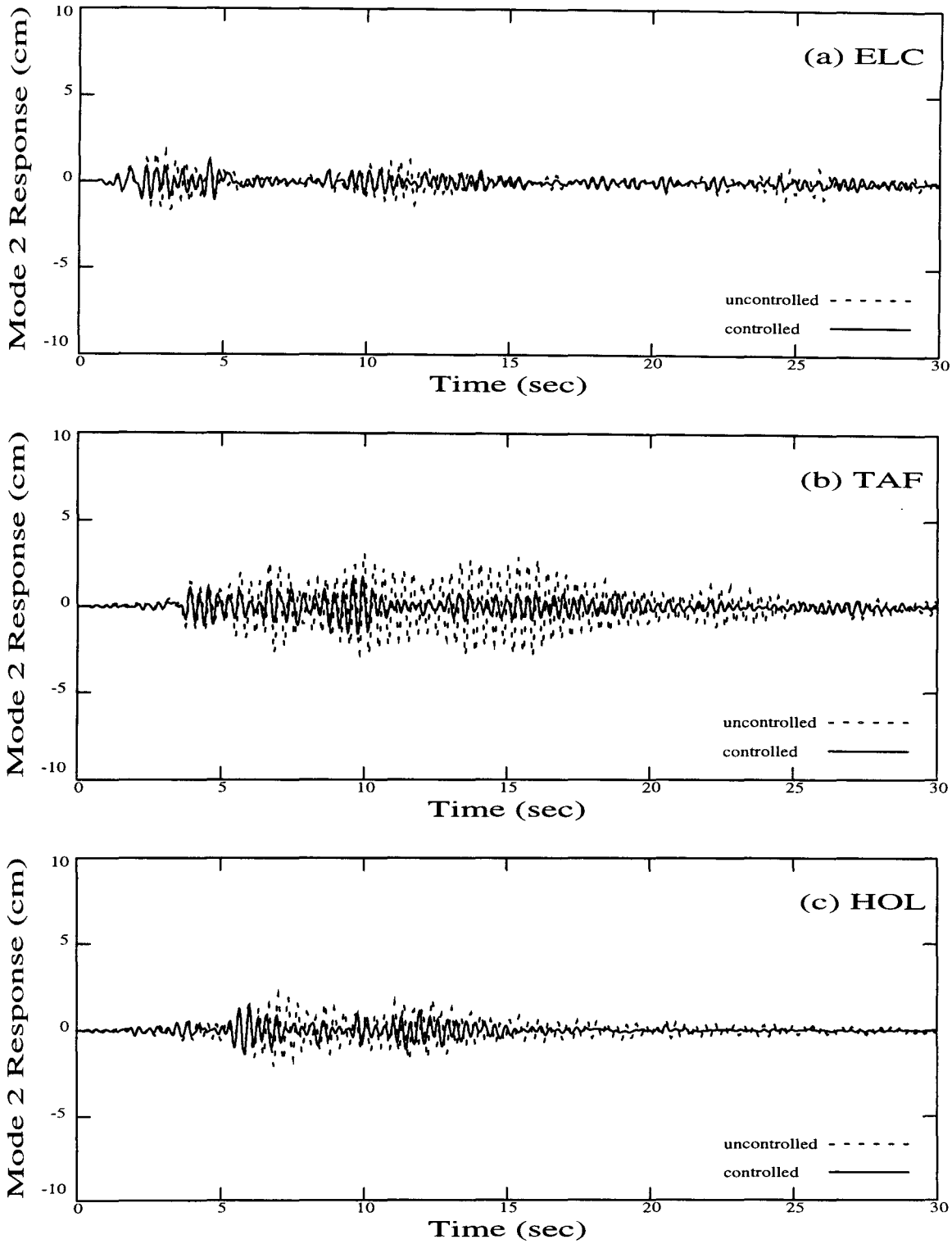

Figure 4.31. Response Time-History of Mode 2 for a 6-Story Category 3(a) Controlled Primary System Subjected to the (a) El Centro, (b) Taft Lincoln School Tunnel, and (c) Holiday Inn Excitation Records. Type 1 elements are used, with $\mu = 1.00$. $\alpha = 1.00$ and $\beta = 0.15$. All elements participate. Primary-Auxiliary System Configuration: 6–6.

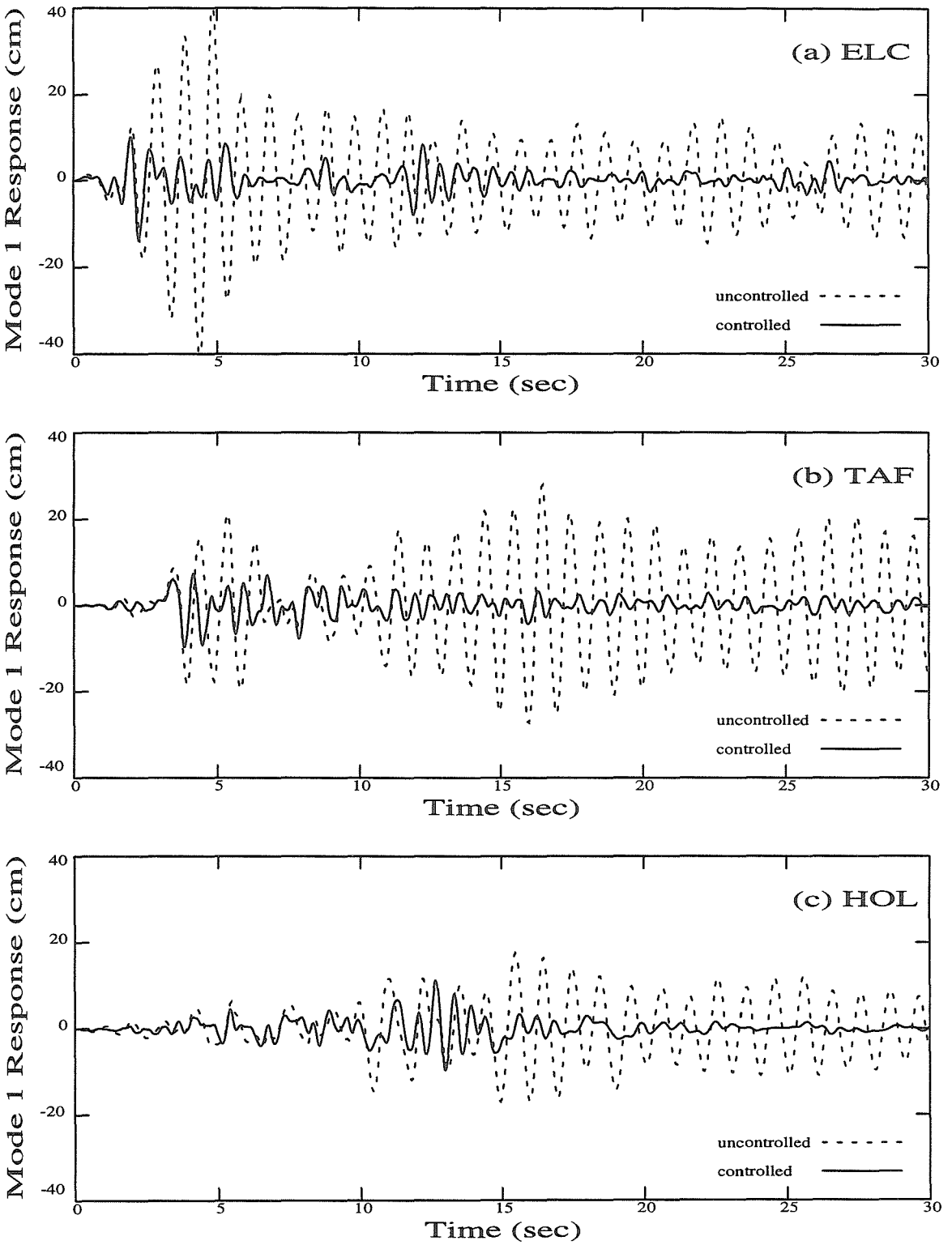

Figure 4.32. Response Time-History of Mode 1 for a 6-Story Category 3(*a*) Controlled Primary System Subjected to the (a) El Centro, (b) Taft Lincoln School Tunnel, and (c) Holiday Inn Excitation Records. Type 2 elements are used, with $\mu = 1.00$ and $\delta_l = 5.00$. $\alpha = 1.00$ and $\beta = 0.15$. All elements participate. Primary-Auxiliary System Configuration: 6–6.

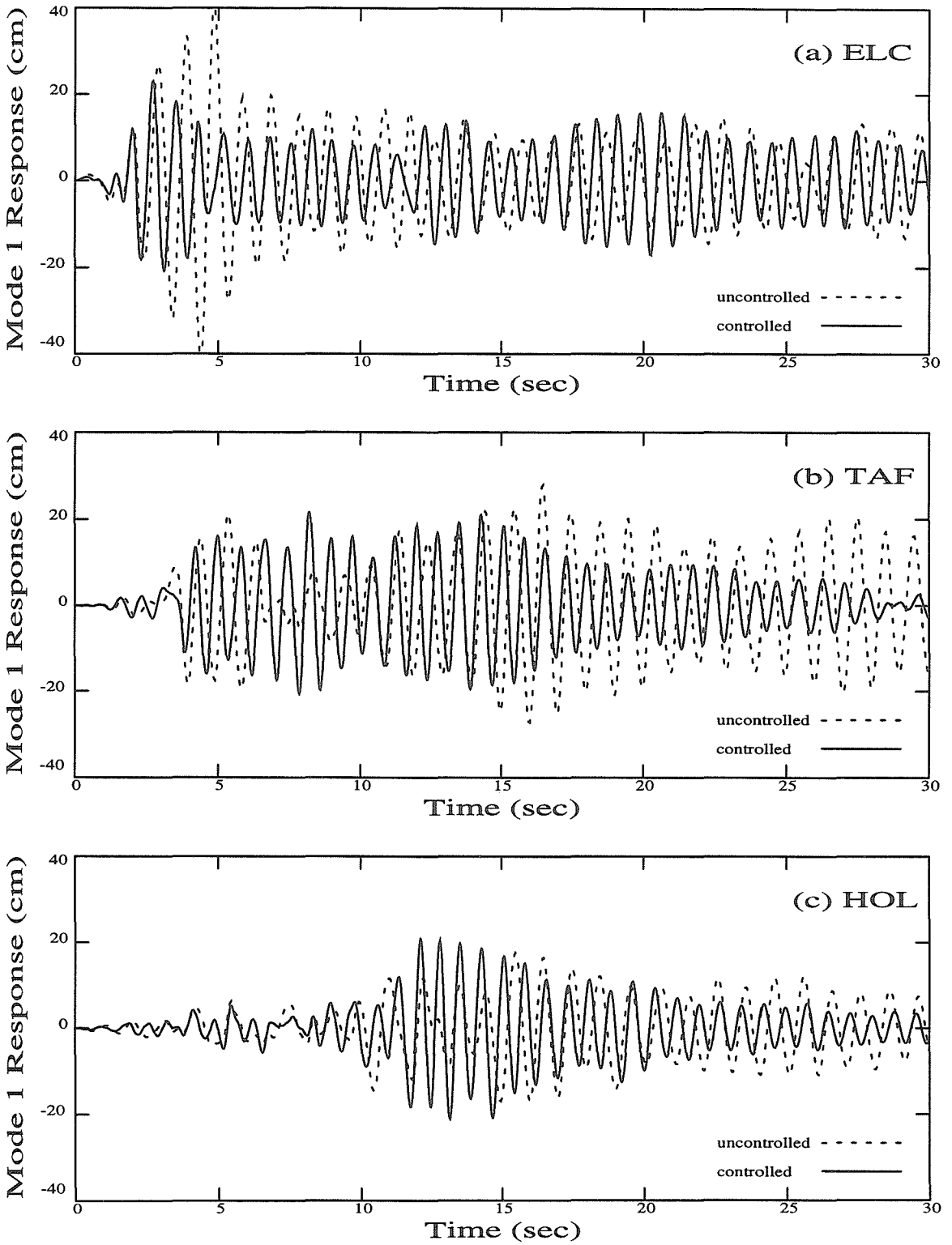

Figure 4.33. Response Time-History of Mode 1 for a 6-Story Category 3(*a*) Controlled Primary System Subjected to the (a) El Centro, (b) Taft Lincoln School Tunnel, and (c) Holiday Inn Excitation Records. Type 1 elements are used, with $\mu = 1.00$, and are locked in the activated state. $\alpha = 1.00$ and $\beta = 0.15$. All elements participate. Primary-Auxiliary System Configuration: 6–6.

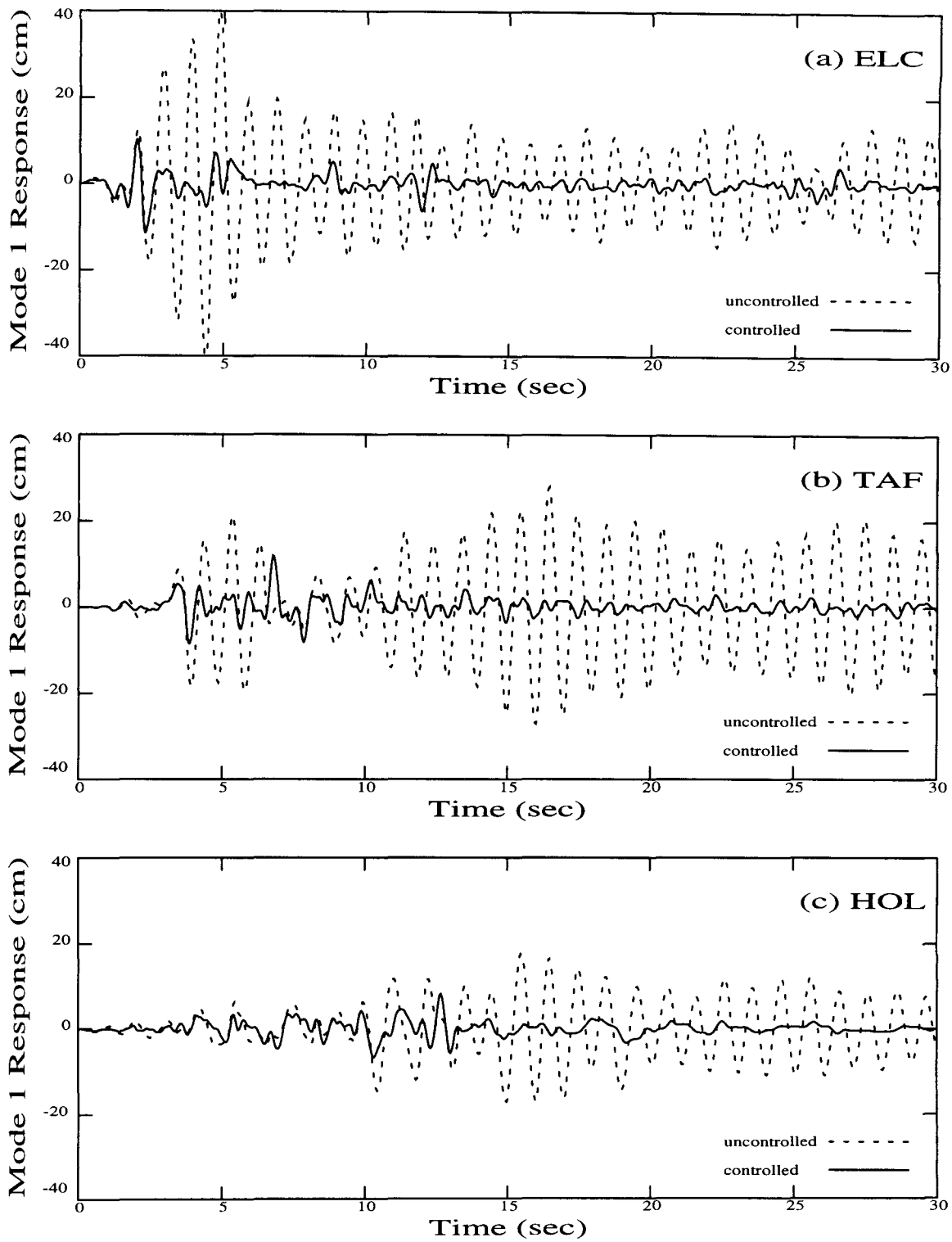

Figure 4.34. Response Time-History of Mode 1 for a 6-Story Category 3(*a*) Controlled Primary System Subjected to the (a) El Centro, (b) Taft Lincoln School Tunnel, and (c) Holiday Inn Excitation Records. Type 1 elements are used, with $\mu = 1.00$. $\alpha = 1.00$ and $\beta = 0.15$. Only bottom three elements participate. Primary-Auxiliary System Configuration: 6–3.

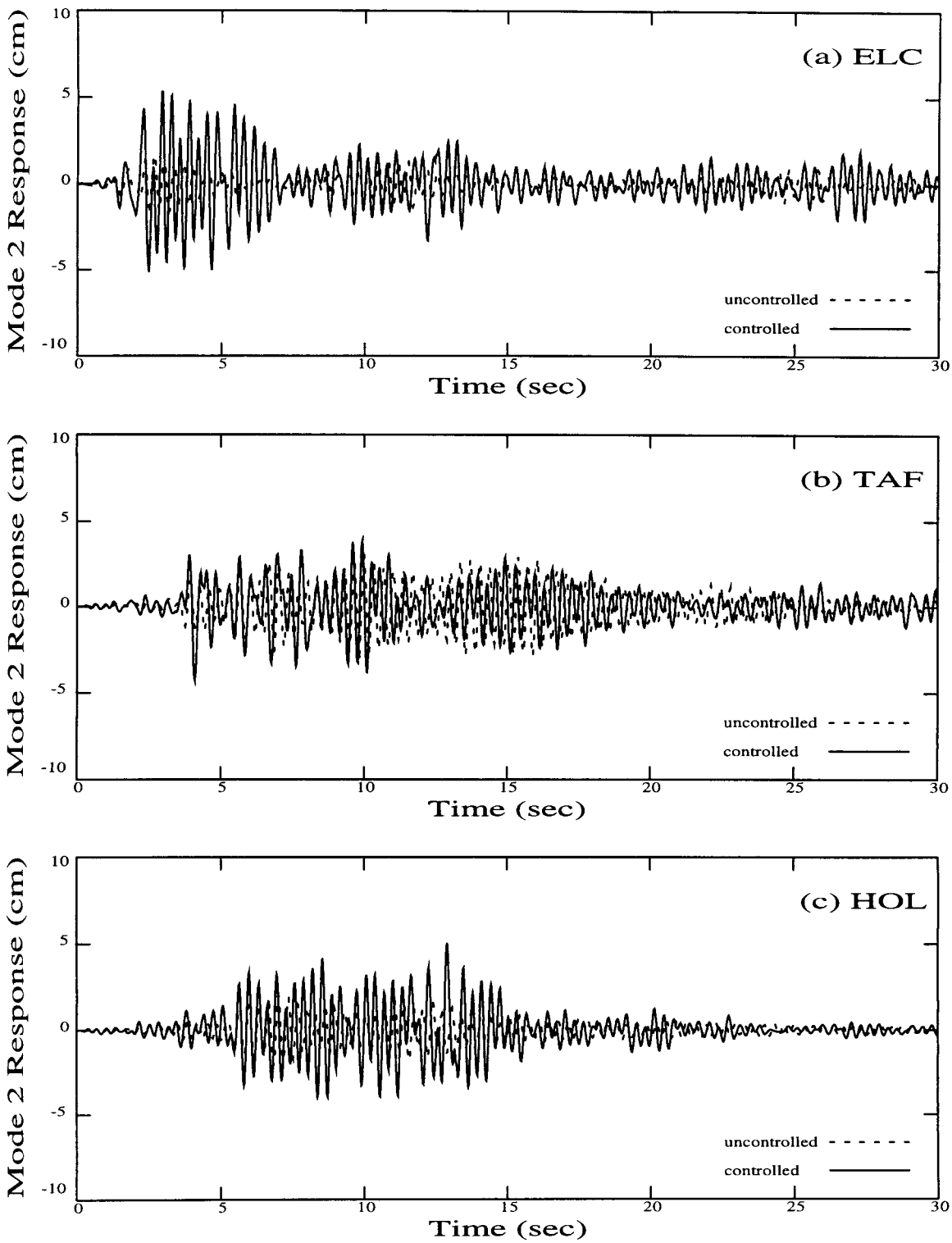

Figure 4.35. Response Time-History of Mode 2 for a 6-Story Category 3(a) Controlled Primary System Subjected to the (a) El Centro, (b) Taft Lincoln School Tunnel, and (c) Holiday Inn Excitation Records. Type 1 elements are used, with $\mu = 1.00$. $\alpha = 1.00$ and $\beta = 0.15$. Only bottom three elements participate. Primary-Auxiliary System Configuration: 6–3.

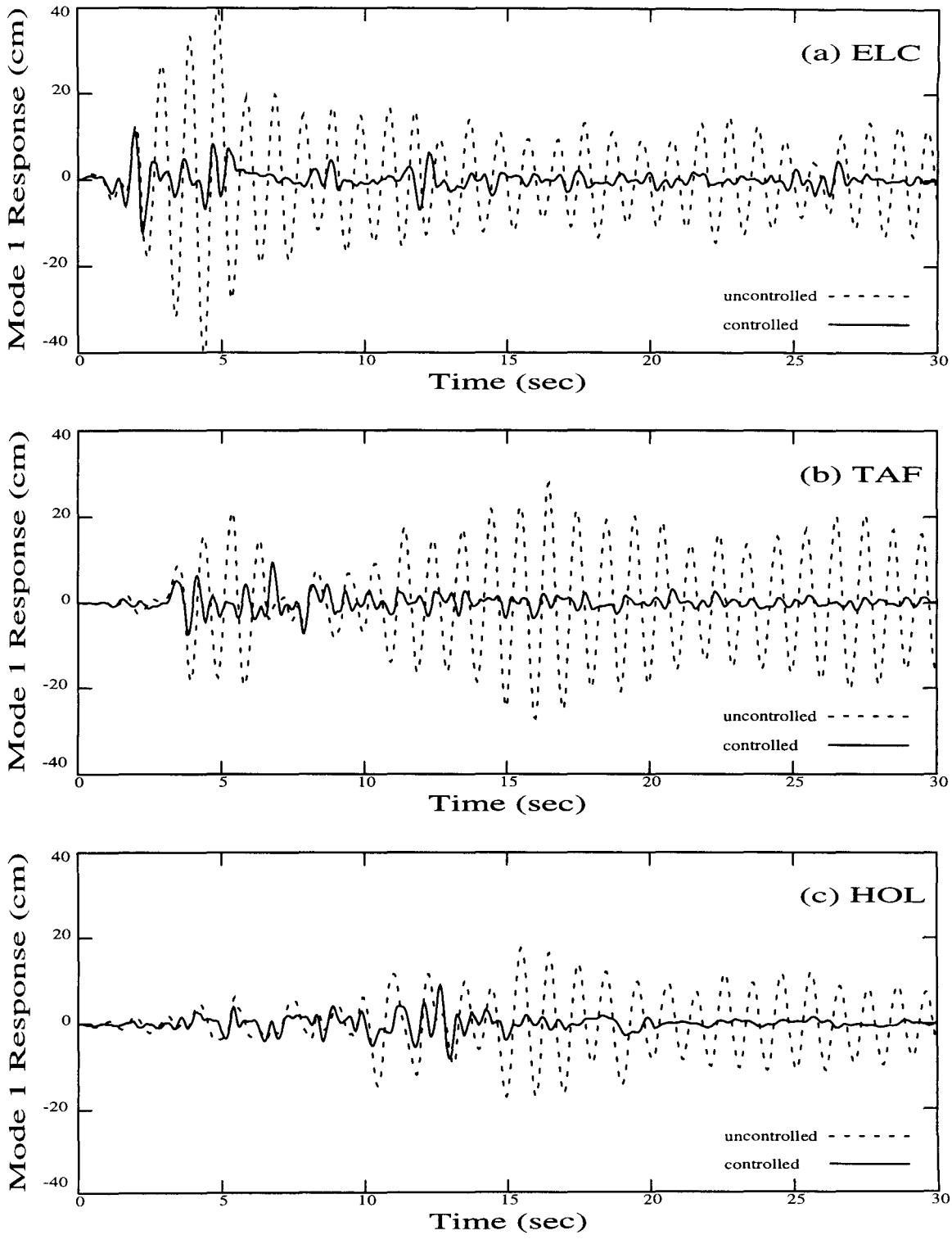

Figure 4.36. Response Time-History of Mode 1 for a 6-Story Category 3(a) Controlled Primary System Subjected to the (a) El Centro, (b) Taft Lincoln School Tunnel, and (c) Holiday Inn Excitation Records. Type 1 elements are used, with $\mu = 1.00$. $\alpha = 1.00$ and $\beta = 0.15$. Only top three elements participate. Primary-Auxiliary System Configuration: 6–6.

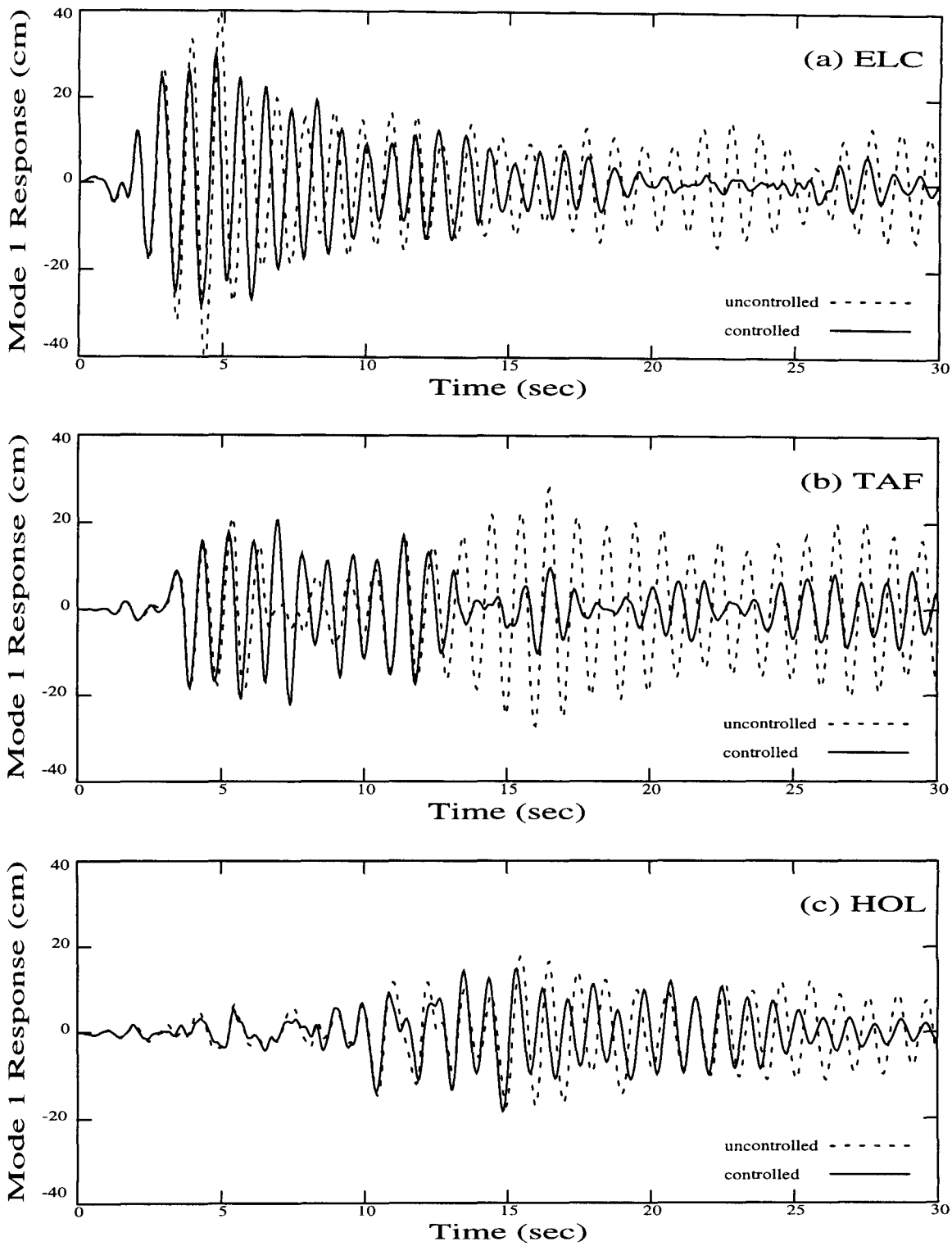

Figure 4.37. Response Time-History of Mode 1 for a 6-Story Category 3(*b*) Controlled Primary System Subjected to the (a) El Centro, (b) Taft Lincoln School Tunnel, and (c) Holiday Inn Excitation Records. Type 1 elements are used, with $\mu = 0.05$. $\alpha = 6.50$ and $\beta = 5.00$. All elements participate. Primary-Auxiliary System Configuration: 6–6.

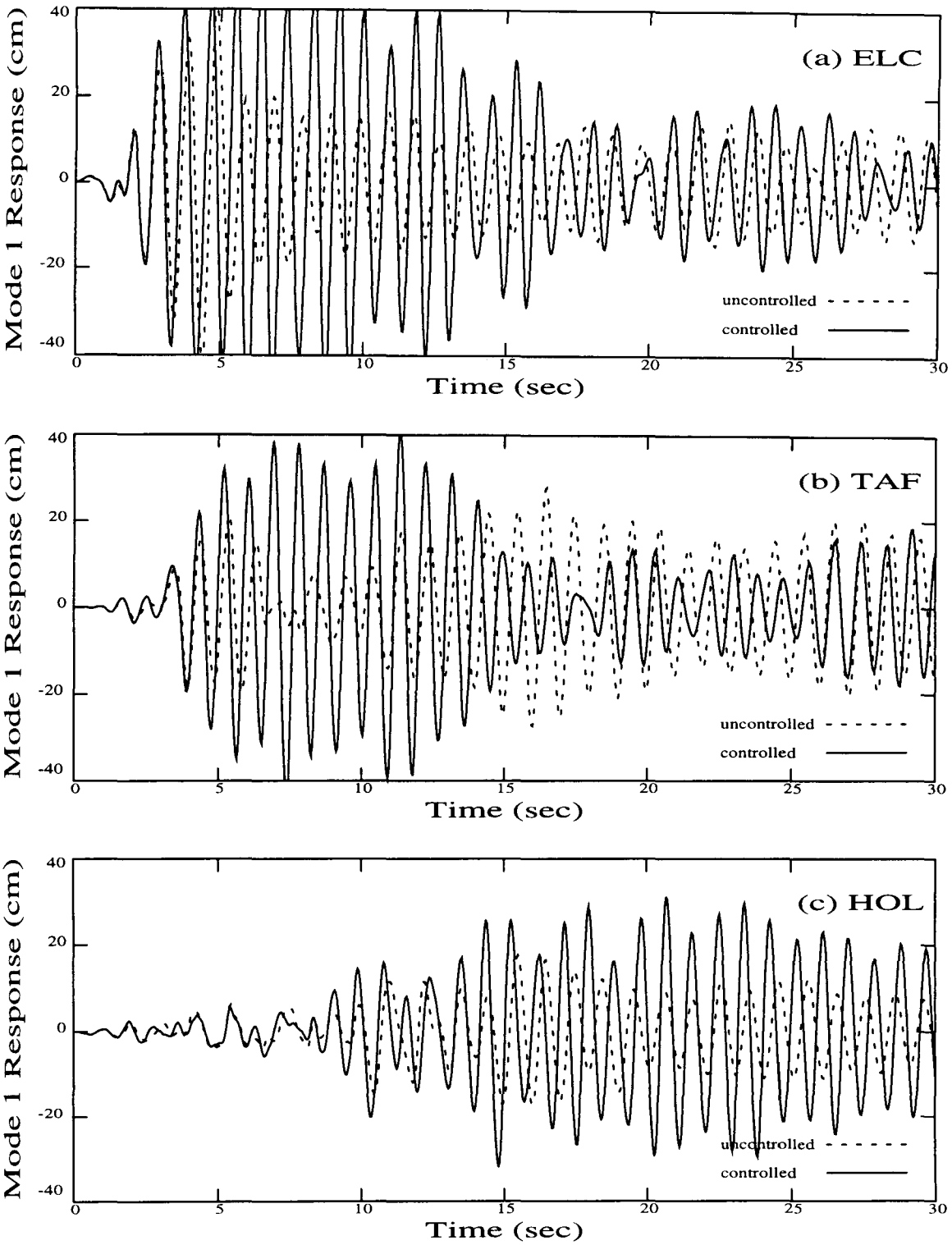

Figure 4.38. Response Time-History of Mode 1 for a 6-Story Category 3(*b*) Controlled Primary System Subjected to the (a) El Centro, (b) Taft Lincoln School Tunnel, and (c) Holiday Inn Excitation Records. Type 1 elements are used, with $\mu = 0.05$, and are locked in the activated state. $\alpha = 6.50$ and $\beta = 5.00$. All elements participate. Primary-Auxiliary System Configuration: 6–6.

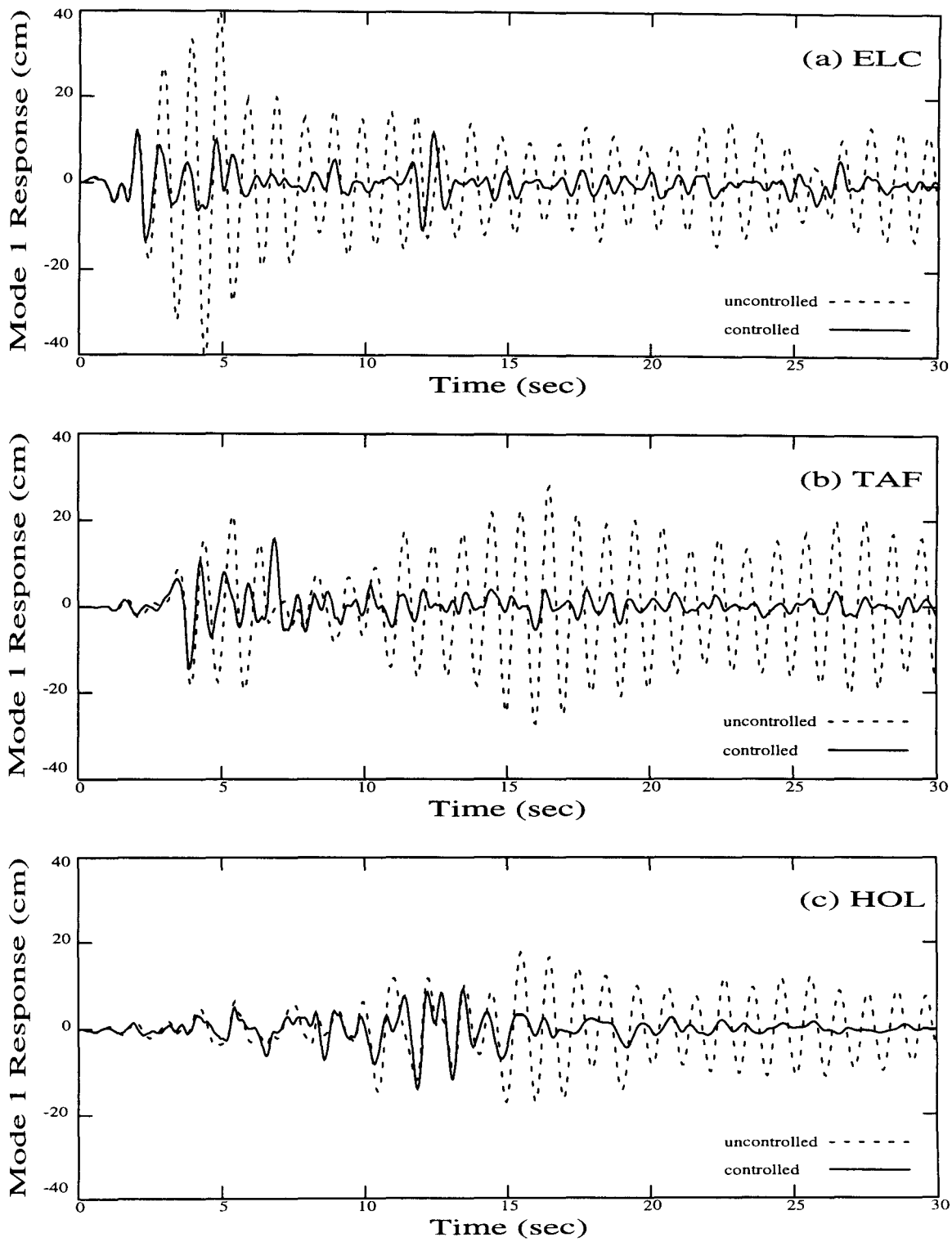

Figure 4.39. Response Time-History of Mode 1 for a 6-Story Category 3(*b*) Controlled Primary System Subjected to the (a) El Centro, (b) Taft Lincoln School Tunnel, and (c) Holiday Inn Excitation Records. Type 1 elements are used, with $\mu = 0.10$. $\alpha = 6.50$ and $\beta = 5.00$. All elements participate. Primary-Auxiliary System Configuration: 6–3.

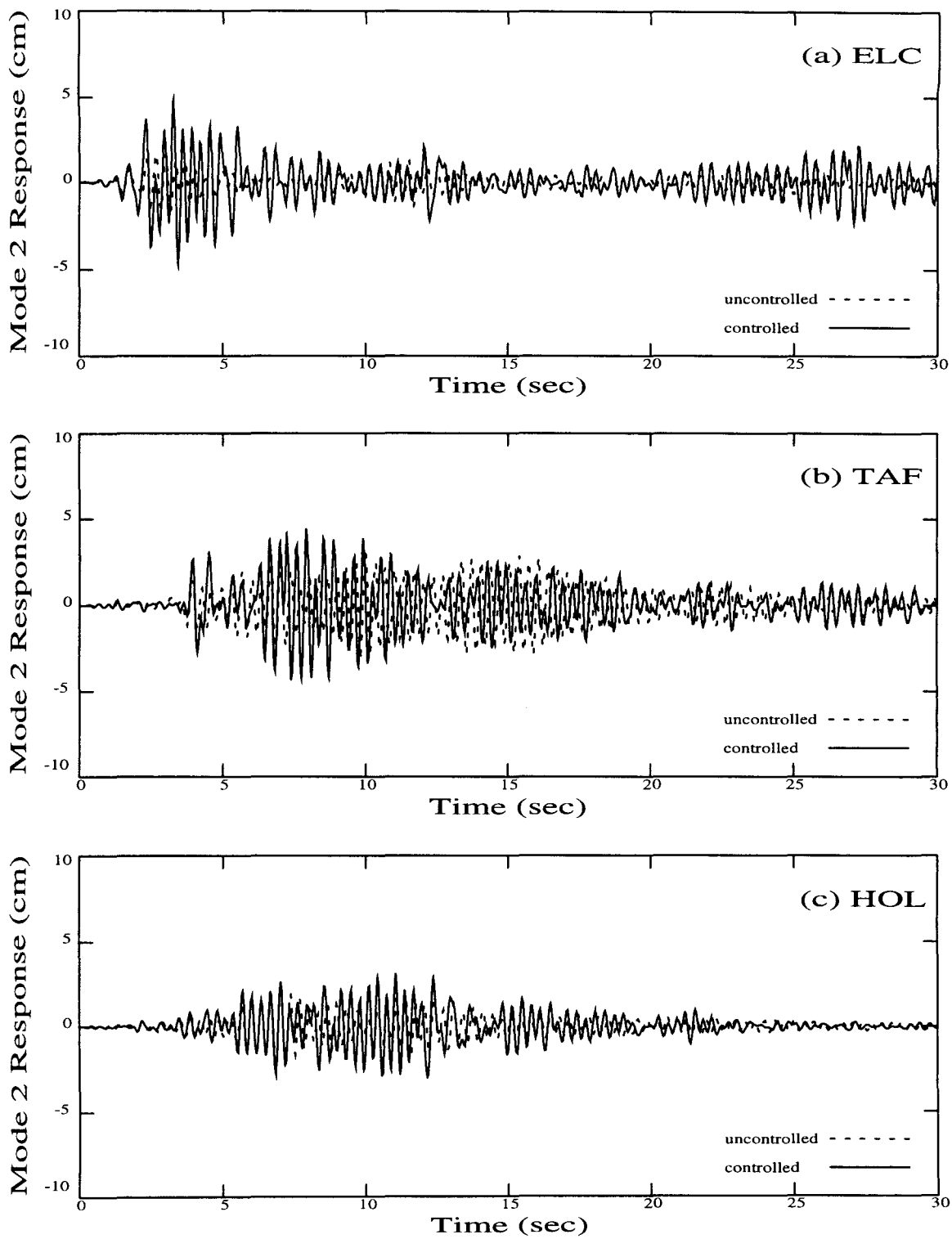

Figure 4.40. Response Time-History of Mode 2 for a 6-Story Category 3(*b*) Controlled Primary System Subjected to the (a) El Centro, (b) Taft Lincoln School Tunnel, and (c) Holiday Inn Excitation Records. Type 1 elements are used, with $\mu = 0.10$. $\alpha = 6.50$ and $\beta = 5.00$. All elements participate. Primary-Auxiliary System Configuration: 6–3.

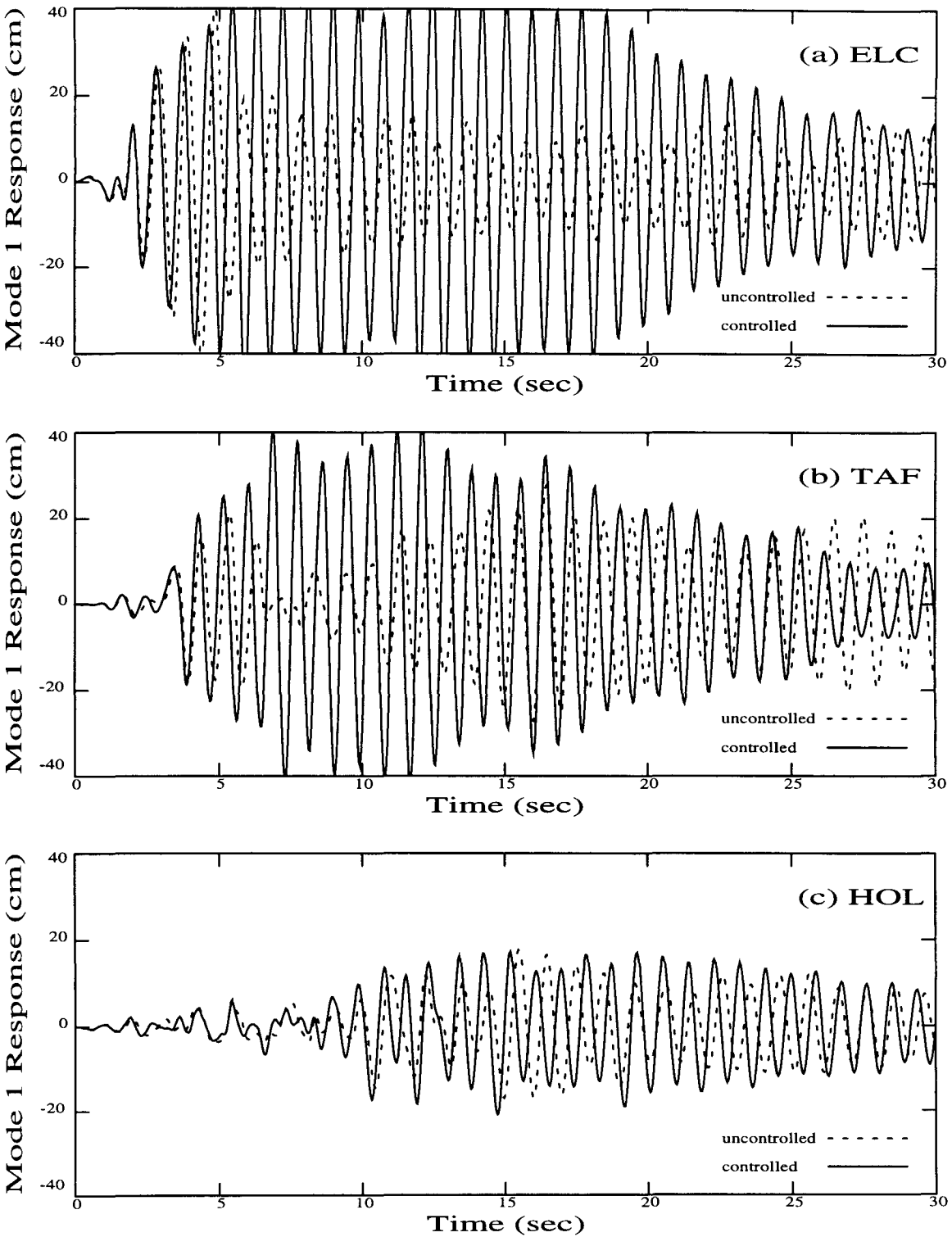

Figure 4.41. Response Time-History of Mode 1 for a 6-Story Category 3(*b*) Controlled Primary System Subjected to the (a) El Centro, (b) Taft Lincoln School Tunnel, and (c) Holiday Inn Excitation Records. Type 1 elements are used, with $\mu = 0.10$, and are locked in the activated state. $\alpha = 6.50$ and $\beta = 5.00$. All elements participate. Primary-Auxiliary System Configuration: 6–3.

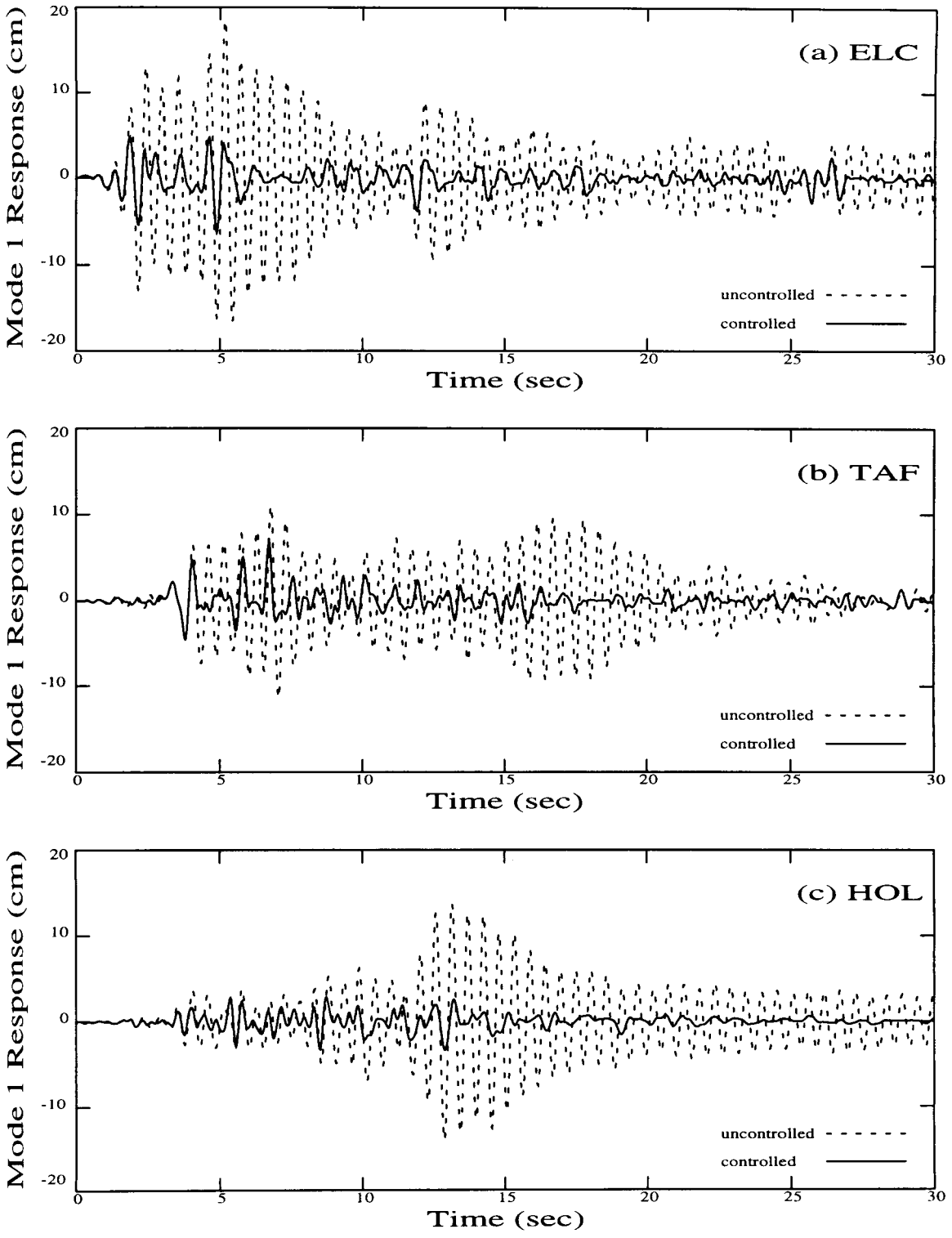

Figure 4.42. Response Time-History of Mode 1 for a 3-Story Category 3(*b*) Controlled Primary System Subjected to the (a) El Centro, (b) Taft Lincoln School Tunnel, and (c) Holiday Inn Excitation Records. Type 1 elements are used, with $\mu = 0.05$. $\alpha = 6.50$ and $\beta = 5.00$. All elements participate. Primary-Auxiliary System Configuration: 3–6.

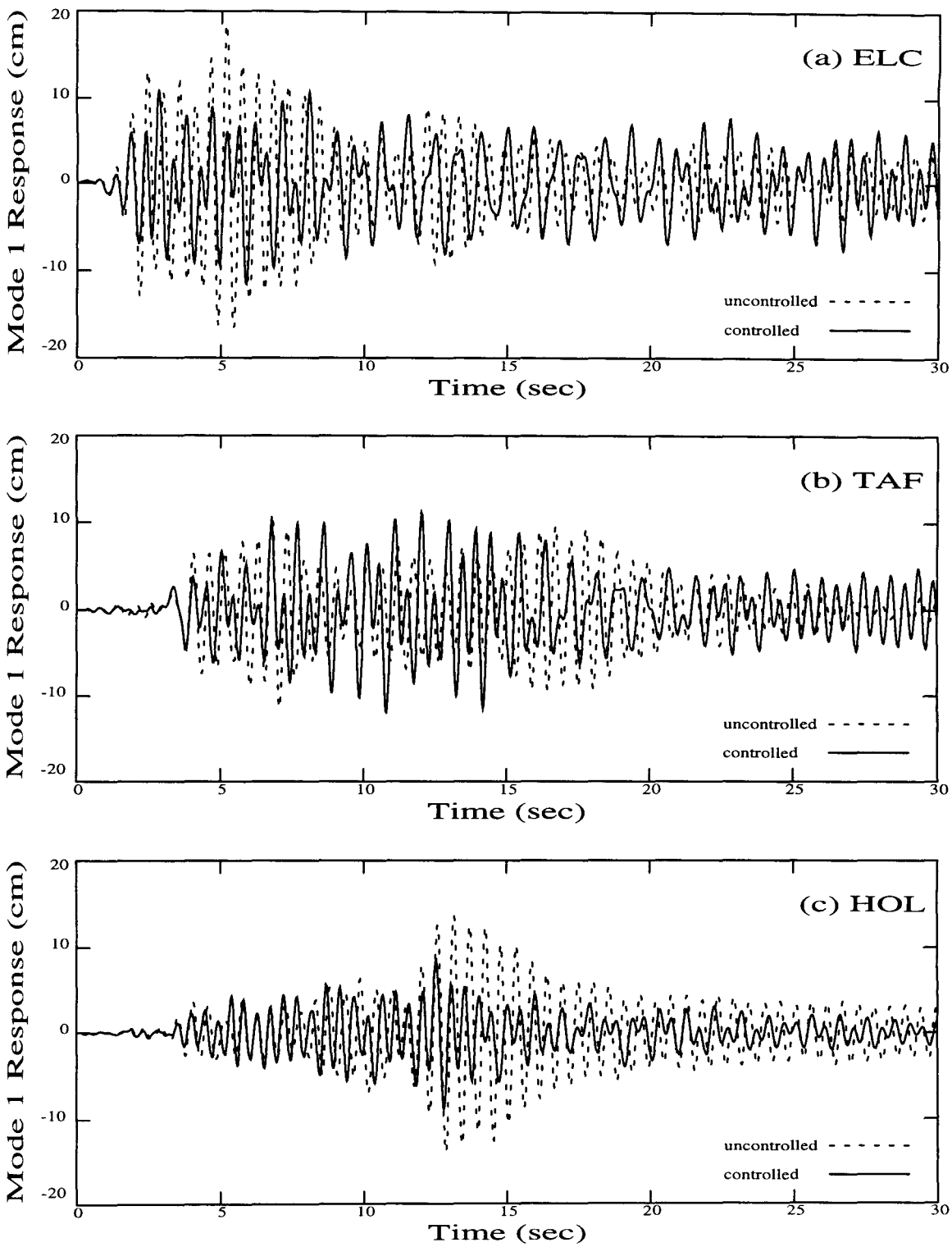

Figure 4.43. Response Time-History of Mode 1 for a 3-Story Category 3(*b*) Controlled Primary System Subjected to the (a) El Centro, (b) Taft Lincoln School Tunnel, and (c) Holiday Inn Excitation Records. Type 1 elements are used, with $\mu = 0.05$, and are locked in the activated state. $\alpha = 6.50$ and $\beta = 5.00$. All elements participate. Primary-Auxiliary System Configuration: 3–6.

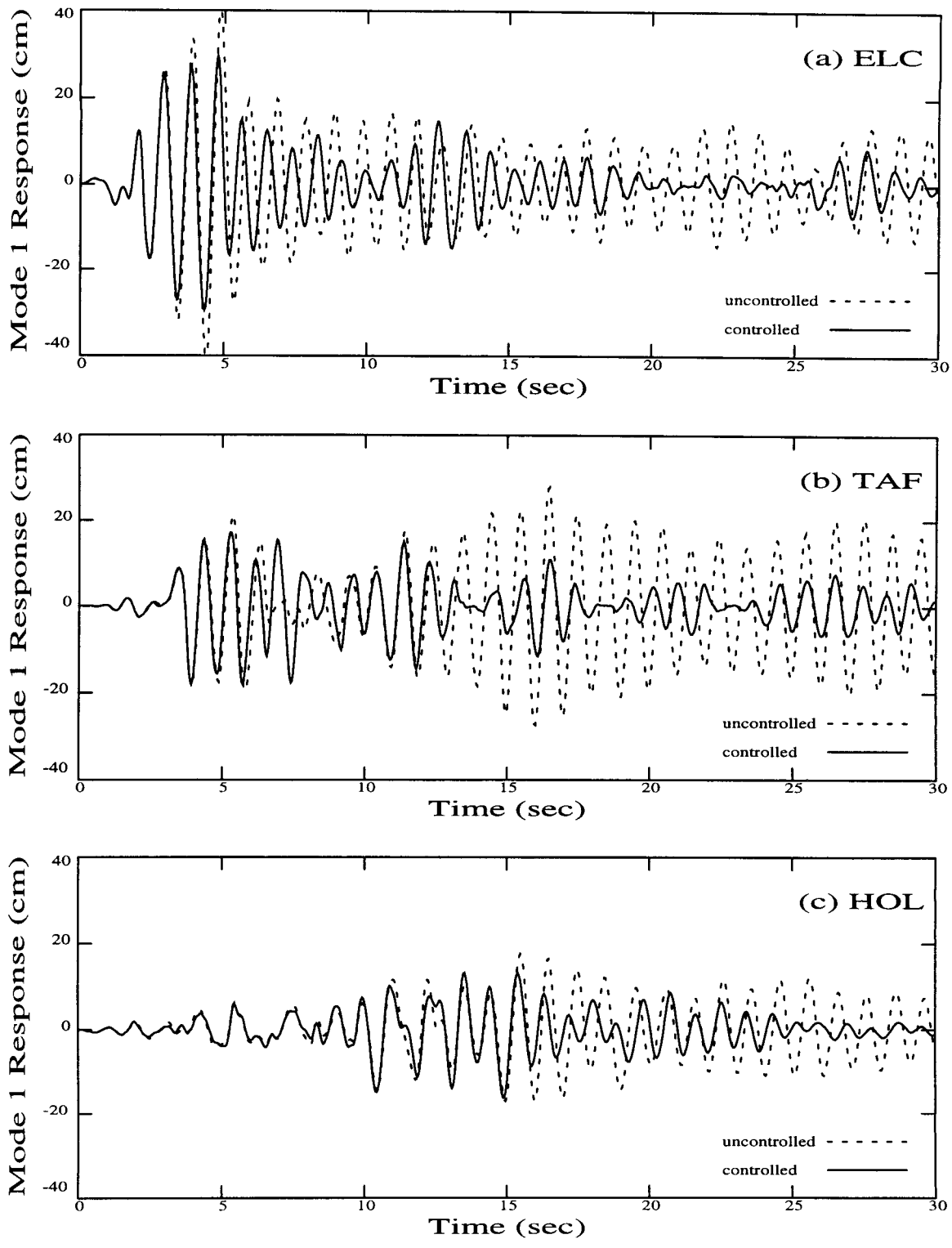

Figure 4.44. Response Time-History of Mode 1 for a 6-Story Category 4 Controlled Primary System Subjected to the (a) El Centro, (b) Taft Lincoln School Tunnel, and (c) Holiday Inn Excitation Records. Type 3 elements are used, with $\delta_h = 10.00$. $\alpha = 6.50$ and $\beta = 5.00$. All elements participate. Primary-Auxiliary System Configuration: 6–6.

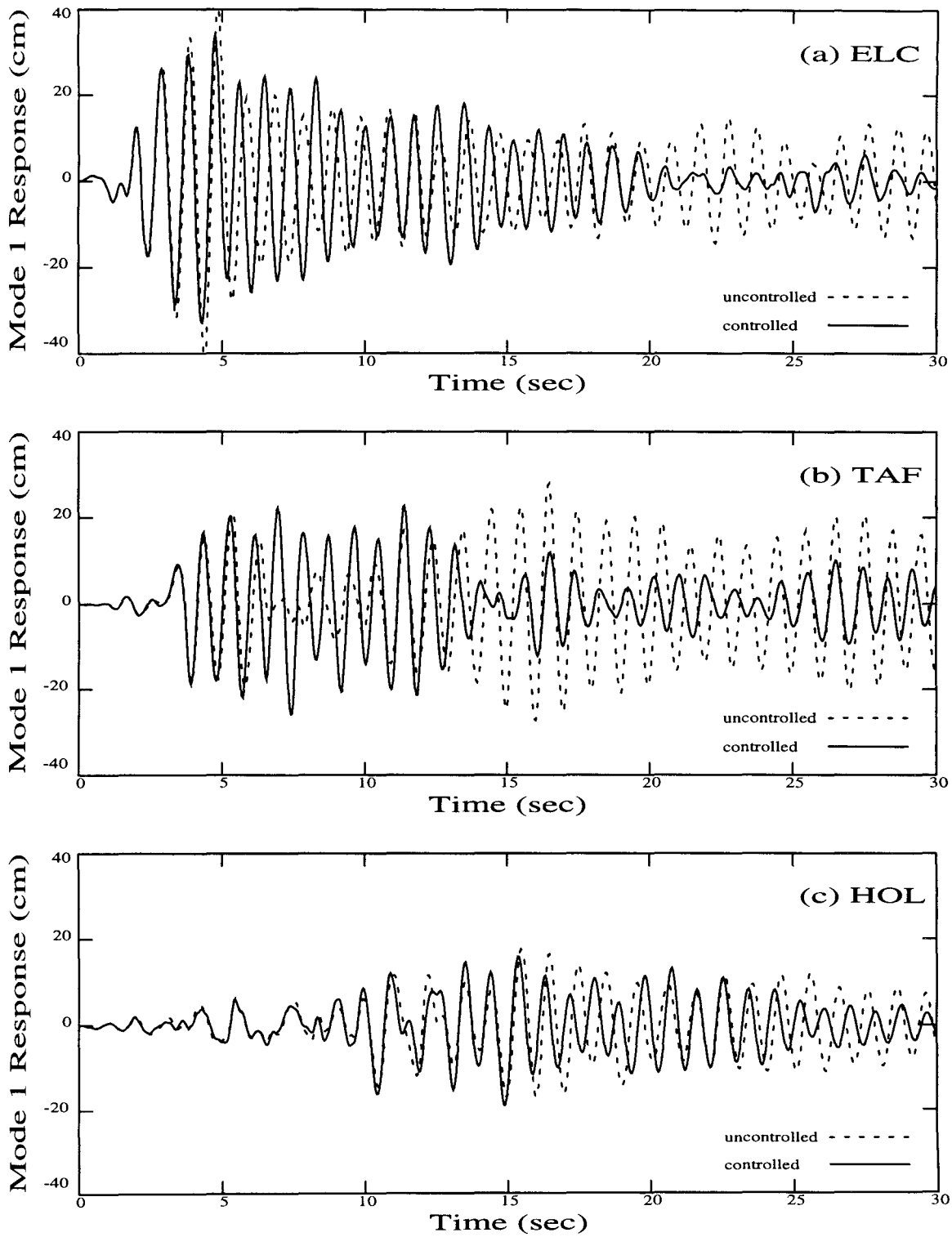

Figure 4.45. Response Time-History of Mode 1 for a 6-Story Category 4 Controlled Primary System Subjected to the (a) El Centro, (b) Taft Lincoln School Tunnel, and (c) Holiday Inn Excitation Records. Type 3 elements are used, with $\delta_h = 10.00$, and are locked in the activated state. $\alpha = 6.50$ and $\beta = 5.00$. All elements participate. Primary-Auxiliary System Configuration: 6–6.

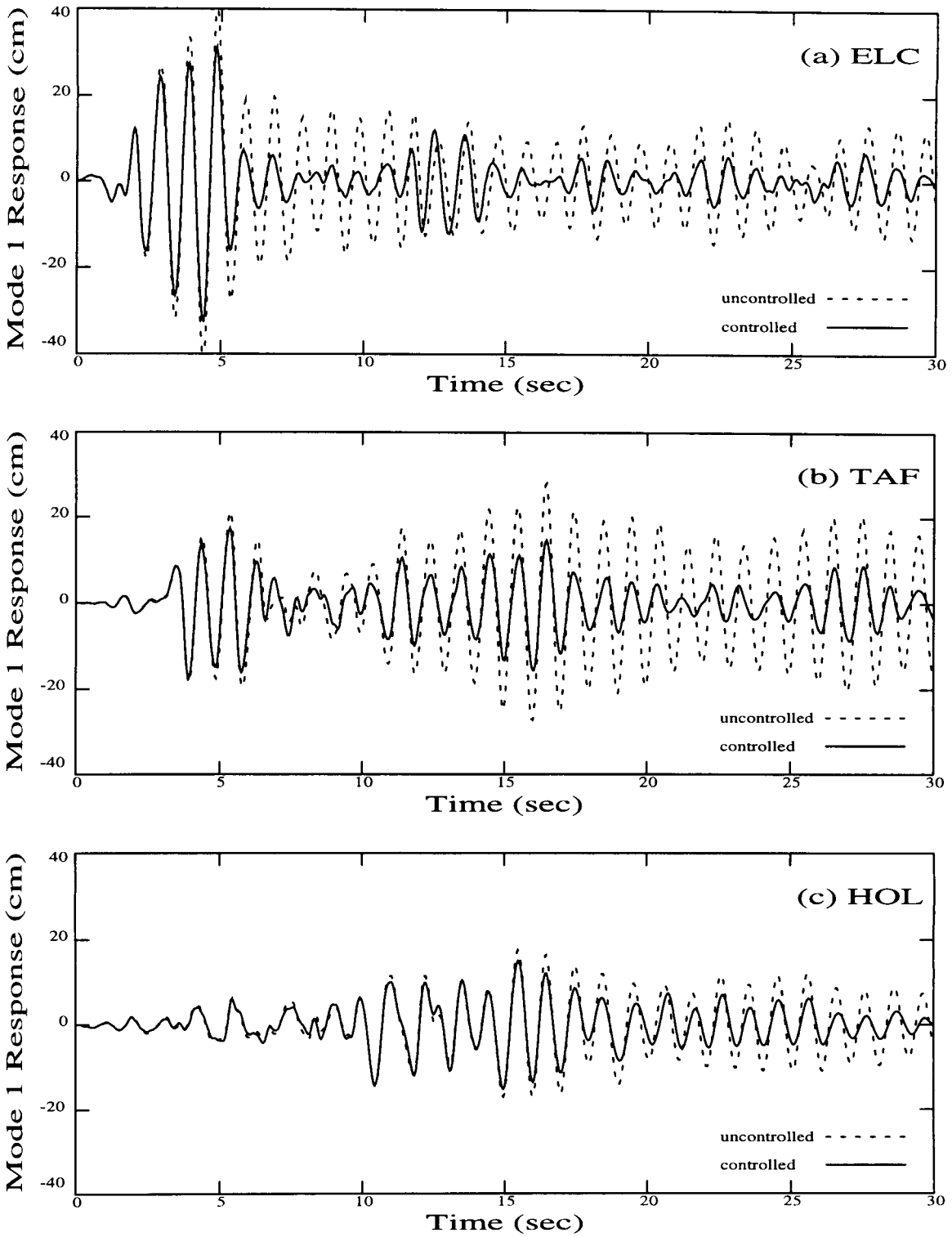

Figure 4.46. Response Time-History of Mode 1 for a 6-Story Category 4 Controlled Primary System Subjected to the (a) El Centro, (b) Taft Lincoln School Tunnel, and (c) Holiday Inn Excitation Records. Type 3 elements are used, with $\delta_h = 10.00$. $\alpha = 6.50$ and $\beta = 5.00$. All elements participate. Primary-Auxiliary System Configuration: 6–3.

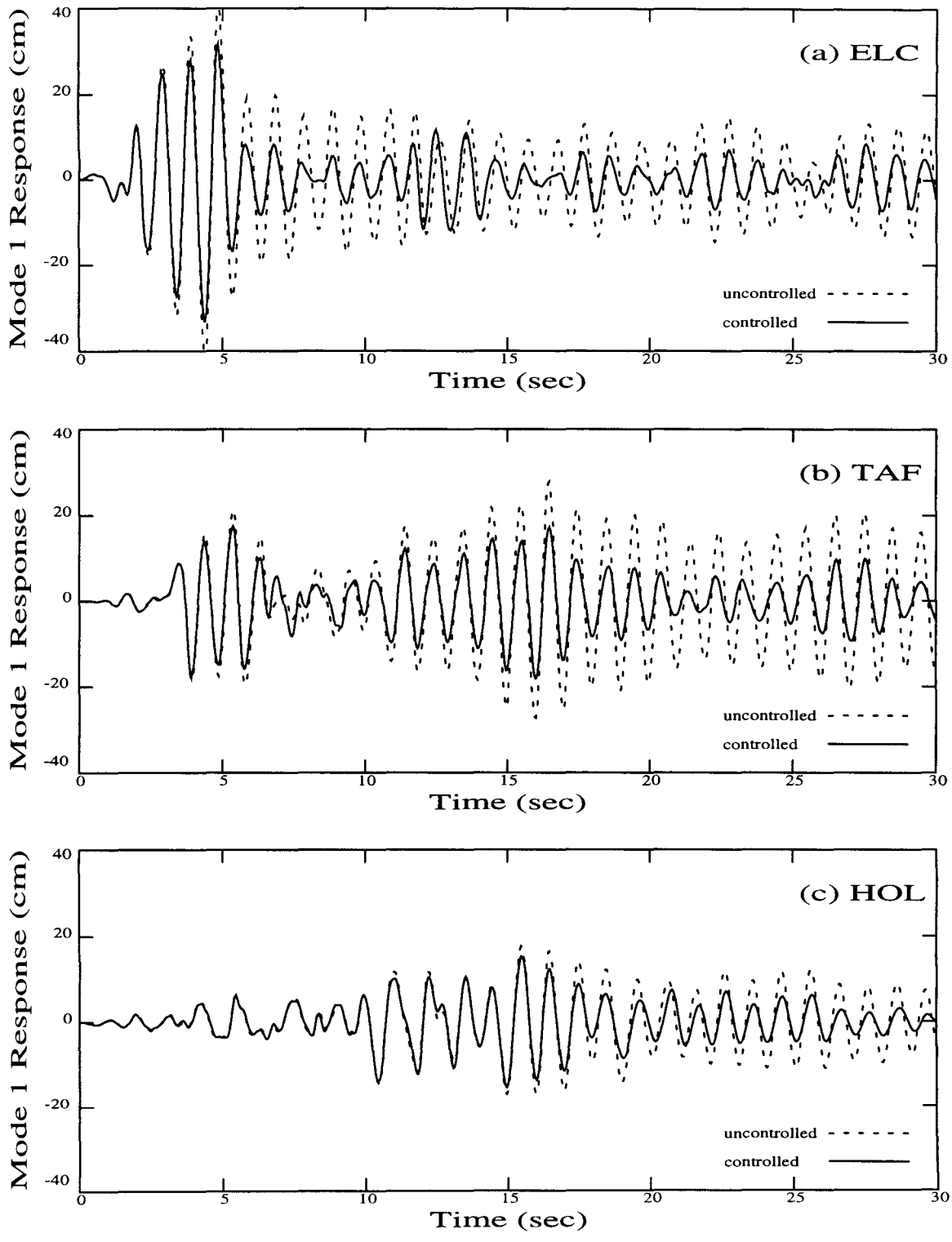

Figure 4.47. Response Time-History of Mode 1 for a 6-Story Category 4 Controlled Primary System Subjected to the (a) El Centro, (b) Taft Lincoln School Tunnel, and (c) Holiday Inn Excitation Records. Type 3 elements are used, with $\delta_h = 10.00$, and are locked in the activated state. $\alpha = 6.50$ and $\beta = 5.00$. All elements participate. Primary-Auxiliary System Configuration: 6–3.

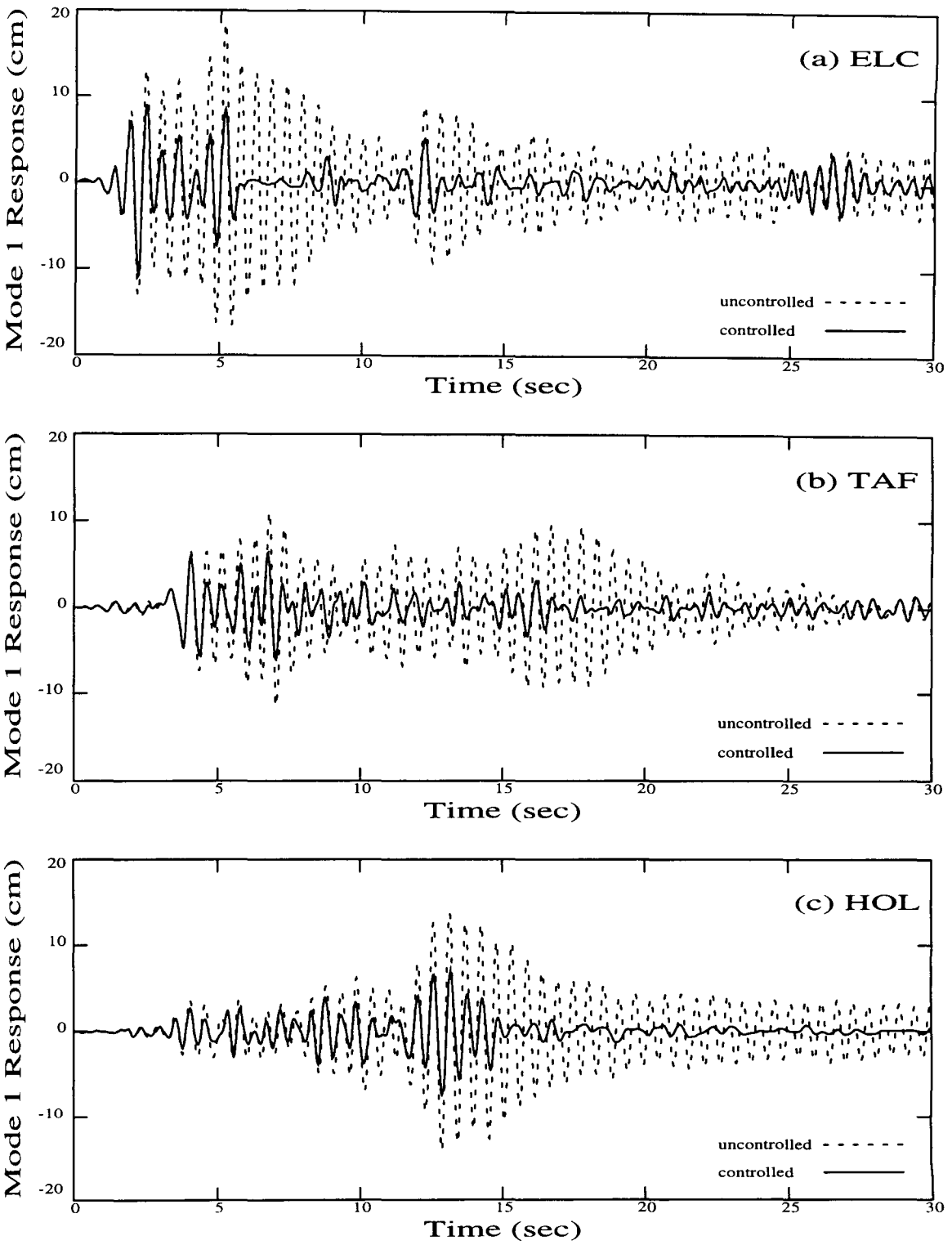

Figure 4.48. Response Time-History of Mode 1 for a 3-Story Category 4 Controlled Primary System Subjected to the (a) El Centro, (b) Taft Lincoln School Tunnel, and (c) Holiday Inn Excitation Records. Type 3 elements are used, with $\delta_h = 5.42$. $\alpha = 6.50$ and $\beta = 5.00$. All elements participate. Primary-Auxiliary System Configuration: 3–6.

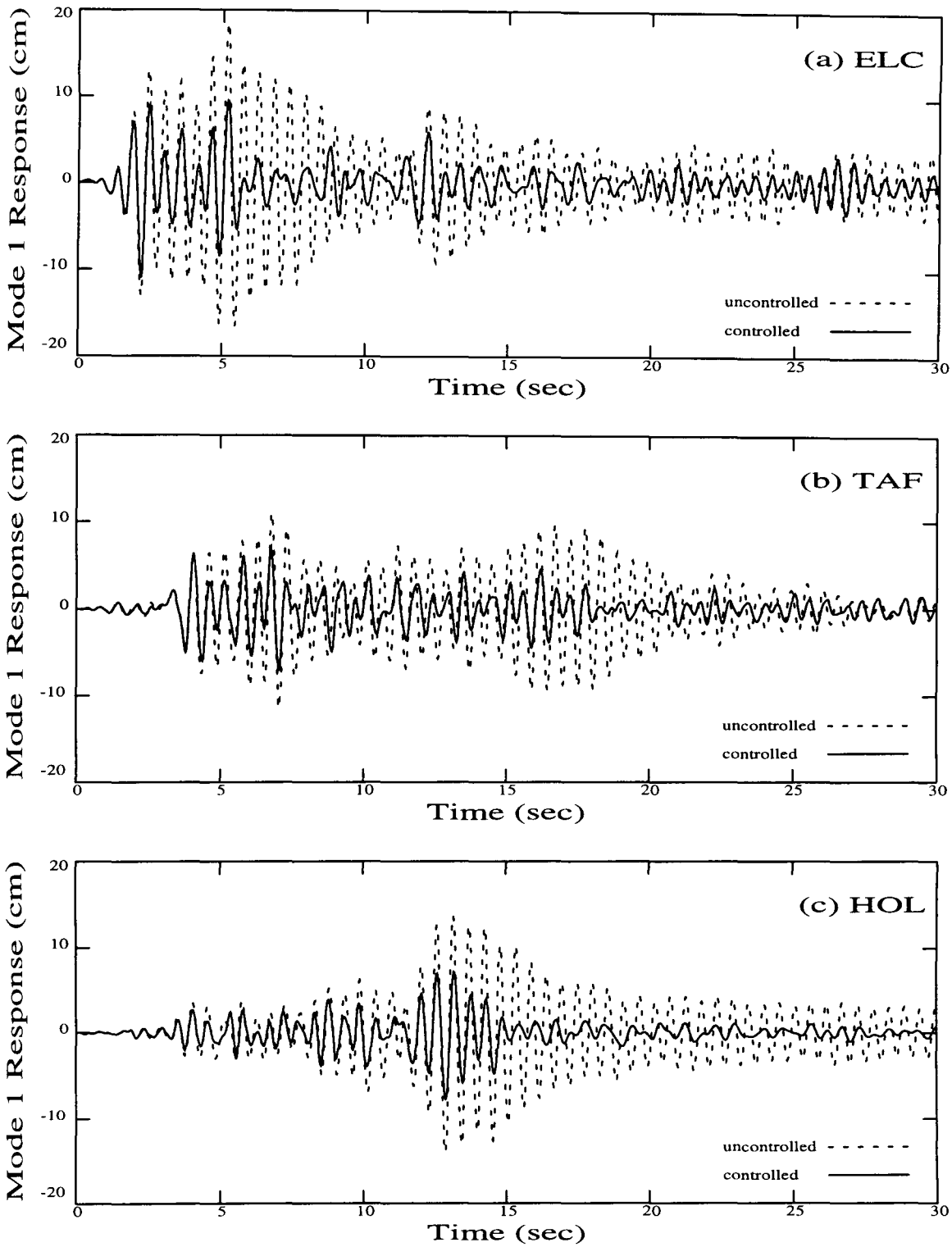

Figure 4.49. Response Time-History of Mode 1 for a 3-Story Category 4 Controlled Primary System Subjected to the (a) El Centro, (b) Taft Lincoln School Tunnel, and (c) Holiday Inn Excitation Records. Type 3 elements are used, with $\delta_h = 5.42$, and are locked in the activated state. $\alpha = 6.50$ and $\beta = 5.00$. All elements participate. Primary-Auxiliary System Configuration: 3–6.

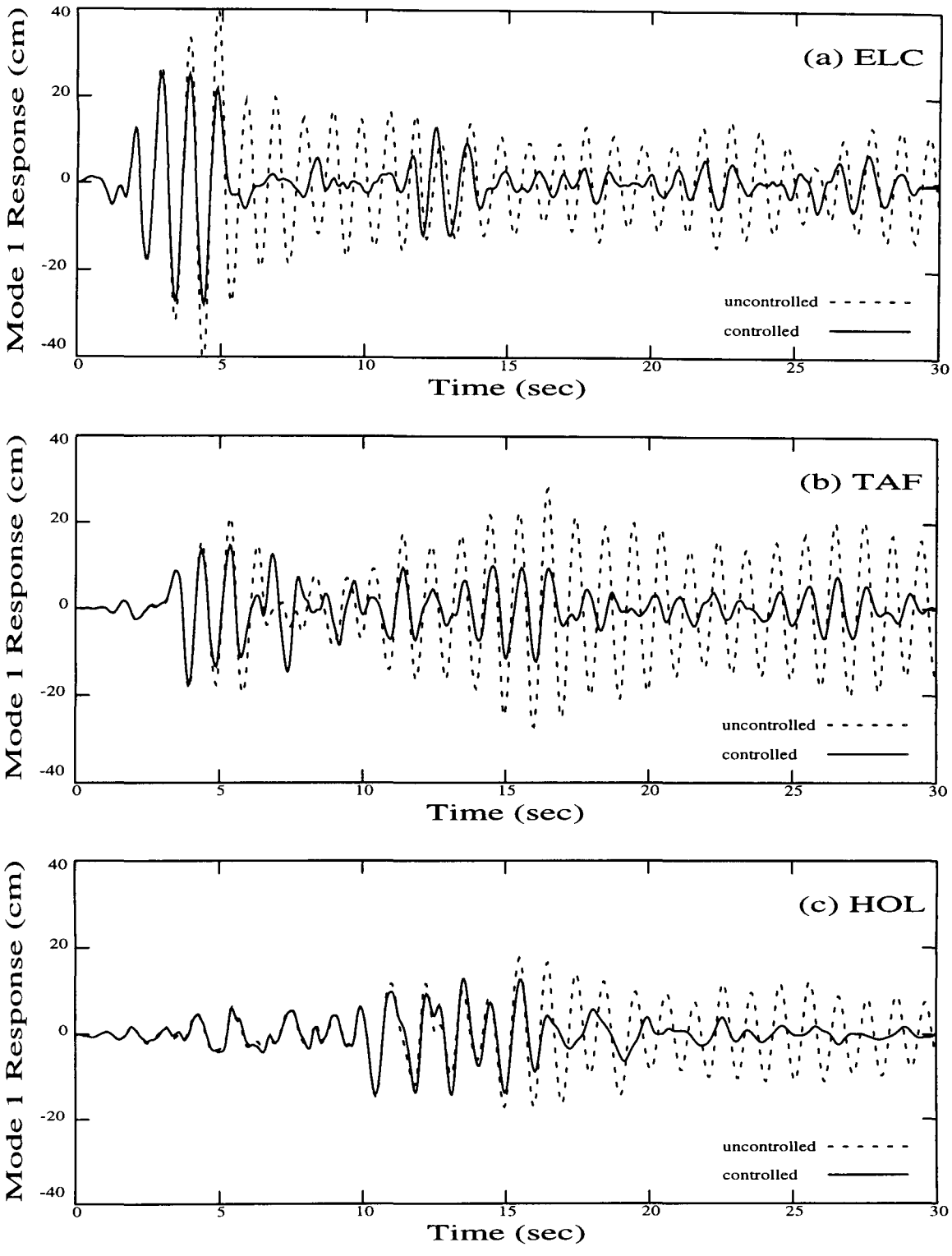

Figure 4.50. Response Time-History of Mode 1 for a 6-Story Category 5 Controlled Primary System Subjected to the (a) El Centro, (b) Taft Lincoln School Tunnel, and (c) Holiday Inn Excitation Records. A Type 1 element is used, with $\mu = 0.005$. $\alpha = 0.00$ and $\beta = 0.06$. Only top element participates.

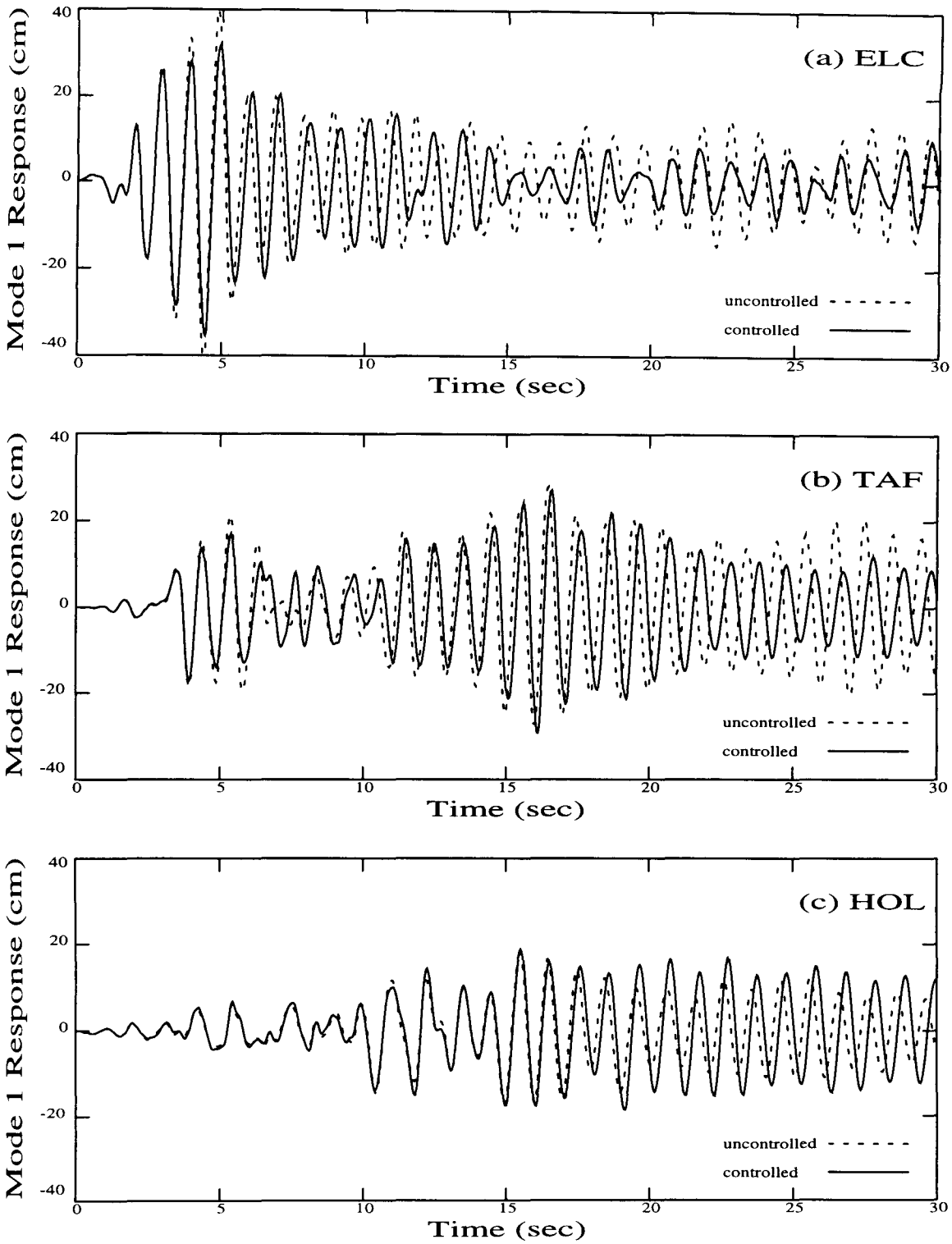

Figure 4.51. Response Time-History of Mode 1 for a 6-Story Category 5 Controlled Primary System Subjected to the (a) El Centro, (b) Taft Lincoln School Tunnel, and (c) Holiday Inn Excitation Records. A Type 1 element is used, with $\mu = 0.005$, and is locked in the activated state. $\alpha = 0.00$ and $\beta = 0.06$. Only top element participates.

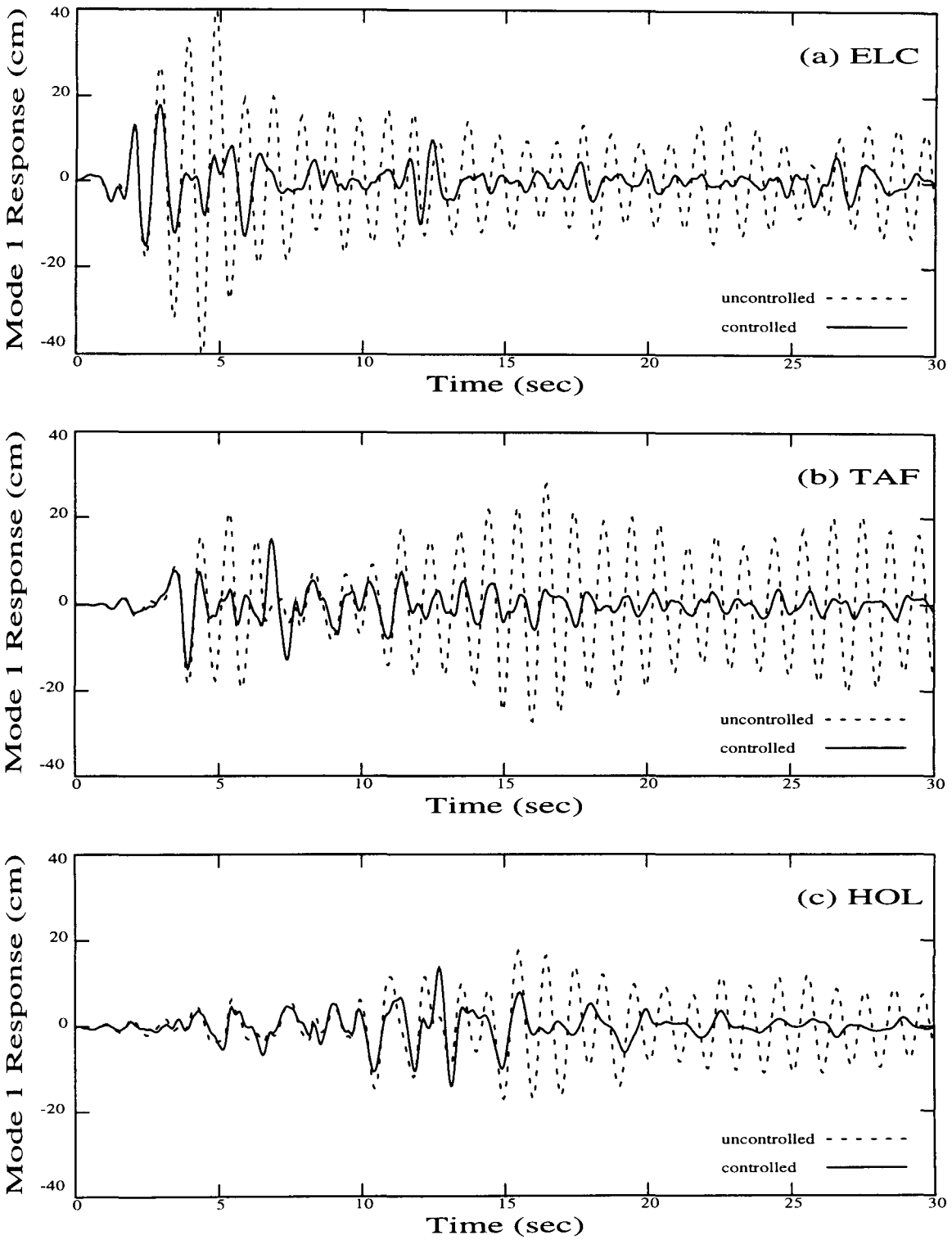

Figure 4.52. Response Time-History of Mode 1 for a 6-Story Category 5 Controlled Primary System Subjected to the (a) El Centro, (b) Taft Lincoln School Tunnel, and (c) Holiday Inn Excitation Records. A Type 1 element is used, with $\mu = 0.025$. $\alpha = 0.00$ and $\beta = 0.30$. Only top element participates.

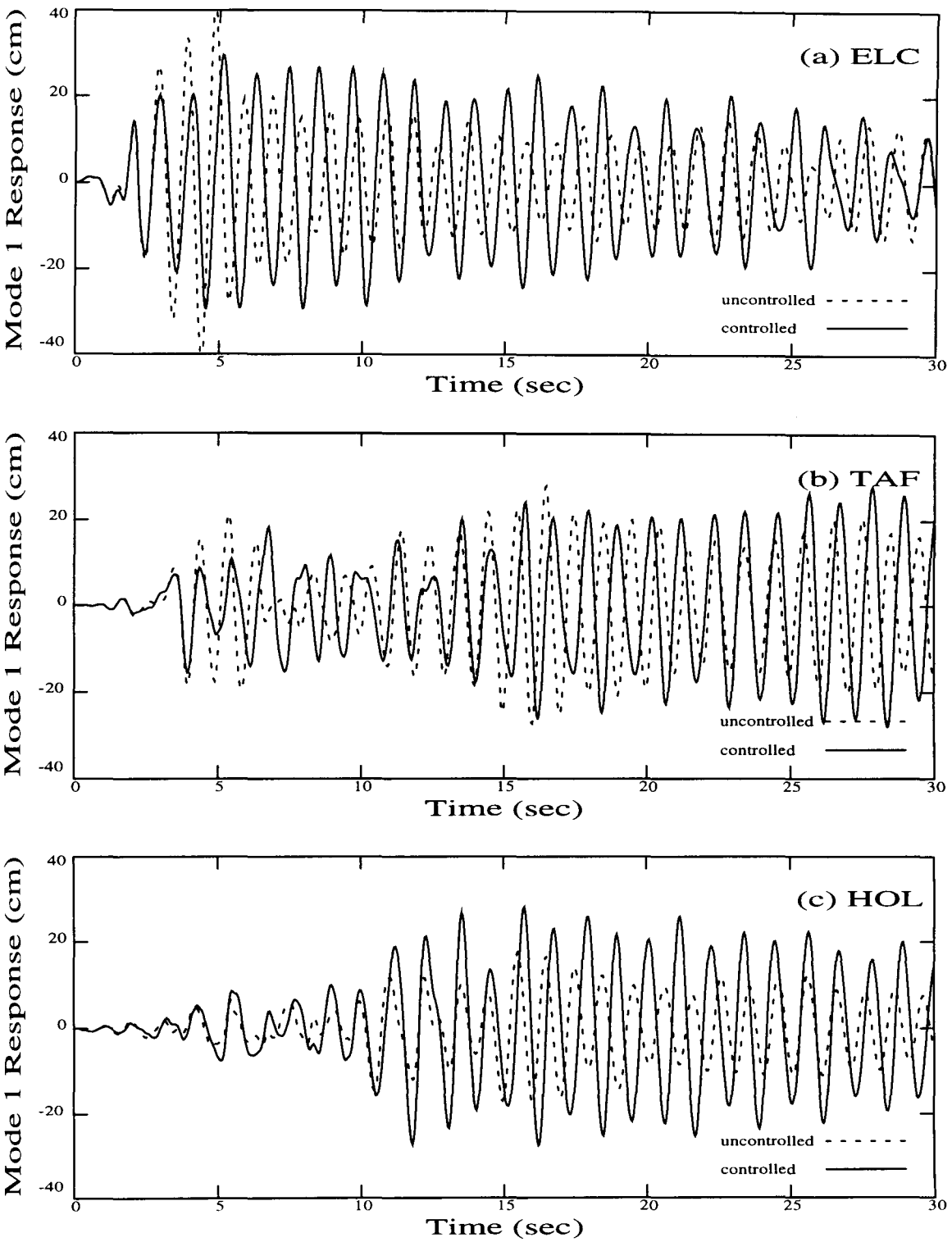

Figure 4.53. Response Time-History of Mode 1 for a 6-Story Category 5 Controlled Primary System Subjected to the (a) El Centro, (b) Taft Lincoln School Tunnel, and (c) Holiday Inn Excitation Records. A Type 1 element is used, with $\mu = 0.025$, and is locked in the activated state. $\alpha = 0.00$ and $\beta = 0.30$. Only top element participates.

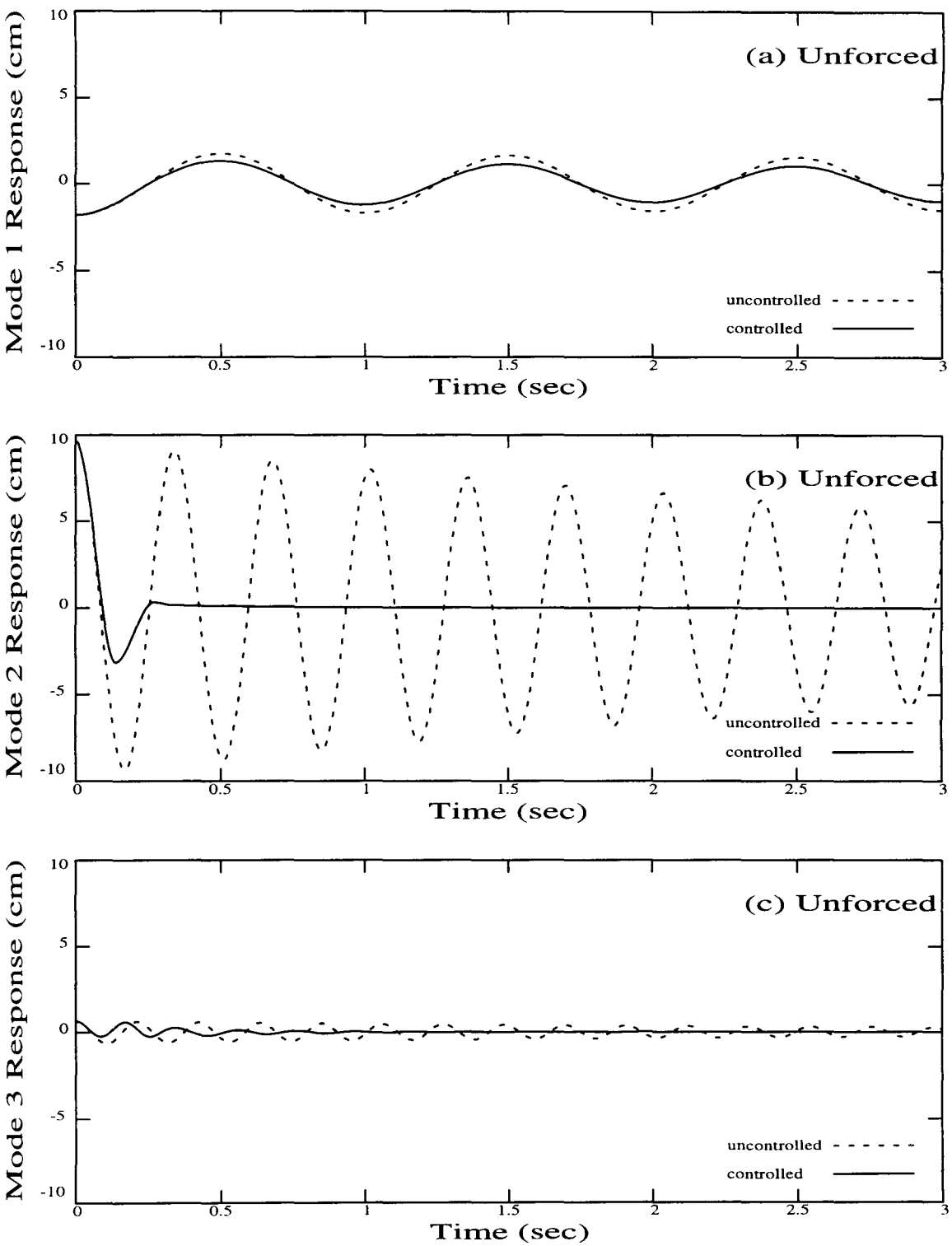

Figure 4.54. Response Time-History of (a) Mode 1, (b) Mode 2, and (c) Mode 3 for a 6-Story Category 1 Controlled Primary System which is Unforced, Initially at Rest, but Given Initial Displacements. Type 1 elements are used, with $\mu = 0.50$. All elements participate. Targeted Response Mode: 2.

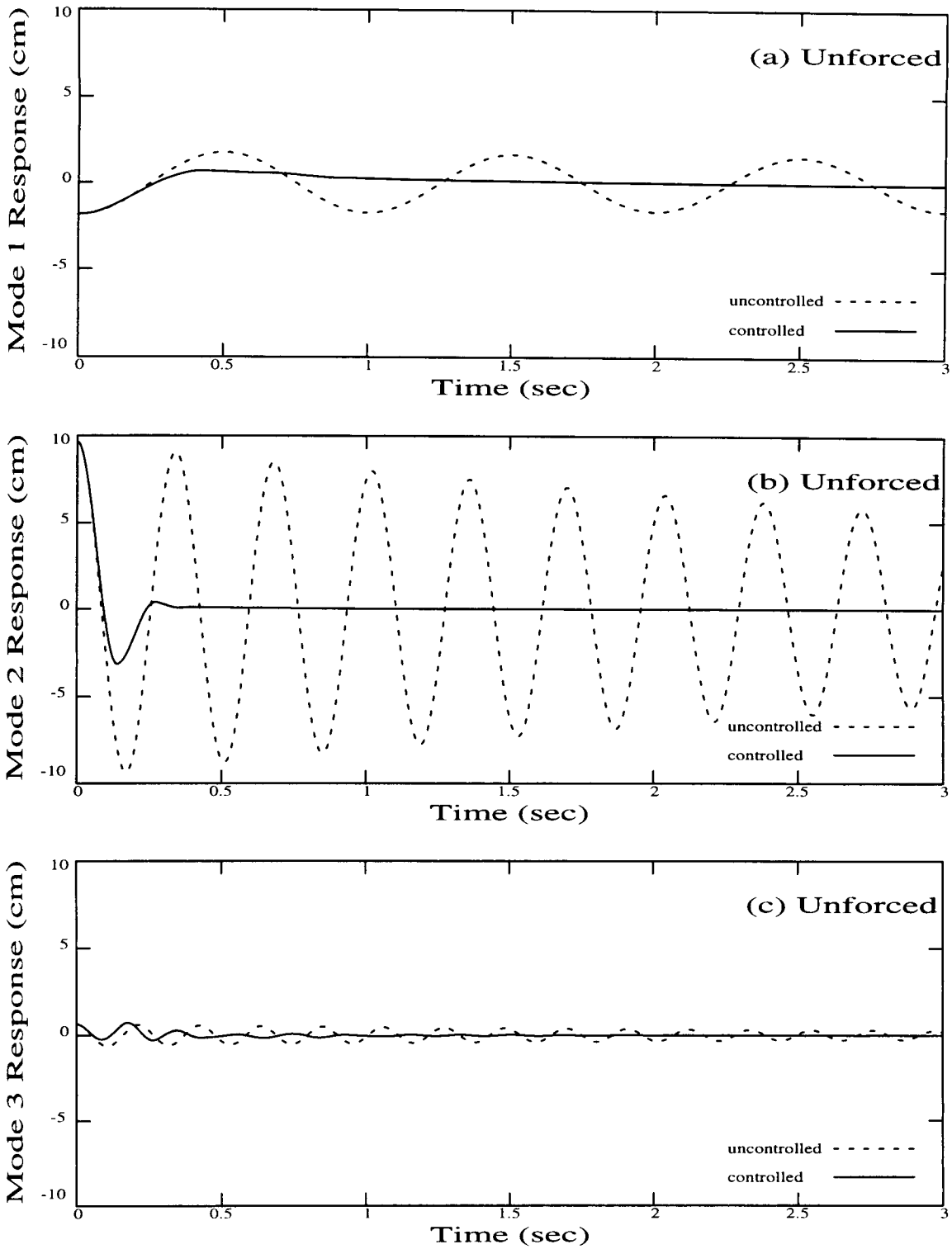

Figure 4.55. Response Time-History of (a) Mode 1, (b) Mode 2, and (c) Mode 3 for a 6-Story Category 1 Controlled Primary System which is Unforced, Initially at Rest, but Given Initial Displacements. Type 1 elements are used, with $\mu = 0.50$. All elements participate. Targeted Response Mode: 1 and 2.

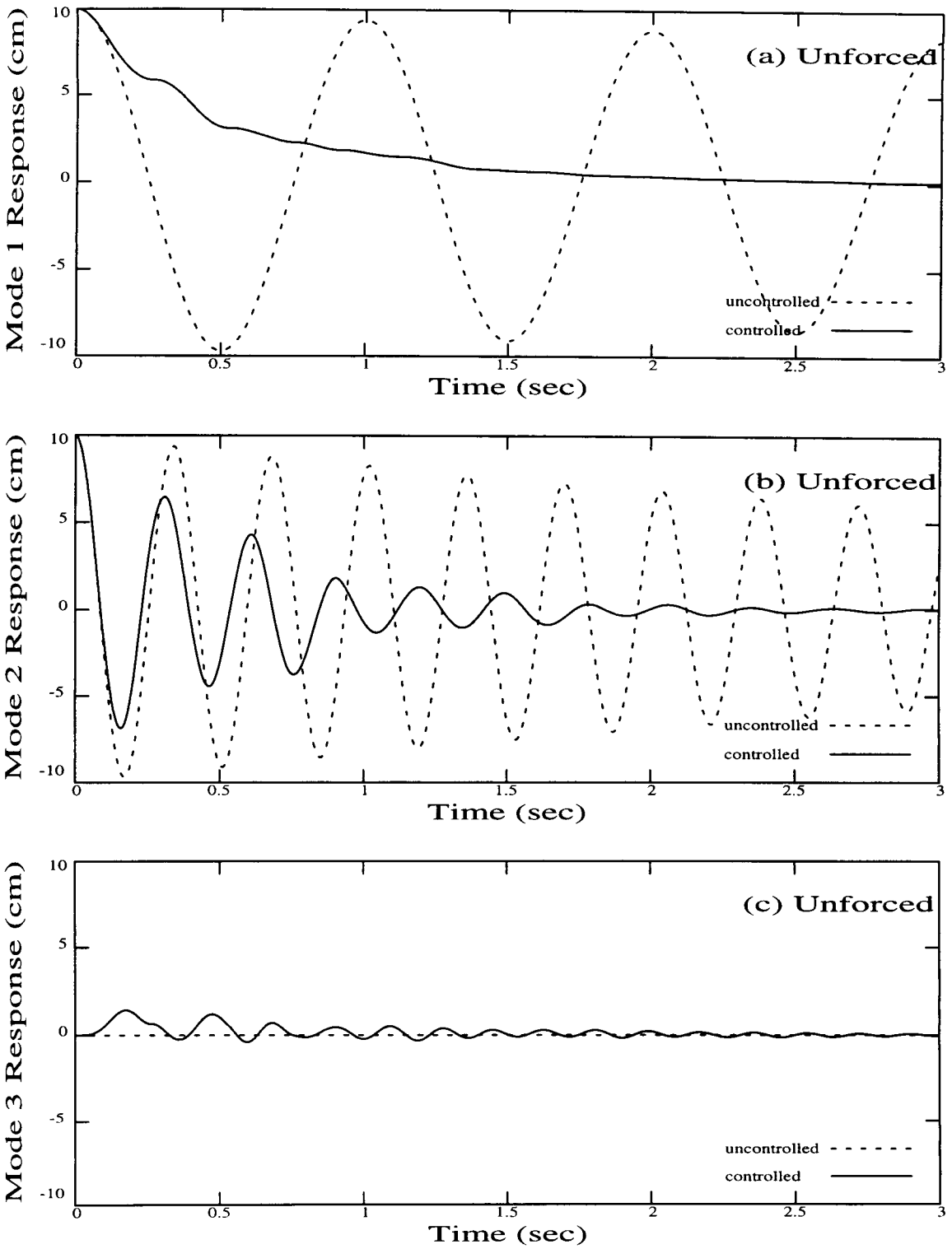

Figure 4.56. Response Time-History of (a) Mode 1, (b) Mode 2, and (c) Mode 3 for a 6-Story Category 1 Controlled Primary System which is Unforced, Initially at Rest, but Given Initial Displacements. Type 1 elements are used, with $\mu = 0.50$. All elements participate. Targeted Response Mode: 1.

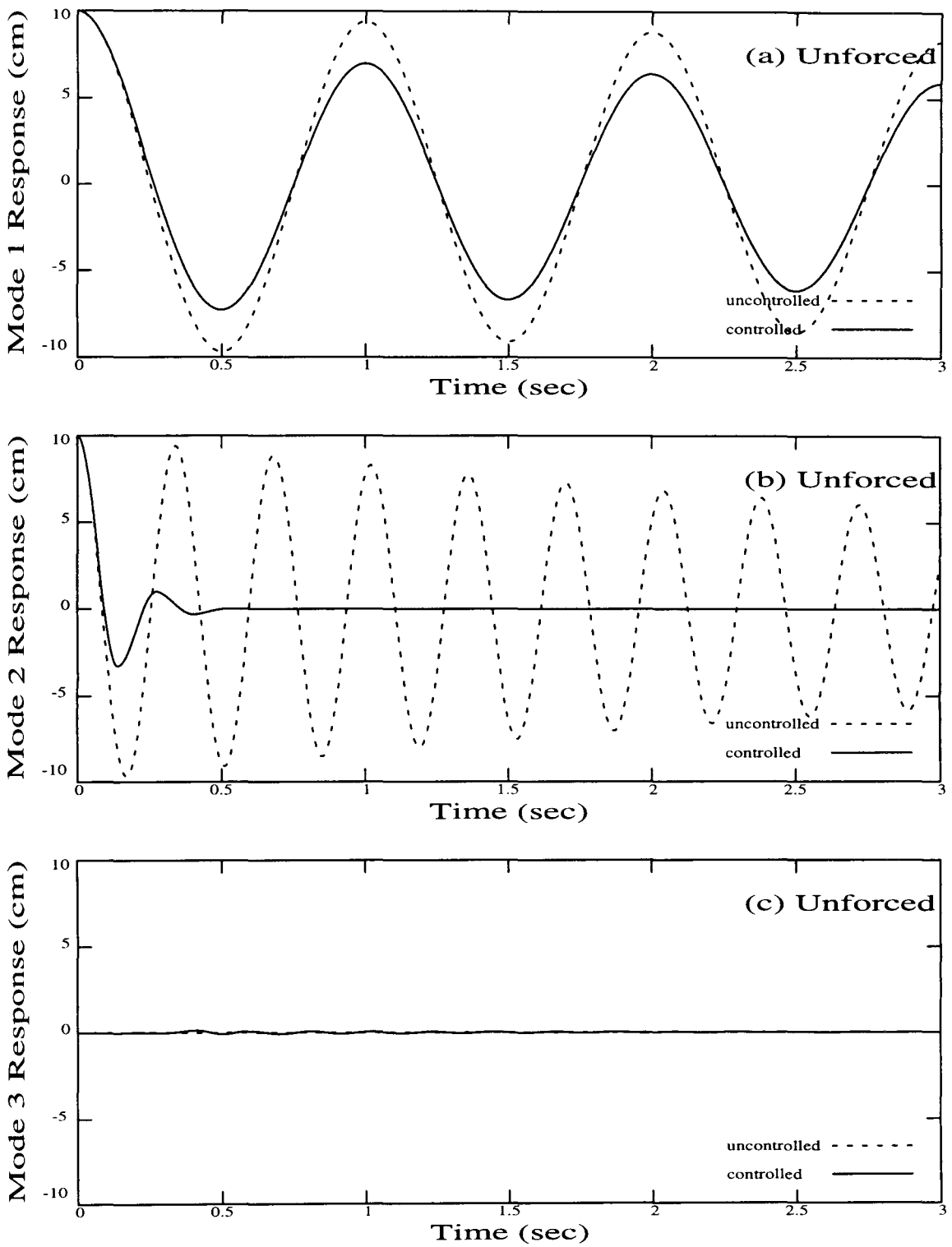

Figure 4.57. Response Time-History of (a) Mode 1, (b) Mode 2, and (c) Mode 3 for a 6-Story Category 1 Controlled Primary System which is Unforced, Initially at Rest, but Given Initial Displacements. Type 1 elements are used, with $\mu = 0.50$. All elements participate. Targeted Response Mode: 2.

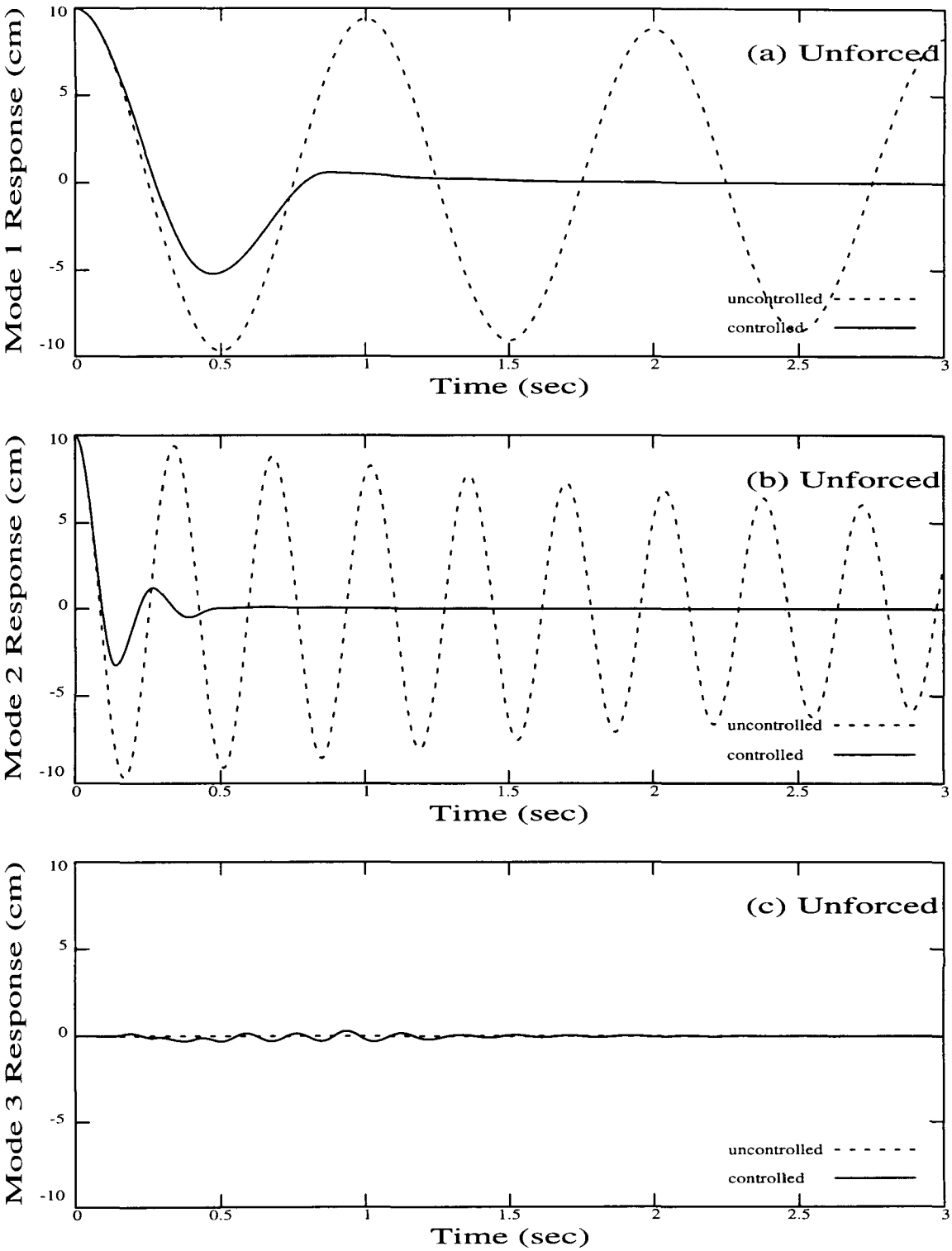

Figure 4.58. Response Time-History of (a) Mode 1, (b) Mode 2, and (c) Mode 3 for a 6-Story Category 1 Controlled Primary System which is Unforced, Initially at Rest, but Given Initial Displacements. Type 1 elements are used, with $\mu = 0.50$. All elements participate. Targeted Response Mode: 1 and 2.

Table 4.1. Descriptive Summary of Control Category Features for MDOF System Study.

Control Category	Primary-Auxiliary System Configuration	Interaction Element Types	Interaction Element Participation	$\alpha \equiv \frac{k_2}{k_1}$	$\beta \equiv \frac{m_2}{m_1}$	$\mu \equiv \frac{k_{int}}{k_1}$	$\delta_h \equiv \frac{c_h}{c_1}$	$\delta_l \equiv \frac{c_l}{c_1}$
1	N/A	1, 2	All, 1 – 3, 4 – 6	—	—	0.50, 1.00	$\rightarrow \infty$	$\rightarrow 0$, 5.00
2	6–6	1, 2	All, 1 – 3, 4 – 6	1.00, 2.00	—	—	$\rightarrow \infty$	$\rightarrow 0$, 5.00
3(*a*)	6–6	1, 2	All, 1 – 3, 4 – 6	1.00, 2.00	0.15, 0.30	1.00, 2.00	$\rightarrow \infty$	$\rightarrow 0$, 5.00
3(*b*)	6–6, 6–3, 3–6	1	All	6.50	5.00	Various	$\rightarrow \infty$	$\rightarrow 0$, 5.00
4	6–6, 6–3, 3–6	3	All	6.50	5.00	—	Various	0.00
5	N/A	1	All	0.00	0.06, 0.30	Various	$\rightarrow \infty$	$\rightarrow 0$, 5.00

Table 4.2. Normalized Mode Shapes (Columns of Φ) for a 6-Story Primary System.

	Mode 1 ($j=1$)	Mode 2 ($j=2$)	Mode 3 ($j=3$)	Mode 4 ($j=4$)	Mode 5 ($j=5$)	Mode 6 ($j=6$)
φ_{6j}	0.55066	– 0.51865	0.45651	– 0.36783	0.25778	– 0.13275
φ_{5j}	0.51865	– 0.25778	– 0.13275	0.45651	– 0.55066	0.36783
φ_{4j}	0.45651	0.13275	– 0.55066	0.25778	0.36783	– 0.51865
φ_{3j}	0.36783	0.45651	– 0.25778	– 0.51865	0.13275	0.55066
φ_{2j}	0.25778	0.55066	0.36783	– 0.13275	– 0.51865	– 0.45651
φ_{1j}	0.13275	0.36783	0.51865	0.55066	0.45651	0.25778

Table 4.3. Normalized Mode Shapes (Columns of Φ) for a 3-Story Primary System.

	Mode 1 ($j=1$)	Mode 2 ($j=2$)	Mode 3 ($j=3$)
φ_{3j}	0.73698	– 0.59101	0.32798
φ_{2j}	0.59101	0.32798	– 0.73698
φ_{1j}	0.32798	0.73698	0.59101

Table 4.4. Peak and Root-Mean-Square Values of Nodal Mass Acceleration (Absolute) for a 6-Story Uncontrolled Primary System. Units are in g.

Primary-Auxiliary System Configuration: N/A						Peak Nodal Mass Acceleration (RMS Nodal Mass Acceleration)					
Excitation	$\alpha \equiv \frac{k_2}{k_1}$	$\beta \equiv \frac{m_2}{m_1}$	$\mu \equiv \frac{k_{int}}{k_1}$	$\delta_h \equiv \frac{c_h}{c_1}$	$\delta_l \equiv \frac{c_l}{c_1}$	Mass 1	Mass 2	Mass 3	Mass 4	Mass 5	Mass 6
ELC	—	—	—	—	—	0.43 (0.11)	0.61 (0.15)	0.65 (0.19)	0.83 (0.22)	0.90 (0.25)	1.05 (0.27)
TAF	—	—	—	—	—	0.63 (0.18)	0.77 (0.25)	0.87 (0.25)	0.73 (0.24)	0.76 (0.26)	1.03 (0.33)
HOL	—	—	—	—	—	0.46 (0.11)	0.49 (0.14)	0.54 (0.14)	0.45 (0.14)	0.39 (0.15)	0.65 (0.19)

Table 4.5. Peak and Root-Mean-Square Values of Story Drift for a 6-Story Uncontrolled Primary System. Units are in cm.

Primary-Auxiliary System Configuration: N/A						Peak Story Drift (RMS Story Drift)					
Excitation	$\alpha \equiv \frac{k_2}{k_1}$	$\beta \equiv \frac{m_2}{m_1}$	$\mu \equiv \frac{k_{int}}{k_1}$	$\delta_h \equiv \frac{c_h}{c_1}$	$\delta_l \equiv \frac{c_l}{c_1}$	Story 1	Story 2	Story 3	Story 4	Story 5	Story 6
ELC	—	—	—	—	—	5.29 (1.51)	5.23 (1.43)	4.69 (1.26)	3.75 (1.03)	2.60 (0.74)	1.51 (0.39)
TAF	—	—	—	—	—	4.28 (1.58)	3.82 (1.46)	3.11 (1.28)	2.95 (1.08)	2.59 (0.84)	1.49 (0.48)
HOL	—	—	—	—	—	2.62 (0.92)	2.31 (0.84)	1.89 (0.74)	1.55 (0.62)	1.45 (0.47)	0.94 (0.27)

Table 4.6. Peak and Root-Mean-Square Values of Nodal Mass Acceleration (Absolute) for a 3-Story Uncontrolled Primary System. Units are in g.

Primary-Auxiliary System Configuration: N/A						Peak Nodal Mass Acceleration (RMS Nodal Mass Acceleration)					
Excitation	$\alpha \equiv \frac{k_2}{k_1}$	$\beta \equiv \frac{m_2}{m_1}$	$\mu \equiv \frac{k_{int}}{k_1}$	$\delta_h \equiv \frac{c_h}{c_1}$	$\delta_l \equiv \frac{c_l}{c_1}$	Mass 1	Mass 2	Mass 3	Mass 4	Mass 5	Mass 6
ELC	—	—	—	—	—	1.16 (0.26)	1.52 (0.42)	1.78 (0.52)	— —	— —	— —
TAF	—	—	—	—	—	0.64 (0.18)	0.92 (0.25)	1.25 (0.25)	— —	— —	— —
HOL	—	—	—	—	—	0.79 (0.21)	1.19 (0.32)	1.32 (0.40)	— —	— —	— —

Table 4.7. Peak and Root-Mean-Square Values of Story Drift for a 3-Story Uncontrolled Primary System. Units are in cm.

Primary-Auxiliary System Configuration: N/A						Peak Story Drift (RMS Story Drift)					
Excitation	$\alpha \equiv \frac{k_2}{k_1}$	$\beta \equiv \frac{m_2}{m_1}$	$\mu \equiv \frac{k_{int}}{k_1}$	$\delta_h \equiv \frac{c_h}{c_1}$	$\delta_l \equiv \frac{c_l}{c_1}$	Story 1	Story 2	Story 3	Story 4	Story 5	Story 6
ELC	—	—	—	—	—	6.31 (1.67)	4.67 (1.33)	2.56 (0.75)	— —	— —	— —
TAF	—	—	—	—	—	3.68 (1.26)	3.07 (1.01)	1.81 (0.58)	— —	— —	— —
HOL	—	—	—	—	—	2.62 (1.30)	2.31 (1.03)	1.89 (0.58)	— —	— —	— —

Table 4.8. Peak and Root-Mean-Square Values of Nodal Mass Acceleration (Absolute) for a 6-Story Category 1 Controlled Primary System Using Type 1 Elements. Units are in g. All elements participate.

Primary-Auxiliary System Configuration: N/A						Peak Nodal Mass Acceleration (RMS Nodal Mass Acceleration)					
Excitation	$\alpha \equiv \frac{k_2}{k_1}$	$\beta \equiv \frac{m_2}{m_1}$	$\mu \equiv \frac{k_{int}}{k_1}$	$\delta_h \equiv \frac{c_h}{c_1}$	$\delta_l \equiv \frac{c_l}{c_1}$	Mass 1	Mass 2	Mass 3	Mass 4	Mass 5	Mass 6
ELC	—	—	0.50	$\to \infty$	$\to 0$	0.40 (0.08)	0.40 (0.09)	0.55 (0.10)	0.52 (0.10)	0.68 (0.11)	0.80 (0.13)
ELC	—	—	1.00	$\to \infty$	$\to 0$	0.39 (0.08)	0.55 (0.09)	0.49 (0.09)	0.49 (0.10)	0.75 (0.10)	0.87 (0.12)
TAF	—	—	0.50	$\to \infty$	$\to 0$	0.39 (0.09)	0.48 (0.09)	0.40 (0.09)	0.43 (0.09)	0.51 (0.10)	0.61 (0.12)
TAF	—	—	1.00	$\to \infty$	$\to 0$	0.32 (0.08)	0.35 (0.09)	0.46 (0.09)	0.55 (0.10)	0.74 (0.10)	0.81 (0.12)
HOL	—	—	0.50	$\to \infty$	$\to 0$	0.28 (0.06)	0.38 (0.07)	0.42 (0.07)	0.39 (0.07)	0.45 (0.08)	0.51 (0.10)
HOL	—	—	1.00	$\to \infty$	$\to 0$	0.31 (0.06)	0.35 (0.07)	0.33 (0.07)	0.42 (0.08)	0.52 (0.08)	0.59 (0.09)

Table 4.9. Peak and Root-Mean-Square Values of Story Drift for a 6-Story Category 1 Controlled Primary System Using Type 1 Elements. Units are in cm. All elements participate.

Primary-Auxiliary System Configuration: N/A						Peak Story Drift (RMS Story Drift)					
Excitation	$\alpha \equiv \frac{k_2}{k_1}$	$\beta \equiv \frac{m_2}{m_1}$	$\mu \equiv \frac{k_{int}}{k_1}$	$\delta_h \equiv \frac{c_h}{c_1}$	$\delta_l \equiv \frac{c_l}{c_1}$	Story 1	Story 2	Story 3	Story 4	Story 5	Story 6
ELC	—	—	0.50	$\rightarrow \infty$	$\rightarrow 0$	1.45 (0.37)	1.47 (0.34)	1.50 (0.30)	1.32 (0.26)	1.18 (0.20)	0.69 (0.12)
ELC	—	—	1.00	$\rightarrow \infty$	$\rightarrow 0$	1.25 (0.26)	1.22 (0.24)	1.16 (0.21)	1.11 (0.18)	0.90 (0.14)	0.51 (0.09)
TAF	—	—	0.50	$\rightarrow \infty$	$\rightarrow 0$	1.34 (0.32)	1.50 (0.30)	1.48 (0.27)	1.27 (0.23)	0.99 (0.19)	0.55 (0.12)
TAF	—	—	1.00	$\rightarrow \infty$	$\rightarrow 0$	1.06 (0.25)	1.11 (0.22)	1.20 (0.20)	1.04 (0.18)	0.80 (0.14)	0.48 (0.09)
HOL	—	—	0.50	$\rightarrow \infty$	$\rightarrow 0$	1.58 (0.31)	1.34 (0.28)	1.13 (0.25)	0.97 (0.21)	0.80 (0.16)	0.47 (0.09)
HOL	—	—	1.00	$\rightarrow \infty$	$\rightarrow 0$	1.08 (0.23)	1.09 (0.21)	1.04 (0.18)	0.91 (0.15)	0.66 (0.11)	0.36 (0.06)

Table 4.10. Peak and Root-Mean-Square Values of Nodal Mass Acceleration (Absolute) for a 6-Story Category 1 Controlled Primary System Using Type 2 Elements. Units are in g. All elements participate.

Primary-Auxiliary System Configuration: N/A						Peak Nodal Mass Acceleration (RMS Nodal Mass Acceleration)					
Excitation	$\alpha \equiv \frac{k_2}{k_1}$	$\beta \equiv \frac{m_2}{m_1}$	$\mu \equiv \frac{k_{int}}{k_1}$	$\delta_h \equiv \frac{c_h}{c_1}$	$\delta_l \equiv \frac{c_l}{c_1}$	Mass 1	Mass 2	Mass 3	Mass 4	Mass 5	Mass 6
ELC	—	—	0.50	$\rightarrow \infty$	5.00	0.37 (0.08)	0.40 (0.09)	0.50 (0.10)	0.46 (0.10)	0.66 (0.11)	0.78 (0.13)
ELC	—	—	1.00	$\rightarrow \infty$	5.00	0.42 (0.08)	0.58 (0.10)	0.57 (0.10)	0.60 (0.10)	0.78 (0.11)	0.89 (0.13)
TAF	—	—	0.50	$\rightarrow \infty$	5.00	0.37 (0.09)	0.47 (0.10)	0.46 (0.10)	0.49 (0.09)	0.56 (0.10)	0.62 (0.13)
TAF	—	—	1.00	$\rightarrow \infty$	5.00	0.42 (0.09)	0.42 (0.10)	0.65 (0.10)	0.71 (0.11)	0.96 (0.12)	0.98 (0.13)
HOL	—	—	0.50	$\rightarrow \infty$	5.00	0.30 (0.07)	0.41 (0.08)	0.44 (0.08)	0.38 (0.08)	0.54 (0.08)	0.56 (0.10)
HOL	—	—	1.00	$\rightarrow \infty$	5.00	0.31 (0.06)	0.41 (0.07)	0.44 (0.07)	0.42 (0.08)	0.53 (0.09)	0.58 (0.10)

Table 4.11. Peak and Root-Mean-Square Values of Story Drift for a 6-Story Category 1 Controlled Primary System Using Type 2 Elements. Units are in cm. All elements participate.

Primary-Auxiliary System Configuration: N/A						Peak Story Drift (RMS Story Drift)					
Excitation	$\alpha \equiv \frac{k_2}{k_1}$	$\beta \equiv \frac{m_2}{m_1}$	$\mu \equiv \frac{k_{int}}{k_1}$	$\delta_h \equiv \frac{c_h}{c_1}$	$\delta_l \equiv \frac{c_l}{c_1}$	Story 1	Story 2	Story 3	Story 4	Story 5	Story 6
ELC	—	—	0.50	$\rightarrow \infty$	5.00	1.50 (0.40)	1.41 (0.36)	1.47 (0.32)	1.38 (0.27)	1.18 (0.21)	0.65 (0.12)
ELC	—	—	1.00	$\rightarrow \infty$	5.00	1.25 (0.29)	1.18 (0.26)	1.22 (0.22)	1.18 (0.19)	0.98 (0.16)	0.55 (0.10)
TAF	—	—	0.50	$\rightarrow \infty$	5.00	1.44 (0.35)	1.49 (0.32)	1.51 (0.28)	1.33 (0.25)	1.02 (0.20)	0.55 (0.12)
TAF	—	—	1.00	$\rightarrow \infty$	5.00	1.05 (0.28)	1.29 (0.25)	1.19 (0.22)	1.11 (0.19)	0.94 (0.16)	0.74 (0.11)
HOL	—	—	0.50	$\rightarrow \infty$	5.00	1.77 (0.33)	1.48 (0.29)	1.29 (0.26)	1.22 (0.22)	0.94 (0.17)	0.51 (0.10)
HOL	—	—	1.00	$\rightarrow \infty$	5.00	1.17 (0.25)	1.10 (0.22)	1.04 (0.19)	0.89 (0.16)	0.68 (0.12)	0.35 (0.07)

Table 4.12. Peak and Root-Mean-Square Values of Nodal Mass Acceleration (Absolute) for a 6-Story Category 2 Controlled Primary System Using Type 1 Elements. Units are in g. All elements participate.

Primary-Auxiliary System Configuration: 6–6						Peak Nodal Mass Acceleration (RMS Nodal Mass Acceleration)					
Excitation	$\alpha \equiv \frac{k_2}{k_1}$	$\beta \equiv \frac{m_2}{m_1}$	$\mu \equiv \frac{k_{int}}{k_1}$	$\delta_h \equiv \frac{c_h}{c_1}$	$\delta_l \equiv \frac{c_l}{c_1}$	Mass 1	Mass 2	Mass 3	Mass 4	Mass 5	Mass 6
ELC	1.00	—	—	$\to \infty$	$\to 0$	0.58 (0.08)	0.93 (0.10)	0.87 (0.10)	0.53 (0.10)	0.75 (0.10)	0.85 (0.11)
ELC	2.00	—	—	$\to \infty$	$\to 0$	1.74 (0.10)	0.77 (0.10)	0.66 (0.10)	0.80 (0.10)	0.68 (0.11)	1.05 (0.12)
TAF	1.00	—	—	$\to \infty$	$\to 0$	0.49 (0.09)	0.75 (0.10)	0.54 (0.09)	0.50 (0.09)	0.61 (0.10)	0.66 (0.11)
TAF	2.00	—	—	$\to \infty$	$\to 0$	1.48 (0.12)	1.11 (0.12)	0.82 (0.11)	0.66 (0.11)	0.69 (0.12)	0.90 (0.13)
HOL	1.00	—	—	$\to \infty$	$\to 0$	0.36 (0.07)	0.46 (0.07)	0.38 (0.07)	0.40 (0.07)	0.45 (0.08)	0.56 (0.09)
HOL	2.00	—	—	$\to \infty$	$\to 0$	0.77 (0.07)	0.47 (0.07)	0.46 (0.08)	0.43 (0.08)	0.50 (0.08)	0.55 (0.09)

Table 4.13. Peak and Root-Mean-Square Values of Story Drift for a 6-Story Category 2 Controlled Primary System Using Type 1 Elements. Units are in cm. All elements participate.

Primary-Auxiliary System Configuration: 6–6						Peak Story Drift (RMS Story Drift)					
Excitation	$\alpha \equiv \frac{k_2}{k_1}$	$\beta \equiv \frac{m_2}{m_1}$	$\mu \equiv \frac{k_{int}}{k_1}$	$\delta_h \equiv \frac{c_h}{c_1}$	$\delta_l \equiv \frac{c_l}{c_1}$	Story 1	Story 2	Story 3	Story 4	Story 5	Story 6
ELC	1.00	—	—	$\to \infty$	$\to 0$	1.20 (0.25)	1.12 (0.23)	1.48 (0.21)	1.12 (0.18)	0.88 (0.15)	0.55 (0.09)
ELC	2.00	—	—	$\to \infty$	$\to 0$	0.93 (0.20)	1.02 (0.18)	0.77 (0.15)	0.74 (0.13)	0.44 (0.10)	0.36 (0.06)
TAF	1.00	—	—	$\to \infty$	$\to 0$	1.20 (0.25)	1.27 (0.23)	1.21 (0.21)	1.00 (0.19)	0.70 (0.15)	0.50 (0.10)
TAF	2.00	—	—	$\to \infty$	$\to 0$	1.05 (0.19)	1.56 (0.18)	0.97 (0.16)	0.72 (0.13)	0.47 (0.11)	0.37 (0.08)
HOL	1.00	—	—	$\to \infty$	$\to 0$	1.13 (0.23)	1.05 (0.20)	0.96 (0.18)	0.86 (0.15)	0.64 (0.12)	0.34 (0.07)
HOL	2.00	—	—	$\to \infty$	$\to 0$	0.74 (0.18)	0.66 (0.16)	0.61 (0.14)	0.54 (0.11)	0.40 (0.08)	0.31 (0.05)

Table 4.14. Peak and Root-Mean-Square Values of Nodal Mass Acceleration (Absolute) for a 6-Story Category 2 Controlled Primary System Using Type 2 Elements. Units are in g. All elements participate.

Primary-Auxiliary System Configuration: 6–6						Peak Nodal Mass Acceleration (RMS Nodal Mass Acceleration)					
Excitation	$\alpha \equiv \frac{k_2}{k_1}$	$\beta \equiv \frac{m_2}{m_1}$	$\mu \equiv \frac{k_{int}}{k_1}$	$\delta_h \equiv \frac{c_h}{c_1}$	$\delta_l \equiv \frac{c_l}{c_1}$	Mass 1	Mass 2	Mass 3	Mass 4	Mass 5	Mass 6
ELC	1.00	—	—	$\rightarrow \infty$	5.00	0.58 (0.09)	0.99 (0.10)	0.88 (0.10)	0.64 (0.10)	0.81 (0.11)	0.87 (0.12)
ELC	2.00	—	—	$\rightarrow \infty$	5.00	0.46 (0.09)	0.56 (0.09)	0.57 (0.10)	0.61 (0.10)	0.68 (0.11)	0.73 (0.11)
TAF	1.00	—	—	$\rightarrow \infty$	5.00	0.48 (0.09)	0.70 (0.09)	0.46 (0.09)	0.54 (0.10)	0.70 (0.11)	0.78 (0.12)
TAF	2.00	—	—	$\rightarrow \infty$	5.00	0.87 (0.10)	0.75 (0.10)	0.60 (0.11)	0.65 (0.11)	0.92 (0.12)	0.95 (0.13)
HOL	1.00	—	—	$\rightarrow \infty$	5.00	0.46 (0.07)	0.37 (0.07)	0.41 (0.08)	0.49 (0.08)	0.54 (0.09)	0.61 (0.10)
HOL	2.00	—	—	$\rightarrow \infty$	5.00	0.40 (0.07)	0.55 (0.08)	0.48 (0.08)	0.56 (0.08)	0.55 (0.09)	0.61 (0.09)

Table 4.15. Peak and Root-Mean-Square Values of Story Drift for a 6-Story Category 2 Controlled Primary System Using Type 2 Elements. Units are in cm. All elements participate.

Primary-Auxiliary System Configuration: 6–6						Peak Story Drift (RMS Story Drift)					
Excitation	$\alpha \equiv \frac{k_2}{k_1}$	$\beta \equiv \frac{m_2}{m_1}$	$\mu \equiv \frac{k_{int}}{k_1}$	$\delta_h \equiv \frac{c_h}{c_1}$	$\delta_l \equiv \frac{c_l}{c_1}$	Story 1	Story 2	Story 3	Story 4	Story 5	Story 6
ELC	1.00	—	—	$\rightarrow \infty$	5.00	1.33 (0.28)	1.34 (0.25)	1.46 (0.23)	1.31 (0.20)	1.04 (0.16)	0.59 (0.10)
ELC	2.00	—	—	$\rightarrow \infty$	5.00	0.97 (0.20)	0.83 (0.17)	0.88 (0.15)	0.74 (0.13)	0.54 (0.10)	0.35 (0.07)
TAF	1.00	—	—	$\rightarrow \infty$	5.00	1.20 (0.26)	1.23 (0.24)	1.17 (0.22)	1.05 (0.20)	0.73 (0.16)	0.52 (0.10)
TAF	2.00	—	—	$\rightarrow \infty$	5.00	1.06 (0.20)	1.02 (0.18)	0.98 (0.16)	0.79 (0.14)	0.44 (0.11)	0.52 (0.08)
HOL	1.00	—	—	$\rightarrow \infty$	5.00	1.25 (0.25)	1.18 (0.23)	1.09 (0.20)	0.97 (0.17)	0.78 (0.13)	0.43 (0.08)
HOL	2.00	—	—	$\rightarrow \infty$	5.00	0.77 (0.18)	0.68 (0.16)	0.64 (0.14)	0.55 (0.11)	0.57 (0.08)	0.28 (0.05)

Table 4.16. Peak and Root-Mean-Square Values of Nodal Mass Acceleration (Absolute) for a 6-Story Category 3(a) Controlled Primary System Using Type 1 Elements. Units are in g. All elements participate.

Primary-Auxiliary System Configuration: 6–6						Peak Nodal Mass Acceleration (RMS Nodal Mass Acceleration)					
Excitation	$\alpha \equiv \frac{k_2}{k_1}$	$\beta \equiv \frac{m_2}{m_1}$	$\mu \equiv \frac{k_{int}}{k_1}$	$\delta_h \equiv \frac{c_h}{c_1}$	$\delta_l \equiv \frac{c_l}{c_1}$	Mass 1	Mass 2	Mass 3	Mass 4	Mass 5	Mass 6
ELC	1.00	0.15	1.00	$\rightarrow \infty$	$\rightarrow 0$	0.56 (0.09)	0.81 (0.11)	1.12 (0.13)	1.23 (0.15)	1.31 (0.17)	1.56 (0.19)
ELC	2.00	0.30	2.00	$\rightarrow \infty$	$\rightarrow 0$	0.97 (0.09)	1.39 (0.12)	2.05 (0.15)	2.27 (0.18)	2.38 (0.21)	2.40 (0.23)
TAF	1.00	0.15	1.00	$\rightarrow \infty$	$\rightarrow 0$	0.66 (0.10)	0.78 (0.12)	0.77 (0.12)	0.82 (0.13)	0.97 (0.15)	1.20 (0.18)
TAF	2.00	0.30	2.00	$\rightarrow \infty$	$\rightarrow 0$	0.68 (0.10)	0.76 (0.12)	0.94 (0.14)	1.31 (0.15)	1.56 (0.17)	1.84 (0.20)
HOL	1.00	0.15	1.00	$\rightarrow \infty$	$\rightarrow 0$	0.48 (0.08)	0.95 (0.10)	1.23 (0.11)	1.37 (0.12)	1.55 (0.14)	1.56 (0.15)
HOL	2.00	0.30	2.00	$\rightarrow \infty$	$\rightarrow 0$	0.60 (0.08)	0.99 (0.10)	1.35 (0.11)	1.67 (0.13)	1.99 (0.14)	1.83 (0.16)

Table 4.17. Peak and Root-Mean-Square Values of Story Drift for a 6-Story Category 3(a) Controlled Primary System Using Type 1 Elements. Units are in cm. All elements participate.

Primary-Auxiliary System Configuration: 6–6						Peak Story Drift (RMS Story Drift)					
Excitation	$\alpha \equiv \frac{k_2}{k_1}$	$\beta \equiv \frac{m_2}{m_1}$	$\mu \equiv \frac{k_{int}}{k_1}$	$\delta_h \equiv \frac{c_h}{c_1}$	$\delta_l \equiv \frac{c_l}{c_1}$	Story 1	Story 2	Story 3	Story 4	Story 5	Story 6
ELC	1.00	0.15	1.00	$\rightarrow \infty$	$\rightarrow 0$	1.81 (0.31)	1.66 (0.29)	1.65 (0.26)	1.45 (0.23)	1.02 (0.18)	0.58 (0.12)
ELC	2.00	0.30	2.00	$\rightarrow \infty$	$\rightarrow 0$	1.80 (0.27)	1.64 (0.24)	1.41 (0.22)	1.24 (0.20)	1.06 (0.16)	0.63 (0.10)
TAF	1.00	0.15	1.00	$\rightarrow \infty$	$\rightarrow 0$	1.13 (0.28)	1.19 (0.25)	1.32 (0.24)	1.22 (0.23)	0.85 (0.21)	0.52 (0.14)
TAF	2.00	0.30	2.00	$\rightarrow \infty$	$\rightarrow 0$	1.38 (0.26)	1.31 (0.23)	1.10 (0.21)	1.09 (0.19)	0.77 (0.16)	0.49 (0.11)
HOL	1.00	0.15	1.00	$\rightarrow \infty$	$\rightarrow 0$	1.50 (0.25)	1.29 (0.22)	1.06 (0.20)	0.99 (0.19)	0.86 (0.16)	0.54 (0.10)
HOL	2.00	0.30	2.00	$\rightarrow \infty$	$\rightarrow 0$	1.04 (0.23)	0.77 (0.20)	0.63 (0.17)	0.59 (0.15)	0.62 (0.13)	0.42 (0.08)

Table 4.18. Peak and Root-Mean-Square Values of Nodal Mass Acceleration (Absolute) for a 6-Story Category 3(a) Controlled Primary System Using Type 2 Elements. Units are in g. All elements participate.

Primary-Auxiliary System Configuration: 6–6						Peak Nodal Mass Acceleration (RMS Nodal Mass Acceleration)					
Excitation	$\alpha \equiv \frac{k_2}{k_1}$	$\beta \equiv \frac{m_2}{m_1}$	$\mu \equiv \frac{k_{int}}{k_1}$	$\delta_h \equiv \frac{c_h}{c_1}$	$\delta_l \equiv \frac{c_l}{c_1}$	Mass 1	Mass 2	Mass 3	Mass 4	Mass 5	Mass 6
ELC	1.00	0.15	1.00	$\rightarrow \infty$	5.00	0.43 (0.08)	0.62 (0.09)	0.69 (0.11)	0.86 (0.12)	1.02 (0.14)	1.20 (0.16)
ELC	2.00	0.30	2.00	$\rightarrow \infty$	5.00	0.50 (0.09)	0.74 (0.11)	0.92 (0.13)	1.30 (0.15)	1.49 (0.17)	1.56 (0.19)
TAF	1.00	0.15	1.00	$\rightarrow \infty$	5.00	0.45 (0.09)	0.61 (0.10)	0.62 (0.11)	0.89 (0.11)	1.00 (0.13)	1.01 (0.15)
TAF	2.00	0.30	2.00	$\rightarrow \infty$	5.00	0.41 (0.09)	0.61 (0.10)	0.73 (0.11)	0.94 (0.12)	0.83 (0.14)	0.91 (0.16)
HOL	1.00	0.15	1.00	$\rightarrow \infty$	5.00	0.46 (0.08)	0.60 (0.09)	0.67 (0.10)	0.84 (0.11)	1.09 (0.12)	1.09 (0.14)
HOL	2.00	0.30	2.00	$\rightarrow \infty$	5.00	0.56 (0.07)	0.74 (0.09)	1.00 (0.10)	1.19 (0.11)	1.38 (0.13)	1.46 (0.14)

Table 4.19. Peak and Root-Mean-Square Values of Story Drift for a 6-Story Category 3(a) Controlled Primary System Using Type 2 Elements. Units are in cm. All elements participate.

Primary-Auxiliary System Configuration: 6–6						Peak Story Drift (RMS Story Drift)					
Excitation	$\alpha \equiv \frac{k_2}{k_1}$	$\beta \equiv \frac{m_2}{m_1}$	$\mu \equiv \frac{k_{int}}{k_1}$	$\delta_h \equiv \frac{c_h}{c_1}$	$\delta_l \equiv \frac{c_l}{c_1}$	Story 1	Story 2	Story 3	Story 4	Story 5	Story 6
ELC	1.00	0.15	1.00	$\rightarrow \infty$	5.00	1.68 (0.34)	1.66 (0.32)	1.70 (0.28)	1.54 (0.24)	1.17 (0.18)	0.63 (0.11)
ELC	2.00	0.30	2.00	$\rightarrow \infty$	5.00	1.76 (0.28)	1.61 (0.26)	1.52 (0.23)	1.27 (0.20)	1.05 (0.16)	0.68 (0.09)
TAF	1.00	0.15	1.00	$\rightarrow \infty$	5.00	1.34 (0.30)	1.22 (0.28)	1.18 (0.26)	1.12 (0.24)	0.88 (0.20)	0.50 (0.13)
TAF	2.00	0.30	2.00	$\rightarrow \infty$	5.00	1.29 (0.25)	1.19 (0.22)	1.11 (0.21)	0.88 (0.19)	0.70 (0.16)	0.47 (0.10)
HOL	1.00	0.15	1.00	$\rightarrow \infty$	5.00	1.46 (0.31)	1.52 (0.28)	1.28 (0.25)	1.12 (0.22)	1.16 (0.18)	0.67 (0.11)
HOL	2.00	0.30	2.00	$\rightarrow \infty$	5.00	1.18 (0.24)	0.90 (0.21)	0.69 (0.18)	0.59 (0.14)	0.57 (0.11)	0.32 (0.07)

Table 4.20. Peak and Root-Mean-Square Values of Nodal Mass Acceleration (Absolute) for a 6-Story Category 3(b) Controlled Primary System Using Type 1 Elements. Units are in g. All elements participate.

Primary-Auxiliary System Configuration: 6–6						Peak Nodal Mass Acceleration (RMS Nodal Mass Acceleration)					
Excitation	$\alpha \equiv \frac{k_2}{k_1}$	$\beta \equiv \frac{m_2}{m_1}$	$\mu \equiv \frac{k_{int}}{k_1}$	$\delta_h \equiv \frac{c_h}{c_1}$	$\delta_l \equiv \frac{c_l}{c_1}$	Mass 1	Mass 2	Mass 3	Mass 4	Mass 5	Mass 6
ELC	6.50	5.00	0.10	$\to \infty$	$\to 0$	0.63 (0.13)	0.75 (0.18)	0.94 (0.21)	1.03 (0.24)	1.41 (0.27)	1.58 (0.31)
ELC	6.50	5.00	0.05	$\to \infty$	$\to 0$	0.46 (0.12)	0.67 (0.16)	0.66 (0.19)	0.83 (0.22)	1.20 (0.25)	1.44 (0.28)
TAF	6.50	5.00	0.10	$\to \infty$	$\to 0$	0.70 (0.16)	0.96 (0.21)	1.06 (0.21)	0.79 (0.20)	0.91 (0.22)	1.20 (0.28)
TAF	6.50	5.00	0.05	$\to \infty$	$\to 0$	0.90 (0.17)	1.11 (0.23)	0.90 (0.22)	0.79 (0.19)	0.80 (0.21)	1.27 (0.29)
HOL	6.50	5.00	0.10	$\to \infty$	$\to 0$	0.54 (0.13)	0.62 (0.18)	0.68 (0.18)	0.53 (0.16)	0.62 (0.17)	0.82 (0.22)
HOL	6.50	5.00	0.05	$\to \infty$	$\to 0$	0.41 (0.11)	0.52 (0.14)	0.56 (0.15)	0.51 (0.14)	0.52 (0.15)	0.62 (0.19)

Table 4.21. Peak and Root-Mean-Square Values of Story Drift for a 6-Story Category 3(b) Controlled Primary System Using Type 1 Elements. Units are in cm. All elements participate.

Primary-Auxiliary System Configuration: 6–6						Peak Story Drift (RMS Story Drift)					
Excitation	$\alpha \equiv \frac{k_2}{k_1}$	$\beta \equiv \frac{m_2}{m_1}$	$\mu \equiv \frac{k_{int}}{k_1}$	$\delta_h \equiv \frac{c_h}{c_1}$	$\delta_l \equiv \frac{c_l}{c_1}$	Story 1	Story 2	Story 3	Story 4	Story 5	Story 6
ELC	6.50	5.00	0.10	$\rightarrow \infty$	$\rightarrow 0$	3.80 (1.22)	3.70 (1.14)	3.54 (1.02)	3.47 (0.84)	2.75 (0.62)	1.47 (0.34)
ELC	6.50	5.00	0.05	$\rightarrow \infty$	$\rightarrow 0$	3.60 (1.16)	3.47 (1.09)	3.55 (0.97)	3.39 (0.80)	2.55 (0.59)	1.45 (0.33)
TAF	6.50	5.00	0.10	$\rightarrow \infty$	$\rightarrow 0$	3.48 (0.98)	3.28 (0.90)	2.89 (0.80)	2.58 (0.70)	2.36 (0.57)	1.40 (0.34)
TAF	6.50	5.00	0.05	$\rightarrow \infty$	$\rightarrow 0$	3.24 (0.98)	3.01 (0.88)	2.50 (0.79)	2.26 (0.71)	2.29 (0.60)	1.61 (0.36)
HOL	6.50	5.00	0.10	$\rightarrow \infty$	$\rightarrow 0$	2.51 (0.78)	2.14 (0.70)	1.91 (0.62)	1.80 (0.54)	1.75 (0.45)	1.09 (0.27)
HOL	6.50	5.00	0.05	$\rightarrow \infty$	$\rightarrow 0$	2.69 (0.74)	2.34 (0.67)	1.93 (0.59)	1.51 (0.50)	1.38 (0.40)	0.85 (0.24)

Table 4.22. Peak and Root-Mean-Square Values of Nodal Mass Acceleration (Absolute) for a 6-Story Category 3(b) Controlled Primary System Using Type 1 Elements. Units are in g. Only bottom three elements participate.

Primary-Auxiliary System Configuration: 6–3						Peak Nodal Mass Acceleration (RMS Nodal Mass Acceleration)					
Excitation	$\alpha \equiv \frac{k_2}{k_1}$	$\beta \equiv \frac{m_2}{m_1}$	$\mu \equiv \frac{k_{int}}{k_1}$	$\delta_h \equiv \frac{c_h}{c_1}$	$\delta_l \equiv \frac{c_l}{c_1}$	Mass 1	Mass 2	Mass 3	Mass 4	Mass 5	Mass 6
ELC	6.50	5.00	0.20	$\rightarrow \infty$	$\rightarrow 0$	1.17 (0.27)	1.10 (0.22)	1.26 (0.26)	1.37 (0.21)	1.29 (0.24)	1.29 (0.28)
ELC	6.50	5.00	0.10	$\rightarrow \infty$	$\rightarrow 0$	0.78 (0.19)	0.98 (0.22)	0.88 (0.21)	0.93 (0.17)	0.71 (0.16)	1.17 (0.24)
TAF	6.50	5.00	0.20	$\rightarrow \infty$	$\rightarrow 0$	1.09 (0.23)	1.27 (0.24)	1.06 (0.23)	0.98 (0.21)	0.90 (0.17)	1.39 (0.26)
TAF	6.50	5.00	0.10	$\rightarrow \infty$	$\rightarrow 0$	1.19 (0.23)	1.11 (0.26)	1.07 (0.24)	0.86 (0.19)	0.95 (0.17)	1.17 (0.28)
HOL	6.50	5.00	0.20	$\rightarrow \infty$	$\rightarrow 0$	0.80 (0.17)	0.67 (0.18)	0.86 (0.17)	0.84 (0.16)	0.67 (0.14)	0.85 (0.20)
HOL	6.50	5.00	0.10	$\rightarrow \infty$	$\rightarrow 0$	0.61 (0.15)	0.76 (0.18)	0.72 (0.17)	0.56 (0.12)	0.56 (0.13)	0.77 (0.19)

Table 4.23. Peak and Root-Mean-Square Values of Story Drift for a 6-Story Category 3(b) Controlled Primary System Using Type 1 Elements. Units are in cm. Only bottom three elements participate.

Primary-Auxiliary System Configuration: 6–3						Peak Story Drift (RMS Story Drift)					
Excitation	$\alpha \equiv \frac{k_2}{k_1}$	$\beta \equiv \frac{m_2}{m_1}$	$\mu \equiv \frac{k_{int}}{k_1}$	$\delta_h \equiv \frac{c_h}{c_1}$	$\delta_l \equiv \frac{c_l}{c_1}$	Story 1	Story 2	Story 3	Story 4	Story 5	Story 6
ELC	6.50	5.00	0.20	$\rightarrow \infty$	$\rightarrow 0$	2.33 (0.44)	1.69 (0.35)	2.13 (0.40)	3.73 (0.62)	2.38 (0.54)	1.86 (0.40)
ELC	6.50	5.00	0.10	$\rightarrow \infty$	$\rightarrow 0$	2.35 (0.48)	1.71 (0.38)	1.86 (0.39)	2.99 (0.54)	2.39 (0.50)	1.70 (0.34)
TAF	6.50	5.00	0.20	$\rightarrow \infty$	$\rightarrow 0$	1.83 (0.43)	1.57 (0.32)	1.93 (0.37)	2.49 (0.53)	2.31 (0.50)	2.02 (0.37)
TAF	6.50	5.00	0.10	$\rightarrow \infty$	$\rightarrow 0$	2.38 (0.54)	2.11 (0.39)	2.31 (0.40)	2.97 (0.57)	2.35 (0.56)	1.69 (0.40)
HOL	6.50	5.00	0.20	$\rightarrow \infty$	$\rightarrow 0$	1.68 (0.37)	1.33 (0.30)	1.74 (0.34)	2.30 (0.45)	1.74 (0.40)	1.23 (0.28)
HOL	6.50	5.00	0.10	$\rightarrow \infty$	$\rightarrow 0$	2.07 (0.43)	1.80 (0.35)	1.57 (0.34)	1.88 (0.43)	1.76 (0.41)	1.11 (0.28)

Table 4.24. Peak and Root-Mean-Square Values of Nodal Mass Acceleration (Absolute) for a 3-Story Category 3(b) Controlled Primary System Using Type 1 Elements. Units are in g. Only bottom three elements participate.

Primary-Auxiliary System Configuration: 3–6						Peak Nodal Mass Acceleration (RMS Nodal Mass Acceleration)					
Excitation	$\alpha \equiv \frac{k_2}{k_1}$	$\beta \equiv \frac{m_2}{m_1}$	$\mu \equiv \frac{k_{int}}{k_1}$	$\delta_h \equiv \frac{c_h}{c_1}$	$\delta_l \equiv \frac{c_l}{c_1}$	Mass 1	Mass 2	Mass 3	Mass 4	Mass 5	Mass 6
ELC	6.50	5.00	0.10	$\to \infty$	$\to 0$	0.56 (0.13)	0.70 (0.12)	0.92 (0.15)	— —	— —	— —
ELC	6.50	5.00	0.05	$\to \infty$	$\to 0$	0.56 (0.15)	0.73 (0.13)	0.93 (0.17)	— —	— —	— —
TAF	6.50	5.00	0.10	$\to \infty$	$\to 0$	0.60 (0.14)	0.64 (0.12)	0.72 (0.16)	— —	— —	— —
TAF	6.50	5.00	0.05	$\to \infty$	$\to 0$	0.52 (0.14)	0.61 (0.12)	0.70 (0.16)	— —	— —	— —
HOL	6.50	5.00	0.10	$\to \infty$	$\to 0$	0.49 (0.11)	0.51 (0.09)	0.66 (0.12)	— —	— —	— —
HOL	6.50	5.00	0.05	$\to \infty$	$\to 0$	0.50 (0.11)	0.48 (0.09)	0.71 (0.12)	— —	— —	— —

Table 4.25. Peak and Root-Mean-Square Values of Story Drift for a 3-Story Category 3(b) Controlled Primary System Using Type 1 Elements. Units are in cm. Only bottom three elements participate.

Primary-Auxiliary System Configuration: 3–6						Peak Story Drift (RMS Story Drift)					
Excitation	$\alpha \equiv \frac{k_2}{k_1}$	$\beta \equiv \frac{m_2}{m_1}$	$\mu \equiv \frac{k_{int}}{k_1}$	$\delta_h \equiv \frac{c_h}{c_1}$	$\delta_l \equiv \frac{c_l}{c_1}$	Story 1	Story 2	Story 3	Story 4	Story 5	Story 6
ELC	6.50	5.00	0.10	$\to \infty$	$\to 0$	2.29 (0.38)	1.52 (0.30)	1.02 (0.20)	— —	— —	— —
ELC	6.50	5.00	0.05	$\to \infty$	$\to 0$	2.36 (0.42)	1.58 (0.32)	1.00 (0.23)	— —	— —	— —
TAF	6.50	5.00	0.10	$\to \infty$	$\to 0$	2.28 (0.39)	1.84 (0.31)	1.00 (0.22)	— —	— —	— —
TAF	6.50	5.00	0.05	$\to \infty$	$\to 0$	2.26 (0.38)	1.84 (0.30)	1.04 (0.21)	— —	— —	— —
HOL	6.50	5.00	0.10	$\to \infty$	$\to 0$	1.11 (0.25)	0.80 (0.20)	0.73 (0.15)	— —	— —	— —
HOL	6.50	5.00	0.05	$\to \infty$	$\to 0$	1.28 (0.28)	1.00 (0.21)	0.84 (0.16)	— —	— —	— —

Table 4.26. Peak and Root-Mean-Square Values of Nodal Mass Acceleration (Absolute) for a 6-Story Category 4 Controlled Primary System Using Type 3 Elements. Units are in g. All elements participate.

Primary-Auxiliary System Configuration: 6–6						Peak Nodal Mass Acceleration (RMS Nodal Mass Acceleration)					
Excitation	$\alpha \equiv \frac{k_2}{k_1}$	$\beta \equiv \frac{m_2}{m_1}$	$\mu \equiv \frac{k_{int}}{k_1}$	$\delta_h \equiv \frac{c_h}{c_1}$	$\delta_l \equiv \frac{c_l}{c_1}$	Mass 1	Mass 2	Mass 3	Mass 4	Mass 5	Mass 6
ELC	6.50	5.00	—	5.00	0.00	0.41 (0.09)	0.58 (0.12)	0.61 (0.14)	0.66 (0.16)	0.83 (0.18)	0.94 (0.21)
ELC	6.50	5.00	—	10.00	0.00	0.42 (0.09)	0.55 (0.12)	0.61 (0.14)	0.66 (0.17)	0.89 (0.19)	0.95 (0.22)
TAF	6.50	5.00	—	5.00	0.00	0.57 (0.14)	0.69 (0.18)	0.53 (0.17)	0.61 (0.14)	0.56 (0.16)	0.90 (0.22)
TAF	6.50	5.00	—	10.00	0.00	0.56 (0.13)	0.71 (0.17)	0.59 (0.17)	0.59 (0.15)	0.59 (0.16)	0.92 (0.22)
HOL	6.50	5.00	—	5.00	0.00	0.39 (0.09)	0.42 (0.10)	0.42 (0.10)	0.38 (0.11)	0.41 (0.11)	0.60 (0.14)
HOL	6.50	5.00	—	10.00	0.00	0.36 (0.08)	0.39 (0.10)	0.36 (0.10)	0.37 (0.11)	0.43 (0.11)	0.58 (0.14)

Table 4.27. Peak and Root-Mean-Square Values of Story Drift for a 6-Story Category 4 Controlled Primary System Using Type 3 Elements. Units are in cm. All elements participate.

Primary-Auxiliary System Configuration: 6–6						Peak Story Drift (RMS Story Drift)					
Excitation	$\alpha \equiv \frac{k_2}{k_1}$	$\beta \equiv \frac{m_2}{m_1}$	$\mu \equiv \frac{k_{int}}{k_1}$	$\delta_h \equiv \frac{c_h}{c_1}$	$\delta_l \equiv \frac{c_l}{c_1}$	Story 1	Story 2	Story 3	Story 4	Story 5	Story 6
ELC	6.50	5.00	—	5.00	0.00	4.53 (1.00)	4.24 (0.95)	3.64 (0.84)	2.97 (0.69)	2.25 (0.50)	1.25 (0.27)
ELC	6.50	5.00	—	10.00	0.00	4.21 (1.00)	3.74 (0.95)	3.31 (0.84)	2.91 (0.69)	2.17 (0.50)	1.19 (0.27)
TAF	6.50	5.00	—	5.00	0.00	2.89 (0.80)	2.42 (0.72)	2.18 (0.64)	2.08 (0.58)	1.90 (0.49)	1.21 (0.30)
TAF	6.50	5.00	—	10.00	0.00	2.64 (0.81)	2.27 (0.74)	2.09 (0.66)	2.07 (0.58)	1.90 (0.48)	1.19 (0.29)
HOL	6.50	5.00	—	5.00	0.00	2.31 (0.63)	2.11 (0.57)	1.80 (0.50)	1.54 (0.42)	1.38 (0.33)	0.82 (0.19)
HOL	6.50	5.00	—	10.00	0.00	2.24 (0.62)	2.07 (0.57)	1.76 (0.50)	1.52 (0.42)	1.32 (0.32)	0.76 (0.18)

Table 4.28. Peak and Root-Mean-Square Values of Nodal Mass Acceleration (Absolute) for a 6-Story Category 4 Controlled Primary System Using Type 3 Elements. Units are in g. Only bottom three elements participate.

Primary-Auxiliary System Configuration: 6–3						Peak Absolute Acceleration (RMS Absolute Acceleration)					
Excitation	$\alpha \equiv \frac{k_2}{k_1}$	$\beta \equiv \frac{m_2}{m_1}$	$\mu \equiv \frac{k_{int}}{k_1}$	$\delta_h \equiv \frac{c_h}{c_1}$	$\delta_l \equiv \frac{c_l}{c_1}$	Mass 1	Mass 2	Mass 3	Mass 4	Mass 5	Mass 6
ELC	6.50	5.00	—	5.00	0.00	0.42 (0.09)	0.52 (0.12)	0.63 (0.14)	0.74 (0.17)	0.83 (0.18)	0.98 (0.21)
ELC	6.50	5.00	—	10.00	0.00	0.43 (0.09)	0.50 (0.12)	0.65 (0.13)	0.67 (0.14)	0.78 (0.16)	0.94 (0.19)
TAF	6.50	5.00	—	5.00	0.00	0.52 (0.14)	0.62 (0.18)	0.64 (0.18)	0.59 (0.16)	0.59 (0.18)	0.88 (0.23)
TAF	6.50	5.00	—	10.00	0.00	0.45 (0.13)	0.59 (0.15)	0.51 (0.15)	0.54 (0.13)	0.53 (0.14)	0.81 (0.19)
HOL	6.50	5.00	—	5.00	0.00	0.39 (0.09)	0.44 (0.11)	0.45 (0.11)	0.39 (0.12)	0.39 (0.12)	0.59 (0.15)
HOL	6.50	5.00	—	10.00	0.00	0.33 (0.08)	0.42 (0.10)	0.38 (0.10)	0.36 (0.10)	0.37 (0.11)	0.55 (0.13)

Table 4.29. Peak and Root-Mean-Square Values of Story Drift for a 6-Story Category 4 Controlled Primary System Using Type 3 Elements. Units are in cm. Only bottom three elements participate.

Primary-Auxiliary System Configuration: 6–3						Peak Story Drift (RMS Story Drift)					
Excitation	$\alpha \equiv \frac{k_2}{k_1}$	$\beta \equiv \frac{m_2}{m_1}$	$\mu \equiv \frac{k_{int}}{k_1}$	$\delta_h \equiv \frac{c_h}{c_1}$	$\delta_l \equiv \frac{c_l}{c_1}$	Story 1	Story 2	Story 3	Story 4	Story 5	Story 6
ELC	6.50	5.00	—	5.00	0.00	4.86 (1.11)	4.68 (1.05)	4.13 (0.93)	3.24 (0.77)	2.43 (0.56)	1.42 (0.30)
ELC	6.50	5.00	—	10.00	0.00	4.43 (0.94)	4.22 (0.89)	3.66 (0.79)	2.99 (0.67)	2.32 (0.49)	1.36 (0.27)
TAF	6.50	5.00	—	5.00	0.00	3.11 (1.01)	2.60 (0.93)	2.24 (0.82)	2.32 (0.71)	2.13 (0.57)	1.27 (0.34)
TAF	6.50	5.00	—	10.00	0.00	2.90 (0.78)	2.30 (0.71)	2.03 (0.64)	2.09 (0.57)	1.77 (0.46)	1.15 (0.28)
HOL	6.50	5.00	—	5.00	0.00	2.29 (0.75)	2.08 (0.69)	1.75 (0.60)	1.54 (0.50)	1.42 (0.38)	0.86 (0.22)
HOL	6.50	5.00	—	10.00	0.00	2.09 (0.66)	1.93 (0.61)	1.66 (0.54)	1.51 (0.45)	1.34 (0.34)	0.80 (0.19)

Table 4.30. Peak and Root-Mean-Square Values of Nodal Mass Acceleration (Absolute) for a 3-Story Category 4 Controlled Primary System Using Type 3 Elements. Units are in g. Only bottom three elements participate.

Primary-Auxiliary System Configuration: 3–6						Peak Nodal Mass Acceleration (RMS Nodal Mass Acceleration)					
Excitation	$\alpha \equiv \frac{k_2}{k_1}$	$\beta \equiv \frac{m_2}{m_1}$	$\mu \equiv \frac{k_{int}}{k_1}$	$\delta_h \equiv \frac{c_h}{c_1}$	$\delta_l \equiv \frac{c_l}{c_1}$	Mass 1	Mass 2	Mass 3	Mass 4	Mass 5	Mass 6
ELC	6.50	5.00	—	2.71	0.00	0.78 (0.15)	1.00 (0.21)	1.15 (0.26)	— —	— —	— —
ELC	6.50	5.00	—	5.42	0.00	0.68 (0.12)	0.94 (0.15)	1.03 (0.19)	— —	— —	— —
TAF	6.50	5.00	—	2.71	0.00	0.50 (0.13)	0.65 (0.16)	0.81 (0.20)	— —	— —	— —
TAF	6.50	5.00	—	5.42	0.00	0.47 (0.11)	0.56 (0.12)	0.64 (0.16)	— —	— —	— —
HOL	6.50	5.00	—	2.71	0.00	0.55 (0.12)	0.79 (0.16)	0.85 (0.20)	— —	— —	— —
HOL	6.50	5.00	—	5.42	0.00	0.46 (0.10)	0.63 (0.12)	0.68 (0.15)	— —	— —	— —

Table 4.31. Peak and Root-Mean-Square Values of Story Drift for a 3-Story Category 4 Controlled Primary System Using Type 3 Elements. Units are in cm. Only bottom three elements participate.

Primary-Auxiliary System Configuration: 3–6						Peak Story Drift (RMS Story Drift)					
Excitation	$\alpha \equiv \frac{k_2}{k_1}$	$\beta \equiv \frac{m_2}{m_1}$	$\mu \equiv \frac{k_{int}}{k_1}$	$\delta_h \equiv \frac{c_h}{c_1}$	$\delta_l \equiv \frac{c_l}{c_1}$	Story 1	Story 2	Story 3	Story 4	Story 5	Story 6
ELC	6.50	5.00	—	2.71	0.00	4.05 (0.83)	3.04 (0.66)	1.62 (0.38)	— —	— —	— —
ELC	6.50	5.00	—	5.42	0.00	3.68 (0.63)	2.82 (0.50)	1.48 (0.29)	— —	— —	— —
TAF	6.50	5.00	—	2.71	0.00	2.57 (0.61)	2.04 (0.49)	1.20 (0.29)	— —	— —	— —
TAF	6.50	5.00	—	5.42	0.00	2.15 (0.48)	1.72 (0.38)	0.94 (0.24)	— —	— —	— —
HOL	6.50	5.00	—	2.71	0.00	3.17 (0.64)	2.38 (0.50)	1.24 (0.29)	— —	— —	— —
HOL	6.50	5.00	—	5.42	0.00	2.54 (0.49)	1.88 (0.38)	0.98 (0.22)	— —	— —	— —

Table 4.32. Peak and Root-Mean-Square Values of Nodal Mass Acceleration (Absolute) for a 6-Story Category 5 Controlled Primary System Using Type 1 Elements. Units are in g. Only top element participates.

Primary-Auxiliary System Configuration: N/A						Peak Nodal Mass Acceleration (RMS Nodal Mass Acceleration)					
Excitation	$\alpha \equiv \frac{k_2}{k_1}$	$\beta \equiv \frac{m_2}{m_1}$	$\mu \equiv \frac{k_{int}}{k_1}$	$\delta_h \equiv \frac{c_h}{c_1}$	$\delta_l \equiv \frac{c_l}{c_1}$	Mass 1	Mass 2	Mass 3	Mass 4	Mass 5	Mass 6
ELC	0.00	0.06	0.010	$\to \infty$	$\to 0$	0.68 (0.16)	0.83 (0.22)	0.69 (0.20)	0.59 (0.14)	0.80 (0.17)	0.97 (0.24)
ELC	0.00	0.06	0.005	$\to \infty$	$\to 0$	0.43 (0.11)	0.58 (0.13)	0.59 (0.13)	0.59 (0.14)	0.79 (0.14)	0.79 (0.18)
TAF	0.00	0.06	0.010	$\to \infty$	$\to 0$	0.53 (0.16)	0.70 (0.22)	0.56 (0.19)	0.43 (0.13)	0.54 (0.14)	0.82 (0.23)
TAF	0.00	0.06	0.005	$\to \infty$	$\to 0$	0.55 (0.17)	0.64 (0.23)	0.62 (0.20)	0.53 (0.14)	0.52 (0.15)	0.84 (0.24)
HOL	0.00	0.06	0.010	$\to \infty$	$\to 0$	0.48 (0.12)	0.48 (0.16)	0.56 (0.14)	0.46 (0.11)	0.50 (0.11)	0.73 (0.17)
HOL	0.00	0.06	0.005	$\to \infty$	$\to 0$	0.46 (0.11)	0.48 (0.12)	0.52 (0.11)	0.44 (0.11)	0.41 (0.10)	0.62 (0.15)

Table 4.33. Peak and Root-Mean-Square Values of Story Drift for a 6-Story Category 5 Controlled Primary System Using Type 1 Elements. Units are in cm. Only top element participates.

Primary-Auxiliary System Configuration: N/A						Peak Story Drift (RMS Story Drift)					
Excitation	$\alpha \equiv \frac{k_2}{k_1}$	$\beta \equiv \frac{m_2}{m_1}$	$\mu \equiv \frac{k_{int}}{k_1}$	$\delta_h \equiv \frac{c_h}{c_1}$	$\delta_l \equiv \frac{c_l}{c_1}$	Story 1	Story 2	Story 3	Story 4	Story 5	Story 6
ELC	0.00	0.06	0.010	$\rightarrow \infty$	$\rightarrow 0$	3.96 (0.92)	3.59 (0.82)	3.37 (0.73)	2.93 (0.68)	2.34 (0.60)	1.38 (0.39)
ELC	0.00	0.06	0.005	$\rightarrow \infty$	$\rightarrow 0$	3.68 (0.85)	3.46 (0.79)	3.25 (0.71)	2.83 (0.60)	2.02 (0.46)	1.14 (0.28)
TAF	0.00	0.06	0.010	$\rightarrow \infty$	$\rightarrow 0$	2.48 (0.73)	1.92 (0.62)	2.00 (0.55)	2.02 (0.56)	1.96 (0.53)	1.18 (0.35)
TAF	0.00	0.06	0.005	$\rightarrow \infty$	$\rightarrow 0$	2.38 (0.75)	1.94 (0.64)	2.01 (0.56)	2.03 (0.57)	1.91 (0.54)	1.20 (0.35)
HOL	0.00	0.06	0.010	$\rightarrow \infty$	$\rightarrow 0$	2.18 (0.65)	2.01 (0.57)	2.01 (0.50)	2.06 (0.46)	1.75 (0.41)	1.05 (0.27)
HOL	0.00	0.06	0.005	$\rightarrow \infty$	$\rightarrow 0$	2.05 (0.59)	1.83 (0.52)	1.77 (0.46)	1.68 (0.41)	1.41 (0.34)	0.88 (0.28)

Table 4.34. Peak and Root-Mean-Square Values of Nodal Mass Acceleration (Absolute) for a 6-Story Category 5 Controlled Primary System Using Type 1 Elements. Units are in g. Only top element participates.

Primary-Auxiliary System Configuration: N/A						Peak Nodal Mass Acceleration (RMS Nodal Mass Acceleration)					
Excitation	$\alpha \equiv \frac{k_2}{k_1}$	$\beta \equiv \frac{m_2}{m_1}$	$\mu \equiv \frac{k_{int}}{k_1}$	$\delta_h \equiv \frac{c_h}{c_1}$	$\delta_l \equiv \frac{c_l}{c_1}$	Mass 1	Mass 2	Mass 3	Mass 4	Mass 5	Mass 6
ELC	0.00	0.30	0.050	$\rightarrow \infty$	$\rightarrow 0$	0.84 (0.20)	1.03 (0.24)	0.86 (0.20)	0.57 (0.16)	0.68 (0.14)	1.11 (0.24)
ELC	0.00	0.30	0.025	$\rightarrow \infty$	$\rightarrow 0$	0.52 (0.11)	0.57 (0.12)	0.48 (0.11)	0.47 (0.11)	0.65 (0.11)	0.70 (0.15)
TAF	0.00	0.30	0.050	$\rightarrow \infty$	$\rightarrow 0$	0.67 (0.19)	0.92 (0.23)	0.86 (0.20)	0.56 (0.14)	0.53 (0.14)	0.91 (0.24)
TAF	0.00	0.30	0.025	$\rightarrow \infty$	$\rightarrow 0$	0.60 (0.18)	0.66 (0.22)	0.59 (0.20)	0.44 (0.13)	0.50 (0.14)	0.75 (0.23)
HOL	0.00	0.30	0.050	$\rightarrow \infty$	$\rightarrow 0$	1.13 (0.19)	1.04 (0.23)	1.05 (0.20)	0.63 (0.13)	0.92 (0.14)	1.17 (0.24)
HOL	0.00	0.30	0.025	$\rightarrow \infty$	$\rightarrow 0$	0.38 (0.11)	0.42 (0.13)	0.44 (0.12)	0.34 (0.10)	0.37 (0.09)	0.49 (0.14)

Table 4.35. Peak and Root-Mean-Square Values of Story Drift for a 6-Story Category 5 Controlled Primary System Using Type 1 Elements. Units are in cm. Only top element participates.

Primary-Auxiliary System Configuration: N/A						Peak Story Drift (RMS Story Drift)					
Excitation	$\alpha \equiv \frac{k_2}{k_1}$	$\beta \equiv \frac{m_2}{m_1}$	$\mu \equiv \frac{k_{int}}{k_1}$	$\delta_h \equiv \frac{c_h}{c_1}$	$\delta_l \equiv \frac{c_l}{c_1}$	Story 1	Story 2	Story 3	Story 4	Story 5	Story 6
ELC	0.00	0.30	0.050	$\rightarrow \infty$	$\rightarrow 0$	2.65 (0.63)	2.37 (0.49)	1.97 (0.45)	2.12 (0.51)	2.54 (0.54)	2.19 (0.41)
ELC	0.00	0.30	0.025	$\rightarrow \infty$	$\rightarrow 0$	2.56 (0.54)	2.22 (0.49)	2.14 (0.44)	2.05 (0.40)	1.56 (0.35)	1.32 (0.26)
TAF	0.00	0.30	0.050	$\rightarrow \infty$	$\rightarrow 0$	2.40 (0.62)	2.03 (0.49)	2.05 (0.44)	1.96 (0.50)	1.99 (0.52)	1.60 (0.38)
TAF	0.00	0.30	0.025	$\rightarrow \infty$	$\rightarrow 0$	1.89 (0.60)	1.83 (0.47)	1.86 (0.40)	1.79 (0.47)	1.62 (0.49)	1.18 (0.35)
HOL	0.00	0.30	0.050	$\rightarrow \infty$	$\rightarrow 0$	2.85 (0.63)	2.32 (0.48)	1.72 (0.42)	2.24 (0.50)	2.19 (0.52)	1.83 (0.38)
HOL	0.00	0.30	0.025	$\rightarrow \infty$	$\rightarrow 0$	1.92 (0.49)	1.74 (0.42)	1.65 (0.37)	1.50 (0.35)	1.17 (0.32)	0.83 (0.24)

Table 4.36. Qualitative Performance Assessment for Control Categories Used in MDOF System Study.

	Performance Assessment Based Upon:	
Control Category	Story Drift	Nodal Mass Acceleration
1	E	G
2	E	S
3(*a*)	E	P to S
3(*b*)	S to E	P to G
4	S to G	S to G
5	S to G	G

Note: E = Excellent, G = Good, S = Satisfactory, P = Poor

Chapter 5

Conclusions and Future Work

5.1 Summary and Conclusions

As the field of structural control continues to mature, a consensus is emerging as to the essential attributes of an effective and acceptable control system or approach for application to structural systems. Reduction of selected maximum response quantities is certainly mandatory; but simplicity, reliability, and ability to function without substantial amounts of externally-supplied power are also desirable features.

The studies presented herein have examined a semi-active control approach which involves controlled interactions between two distinct structural systems — or different components of a single structural system — in order to reduce the resonance buildup that develops during an external excitation. This approach utilizes certain types of elements to physically produce the interactions, which consist of reaction forces that are applied to the systems. The mechanical properties of the interaction elements may be altered in real time through the use of switching components to effect changes in the reaction forces which are favorable to the control strategy. The major advantage of this semi-active control technology is that relatively large control forces can be generated with minimal power requirements.

A preliminary study involving two interacting SDOF systems has been conducted to examine the effectiveness of the proposed control approach. This study was exploratory in nature and involved very simplistic models of structural systems. However, it was crucial in the development of a methodology for implementation of the control strategy (*i.e.*, Method 1) that could be extended for application to MDOF systems. At present, it has been demonstrated that such an extension is only possible for linear systems, whose response can be decomposed into particular modes of vibration. The response control of

one or several of these modes, each of which behaves like a SDOF system, then naturally follows from the previous work. However, because the control strategy focuses on the so-called relative vibrational energy associated with the linear system (in particular, the components of this energy contributed by certain modes), it may also be possible to further extend the approach to nonlinear systems which exhibit *mode-like* properties, since this kind of system also has a relative vibrational energy associated with it.

In addition, the results of the preliminary study were instrumental in the conception and development of new interaction elements (*i.e.*, Types 1 and 2) for use in the follow-on study involving MDOF systems. As may be recalled, these elements consist of an elastic element which is placed in series with a component that may be activated or deactivated in real time. When activated, the component behaves as a rigid connecting member. When deactivated, the component yields in an extremely-fast manner, rapidly dissipating the strain energy that is stored in the elastic element. In fact, of all the control cases examined, the greatest degree of response reduction is achieved when these types of elements are utilized. Finally, the results of the Category 1 cases in the preliminary study indicate that a significant improvement in response control effectiveness may be obtained if the proposed control algorithm is used instead of algorithm developed by Kobori *et al.* for the Active Variable Stiffness control method [1].

The follow-on study considered MDOF models of structural systems to examine the effectiveness of the proposed control approach and investigated various interaction arrangements involving what may be interpreted as: two adjacent multi-story buildings that interact with one another; or a single multi-story building that interacts with either itself and its base, an externally-situated resilient frame, or an unrestrained, relatively small mass located on top of the multi-story building. In each of these situations, the response control effort is directed at controlling only one multi-story building, which is designated the primary system; the other multi-story building, resilient frame, or small mass is referred to as the auxiliary system.

The following list summarizes the main conclusions for the MDOF system study:

1) Under appropriate conditions, the proposed control method and algorithm are capable of achieving a substantial decrease in the story drift levels associated with the primary system. Depending upon the particular interaction arrangement, the nodal mass acceleration levels may either be reduced or elevated.

2) For the five categories of control cases previously considered, the best response reduction results are obtained when interaction elements capable of continuous energy storage and sudden energy dissipation (Types 1 and 2) are utilized.

3) The proposed control approach is most effective when these types of interaction elements are either: internally mounted within the primary system, between adjacent nodal masses; or attached between the primary system and an auxiliary system intended to resemble an externally-situated elastic frame.

4) For these kinds of interaction arrangements, very significant response reduction is achieved (a 50 to 75 percent decrease in the peak values of the first mode response, which provides the largest contribution to the story drift levels for the ensemble of excitation records considered) when stiffness ratios of order unity are used ($\mu = 0.50$ for Category 1 cases; $\alpha = 1.00$ and $\mu = 1.00$ for Category 2 and 3(a) cases).

5) For the cases in Categories 1, 2, and 3(a), the results generally indicate that it is better to employ the full complement of available interaction elements rather than a partial complement. Such a policy enables effective reduction of the first mode response and prevents the excitation of higher modes by the control effort.

6) Because the more-idealized Type 1 elements produce nearly the same controlled response behavior for the primary system as does the less-idealized Type 2 elements, as is verified by the results of the Category 1, 2, and 3(a) cases, it is acceptable to use Type 1 elements for further exploratory investigation which involves these types of interaction elements. This course of action permits a substantial savings in computational effort.

7) The proposed control approach appears to be less effective for the situation in which the primary and auxiliary systems represent two existing structures (*i.e.*, two adjacent buildings), in which the auxiliary system is presumed to be much stronger and more massive than the primary system. However, significant response reduction may still be achieved if a *low-high* primary-auxiliary system configuration exists.

8) When the results of cases in Categories 3(*b*) and 4 which involve the same primary-auxiliary configuration are compared, it is generally observed that the response reduction obtained for the cases in Category 4 is less than that for the cases in Category 3(*b*). Hence, Type 3 elements are less effective at implementing the control strategy for this interaction arrangement and the assumed conditions associated with the auxiliary system.

9) The cases in Category 5 show remarkable response reduction capability in view of the facts that only a single interaction element is utilized and an auxiliary system consisting of a relatively small, unrestrained mass is employed. Although the control effectiveness of these cases is not as great as that of some cases in other categories, such an interaction arrangement might prove useful for applications involving wind gust excitation, such as has been previously considered for tuned mass dampers and active mass drivers.

10) The cases in Categories 3(*b*) and 5 reveal that response control effectiveness is highly dependent upon the value selected for μ, the parameter associated with the Type 1 elements used.

11) For each of the categories previously considered, a comparison of the results of special reference cases, in which the interaction elements are locked in the activated operating state, with the results of the cases that use the proposed control method indicates both the efficacy of the switching process and the necessity of a control algorithm for the operation of the interaction elements.

12) Several examples of a Category 1 controlled primary system — which is

initially given certain nonequilibrium displacements but is externally unforced — show that the proposed control method is capable of reducing the response of higher frequency modes and suppressing the response of several dominant modes. These results suggest that such a capability may also be possible for a primary system which is externally forced.

5.2 Topics for Future Work

Some questions may be raised regarding the simplistic nature of the models used to represent actual structural systems and the idealistic conditions assumed for the behavior and operation of the interaction elements. These are legitimate concerns. The studies presented herein are based upon a very fundamental treatment of the structural control problem, in which the structural systems are represented by discrete mechanical systems. Such models were chosen for two reasons: to reduce the number of parameters necessary to characterize the systems; and to obtain exact expressions for the natural frequencies and mode shapes of vibration, with the number of degrees of freedom (*i.e.*, the number of structural stories) appearing as a parameter, a feature that greatly facilitated the study.

Perhaps, in more detailed and extensive studies, it would be desirable to include additional factors that could be expected in a real-world setting. Some of these factors might be:

- Constitutive and Geometric Nonlinearities
- Three-Dimensional Effects (*e.g.*: variation in the directional orientation of the external excitation; presence of rotational, other translational, or even vertical modes of vibration; *etc.*)
- Controllability and Observability Issues
- Parameter Identification and Uncertainties
- Thermal Loading of Control Devices
- Time Delays in Switching Processes
- Ground/Structure Interaction Effects

The next steps which should most likely be taken in further investigation include: development of more realistic models for the structural systems and interaction elements utilized in simulations, which would more accurately capture the dynamics (both thermal and mechanical) of the actual systems and devices involved; and incorporation of the capability to identify and target the most dominant response modes in real time. In addition, verification of the proposed control approach through experiments on reduced-scale physical models of structural systems should be accomplished.

Also, it has not been rigorously established that the control algorithm used in the proposed approach guarantees the stability of the controlled system. Because the uncontrolled system is assumed to be asymptotically stable and the excitation input is assumed to be bounded and of finite duration, it would intuitively seem that the proposed approach preserves the stability of the system since the strategy of the approach is to remove relative vibrational energy from the system, and it has already been shown that this kind of energy provides an upper bound for the response quantities of interest. However, it would be preferable to mathematically demonstrate that the proposed approach preserves the stability of the system, and perhaps such a demonstration can be carried out in future work.

Lately, earthquake engineering investigators have expressed concerns regarding the so-called *near-field* effects which have been manifested in recent seismic episodes, such as the 1992 Landers and 1994 Northridge earthquake events. These effects generally occur at locations geographically near to the faulting mechanisms responsible for the earthquake, and they are characterized by much greater peak ground velocities and permanent ground displacements than are experienced at more remote locations. It can be shown that such effects have a tendency to place high demands on the ability of multi-story structures to withstand sudden and pronounced story drifts [2, 3]. These kinds of ground motions are very different from those exhibited by traditional earthquake records, such as the ones employed as excitation input for the studies presented herein, which

typically produce a more gradual buildup in the response of the structure. For such reasons, it would be wise to examine the control effectiveness of the proposed approach in cases that employ these kinds of ground motions.

In each of the control categories previously considered, it has been assumed that the auxiliary system is capable of absorbing any additional energy received as a result of the control effort, and so attention need not be given to its response. In future work, it would be prudent to directly examine the response of the auxiliary system in various cases to verify such an assumption, and perhaps provide the results of some simple calculations involving the strength of materials to substantiate this claim. Also, it is worth reiterating that the parameters characterizing the auxiliary system were selected with the intention that one of the following conditions holds: the effects upon the auxiliary system resulting from interaction with the primary system are minimal (*e.g.*, interaction between two existing structures); or the auxiliary system does not represent a load-carrying structure and can withstand large deflections or excursions (*e.g.*, an externally-situated resilient frame or an unrestrained, relatively small mass).

Finally, it should be mentioned that because most of the dynamic activity for the control cases in the MDOF system study occurs in a single response mode, it should be possible to perform further analysis using reduced-order models for the structural systems. A few situations for which this analysis approach could be helpful are the control cases considered in Categories 3(*b*) and 5, in which there appeared to be optimal values for μ given specified values of α and β. Perhaps, if it were reasonable to model the external excitation as a random process (*e.g.*, filtered, stationary Gaussian white noise), a technique such as *statistical linearization* [4] could be used to find equivalent elements and systems to which approximate analysis may be applied in order to facilitate analytical determination of optimal values for μ in terms of the other parameters.

It is believed that the studies which have been presented herein provide a solid basis for more detailed and advanced investigations of a control approach that uses semi-

actively controlled interactions for the response control of structural systems subjected to external excitations. Although originally intended for multi-story buildings undergoing seismic excitation, it is hoped that these research efforts can also be utilized for general areas of application such as vibration suppression in mechanical systems, vehicles, and other kinds of structures that are exposed to external excitations.

References for Chapter 5

1. T. Kobori and S. Kamagata, "Dynamic Intelligent Buildings — Active Seismic Response Control," *Intelligent Structures – 2: Monitoring and Control, Proc. of Intnl. Workshop on Intel. Systems*, ed. by Y. K. Wen, Perugia, Italy, 1991, London: Elsevier Science Pub. Ltd., 1992, pp. 279–292.

2. W. D. Iwan, "Near-Field Considerations in Specification of Seismic Design Motions for Structures," *Proc. of Tenth European Conf. on Earthquake Engrg.*, Vienna, Austria, Aug. 1994, accepted for publication.

3. T. H. Heaton, J. F. Hall, D. J. Wald, and M. W. Halling, "Response of High-Rise and Base-Isolated Buildings to Hypothetical M_W 7.0 Blind Thrust Earthquake," *Science*, Vol. 267, 13 Jan. 1995, pp. 206-211.

4. J. B. Roberts and P. D. Spanos, *Random Vibration and Statistical Linearization*, New York: John Wiley and Sons, Inc., 1990, Chap. 5 and 6.

Appendix A

A Generalized Form of Pontryagin's Minimum Principle

A.1 Introduction

In Chapter 2, attention is given to a particular form for the integrand L of the performance index J associated with the optimal control problem formulated in Section 2.2. This form is one for which

$$L = L(\dot{z}, z, \boldsymbol{u}, t) \tag{A-1}$$

(*i.e.*, L explicitly depends upon the argument $\dot{z}$). But such a problem can always be converted into one for which the integrand has an explicit functional dependence only upon z, $\boldsymbol{u}$, and t, by virtue of the constraint relation

$$\dot{z} = \boldsymbol{g}(z, \boldsymbol{u}, t) \tag{A-2}$$

in which case, the modified form for the integrand, denoted by $\overline{L}$, is

$$\overline{L} = \overline{L}(z, \boldsymbol{u}, t) \equiv L(\boldsymbol{g}(z, \boldsymbol{u}, t), z, \boldsymbol{u}, t) \tag{A-3}$$

$\overline{L}$ may then be used to formulate the Hamiltonian $\overline{H}$, given by

$$\overline{H} = \overline{H}(\overline{\lambda}, z, \boldsymbol{u}, t) \equiv \overline{\lambda}^{\mathrm{T}} \boldsymbol{g}(z, \boldsymbol{u}, t) + \overline{L}(z, \boldsymbol{u}, t) \tag{A-4}$$

If a solution to the optimal control problem formulated in Section 2.2 exists, then the following necessary conditions, rigorously proved in [1], must be satisfied:

$$\dot{z} = \frac{\partial \overline{H}}{\partial \overline{\lambda}}, \quad -\dot{\overline{\lambda}} = \frac{\partial \overline{H}}{\partial z}; \quad \forall t \in [t_a, t_b] \tag{A-5}$$

and

$$\overline{H}(\overline{\lambda}, z, \boldsymbol{u}, t) \leq \overline{H}(\overline{\lambda}, z, \boldsymbol{v}, t); \quad \forall \boldsymbol{v} \in \Omega, \quad \forall t \in [t_a, t_b] \tag{A-6}$$

subject to the boundary conditions

$$\left[\frac{\partial \varphi}{\partial z} - \overline{\lambda}\right]^{\mathrm{T}}\Bigg|_{t_b} dz_b = 0, \quad \left[\frac{\partial \varphi}{\partial t} + \overline{H}\right]\Bigg|_{t_b} dt_b = 0 \tag{A-7}$$

It is now shown that, for the assumed functional form of L as given in (A-1), an alternative set of necessary conditions to (A-5) and (A-6) is available. These conditions are considered more useful because they directly involve L instead of $\overline{L}$. The path taken to obtain these conditions starts from those given in (A-5) through (A-7), which have already been established. A transformation is then used to modify the system costate $\overline{\lambda}$. It is finally demonstrated that the condition in (A-6), although still valid, may be replaced by an equally valid yet more convenient condition. The following derivation is partially based upon the developments given in [2, 3].

A.2 Derivation

To begin, it is assumed that an admissible control $\boldsymbol{u}$ is a bounded, piecewise continuous function of t on the interval $[t_a, t_b]$. Furthermore, it is required that $\boldsymbol{u}(t) \in \Omega$, $\forall t \in [t_a, t_b]$, where Ω is a specified (possibly closed) subset of E^r, the Euclidean space associated with R^r.

Moreover, it is assumed that $\boldsymbol{g}$ satisfies the uniform Lipshitz condition

$$\|\boldsymbol{g}(z, \boldsymbol{u}, t) - \boldsymbol{g}(\boldsymbol{a}, \boldsymbol{v}, t)\| \le m\left[\|z - \boldsymbol{a}\| + c\|\boldsymbol{u} - \boldsymbol{v}\|\right]; \quad \forall t \in [t_a, t_b] \tag{A-8}$$

where m and c are positive constants and $\|\cdot\|$ denotes an appropriate finite-dimensional norm (*e.g.*, the Euclidean norm). In addition, the auxiliary Lipshitz condition

$$\|z - \boldsymbol{a}\|_z \le k\|\boldsymbol{u} - \boldsymbol{v}\|_u \tag{A-9}$$

will be shown to hold, where

$$\dot{z} = \boldsymbol{g}(z, \boldsymbol{u}, t), \quad \dot{\boldsymbol{a}} = \boldsymbol{g}(\boldsymbol{a}, \boldsymbol{v}, t) \tag{A-10}$$

and

$$\|z\|_z \equiv \max_{t_a \le t \le t_b} \|z(t)\|, \quad \|\boldsymbol{u}\|_u \equiv \frac{1}{T}\int_{t_a}^{t_b} \|\boldsymbol{u}(t)\| dt \tag{A-11}$$

where T is some characteristic time for the problem.

Let z be the system state (*i.e.*, the entire trajectory) corresponding to the optimal control $\boldsymbol{u}$. Suppose that a class of controls neighboring $\boldsymbol{u}$ are considered, and denote an arbitrary member of this class by $\boldsymbol{v} = \boldsymbol{u} + \delta\boldsymbol{u}$, where $\delta\boldsymbol{u}$ is an admissible (not necessarily infinitesimal) variation to the optimal control. Let the system state corresponding to such a member be denoted by $\boldsymbol{a} = z + \delta z$, where δz is the variation in z due to $\delta\boldsymbol{u}$. The class of neighboring controls considered includes only those controls which take the system state from z_a at time t_a to z_b at time t_b, where z_b and t_b are either specified or determined from the conditions given in (A-7). Using (A-10), it is then clear that

$$\frac{d}{dt}[\delta z] = \boldsymbol{g}(\boldsymbol{a},\, \boldsymbol{v},\, t) - \boldsymbol{g}(z,\, \boldsymbol{u},\, t) \tag{A-12}$$

in which case

$$\delta z(t) = \int_{t_a}^{t} [\boldsymbol{g}(\boldsymbol{a},\, \boldsymbol{v},\, \tau) - \boldsymbol{g}(z,\, \boldsymbol{u},\, \tau)]\, d\tau \tag{A-13}$$

where the fact that $\delta z(t_a) = \delta z_a = 0$ has been invoked. It is also clear that

$$\| \delta z(t) \| \le \int_{t_a}^{t} \| \boldsymbol{g}(z,\, \boldsymbol{u},\, \tau) - \boldsymbol{g}(\boldsymbol{a},\, \boldsymbol{v},\, \tau) \|\, d\tau \tag{A-14}$$

Using (A-8) yields

$$\| \delta z(t) \| \le \int_{t_a}^{t} m\left[\| \delta z(\tau) \| + c \| \delta\boldsymbol{u}(\tau) \| \right] d\tau \tag{A-15}$$

Recall the *Gronwall-Bellman lemma* [4], which asserts that if

$$\xi(t) \le \sigma + \int_{t_o}^{t} [\rho(\tau)\xi(\tau) + \mu(\tau)]\, d\tau;\;\; \rho(\tau) \ge 0 \tag{A-16}$$

where σ is a constant, then

$$\xi(t) \le \left[\sigma + \int_{t_o}^{t} e^{-\int_{t_o}^{\tau} \rho(\eta)\, d\eta} \mu(\tau)\, d\tau \right] e^{\int_{t_o}^{t} \rho(\tau)\, d\tau} \tag{A-17}$$

Applying this result to (A-15) gives

$$\| \delta z(t) \| \le m c e^{m(t - t_a)} \int_{t_a}^{t} e^{-m(\tau - t_a)} \| \delta\boldsymbol{u}(\tau) \|\, d\tau \tag{A-18}$$

$\forall t \in [t_a,\, t_b]$, for which

$$\| \delta z(t) \|_z \le m c T e^{m(t_b - t_a)} \frac{1}{T} \int_{t_a}^{t_b} \| \delta\boldsymbol{u}(\tau) \|\, d\tau \tag{A-19}$$

Thus,

$$\| z - a \|_z \leq k \| u - v \|_u \tag{A-20}$$

where $k = mcTe^{m(t_b - t_a)}$, and (A-9) is verified.

Now,

$$L(\dot{z}, z, u, t) - L(\dot{a}, a, v, t) = L(\dot{z}, z, u, t) - L(\dot{z}, z, v, t) \tag{A-21}$$

$$+ L(\dot{z}, z, v, t) - L(\dot{a}, a, v, t)$$

But

$$L(\dot{a}, a, v, t) = \left[\frac{\partial L}{\partial \dot{z}}(\dot{z}, z, v, t)\right]^{\mathsf{T}} (\dot{a} - \dot{z}) + \left[\frac{\partial L}{\partial z}(\dot{z}, z, v, t)\right]^{\mathsf{T}} (a - z) \tag{A-22}$$

$$+ L(\dot{z}, z, v, t) + O(\| \dot{z} - \dot{a} \|_z^2 + \| z - a \|_z^2)$$

Also,

$$\frac{\partial L}{\partial \dot{z}}(\dot{z}, z, v, t) = \frac{\partial L}{\partial \dot{z}}(\dot{z}, z, u, t) + \left[\frac{\partial^2 L}{\partial \dot{z}\, \partial u}(\dot{z}, z, u, t)\right](v - u) + O(\| u - v \|_u^2) \tag{A-23}$$

and

$$\frac{\partial L}{\partial z}(\dot{z}, z, v, t) = \frac{\partial L}{\partial z}(\dot{z}, z, u, t) + \left[\frac{\partial^2 L}{\partial z\, \partial u}(\dot{z}, z, u, t)\right](v - u) + O(\| u - v \|_u^2) \tag{A-24}$$

In addition,

$$\| \dot{z} - \dot{a} \| = \| g(z, u, t) - g(a, v, t) \| \leq m(k + c) \| u - v \|_u \tag{A-25}$$

so that

$$O(\| \dot{z} - \dot{a} \|_z^2 + \| z - a \|_z^2) = O(\| u - v \|_u^2) \tag{A-26}$$

Hence,

$$L(\dot{z}, z, u, t) - L(\dot{a}, a, v, t) = L(\dot{z}, z, u, t) - L(\dot{z}, z, v, t) \tag{A-27}$$

$$+ \left[\frac{\partial L}{\partial \dot{z}}(\dot{z}, z, u, t)\right]^{\mathsf{T}} (\dot{z} - \dot{a}) + \left[\frac{\partial L}{\partial z}(\dot{z}, z, u, t)\right]^{\mathsf{T}} (z - a) + O(\| u - v \|_u^2)$$

Likewise,

$$\dot{z} - \dot{a} = g(z, u, t) - g(a, v, t) = g(z, u, t) - g(z, v, t) \tag{A-28}$$

$$+\left[\frac{\partial g}{\partial z}(z, u, t)\right](z - a) + O(\|u - v\|_u^2)$$

Therefore, for the class of neighboring controls considered,

$$J[U] - J[V] = \int_{t_a}^{t_b} [L(\dot{z}, z, u, t) - L(\dot{a}, a, v, t)]dt \tag{A-29}$$

$$+\int_{t_a}^{t_b} \left[\lambda^T(g(z, u, t) - g(a, v, t)) - \lambda^T(\dot{z} - \dot{a})\right]dt$$

which is valid for any λ.

Now, let

$$H = H(\dot{z}, z, u, t) \equiv \lambda^T g(z, u, t) + L(\dot{z}, z, u, t) \tag{A-30}$$

Using (A-27) and (A-30), (A-29) becomes (after some manipulation)

$$J[U] - J[V] = \int_{t_a}^{t_b} \left[H(\lambda, \dot{z}, z, u, t) - H(\lambda, \dot{z}, z, v, t) + \frac{\partial H}{\partial z}^T (z - a)\right]dt \tag{A-31}$$

$$+\int_{t_a}^{t_b} \left[\frac{\partial L}{\partial \dot{z}}^T (\dot{z} - \dot{a}) - \lambda^T(\dot{z} - \dot{a})\right]dt + O(\|u - v\|_u^2)$$

where the two partial derivatives in (A-31) are both evaluated at $(\dot{z}, z, u, t)$.

Also, let

$$\overline{\lambda} \equiv \lambda - \frac{\partial L}{\partial \dot{z}}(\dot{z}, z, u, t) \tag{A-32}$$

which is actually a defining relation for λ, since $\overline{\lambda}$ is governed by (A-5). It can then be shown that

$$\frac{\partial \overline{H}}{\partial z}(\overline{\lambda}, z, u, t) = \frac{\partial H}{\partial z}(\lambda, \dot{z}, z, u, t) \tag{A-33}$$

where $\overline{H}$ and H are as defined in (A-4) and (A-30), respectively, and $\dot{z}$ is evaluated according to (A-2). Thus, (A-5), together with (A-32) and (A-33), becomes

$$\dot{\lambda} = \frac{d}{dt}\left[\frac{\partial L}{\partial \dot{z}}\right] - \frac{\partial H}{\partial z} \tag{A-34}$$

In addition, using (A-32), it easily shown that

$$\overline{H} = H - \frac{\partial L}{\partial \dot{z}}^T g \tag{A-35}$$

Using (A-34) to substitute for $\partial H/\partial z$ in (A-31), integrating some terms by parts, and cancelling other terms yields

$$J[U]-J[V]=\int_{t_a}^{t_b}\left[H(\lambda,\dot{z},z,\boldsymbol{u},t)-H(\lambda,\dot{z},z,\boldsymbol{v},t)\right]dt+O(\|\boldsymbol{u}-\boldsymbol{v}\|_u^2) \qquad \text{(A-36)}$$

$$+\left[\frac{\partial L}{\partial \dot{z}}-\lambda\right](z-\boldsymbol{a})\Bigg|_{t_a}^{t_b}$$

The last term in (A-36) vanishes because only neighboring controls are considered for which $\boldsymbol{a}(t_a)=z(t_a)$ and $\boldsymbol{a}(t_b)=z(t_b)$. Hence, (A-36) becomes

$$J[U]-J[V]=\int_{t_a}^{t_b}\left[H(\lambda,\dot{z},z,\boldsymbol{u},t)-H(\lambda,\dot{z},z,\boldsymbol{v},t)\right]dt+O(\|\boldsymbol{u}-\boldsymbol{v}\|_u^2) \qquad \text{(A-37)}$$

Consider the following claim:

Claim:

Suppose an admissible control $\boldsymbol{u}$, having corresponding system state z, is optimal on $[t_a,\ t_b]$. Then

$$H(\lambda,\dot{z},z,\boldsymbol{u},t)\le H(\lambda,\dot{z},z,\boldsymbol{v},t);\ \ \forall \boldsymbol{v}\in\Omega,\ \ \forall t\in[t_a,\ t_b] \qquad \text{(A-38)}$$

Proof:

The assertion in (A-38) will be proven by contradiction. Assume there exists a time $\bar{t}\in[t_a,\ t_b]$ and a control $\boldsymbol{w}\in\Omega$ such that

$$H(\lambda(\bar{t}),\dot{z}(\bar{t}),z(\bar{t}),\boldsymbol{u}(\bar{t}),\bar{t})>H(\lambda(\bar{t}),\dot{z}(\bar{t}),z(\bar{t}),\boldsymbol{w},\bar{t}) \qquad \text{(A-39)}$$

The piecewise continuity of $\boldsymbol{u}$ and the continuity of λ, $\boldsymbol{g}$, z, and L imply that an interval $[t_c,\ t_d]\subset[t_a,\ t_b]$, with $\bar{t}\in[t_c,\ t_d]$, and an $\varepsilon>0$ exist, such that

$$H(\lambda(t),\dot{z}(t),z(t),\boldsymbol{u}(t),t)-H(\lambda(t),\dot{z}(t),z(t),\boldsymbol{w},t)>\varepsilon \qquad \text{(A-40)}$$

$\forall t\in[t_c,\ t_d]$. Consequently, let $\boldsymbol{v}$ be chosen so that

$$\boldsymbol{v}(t)=\boldsymbol{w} \quad ,\ t\in[t_c,\ t_d] \qquad \text{(A-41)}$$

$$\boldsymbol{v}(t)=\boldsymbol{u}(t) \quad ,\ t\notin[t_c,\ t_d]$$

Then

$$J[U] - J[V] > \varepsilon(t_d - t_c) + O(\|\boldsymbol{u} - \boldsymbol{v}\|_u^2) \tag{A-42}$$

But

$$\|\boldsymbol{u} - \boldsymbol{v}\|_u = O(|t_d - t_c|) \tag{A-43}$$

Thus, selection of $t_d - t_c$ small enough forces $J[U] - J[V] > 0$, which contradicts the optimality of $\boldsymbol{u}$. Hence, the assertion in (A-38) is proved. ■

Having concluded the immediate derivation, it should be noted that the procedure followed above may be repeated while allowing for z_b and t_b to vary. In addition to the foregoing results, which must be satisfied independent of whether or not z_b and t_b are allowed to vary, boundary conditions equivalent to those given in (A-7) will also be obtained. Thus, using the relations provided in (A-33) and (A-35), and noting that $\partial L/\partial \dot{z} = \partial H/\partial \dot{z}$ (since $\boldsymbol{g}$ does not explicitly depend upon $\dot{z}$), the resulting necessary conditions are

$$\dot{z} = \frac{\partial H}{\partial \lambda}, \quad \dot{\lambda} = \frac{d}{dt}\left[\frac{\partial H}{\partial \dot{z}}\right] - \frac{\partial H}{\partial z}; \quad \forall t \in [t_a, t_b] \tag{A-44}$$

and

$$H(\lambda, \dot{z}, z, \boldsymbol{u}, t) \le H(\lambda, \dot{z}, z, \boldsymbol{v}, t); \quad \forall \boldsymbol{v} \in \Omega, \quad \forall t \in [t_a, t_b] \tag{A-45}$$

subject to the boundary conditions

$$\left[\frac{\partial \varphi}{\partial z} - \lambda + \frac{\partial H}{\partial \dot{z}}\right]^{\mathsf{T}}\Bigg|_{t_b} dz_b = 0, \quad \left[\frac{\partial \varphi}{\partial t} + H - \frac{\partial H}{\partial \dot{z}}^{\mathsf{T}}\, \boldsymbol{g}\right]\Bigg|_{t_b} dt_b = 0 \tag{A-46}$$

where $\boldsymbol{g}$ is as indicated in (A-30). It is worth mentioning that for the case when $\Omega \equiv R^r$, the condition in (A-45) can be replaced by

$$\frac{\partial H}{\partial \boldsymbol{u}}(\lambda, \dot{z}, z, \boldsymbol{u}, t) = 0 \tag{A-47}$$

The conditions given in (A-44), (A-46), and (A-47) may then be independently verified by using the calculus of variations, which lends further support for the validity of the conditions in (A-44) through (A-46).

References for Appendix A

1. L. S. Pontryagin, V. G. Boltyanskii, R. V. Gamkrelidze, and E. F. Mishchenko, *The Mathematical Theory of Optimal Processes*, trans. by K. N. Trirogoff and ed. by L. W. Neustadt, New York: John Wiley and Sons, Inc., 1962, Chap. 1 and 2.
2. D. G. Luenberger, *Optimization Methods by Vector Space Methods*, Series in Decision and Control, New York: John Wiley and Sons, Inc., 1969, Chap. 9.
3. A. P. Sage and C. C. White, *Optimum Systems Control*, 2nd ed., Englewood Cliffs, N.J.: Prentice-Hall, Inc., 1977, Chap. 4.
4. D. M. Wiberg, *State Space and Linear Systems*, Schaum's Outline Series in Engineering, New York: McGraw-Hill, Inc., 1971, Chap. 9.

Appendix B

Some Mathematical Relationships and Derivations

B.1 The $O(\cdot)$ Notation

A scalar, vector, or tensor function $f(h)$ is said to be *order of magnitude* $g(h)$ as $h \to 0$ if the condition

$$\lim_{h \to 0} \frac{f(h)}{g(h)} = b \tag{B-1}$$

holds, where $g(h)$ is a nonnegative scalar function, b is a scalar, vector, or tensor quantity, and h is a nonnegative scalar variable. This is expressed by

$$f(h) = O(g(h)) \text{ as } h \to 0 \tag{B-2}$$

Furthermore, it can also be shown that if

$$f_1(h) = O(g_1(h)) \text{ and } f_2(h) = O(g_2(h)) \tag{B-3}$$

then

$$f_1(h) + f_2(h) = O(g_1(h) + g_2(h)) \text{ as } h \to 0 \tag{B-4}$$

Moreover, if c is a scalar constant, then

$$c f(h) = O(g(h)) \text{ as } h \to 0 \tag{B-5}$$

B.2 Derivation of Equations (3-28) and (3-29)

$$\frac{\left|\Delta E_1(t_k)\right|}{E_1(t_k^-)}$$

$$= \frac{\left|\frac{1}{2} m_1 \omega_1^2 \Delta \left| x_1(t_k) \right|_{sup}^2 \right|}{\frac{1}{2} m_1 \omega_1^2 \left| x_1(t_k^-) \right|_{sup}^2}$$

$$
\begin{aligned}
&= \frac{\left| \Delta \left| x_1(t_k) \right|_{sup}^2 \right|}{\left| x_1(t_k^-) \right|_{sup}^2} \\
&= \frac{\left| \left| x_1(t_k^+) \right|_{sup}^2 - \left| x_1(t_k^-) \right|_{sup}^2 \right|}{\left| x_1(t_k^-) \right|_{sup}^2} \\
&= \frac{\left| \left| x_1(t_k^+) \right|_{sup} - \left| x_1(t_k^-) \right|_{sup} \right|}{\left| x_1(t_k^-) \right|_{sup}} \frac{\left| \left| x_1(t_k^+) \right|_{sup} + \left| x_1(t_k^-) \right|_{sup} \right|}{\left| x_1(t_k^-) \right|_{sup}} \\
&= \frac{\left| \Delta \left| x_1(t_k) \right|_{sup} \right|}{\left| x_1(t_k^-) \right|_{sup}} \frac{\left\{ 2 \left| x_1(t_k^-) \right|_{sup} + \Delta \left| x_1(t_k) \right|_{sup} \right\}}{\left| x_1(t_k^-) \right|_{sup}} \\
&= 2 \left(\frac{\left| \Delta \left| x_1(t_k) \right|_{sup} \right|}{\left| x_1(t_k^-) \right|_{sup}} \right) + \left(\frac{\left| \Delta \left| x_1(t_k) \right|_{sup} \right|}{\left| x_1(t_k^-) \right|_{sup}} \right)^2
\end{aligned}
\tag{B-6}
$$

Now, let

$$
\theta \equiv \frac{\left| \Delta \left| x_1(t_k) \right|_{sup} \right|}{\left| x_1(t_k^-) \right|_{sup}} \quad \text{and} \quad \gamma \equiv \frac{\left| \Delta E_1(t_k) \right|}{E_1(t_k^-)} \tag{B-7}
$$

in which case (B-6) becomes

$$
\theta^2 + 2\theta - \gamma = 0 \tag{B-8}
$$

It is then easily verified that

$$
\theta = \sqrt{1+\gamma} - 1 \tag{B-9}
$$

since $\theta > 0$. (B-9) may then be expanded as a binomial series of the form

$$
\theta = 1 + \tfrac{1}{2}\gamma - \tfrac{1}{2 \cdot 4}\gamma^2 + \tfrac{1 \cdot 3}{2 \cdot 4 \cdot 6}\gamma^3 - \cdots - 1 \tag{B-10}
$$

from which it is clear that $\theta < \frac{1}{2}\gamma$, since $\gamma < 1$.

B.3 Relationship for a Generalized Performance Index

Consider the generalized performance index

$$
J[z,\ t;\ t_b,\ \boldsymbol{u}(\tau)] = \varphi(z_b,\ t_b) + \int_t^{t_b} L(z(\tau),\ \boldsymbol{u}(\tau),\ \tau)\, d\tau \tag{B-11}
$$

where $z(\tau)$ denotes a trajectory obeying

$$\frac{dz}{d\tau} = \boldsymbol{g}(z(\tau),\ \boldsymbol{u}(\tau),\ \tau) \tag{B-12}$$

on the interval $t \le \tau \le t_b$. For a given initial state $z = z(t)$ at an arbitrary initial time t, but fixed final time t_b and prescribed $\boldsymbol{u}(\tau)$, the derivative of J with respect to t is given by

$$\dot{J} = -L(z(t),\ \boldsymbol{u}(t),\ t) \tag{B-13}$$

as verified by using *Leibnitz's rule* for differentiation of an integral. Alternatively, if the functional form of J were known, $\dot{J}$ could be directly evaluated from

$$\dot{J} = \sum_{i=1}^{n} \frac{\partial J}{\partial z_i} g_i + \frac{\partial J}{\partial t} \tag{B-14}$$

Equating (B-13) and (B-14), and rearranging yields

$$\sum_{i=1}^{n} \frac{\partial J}{\partial z_i} g_i + \frac{\partial J}{\partial t} + L = 0 \tag{B-15}$$

A relation which links λ to J in the formulation of the optimal control problem discussed in Chapter 2 is now derived. The derivation follows the account given in [1]. Consider the equation obtained by taking the partial derivative of (B-15) with respect to z_j, $j \in \{1, \ldots, n\}$,

$$\frac{\partial}{\partial z_j} \sum_{i=1}^{n} \frac{\partial J}{\partial z_i} g_i + \frac{\partial^2 J}{\partial t\, \partial z_j} + \frac{\partial L}{\partial z_j} = 0 \tag{B-16}$$

or, assuming continuous first partial derivatives,

$$\sum_{i=1}^{n} \left[\frac{\partial^2 J}{\partial z_i\, \partial z_j} g_i + \frac{\partial J}{\partial z_i} \frac{\partial g_i}{\partial z_j} \right] + \frac{\partial^2 J}{\partial t\, \partial z_j} + \frac{\partial L}{\partial z_j} = 0 \tag{B-17}$$

Next, consider the derivative of $\partial J / \partial z_j$ with respect to t

$$\frac{d}{dt}\left[\frac{\partial J}{\partial z_j} \right] = \sum_{i=1}^{n} \frac{\partial^2 J}{\partial z_j\, \partial z_i} g_i + \frac{\partial^2 J}{\partial z_j\, \partial t} \tag{B-18}$$

Assuming that the first partial derivatives of J with respect to z_k and t are continuous, $k \in \{1, \ldots, n\}$, the order of differentiation may be interchanged, whereupon

$$\frac{d}{dt}\left[\frac{\partial J}{\partial z_j} \right] = \sum_{i=1}^{n} \frac{\partial^2 J}{\partial z_i\, \partial z_j} g_i + \frac{\partial^2 J}{\partial t\, \partial z_j} \tag{B-19}$$

The relations in (B-17) and (B-19) may be combined to yield

$$-\frac{d}{dt}\left[\frac{\partial J}{\partial z_j}\right]=\frac{\partial L}{\partial z_j}+\sum_{i=1}^{n}\frac{\partial J}{\partial z_i}\frac{\partial g_i}{\partial z_j} \tag{B-20}$$

which holds $\forall j \in \{1, \ldots, n\}$, and so (B-20) is representable in vector form as

$$-\frac{d}{dt}\left[\frac{\partial J}{\partial z}\right]=\frac{\partial L}{\partial z}+\frac{\partial g}{\partial z}^{\mathsf{T}}\frac{\partial J}{\partial z} \tag{B-21}$$

which is the desired relationship.

B.4 Matrix Inversion Lemma

Consider the following claim:

Claim:

$$(I+GH)^{-1}=I-G(I+HG)^{-1}H \tag{B-22}$$

where G and H are assumed to be invertible matrices of the same dimensions, and I is an identity matrix with appropriate dimensions.

Proof:

$$\begin{aligned}
&I-G(I+HG)^{-1}H \\
&=I-\left[H^{-1}(I+HG)G^{-1}\right]^{-1} \\
&=I-\left[I+(GH)^{-1}\right]^{-1} \\
&=\left[I+(GH)^{-1}\right]\left[I+(GH)^{-1}\right]^{-1}-\left[I+(GH)^{-1}\right]^{-1} \\
&=\left\{I+(GH)^{-1}-I\right\}\left[I+(GH)^{-1}\right]^{-1} \\
&=(GH)^{-1}\left[I+(GH)^{-1}\right]^{-1} \\
&=\left\{\left[I+(GH)^{-1}\right](GH)\right\}^{-1} \\
&=(I+GH)^{-1}
\end{aligned}$$

■

Next, it is shown that a series expansion may be obtained for $(I+GH)^{-1}$ through recursive application of (B-22):

$$
\begin{aligned}
&(I+GH)^{-1} \\
&= I - G(I+HG)^{-1}H \\
&= I - G\left[I - H(I+GH)^{-1}G\right]H \\
&= I - G\left\{I - H\left[I - G(I+HG)^{-1}H\right]G\right\}H
\end{aligned}
$$

from which it is apparent that

$$(I+GH)^{-1} = I - GH + (GH)^2 - (GH)^3 + \cdots \tag{B-23}$$

B.5 Natural Frequencies and Mode Shapes for the Free Vibration of a Uniformly-Discretized, Chain-Like Mechanical System

Consider a discrete, undamped mechanical system which consists of n repeated identical units, with the same boundary conditions as that indicated in Figure 4.1. The equation of motion for a representative nodal mass away from the boundaries is given by

$$m\ddot{x}_r - k(x_{r+1} - x_r) + k(x_r - x_{r-1}) = 0 \tag{B-24}$$

where $r \in \{2, \ldots, n-1\}$. The boundary conditions to be enforced are

$$m\ddot{x}_1 - k(x_2 - x_1) + k(x_1 - 0) = 0 \tag{B-25}$$

and

$$m\ddot{x}_n - k(x_n - x_{n-1}) = 0 \tag{B-26}$$

The solutions of interest to (B-24) have the form

$$x_r = A_r \cos(\omega t - \varphi) \tag{B-27}$$

Substituting (B-27) into (B-24), and cancelling common terms yields

$$A_{r+1} + (\alpha - 2)A_r + A_{r-1} = 0 \tag{B-28}$$

where

$$\alpha \equiv \frac{m}{k}\omega^2 \tag{B-29}$$

Similarly, (B-25) and (B-26) become

$$A_2 + (\alpha - 2)A_1 = 0 \tag{B-30}$$

and

$$(\alpha - 1)A_n + A_{n-1} = 0 \tag{B-31}$$

respectively. Equation (B-28) is a *difference equation*, and techniques for its solution may be found in [2, 3].

Elementary solutions to (B-28) exist and are of the form

$$A_r = Be^{\beta r} \tag{B-32}$$

Substituting (B-32) into (B-28), and rearranging terms yields

$$2 - \alpha = e^{\beta} + e^{-\beta} \tag{B-33}$$

in which case

$$2 - \alpha = 2\cosh\beta \tag{B-34}$$

if β is real, or

$$2 - \alpha = 2\cos|\beta| \tag{B-35}$$

if β is imaginary. Equations (B-34) and (B-35) represent a constraint relation between the parameters α and β.

In general, the solution to (B-28) which satisfies the boundary conditions given by (B-30) and (B-31) must be of the form

$$A_r = ae^{\beta r} + be^{-\beta r} \tag{B-36}$$

Substituting (B-36) into (B-30) gives

$$ae^{2\beta} + be^{-2\beta} + (\alpha - 2)\left[ae^{\beta} + be^{-\beta}\right] = 0 \tag{B-37}$$

which, upon using (B-33), becomes

$$a + b = 0 \tag{B-38}$$

Substituting (B-36) into (B-31) gives

$$(\alpha - 1)\left[ae^{n\beta} + be^{-n\beta}\right] + ae^{(n-1)\beta} + be^{-(n-1)\beta} = 0 \tag{B-39}$$

which, upon using (B-33), becomes

$$ae^{(n+1)\beta}(1 - e^{-\beta}) + be^{-(n+1)\beta}(1 - e^{\beta}) = 0 \tag{B-40}$$

Equations (B-38) and (B-40) may be combined into a matrix form as

$$\begin{bmatrix} 1 & 1 \\ e^{(n+1)\beta}(1 - e^{-\beta}) & e^{-(n+1)\beta}(1 - e^{\beta}) \end{bmatrix} \begin{Bmatrix} a \\ b \end{Bmatrix} = \begin{Bmatrix} 0 \\ 0 \end{Bmatrix} \tag{B-41}$$

Clearly, (B-41) yields nontrivial solutions for a and b only when the determinant of the coefficient matrix vanishes, in which case

$$e^{(n+1)\beta}(1 - e^{-\beta}) - e^{-(n+1)\beta}(1 - e^{\beta}) = 0 \tag{B-42}$$

After some manipulation, (B-42) becomes

$$\sin\left[(n+1)\frac{\beta}{i}\right] = \sin\left[n\frac{\beta}{i}\right] \tag{B-43}$$

where $i \equiv \sqrt{-1}$.

There are two classes of roots to consider which satisfy (B-43):

a) $$(n+1)\frac{\beta}{i} = (2s - 2)\pi + n\frac{\beta}{i}; \quad s = 1, 2, \ldots \tag{B-44}$$

in which case

$$\beta = \beta_s = 2s\pi i \tag{B-45}$$

Using (B-45) with (B-35) and (B-36), it is readily shown that

$$\alpha = 0 \;\Rightarrow\; \omega = 0 \tag{B-46}$$

and

$$A_{r,s} = a_s + b_s \tag{B-47}$$

which constitutes a trivial solution.

b)
$$(n+1)\frac{\beta}{i} = (2s-1)\pi - n\frac{\beta}{i};\ \ s = 1,\ 2,\ \ldots \tag{B-48}$$

in which case

$$\beta = \beta_s = \frac{(2s-1)}{(2n+1)}\pi i \tag{B-49}$$

(actually, s terminates at n because for $s > n$, the roots replicate the functional behavior for $s \le n$). Using (B-49) with (B-35) and the trigonometric identity

$$\sin^2\left|\frac{\beta}{2}\right| = \frac{1-\cos|\beta|}{2} \tag{B-50}$$

gives

$$\alpha = \alpha_s = 4\sin^2\left[\frac{(2s-1)}{(2n+1)}\frac{\pi}{2}\right] \tag{B-51}$$

and from (B-29) yields

$$\omega = \omega_s = 2\sqrt{\frac{k}{m}}\sin\left[\frac{(2s-1)}{(2n+1)}\frac{\pi}{2}\right] \tag{B-52}$$

Using (B-49) with (B-36) gives

$$A_r = A_{r,s} = a_s e^{i|\beta_s|r} + b_s e^{-i|\beta_s|r} \tag{B-53}$$

But from the boundary condition in (B-38), (B-53) becomes

$$A_{r,s} = 2ia_s\left[\frac{e^{i|\beta_s|r} - e^{-i|\beta_s|r}}{2i}\right] \tag{B-54}$$

or

$$A_{r,s} = c_s \sin\left[\frac{(2s-1)}{(2n+1)}\pi r\right] \tag{B-55}$$

where $c_s \equiv 2ia_s \in R$, since $A_{r,s}$ must be real from the assumed form in (B-27). Hence, the relations given in (4-7) are established from (B-52) and (B-55).

References for Appendix B

1. D. G. Schultz and J. L. Melsa, *State Functions and Linear Control Systems*, Series in Electronic Systems, New York: McGraw-Hill, Inc., 1967, Chap. 7.

2. M. R. Spiegel, *Calculus of Finite Differences and Difference Equations*, Schaum's Outline Series in Mathematics and Statistics, New York: McGraw-Hill, Inc., 1971, Chap. 6.

3. W. T. Thomson, *Theory of Vibration With Applications*, 2nd ed., Englewood Cliffs, N.J.: Prentice-Hall, Inc., 1981, Chap. 10.